# Density Functional and *Ab Initio* Study of Molecular Response

by

Degao Peng

Department of Chemistry
Duke University

Date: _____

Approved:

_____
Weitao Yang, Supervisor

_____
David N. Beratan

_____
Patrick Charbonneau

_____
Benjamin J. Wiley

Dissertation submitted in partial fulfillment of the requirements for the degree of
Doctor of Philosophy in the Department of Chemistry
in the Graduate School of Duke University
2014

# Abstract

## Density Functional and *Ab Initio* Study of Molecular Response

by

Degao Peng

Department of Chemistry
Duke University

Date: _____

Approved:

_____
Weitao Yang, Supervisor

_____
David N. Beratan

_____
Patrick Charbonneau

_____
Benjamin J. Wiley

An abstract of a dissertation submitted in partial fulfillment of the requirements for the degree of Doctor of Philosophy in the Department of Chemistry in the Graduate School of Duke University
2014

# Abstract

Quantum chemistry methods nowadays reach its maturity with various robust ground state correlation methods. However, many problems related to response do not have satisfactory solutions. Chemical reactivity indexes are some static response to external fields and number of particles change. These chemical reactivity indexes have important chemical significance, yet not all of them have analytical expressions for direct evaluations. By solving coupled perturbed self-consistent field equations, analytical expressions are obtained and verified numerically. In the particle-particle (pp) channel, the response to the pairing field describes $N \pm 2$ excitations, i.e. double ionization potentials and double electron affinities. The linear response time-dependent density-functional theory (DFT) with pairing fields is the response theory in the density-functional theory (DFT) framework to describe $N \pm 2$ excitations. Both adiabatic and dynamic kernels are included in this response theory. The correlation energy based on this response, the particle-particle random phase approximation (pp-RPA) correlation energy, is proven equivalent to the ladder approximation of the well-established coupled-cluster doubles. These connections between the response theory, *ab initio* methods, and Green's function theory will be beneficial for further development. Based on the particle-hole RPA and the pp-RPA, the theory of the second particle-hole RPA and the second pp-RPA with restrictions capture single and double excitations efficiently. We also present a novel method, variational fractional spin DFT, to calculate singlet-triplet energy gaps for diradicals, which are

usually studied through spin-flip response theories.

"I leave no trace of wings in the air, but I am glad I have had my flight."

From *Fireflies* by Rabindranath Tagore (1928)

# Contents

# List of Tables

# List of Figures

# List of Abbreviations and Symbols

## Symbols

| | |
|---|---|
| $\chi$ | An atomic orbital (AO) |
| $\mu,\ \nu,\ \gamma,\ \lambda$ | AO indexes |
| $\phi,\ \varphi$ | A molecular orbital (MO) |
| $i,\ j,\ k,\ l,\ m,\ n$ | Indexes for occupied MOs (with or without spin) |
| $a,\ b,\ c,\ d,\ e,\ f$ | Indexes for virtual MOs (with or without spin) |
| $p,\ q,\ r,\ s,\ u,\ v$ | Indexes for general MOs (with or without spin) |
| $\sigma,\ \tau$ | Spin indexes |
| $(pq\|rs)$ | Chemists' notation of a two-electron integral |
| $\langle pq\|rs\rangle$ | Physicists' notation of a two-electron integral |
| $\langle pq\|\|rs\rangle$ | Physicists' notation of an antisymmetrized two-electron integral |
| $\{\hat{A}\}$ | The normal order of the operator $\hat{A}$ |
| $\epsilon_{p\sigma}$ | The MO eigenvalue of orbital $\phi_{p\sigma}$ |
| $\epsilon_{ij}^{ab}$ | $\epsilon_i + \epsilon_j - \epsilon_a - \epsilon_b$ |

## Abbreviations

| | |
|---|---|
| 2ph-RPA | Second particle-hole random phase approximation |
| 2ph-TDA | Second particle-hole Tamm-Dancoff approximation |
| 2pp-RPA | Second particle-particle random phase approximation |
| 2pp-TDA | Second particle-particle Tamm-Dancoff approximation |

| | |
|---|---|
| 2RDM | Two-electron reduced density matrix |
| 2RPA | Second random phase approximation |
| AO | Atomic orbital |
| B3LYP | Becke-three-parameter exchange and Lee-Yang-Parr correlation functional |
| BNL | Baer-Neuhauser-Livshits |
| BSE | Bethe-Salpeter equation |
| CASSCF | Complete-active-space self-consistent field |
| CASPT2 | Complete-active-space with second order perturbation theory |
| CC | Coupled cluster |
| CCD | Coupled cluster doubles |
| CCSD | Coupled cluster singles and doubles |
| CCSDT | Coupled cluster singles, doubles and triples |
| CCSD(T) | Coupled cluster singles and doubles with perturbative triples |
| CI | Configuration interaction |
| CID | Configuration interaction doubles |
| CIS | Configuration interaction singles |
| CISD | Configuration interaction singles and doubles |
| CISDT | Configuration interaction singles, doubles and triples |
| CISDTQ | Configuration interaction singles, doubles, triples and quadruples |
| CP-SCF | Coupled-perturbed self-consistent field |
| DFA | Density-functional approximation |
| DFT | Density-functional theory |
| DIP/DEA-EOM-CC | Double-ionization-potential/double-electron-affinity equation-of-motion coupled-cluster |
| EE-EOM-CC | Excitation-energy equation-of-motion coupled-cluster |

| | |
|---|---|
| EOM | Equation-of-motion |
| FCI | Full configuration interaction |
| FS-DFT | Fractional-spin density-functional theory |
| GGA | Generalized gradient approximation |
| GKS | Generalized Kohn-Sham |
| HF | Hatree-Fock |
| HK | Hohenberg-Kohn |
| KS | Kohn-Sham |
| KS-DFT | Kohn-Sham density-functional theory |
| lCCD | Ladder coupled cluster doubles |
| LDA | Local density approximation |
| LHS | Left-hand side |
| LYP | Lee-Yang-Parr |
| MC-SCF | Multi-configuration self-consistent field |
| MO | Molecular orbital |
| MP | Møller-Plesset |
| MRPT | Multi-reference perturbation theory |
| MRCC | Multi-reference coupled cluster |
| MRCI | Multi-reference configuration interaction |
| OF-DFT | Orbital-free density-functional theory |
| PBE | Perdew-Burke-Ernzerhof |
| pp-RPA | Particle-particle random phase approximation |
| pp-TDA | Particle-particle Tamm-Dancoff approximation |
| PT | Perturbation theory |
| QED | Quantum electrodynamics |
| QMC | Quantum Monte Carlo |

| | |
|---|---|
| r2ph-RPA | Restricted second particle-hole random phase approximation |
| r2ph-TDA | Restricted second particle-hole Tamm-Dancoff approximation |
| r2pp-TDA | Restricted second particle-particle Tamm-Dancoff approximation |
| RHS | Right-hand side |
| RPA | Random phase approximation |
| SCF | Self-consistent field |
| ST | Singlet-triplet |
| TDA | Tamm-Dancoff approximation |
| TDDFT | Time-dependent density-functional theory |
| TDDFT-P | Time-dependent density-functional theory with pairing fields |
| TMM | Trimethylenemathane |
| VFS-DFT | Variational-fractional-spin density-functional theory |
| VWN | Vosko-Wilk-Nusair |
| WKG | Wacker, Kümmel, and Gross |

# Acknowledgements

I express my greatest gratitude to Weitao Yang, without whom I can never manage to finish my PhD. He is the most encouraging cheer leader to me. The best thing I learned from Weitao is his optimisism. The road of research is so difficult and full of thorns. There were depressed days when I devoted a lot of efforts while seeing no good outcomes. Weitao always found exciting points in the theory and data that guided me though the through.

I also want to thank Xiangqian Hu, as my direct advisor in my early years in the group. He taught me hand on hand about the infrastructure of the group cluster and the code in QM4D. His resourceful mind could alwayas help me out of whatever technical issues I encountered. His pragmatic view also influenced my interpretation of many complicated theories.

I am thankful to great collaborators in and out of the group, including Bo Zhao, Aron J. Cohen, Erin R. Johnson, Daniel N. Ess, Deepa Devarajan, Stephen N. Steinmann, Ali M. Malek, Yang Yang, Helen van Aggelen, Andrew T. Franks, Katherine J. Franz, Robert Balawender, Andrzej Holas, Hao Hu, Yuqian Jiang, Jun Gao, and Peng Zhang. It has always been helpful and inspiring to work with people around the world. I also thank Per Jensen for providing the bending potential of $CH_2$ and $NH_2^+$.

Funding support from National Science Foundation, Office of Naval Research, and William Krigbaum and Marcus Hobbs Fellowship from Duke University is greatly

appreciated. I also want to thank travel grants from Duke Graduate School for supporting my conference travels.

# 1

# Introduction

## 1.1 Overview of quantum chemistry

Quantum chemistry[1, 2] is a broad subject to study chemistry in theory using quantum mechanics. As P. A. M. Dirac pointed out in 1929[3], "The underlying physical laws necessary for the mathematical theory of a large part of physics and the whole of chemistry are thus completely known, and the difficulty is only that the exact application of these laws leads to equations much too complicated to be soluble." After almost one century, solving the electronic Schrodinger equation of multiple electrons nowadays is still a nontrivial problem even with non-relativistic and Born-Oppenheimer approximations.[1]

The target problem in quantum chemistry is the time-independent electronic Schrodinger equation, i.e.,

$$\hat{H}\Psi = E\Psi, \tag{1.1}$$

where $\hat{H}$ is the electronic Hamiltonian with nonrelativistic and Born-Oppenheimer

approximations (in atomic units)

$$\hat{H} = -\sum_{i=1}^{N} \frac{1}{2}\nabla_i^2 - \sum_{i=1}^{N}\sum_{A=1}^{N_C} \frac{Z_A}{|\mathbf{r}_i - \mathbf{R}_A|} + \sum_{i=1}^{N}\sum_{j=i+1}^{N} \frac{1}{|\mathbf{r}_i - \mathbf{r}_j|}, \tag{1.2}$$

$\Psi$ is the multi-electron wavefunction, and $E$ is the energy. $N$ is the total number of electrons, while $N_C$ is the number of nuclei in the molecule. The three terms on RHS of Eq. (1.2) is the kinetic energy, the nuclear attraction, and electron-electron repulsion, respectively. The two-electron interaction, the third term on RHS of Eq. (1.2) is the culprit prohibiting the exact solution. Most quantum chemistry methods solve Eq. (1.1) by first projecting the Hamiltonian and the wavefunction into some basis sets, which transforms the differential equation of Eq. (1.1) into a set of algebraic equations. Many methods have been developed to solve the Schrodinger equation, especially for the ground state energy. This section briefly reviewed some major branches of electronic structure theories. Due to the vast quantum chemistry literature, not all methods may be covered in this brief review.

The most well-established branch of quantum chemistry, in the author's perspective, is *ab initio* wavefunction methods. The simplest approximation in *ab initio* methods is the Hartree-Fock (HF) ansatz, which approximates the wavefunction as a single Slater determinant. The difference of the HF energy and the exact one from Eq. (1.1) is the correlation energy. Although the correlation energy only contributes a small portion in the total energy, it is critical to chemical properties. The HF approximation forms the basis of higher order correlation treatment, including configuration interactions (CI), perturbation theory (PT), and coupled-cluster methods (CC). *Ab initio* methods are relatively more matured in theories and algorithms, with systematic improvement to capture all levels of the correlation energies. Coupled-Cluster Singles and Doubles with perturbative Triples (CCSD(T)) becomes the golden standard of quantum chemistry. The main criticism for *ab initio* meth-

ods is the exponentially-growing computational complexity. The straightforward implementation of HF scales as $O(L^4)$, and Møller-Plesset second order perturbation theory (MP2) scales as $O(L^5)$, while CCSD(T) scales as $O(L^7)$, with $L$ being the size of the basis set. Any step forward makes the calculation prohibitive for medium size molecules. Additionally, *ab initio* methods usually require large basis sets to describe wavefunction cusps, which dramatically increases the computational efforts. Yet, *ab initio* methods are still considered robust and reliable methods for molecules of medium sizes in general.

Density / density matrix functional theories take the approach to calculate the correlation energy differently, where wavefunctions are not directly referred to[4]. As a typical density matrix functional theory, the two-electron reduced density matrix (2RDM) theory, treats 2RDM rather than the wavefunction as the basic variable[5]. The 2RDM is a 4-dimensional tensor, a much smaller object compared to the many-body wavefunction which is an $N$-dimensional tensor. This simplification is justified because the electronic Hamiltonian includes only up to two-body interactions. Yet 2RDM suffers from its notorious $N$-representability problem, resulting in too low energies[5]. Density-functional theory (DFT)[4], on the other hand, utilizes electron density rather than the many-body wavefunction as the basic variable to describe the system. It achieves great success in application to a broad range of systems from atoms to molecules to solids with affordable computational complexity and moderate accuracy. The main obstacle for DFT applications is the haunting pathological errors of those widely used functional approximations, including fractional spin errors, fractional charge errors, and the wrong asymptotic description of van der Waals interactions. Despite many efforts invested in these issues, no satisfactory solutions have yet been generally accepted.

Quantum Monte Carlo (QMC) methods[6] solve the Schrodinger equation by stochastic sampling. QMC includes techniques such as variational QMC and diffusion

QMC. QMC can be very accurate if treated properly, however, QMC is far from a black box method due to sophisticated choices of techniques. QMC is mostly, if not exclusively, practiced by QMC developers only.

Besides all that mentioned, there are still novel ongoing developments on electronic structure theories such as density matrix renormalization group[7]. Among all the theories discussed above, the most used methods are *ab initio* wavefunction methods and DFT, since they have been implemented in most quantum chemistry packages (such as Gaussian[8], Gamess[9] and NWChem[10]) as (semi-)black box methods and their behaviors on molecular systems have been tested to be robust. For general purposes, DFT should be used if the system stays within the comfort zones of DFT; otherwise *ab initio* wavefunction methods should be used to correct those pathological errors owing to DFT approximations. In this Dissertation, we only focus on *ab initio* methods and DFT. Readers are encouraged to investigate standard textbooks for details on *ab initio* methods[1, 2, 11, 12], DFT[4], and QMC.[6]

The key concept in this Dissertation is *response*, which is the reaction of a system exposed to an external perturbation. In quantum chemistry, excited states are usually solved within response theories. Therefore, response is essential to understand UV-Vis spectra, excited state dynamics, photochemistry, electron transfer, energy transfer, etc. Different quantum chemistry theories have different methods to calculate response properties. In this Dissertation, we will study response of various types. Chapter 2 with Appendix B is a reproduction of Ref. [13] that presents the static response of a system, which generates many significant chemical reactivity indexes. Chapter 3 with Appendix C is a reproduction of Ref. [14] that establishes the theory for the pairing field response, which studies $N \pm 2$ excitations. Chapter 4 with Appendix D is a reproduction of Ref. [15] that proves an important equivalence between the correlation energy related to the pairing matrix response, i.e. the particle-particle random phase approximation correlation energy, and the ladder ap-

proximation to coupled-cluster doubles. Chapter 5 studies novel response that is capable of capturing single and double excitations with low scaling. Chapter 6 is a reproduction of Ref. [16] that concerns the singlet-triplet energy gaps of diradicals using fractional spin concepts. Although calculations in Chapter 6 are not response based, it does achieve excited state energies which are normally obtained in spin-flip response calculations.

Before we delve deeper into response theories, some introductions on standard quantum chemistry models are reviewed as a starting point.

## 1.2 *Ab initio* methods

### *1.2.1 Hartree-Fock approximation*

The simplest *ab initio* method is the Hartree-Fock approximation, where the wave-function is approximated as a single Slater determinant[1, 17],

$$\Phi_{\mathrm{HF}}(\mathbf{x}_1, \mathbf{x}_2, \cdots \mathbf{x}_N) = \frac{1}{\sqrt{N!}} \begin{vmatrix} \phi_1(\mathbf{x}_1) & \phi_1(\mathbf{x}_2) & \cdots & \phi_1(\mathbf{x}_N) \\ \phi_2(\mathbf{x}_1) & \phi_2(\mathbf{x}_2) & \cdots & \phi_2(\mathbf{x}_N) \\ \vdots & \vdots & & \vdots \\ \phi_N(\mathbf{x}_1) & \phi_N(\mathbf{x}_2) & \cdots & \phi_N(\mathbf{x}_N) \end{vmatrix}, \tag{1.3}$$

where $N$ is the number of electrons in the system, $\mathbf{x}_i$ represents the spatial co-ordinate $\mathbf{r}_i$ and the spin coordinate $\sigma_i$ of the $i$-th electron, and $\phi$'s are molecular orbitals (MO). The Slater determinant guarantees to be antisymmetric with respect to electron transpositions, and is also normalized by construction if all orbitals are orthonormalized,

$$\langle \phi_i | \phi_j \rangle = \int d\mathbf{x} \phi_i^*(\mathbf{x}) \phi_j(\mathbf{x}) = \delta_{ij}. \tag{1.4}$$

The HF determinant is solved by minimizing the total energy with respect to the orbitals,

$$E_{\mathrm{HF}} = \min_{\{\phi_i | i=1..N\}} \langle \Phi_{\mathrm{HF}} | \hat{H} | \Phi_{\mathrm{HF}} \rangle, \tag{1.5}$$

subject to orbital orthonormalization in Eq. (1.4). The expectation value can be evaluated using Slater-Condon rules or second quantization techniques,

$$\langle \Phi_{\mathrm{HF}} | \hat{H} | \Phi_{\mathrm{HF}} \rangle = \sum_{i=1}^{N} h_{ii} + \frac{1}{2} \sum_{i=1}^{N} \sum_{j=1}^{N} \langle ij||ij \rangle, \tag{1.6}$$

where $\hat{h}$ is the core operator which consists of one-body interactions in the Hamiltonian (the kinetic and nuclear attractive part), and the antisymmetrized two-electron integral is

$$\langle pq||sr \rangle = \langle pq|sr \rangle - \langle pq|rs \rangle, \tag{1.7}$$

with the physicists' notation of two electron integrals defined as

$$\langle pq|sr \rangle = \int\int d\mathbf{x}_1 d\mathbf{x}_2 \phi_p^*(\mathbf{x}_1) \phi_q^*(\mathbf{x}_2) \frac{1}{r_{12}} \phi_s(\mathbf{x}_1) \phi_r(\mathbf{x}_2). \tag{1.8}$$

The two electron integral can also be written in a chemists' notation

$$(pq|rs) = \langle pr|qs \rangle. \tag{1.9}$$

Eq. (1.5) with Eq. (1.4) is a standard constrained optimization problem which can be solved by Lagrangian multiplier methods. The resulting equations are the Hartree-Fock equations,

$$\hat{F} \phi_i(\mathbf{x}) = \sum_{j=1}^{N} \phi_j(\mathbf{x}) \epsilon_{ji}, \tag{1.10}$$

with the Fock operator defined as

$$\hat{F} \phi_i(\mathbf{x}) = \hat{h} \phi_i(\mathbf{x}) + \hat{J} \phi_i(\mathbf{x}) - \hat{K} \phi_i(\mathbf{x}), \tag{1.11}$$

where $\hat{J}$ is the Coulomb operator

$$\hat{J} \phi(\mathbf{x}) = \sum_{i=1}^{N} \int d\mathbf{x}' \frac{\phi_i^*(\mathbf{x}') \phi_i(\mathbf{x}')}{|\mathbf{r} - \mathbf{r}'|} \phi(\mathbf{x}), \tag{1.12}$$

and $\hat{K}$ is the Fock exchange operator

$$\hat{K}\phi(\mathbf{x}) = \sum_{i=1}^{N} \int d\mathbf{x}' \frac{\phi_i^*(\mathbf{x}')\phi(\mathbf{x}')}{|\mathbf{r} - \mathbf{r}'|}\phi_i(\mathbf{x}), \tag{1.13}$$

Note that $\hat{K}$ is a nonlocal operator as the result of $\hat{K}\phi(\mathbf{x})$ depends on the whole function $\phi$ rather than just its value at $\mathbf{x}$. $\epsilon_{ji}$'s in Eq. (1.10) are the Lagrangian multipliers controling the orthonormalization of orbitals. Since $E_{\mathrm{HF}}$ is invariant under a unitary transformations among orbitals and $\hat{F}$ is a Hermitian operator, we can choose a set of orbitals such that the Fock operator and the Lagrangian multipliers are diagonal,

$$\hat{F}\phi_i(\mathbf{x}) = \epsilon_i\phi_i(\mathbf{x}). \tag{1.14}$$

Such set of orbitals are called canonical orbitals.

Eq. (1.14) is a differential-integral equation, where the kinetic operator contains a differential operator and the Fock exchange operator contains integral operations. Solving such an equation in real space is very complicated. Therefore, the canonical HF equations are usually solved by expanding the orbitals in terms of a set of basis functions $\{\chi_\mu|\mu = 1..L\}$, which is usually a set of atomic orbitals (AO),

$$\phi_i(\mathbf{x}) = \sum_{\mu=1}^{L} \chi_\mu(\mathbf{x})C_{\mu i}, \tag{1.15}$$

then the differential integral equation of Eq. (1.14) becomes an algebraic equation

$$\sum_{\nu=1}^{L} F_{\mu\nu}C_{\nu i} = \epsilon_i \sum_{\nu=1}^{L} S_{\mu\nu}C_{\nu i}, \tag{1.16}$$

where the overlap matrix is

$$S_{\mu\nu} = \langle\chi_\mu|\chi_\nu\rangle, \tag{1.17}$$

the Fock matrix is

$$F_{\mu\nu} = h_{\mu\nu} + J_{\mu\nu} - K_{\mu\nu}, \tag{1.18}$$

the core matrix is

$$h_{\mu\nu} = \langle \chi_\mu | \hat{h} | \chi_\nu \rangle, \tag{1.19}$$

the Coulomb matrix is

$$J_{\mu\nu} = \sum_{\gamma\lambda} (\mu\nu|\gamma\lambda) P_{\gamma\lambda}, \tag{1.20}$$

the Fock exchange matrix is

$$K_{\mu\nu} = \sum_{\gamma\lambda} (\mu\lambda|\gamma\nu) P_{\gamma\lambda}, \tag{1.21}$$

with the density matrix defined as

$$P_{\mu\nu} = \sum_{i=1}^{N} C^*_{\mu i} C_{\nu i}. \tag{1.22}$$

Rewriting Eq. (1.16) as a matrix equation

$$\mathbf{FC} = \mathbf{SC}\boldsymbol{\epsilon}, \tag{1.23}$$

we recognize that Eq. (1.23) is a generalized eigenvalue equation, while the corresponding orthonormalization condition in Eq. (1.4) is represented as

$$\mathbf{C}^\dagger \mathbf{SC} = \mathbf{I}. \tag{1.24}$$

Note that Eq. (1.23) cannot be solved in one shot, as the Fock matrix $\mathbf{F}$ depends on the Coulomb matrix $\mathbf{J}$ and the Fock exchange matrix $\mathbf{K}$ which depend on the density matrix $\mathbf{P}$ which depends on the coefficients $\mathbf{C}$. Therefore, the HF equation is solved self-consistently, and Eq. (1.23) is usually called the self-consistent field (SCF) equation. The most time consuming process in the SCF procedure is the tensor contraction with the two-electron integrals when building $J$ and $K$ matrices. Since there are $O(L^4)$ two-electron integrals, the time complexity of the SCF procedure scales as $O(L^4)$.

During the derivations above, the mismatch of $N$—the number of electrons—and $L$—the number of basis functions—was not discussed. In order to form $N$ orthogonal spin orbitals, the number of spatial basis functions should be no less than $N/2$. For a practical calculation, $L$ is usually much larger than $N$. The problem arises when we solve Eq. (1.23), where we have $L$ eigenvalues and eigenvectors while we need only $N$ of them. The dilemma is resolved by picking the $N$ eigenvectors with the lowest eigenvalues $\epsilon_i$. This construction scheme is called the Aufbau principle, in which the orbitals should be picked from bottom up according to the eigenvalues. Because the eigenvalues also imply the ordering of MOs, they are also called the MO energies. We call those $N$ orbitals assigned to the Slater determinants the occupied orbitals, and the rest of the orbitals unoccupied or virtual orbitals. Throughout this Dissertation, we use $i$, $j$, $k$, $l\ldots$ to represent occupied orbitals, $a$, $b$, $c$, $d\ldots$ to represent virtual orbitals, and $p$, $q$, $r$, $s$, $u$, $v$ to represent general MOs.

The HF approximation is important not only because it is the simplest *ab initio* methods and serves as the starting point for higher correlation treatments, but also due to its pivotal role in connecting DFT and Green's function methods, which will be discussed subsequently.

The difference between the exact ground state energy in Eq. (1.1) and $E_{\mathrm{HF}}$ at basis set limit is defined as the correlation energy,

$$E_{\mathrm{corr}} = E_{\mathrm{Exact}} - E_{\mathrm{HF}}. \tag{1.25}$$

Due to the variational principle, $E_{\mathrm{corr}}$ is always negative. The correlation energy is the holy grail to all quantum chemistry methods. Traditionally, correlation energies can be categorized in two distinct types: static/nondynamical correlation and dynamical correlation. Static correlation energies arise from bad representation of one single Slater determinant of the system; i.e. the system requires several (nearly) degenerate Slater determinants to have a qualitatively correct picture. This typically

happens when a molecule is stretched, e.g. hydrogen molecule dissociation. Dynamical correlation energies come from dynamic short-range electron depletion due to the Coulomb repulsion that the HF mean-field theory overlooks. Static and dynamical correlations are qualitatively different in their concepts; however, they cannot be exactly partitioned. These concepts are only used to understand the behaviors of different methods. In the next subsection, we will briefly introduce CI, PT, and CC, the main categories to obtain dynamical correlation energies in *ab initio* methods. The way to obtain static correlation is to use multiple references rather than a single reference in the dynamical correlation methods.

### *1.2.2 Second quantization*

The best language to describe the *ab initio* correlation methods is second quantization. The origin of the name "second quantization" is always a puzzle for many quantum chemistry beginners, and is seldom explained clearly in many textbooks. We will explain the naming according to Ref. [18] before going into the details. When we talk about the "first quantization", it means the energy level quantization of particles, such as a particle in a box, a harmonic oscillator, or an electron in a hydrogen-like atom, where we see discrete energy levels. In the "first quantization", particles and fields are treated differently, where particles are quantized and described as wavefunctions while the fields are classical. The "first" "second quantization" occurs in quantum electrodynamics (QED) where the electromagnetic fields are also quantized. In QED, the Coulomb interaction between electrons are described as a photon exchange process, where the field is described as particles—photons. Second quantization language is capable of describing systems with particle number variation. Although the technique was originally developed to work on QED, second quantization turns out to be a very powerful tool in describing quantum particles in classical fields too. And this is the "second quantization" we use in quantum

chemistry, which vaguely relates to its original sense of field quantization.

*Ab initio* correlation methods and Green's function methods make extensive use of second quantization in the derivation. The reader is encouraged to investigate standard textbooks for details about the second quantization, especially Ref. [12] and [19]. Appendix A briefly outlines the conventions and a list of important identities used in this Dissertation.

Using second quantization, the normal ordered Hamiltonian is

$$\hat{H}_N = \hat{F}_N + \hat{G}_N \tag{1.26}$$

$$= \sum_r \epsilon_r \{r^\dagger r\} + \frac{1}{4} \sum_{pqrs} \langle pq||sr\rangle \{p^\dagger q^\dagger rs\}, \tag{1.27}$$

The original Schrodinger equation can be rewritten as

$$\hat{H}_N|\Psi\rangle = E_{\text{corr}}|\Psi\rangle, \tag{1.28}$$

We will discuss various post-HF correlation treatments with second quantization techniques below.

### *1.2.3 Configuration interaction*

The most straightforward post-HF correction is configuration interaction (CI) in terms of formalism. In CI, the wavefunction is approximated by a series of excitation determinants,

$$|\Psi\rangle = (1 + \sum_{ia} t_i^a \{a^\dagger i\} + \frac{1}{2!} \sum_{ijab} t_{ij}^{ab} \{a^\dagger i b^\dagger j\} \cdots)|\Phi_{\text{HF}}\rangle. \tag{1.29}$$

Eq. (1.29) is exact within the one-particle basis set expansion if excitations of all orders are included, which is called full CI (FCI). The computational complexity grows exponentially as the basis set increases in FCI, and thus it is seldom used except for very small systems. By truncating the excitation to a certain order, we

obtain a truncated CI. CI singles (CIS) where only single excitations are included, does not correct the ground state energy due to Brillouin's theorem[1]. Projecting Eq. (1.28) to single excitation determinants, we have an eigenvalue equation, i.e. the CIS equation,

$$\sum_{jb}\langle\Phi_{\rm HF}|\{i^\dagger a\}\hat{H}_N\{b^\dagger j\}|\Phi_{\rm HF}\rangle t_j^b = \omega\sum_{jb}\langle\Phi_{\rm HF}|\{i^\dagger a\}\{b^\dagger j\}|\Phi_{\rm HF}\rangle t_j^b \tag{1.30}$$

$$= \omega\ t_i^a. \tag{1.31}$$

CIS can be used to solve single excitation energies, related to time-dependent Hartree-Fock methods.

The simplest CI with corrections to the ground state is CI doubles (CID), where only $t_{ij}^{ab}$'s are included in Eq. (1.29). A common implementation is CI with singles and doubles (CISD), where all but excitations up to doubles remain. Projecting Eq. (1.28) onto $\langle\Phi_{\rm HF}|$, $\langle\Phi_{\rm HF}|\{i^\dagger a\}$, and $\langle\Phi_{\rm HF}|\{i^\dagger a j^\dagger b\}$ respectively, we have the CISD equation

$$\frac{1}{4}\sum_{ijab} t_{ij}^{ab}\langle\Phi_{\rm HF}|\hat{H}_N\{a^\dagger i b^\dagger j\}|\Phi_{\rm HF}\rangle = E_{\rm corr},$$

$$\sum_{ia} t_i^a\langle\Phi_{\rm HF}|\{k^\dagger c\}\hat{H}_N\{a^\dagger i\}|\Phi_{\rm HF}\rangle + \frac{1}{4}\sum_{ijab} t_{ij}^{ab}\langle\Phi_{\rm HF}|\{k^\dagger c\}\hat{H}_N\{a^\dagger i b^\dagger j\}|\Phi_{\rm HF}\rangle = E_{\rm corr}t_k^c,$$

$$\sum_{ia} t_i^a\langle\Phi_{\rm HF}|\{k^\dagger c l^\dagger d\}\hat{H}_N\{a^\dagger i\}|\Phi_{\rm HF}\rangle + \frac{1}{4}\sum_{ijab} t_{ij}^{ab}\langle\Phi_{\rm HF}|\{k^\dagger c l^\dagger d\}\hat{H}_N\{a^\dagger i b^\dagger j\}|\Phi_{\rm HF}\rangle = E_{\rm corr}t_{kl}^{cd}. \tag{1.32}$$

Although the number of matrix elements in the CISD equation scales as $O(L^8)$, since the number of nonzero elements scales as $O(L^6)$, the computational complexity scales as $O(L^6)$. The CID equation is almost the same as the CISD equation with all $t_i^a$ set zero. Computational complexity of CID is also $O(L^6)$. All truncated CI methods violate size-extensivity. Consequently, truncated CI is usually not preferable in real applications.

### *1.2.4 Perturbation Theory*

This subsection uses special perturbation theory techniques to attain correlation energies order by order. The order here refers to the order of the two-electron interaction. The perturbation theory in a more general sense is outlined in Subsection 1.4.1. Refer to Ref. [12] for details of derivations in this subsection.

It is convenient to introduce the projection operator

$$\hat{P} = |\Phi_{\mathrm{HF}}\rangle\langle\Phi_{\mathrm{HF}}|, \tag{1.33}$$

and

$$\hat{Q} = \hat{I} - \hat{P} = \hat{I} - |\Phi_{\mathrm{HF}}\rangle\langle\Phi_{\mathrm{HF}}|. \tag{1.34}$$

Both $\hat{P}$ and $\hat{Q}$ are idempotent by definition,

$$\hat{P}^2 = \hat{P}, \tag{1.35}$$

$$\hat{Q}^2 = \hat{Q}. \tag{1.36}$$

With intermediate normalization

$$\langle\Phi_{\mathrm{HF}}|\Psi\rangle = 1, \tag{1.37}$$

Eq. (1.27) can be rewritten as

$$E_{\mathrm{corr}} = \langle\Phi_{\mathrm{HF}}|\hat{H}_N|\Psi\rangle, \tag{1.38}$$

and

$$\hat{Q}(\hat{G}_N - E_{\mathrm{corr}})|\Psi\rangle = -\hat{Q}\hat{F}_N|\Psi\rangle. \tag{1.39}$$

Note that

$$\hat{F}_N = \hat{Q}\hat{F}_N\hat{Q}, \tag{1.40}$$

since $\hat{F}_N|\Phi_{\mathrm{HF}}\rangle = \langle\Phi_{\mathrm{HF}}|\hat{F}_N = 0$. We can define a resolvent

$$\hat{R} = \hat{Q}\frac{1}{-\hat{F}_N}\hat{Q}, \tag{1.41}$$

which acts as the negative of the pseudoinverse of $\hat{F}_N$

$$\hat{R}\hat{F}_N = \hat{F}_N\hat{R} = -\hat{Q}. \tag{1.42}$$

Thus, multiplying $\hat{R}$ on both sides of Eq. (1.39), we have

$$\hat{Q}|\Psi\rangle = \hat{R}(\hat{G}_N - E_{\text{corr}})|\Psi\rangle \tag{1.43}$$

$$= \hat{R}(\hat{G}_N - E_{\text{corr}})(\hat{P} + \hat{Q})|\Psi\rangle \tag{1.44}$$

$$= \hat{R}(\hat{G}_N - E_{\text{corr}})|\Phi_{\text{HF}}\rangle + \hat{R}(\hat{G}_N - E_{\text{corr}})\hat{Q}|\Psi\rangle. \tag{1.45}$$

Expanding $\hat{Q}|\Psi\rangle$ repeatedly in Eq. (1.45), we have

$$\hat{Q}|\Psi\rangle = \sum_{m=1}^{\infty}[\hat{R}(\hat{G}_N - E_{\text{corr}})]^m|\Phi_{\text{HF}}\rangle, \tag{1.46}$$

given that the series summation converges. Combining Eqs. (1.38), (1.40) and (1.46) gives the basic working equation for correlation energies in PT

$$E_{\text{corr}} = \langle\Phi_{\text{HF}}|\hat{G}_N\sum_{m=1}^{\infty}[\hat{R}(\hat{G}_N - E_{\text{corr}})]^m|\Phi_{\text{HF}}\rangle. \tag{1.47}$$

We now expand Eq. (1.47), rearranging terms order by order according to $\hat{G}_N$,

$$\begin{aligned}
E_{\text{corr}} &= \langle\Phi_{\text{HF}}|\hat{G}_N\hat{R}\hat{G}_N|\Phi_{\text{HF}}\rangle \\
&\quad + \langle\Phi_{\text{HF}}|\hat{G}_N\hat{R}(\hat{G}_N - E_{\text{corr}})\hat{R}\hat{G}_N|\Phi_{\text{HF}}\rangle \\
&\quad + \cdots && (1.48)\\
&= \langle\Phi_{\text{HF}}|\hat{G}_N\hat{R}\hat{G}_N|\Phi_{\text{HF}}\rangle \\
&\quad + \langle\Phi_{\text{HF}}|\hat{G}_N\hat{R}\hat{G}_N\hat{R}\hat{G}_N|\Phi_{\text{HF}}\rangle - \langle\Phi_{\text{HF}}|\hat{G}_N\hat{R}\langle\Phi_{\text{HF}}|\hat{G}_N\hat{R}\hat{G}_N|\Phi_{\text{HF}}\rangle\hat{R}\hat{G}_N|\Phi_{\text{HF}}\rangle + \cdots \\
&\quad + \cdots && (1.49)\\
&= \langle\Phi_{\text{HF}}|\hat{G}_N\hat{R}\hat{G}_N|\Phi_{\text{HF}}\rangle && (1.50)\\
&\quad + \langle\Phi_{\text{HF}}|\hat{G}_N\hat{R}\hat{G}_N\hat{R}\hat{G}_N|\Phi_{\text{HF}}\rangle && (1.51)\\
&\quad + \cdots . && (1.52)
\end{aligned}$$

Therefore, we have the formal expressions for the second order correlation energy, i.e. MP2 correlation energy,

$$E^{(2)} = \langle \Phi_{\mathrm{HF}} | \hat{G}_N \hat{R} \hat{G}_N | \Phi_{\mathrm{HF}} \rangle \tag{1.53}$$

and the third order correlation energy

$$E^{(3)} = \langle \Phi_{\mathrm{HF}} | \hat{G}_N \hat{R} \hat{G}_N \hat{R} \hat{G}_N | \Phi_{\mathrm{HF}} \rangle. \tag{1.54}$$

PT expressions get very involved to higher order. See Ref. [12] for examples. Using the definition of the resolvent, the detailed expression of $E^{(2)}$ is

$$\begin{aligned}
E^{(2)} &= \langle \Phi_{\mathrm{HF}} | \hat{G}_N \hat{Q} \frac{1}{-\hat{F}_N} \hat{Q} \hat{G}_N | \Phi_{\mathrm{HF}} \rangle \\
&= \langle \Phi_{\mathrm{HF}} | \hat{G}_N \sum_{I \neq 0} |\Phi_I\rangle\langle\Phi_I| \frac{1}{-\hat{F}_N} \sum_{J \neq 0} |\Phi_J\rangle\langle\Phi_J| \hat{G}_N | \Phi_{\mathrm{HF}} \rangle \\
&= \left( \frac{1}{(2!)^2} \right)^2 \sum_{ijabkcld} \langle \Phi_{\mathrm{HF}} | \hat{G}_N \{ a^\dagger i b^\dagger j \} | \Phi_{\mathrm{HF}} \rangle \\
&\quad \times \langle \Phi_{\mathrm{HF}} | \{ j^\dagger b i^\dagger a \} \frac{1}{-\hat{F}_N} \{ c^\dagger k d^\dagger l \} | \Phi_{\mathrm{HF}} \rangle \langle \Phi_{\mathrm{HF}} | \{ l^\dagger d k^\dagger c \} \hat{G}_N | \Phi_{\mathrm{HF}} \rangle \\
&= \frac{1}{16} \sum_{ijab} \langle ab||ij\rangle \frac{4}{\epsilon_{ij}^{ab}} \langle ij||ab\rangle \\
&= \frac{1}{4} \sum_{ijab} \frac{|\langle ab||ij\rangle|^2}{\epsilon_{ij}^{ab}}.
\end{aligned} \tag{1.55}$$

where

$$\epsilon_{ij}^{ab} = \epsilon_i + \epsilon_j - \epsilon_a - \epsilon_b. \tag{1.56}$$

Most post-HF correlation methods works on MOs rather than AOs. The two-electron integral transformation from AO basis to MO basis scales as $O(L^5)$, which is the most time consuming process for MP2 correlation energy calculations. Time complexity of MPx increases dramatically with respect to the order x. For example, MP3 and MP4

scale as $O(L^7)$, and thus are seldom used since CCSD scales as $O(L^6)$ and performs much better.

### *1.2.5 Coupled-cluster theory*

The formalism of coupled-cluster (CC) theory is much more complicated compared to CI and PT. Instead of using a linear excitation operator in CI, CC employs an exponential excitation operator, $\exp(\hat{T})$. The reason for using the exponential operator is not straightforward and is always a puzzle for quantum chemistry beginners. Some reasoning for the choice of the exponential operator can be found in Ref. [12]. One good justification for using exponential operators is that the resulting correlation energy is size-extensive. This subsection only briefly discusses the CC formalism.

In CC theory, the wavefunction is approximated as

$$|\mathrm{CC}\rangle = \exp(\hat{T})|\Phi_{\mathrm{HF}}\rangle, \tag{1.57}$$

where

$$\hat{T} = \hat{T}_1 + \hat{T}_2 + \cdots, \tag{1.58}$$

with $\hat{T}_n$ an $n$-body excitation operator. The CC wavefunction including all level of excitations in $\hat{T}$, namely full CC (interestingly, to the best of my knowledge, no one use the term full CC), is exact, the same as FCI. Note that the number of degrees of freedom in the full CC wavefunction and the FCI wavefunction is the same.

Solving full CC is not practical and we normally need truncations in $\hat{T}$. The simplest CC is CC doubles (CCD), where only $\hat{T}_2$ is included in $\hat{T}$. $\hat{T} = \hat{T}_1 + \hat{T}_2$ makes CC singles and doubles (CCSD). We will derive CCD equations as a heuristic example. Readers are encouraged to refer to Shavitt and Bartlett[12] for details of CC theory.

In CCD, the wavefunction is expressed as

$$|\mathrm{CCD}\rangle = \exp(\hat{T}_2)|\Phi_{\mathrm{HF}}\rangle = \sum_{n=0}^{\infty} \frac{1}{n!}\hat{T}_2^n|\Phi_{\mathrm{HF}}\rangle, \tag{1.59}$$

with

$$\hat{T}_2 = \sum_{i>j,a>b} t_{ij}^{ab}\{a^\dagger i b^\dagger j\} = \frac{1}{4}\sum_{ijab} t_{ij}^{ab}\{a^\dagger i b^\dagger j\}. \tag{1.60}$$

Treating $|\mathrm{CCD}\rangle$ as an eigenvector of $\hat{H}$, we have

$$\hat{H}\exp(\hat{T}_2)|\Phi_{\mathrm{HF}}\rangle = E_{\mathrm{CCD}}\exp(\hat{T}_2)|\Phi_{\mathrm{HF}}\rangle. \tag{1.61}$$

Multiplying $\langle\Phi_{\mathrm{HF}}|$ to Eq. (1.61), we have

$$E_{\mathrm{CCD}} = \langle\Phi_{\mathrm{HF}}|\hat{H}(1+\hat{T}_2)|\Phi_{\mathrm{HF}}\rangle, \tag{1.62}$$

where higher orders in the exponential expansion have zero contributions since $\hat{H}$ contains only one and two body interactions. Multiplying $\langle\Phi_{\mathrm{HF}}|\{i^\dagger a j^\dagger b\}$ to Eq. (1.61), we have

$$E_{\mathrm{CCD}} t_{ij}^{ab} = \langle\Phi_{\mathrm{HF}}|\{i^\dagger a j^\dagger b\}\hat{H}(1+\hat{T}_2+\hat{T}_2^2/2)|\Phi_{\mathrm{HF}}\rangle. \tag{1.63}$$

After some straightforward but tedious algebra, Eqs. (1.62) and (1.63) become the energy equation,

$$E_{\mathrm{CCD}} - E_{\mathrm{HF}} = \frac{1}{4}\sum_{ijab} t_{ij}^{ab}\langle ab||ij\rangle, \tag{1.64}$$

and the amplitude equation,

$$\begin{aligned}
\epsilon_{ij}^{ab} t_{ij}^{ab} = {} & \langle ab||ij\rangle + \frac{1}{2}\sum_{cd}\langle ab||cd\rangle t_{ij}^{cd} + \frac{1}{2}\sum_{kl}\langle ij||kl\rangle t_{kl}^{ab} \\
& - \sum_{kc}(\langle bk||cj\rangle t_{ik}^{ac} - \langle bk||ci\rangle t_{jk}^{ac} - \langle ak||cj\rangle t_{ik}^{bc} + \langle ak||ci\rangle t_{jk}^{bc}) \\
& + \sum_{klcd}\langle kl||cd\rangle[\frac{1}{4}t_{ij}^{cd}t_{kl}^{cd} - \frac{1}{2}(t_{ij}^{ac}t_{kl}^{bd} + t_{ij}^{bd}t_{kl}^{ac}) - \frac{1}{2}(t_{ik}^{ab}t_{jl}^{cd} + t_{ik}^{cd}t_{jl}^{ab}) + (t_{ik}^{ac}t_{jl}^{bd} + t_{ik}^{bd}t_{jl}^{ac})].
\end{aligned} \tag{1.65}$$

The amplitude equation is solved iteratively. The computation of the quadratic term of $t$ is the most time consuming process, which scales as $O(L^6)$. In total, CCD scales as $O(L^6)$, the same as CCSD. CCSD(T) is a post-CCSD treatment with perturbative triple corrections which scales as $O(L^7)$.

### *1.2.6 Remarks on* ab initio *methods*

CI, PT and CC are good ways to capture dynamical correlations. However, in order to capture static correlations, we need multi-reference configuration interactions (MRCI), multi-reference perturbation theory (MRPT), and multi-reference coupled-cluster (MRCC), based on a multi-configuration self-consistent field calculation (MC-SCF)[1, 12]. The mathematics involved in multi-reference methods are much more complicated than the single-reference counterparts.

This short review of *ab initio* wavefunction methods only serves as an appetizer of those standard textbooks on this subject. Through the review we see that for wavefunction methods, we always have a systematic way to approach the FCI result, from CISD to CISDT to CISDTQ, from MP2 to MP3 to MP4, from CCSD to CCSD to CCSDT, etc. However, the computational complexity grows drastically for every step forward. Therefore people try different routes to reach the holy grail. DFT is one of the most famous and widely used route of it.

## 1.3 Density-functional theory

The practice of using density alone to calculate properties of a system predates the formal establishment of density-functional theory (DFT), for solely computational merits. The Thomas-Fermi-Dirac model, the von Wasacker's gradient correction, and Slater's $X\alpha$ model[4] are examples of these pre-Hohenberg-Kohn[20] DFT practice. When we talk about DFT nowadays, implicitly we refer to Kohn-Sham[21] (KS) DFT established by Hohenberg, Kohn, and Sham. Readers are encouraged to investigate

Ref. [4] for details not covered in this brief review.

### *1.3.1 Hohenberg-Kohn theorems*

This subsection proves two important theorems established by Hohenberg and Kohn[20] that set the foundation of DFT.

**Theorem 1.** *(Hohenberg-Kohn Theorem I) For a non-degenerate ground state, the ground state electron density uniquely determines the external potential up to an additive constant.*

*Proof.* Given a Hamiltonian with a non-degenerate ground state

$$\hat{H} = \hat{T} + \hat{v}_{\text{ext}} + \hat{V}_{ee}, \tag{1.66}$$

where $\hat{T}$, $\hat{v}_{\text{ext}}$ and $\hat{V}_{ee}$ are kinetic, external potential (nuclear attractive potential for a molecular system), and two-electron interaction operators, respectively, we have its ground state wavefunction $\Psi$ and density $\rho(\mathbf{r})$. The ground state energy is

$$E_0 = \langle \Psi | \hat{T} + \hat{V}_{ee} | \Psi \rangle + \int d\mathbf{r} v(\mathbf{r}) \rho(\mathbf{r}). \tag{1.67}$$

Assuming there is another Hamiltonian $\hat{H}'$ with another external potential $\hat{v}'_{\text{ext}}$ that produces the same density $\rho(\mathbf{r})$

$$\hat{H}' = \hat{T} + \hat{v}'_{\text{ext}} + \hat{V}_{ee}. \tag{1.68}$$

We then have the ground state energy of $\hat{H}'$,

$$E'_0 = \langle \Psi' | \hat{T} + \hat{V}_{ee} | \Psi' \rangle + \int d\mathbf{r} v(\mathbf{r}) \rho(\mathbf{r}), \tag{1.69}$$

where $|\Psi'\rangle$ is the ground state wavefunction of $\hat{H}'$. According to the variational

principle, we have

$$E_0 = \langle\Psi|\hat{H}|\Psi\rangle \tag{1.70}$$

$$\geqslant \langle\Psi'|\hat{H}|\Psi'\rangle \tag{1.71}$$

$$= \langle\Psi'|\hat{H}'|\Psi'\rangle + \int d\mathbf{r}(v_{\text{ext}}(\mathbf{r}) - v'_{\text{ext}}(\mathbf{r}))\rho(\mathbf{r}) \tag{1.72}$$

$$= E'_0 + \int d\mathbf{r}(v_{\text{ext}}(\mathbf{r}) - v'_{\text{ext}}(\mathbf{r}))\rho(\mathbf{r}). \tag{1.73}$$

Following a similar approach, we also have

$$E'_0 \geqslant E_0 + \int d\mathbf{r}(v'_{\text{ext}}(\mathbf{r}) - v_{\text{ext}}(\mathbf{r}))\rho(\mathbf{r}). \tag{1.74}$$

Therefore, we have

$$E_0 + E'_0 \geqslant E'_0 + E_0, \tag{1.75}$$

indicating the both Eq. (1.71) and (1.74) should use equal signs. Since $|\Psi\rangle$ is non-degenerate, Eq. (1.71) can take equal sign only when $|\Psi'\rangle$ is the same as $|\Psi\rangle$ up to a trivial phase factor. Therefore, $\hat{H}$ and $\hat{H}'$ share the same ground state wavefunction,

$$\hat{H}|\Psi\rangle = E_0|\Psi\rangle, \tag{1.76}$$

$$\hat{H}'|\Psi\rangle = E'_0|\Psi\rangle. \tag{1.77}$$

Subtracting Eq. (1.77) from Eq. (1.76), we have

$$(\hat{v}_{\text{ext}} - \hat{v}'_{\text{ext}})|\Psi\rangle = (E_0 - E'_0)|\Psi\rangle. \tag{1.78}$$

Since $\hat{v}_{\text{ext}} - \hat{v}'_{\text{ext}}$ is a multiplicative operator, $|\Psi\rangle$ is its eigenvector only if it is a constant. Therefore, $\hat{v}_{\text{ext}} - \hat{v}'_{\text{ext}} = \text{const}$. □

HK Theorem I proves that the ground state density determines $v_{\text{ext}}$ (up to a constant) and thus $\hat{H}$ and thus $|\Psi\rangle$ and the ground state energy $E_0$. The dictation of the ground state energy forms a functional

$$E_0 = E_v[\rho] = \langle\Psi|\hat{T} + \hat{V}_{ee}|\Psi\rangle + \int d\mathbf{r}\rho(\mathbf{r})v(\mathbf{r}). \tag{1.79}$$

HK Theorem II provides a variational principle for the ground state energy $E_0$.

**Theorem 2.** *(Hohenberg-Kohn Theorem II) For a trial density $\tilde{\rho}(\mathbf{r})$ such that $\tilde{\rho}(\mathbf{r}) \geqslant 0$ and $\int d\mathbf{r}\tilde{\rho}(\mathbf{r}) = N$, there is a variational principle for the functional in Eq.* (1.79)

$$E_v^{HK}[\tilde{\rho}] \geqslant E_0, \tag{1.80}$$

*where the minimizer is the ground state density $\rho(\mathbf{r})$.*

*Proof.* Following the variational principle from the wavefunction theory,

$$E_v^{\mathrm{HK}}[\tilde{\rho}] = \langle \tilde{\Psi}|\hat{H}|\tilde{\Psi}\rangle \tag{1.81}$$

$$\geqslant \langle \Psi|\hat{H}|\Psi\rangle \tag{1.82}$$

$$= E_0, \tag{1.83}$$

where $\tilde{\Psi}$ is the wavefunction that $\tilde{\rho}$ determines according to HK Theorem I. Since the ground state of $\hat{H}$ is non-degenerate, Eq. (1.82) can take the equal sign if and only if $|\tilde{\Psi}\rangle$ is also the ground state wavefunction of $\hat{H}$. Therefore, the minimizer of this energy functional is the ground state density $\rho$. □

Note that to make use of HK Theorem I, the trial density in HK Theorem II should be a ground state density of some external potential. The set of these densities is called $v$-representable densities in DFT. Additionally, no degeneracy is allowed for the ground state, which means these theorems fail to apply to even a carbon atom. Basically, HK theorems justify the use of electron density as the fundamental variable to describe the system. Later, Levy constrained search formalism solves the $v$-representability and non-degeneracy problems of HK theorems.

### *1.3.2 The Levy constrained-search functional*

Levy present a constrained-search formalism to resolve the $v$-representability and the non-degeneracy issue. The Levy constrained-search functional[22] is defined as

$$E_v^{\mathrm{Levy}}[\tilde{\rho}] = \min_{\Psi\to\tilde{\rho}} \langle \Psi|\hat{T} + \hat{V}_{\mathrm{ee}}|\Psi\rangle + \int d\mathbf{r}\tilde{\rho}(\mathbf{r})v(\mathbf{r}), \tag{1.84}$$

where $\Psi \to \rho$ indicates that the minimization is a constrained optimization within the space $\langle\Psi|\hat{\rho}(\mathbf{r})|\Psi\rangle = \rho(\mathbf{r})$. Therefore, the Levy functional is defined for all $N$-representable densities, i.e. densities that are from some electronic wavefunction, but not necessary of a ground state. The space of $N$-representable densities is a much larger space than that of the $v$-representable densities. The minimizer of the Levy functional is the ground state density

$$\min_{\tilde{\rho}} E_v^{\text{Levy}}[\tilde{\rho}] = \min_{\tilde{\rho}} \min_{\Psi\to\tilde{\rho}} \langle\Psi|\hat{H}|\Psi\rangle \tag{1.85}$$

$$= \min_{\Psi} \langle\Psi|\hat{H}|\Psi\rangle \tag{1.86}$$

$$= E_0 \tag{1.87}$$

Note that although the ground state of $\hat{H}$ is degenerate, the minimization is still justified. Therefore, the Levy constrained-search functional behaves the same as the HK functional, while killing non-degeneracy and $v$-representability issues.

With an energy functional $E_v[\rho]$ in hand, according to the variational principle in DFT, the minimization problem is $\min_\rho E_v[\rho]$ subject to the constraint $\int d\mathbf{r}\rho(\mathbf{r}) = N$. This constrained optimization is solved by Lagrangian multiplier methods. Defining

$$L = E_v[\rho] - \mu(\int d\mathbf{r}\rho(\mathbf{r}) - N) \tag{1.88}$$

then the optimal solution requires

$$\frac{\delta E_v[\rho]}{\delta\rho(\mathbf{r})} = \mu. \tag{1.89}$$

### *1.3.3 Kohn-Sham formalism*

HK theorems are existence theorems but not construction theorems. The difficulty to devise proper functionals that are useful has never been easy. Historically, the kinetic energy has been approximated by Thomas-Fermi (TF) functional from homogeneous

electron gas

$$T_{\mathrm{TF}}[\rho] = C_F \int d\mathbf{r} \rho^{5/3}(\mathbf{r}), \quad \text{with } C_F = \frac{3}{10}(3\pi^2)^{2/3}, \tag{1.90}$$

or TF with a von Weizsacker gradient correction

$$T_W[\rho] = \frac{1}{8} \int d\mathbf{r} \frac{|\nabla \rho|^2}{\rho(\mathbf{r})}. \tag{1.91}$$

Neither kinetic functional works well enough to have actual impact in quantum chemistry. According to the virial theorem, kinetic energy contributes 100% to the total energy[4]. Therefore, errors in kinetic energy will seriously deteriorate the total energy. Kohn and Sham[21] proposed to compromise pure DFT with a little wavefunction contribution by approximating the many-body kinetic energy by the kinetic energy of a non-interacting system with the same electron density. Basically, this is a repartition of the energy

$$\langle \Psi | \hat{T} + \hat{V}_{ee} | \Psi \rangle = T[\rho] + V_{ee}[\rho] = T_s[\rho] + J[\rho] + E_{\mathrm{XC}}[\rho], \tag{1.92}$$

with the exchange-correlation energy defined as

$$E_{\mathrm{XC}}[\rho] = T[\rho] - T_s[\rho] + V_{ee}[\rho] - J[\rho] \tag{1.93}$$

and the classical Coulomb energy (also called the Hartree term in some DFT dialect, although Hartree's theory[17] does not suffer from the self-interaction error as in the Hartree approximation in DFT)

$$J[\rho] = \frac{1}{2} \int \int d\mathbf{r} d\mathbf{r}' \frac{\rho(\mathbf{r})\rho(\mathbf{r}')}{|\mathbf{r} - \mathbf{r}'|}. \tag{1.94}$$

$T_s[\rho]$ is the kinetic energy of a non-interacting system of the density $\rho$. It turns out that $T_s[\rho]$ is a better approximation to $T[\rho]$ than TF and Weiszacker approximations. Since the contribution of $E_{\mathrm{XC}}$ to the total energy is much smaller than that of kinetic

energy, approximations on $E_{\mathrm{XC}}$ is more likely to deliver better total energy. Up to now, Eq. (1.92) only repartitions the energies, thus the formalism is still exact.

With this repartitioning, Eq. (1.89) becomes

$$\frac{\delta T_s[\rho]}{\delta\rho(\mathbf{r})} + v_s(\mathbf{r}) = \mu \tag{1.95}$$

with the effective potential

$$v_s(\mathbf{r}) = v_{\mathrm{ext}}(\mathbf{r}) + v_J(\mathbf{r}) + v_{\mathrm{XC}}(\mathbf{r}), \tag{1.96}$$

the Coulomb potential

$$v_J(\mathbf{r}) = \int d\mathbf{r}' \frac{\rho(\mathbf{r}')}{|\mathbf{r} - \mathbf{r}'|}, \tag{1.97}$$

and the exchange-correlation potential

$$v_{\mathrm{XC}}(\mathbf{r}) = \frac{\delta E_{\mathrm{XC}}[\rho]}{\delta\rho(\mathbf{r})}. \tag{1.98}$$

Directly solving Eq. (1.95) is not straightforward. We observe that a non-interacting system

$$\hat{H}_s|\Psi_s\rangle = (\hat{T} + \hat{v}_s)|\Psi_s\rangle = E_s|\Psi_s\rangle, \tag{1.99}$$

also gives Eq. (1.95) if using the Lagrangian multiplier technique. Since $\hat{H}_s$ has only one-body interaction, the eigenvector is just a Slater determinant. Each orbital is an eigenvector of the effective Hamiltonian

$$\hat{H}_s|\phi_u\rangle = \epsilon_u|\phi_u\rangle. \tag{1.100}$$

When approximating the KS MOs with AO expansions, we also need the Aufbau principle to pick the lowest $N$ orbitals to form the Slater determinant. The resulting density, $\rho_s(\mathbf{r})$, equals the full interacting density $\rho(\mathbf{r})$ as stated in the KS construction. Eq. (1.100) also needs to be solved self-consistently as $\hat{H}_s$ depends on $v_J$ and $v_{\mathrm{XC}}$

which depend on $\rho$ which depends on $|\phi_i\rangle's$. Thus the algorithms of HF and KS are very similar as they both need SCF procedures. By implementing density fitting, KS-DFT scales as $O(L^3)$, which is even better than HF.

Note that $\rho_s(\mathbf{r}) = \rho(\mathbf{r})$ requires that the interacting density $\rho(\mathbf{r})$ can be represented as the ground state density of some $v_s$. This representability is called $v_s$-representability, which has never been proven, although it is generally *conjectured* to be true.

When the quantum chemistry community says DFT, they normally refer to KS-DFT by default, while there is still some development of orbital-free DFT (OF-DFT)[23]. OF-DFT is favorable due to its lower scaling with respect to $L$. However, owing to the low accuracy of the kinetic functional, the practice of OF-DFT is only limited to OF-DFT developers to do dynamics.

### *1.3.4 Exchange-correlation energy*

KS formalism hides anything complicated in the mysterious exchange-correlation energy $E_{\mathrm{XC}}[\rho]$ which still requires approximations. HK theorems only prove the existence of such functional, but there is no prescription of how to construct such functional. Slater's $X\alpha$ method use Slater exchange functional to approximate $E_{\mathrm{XC}}[\rho]$. The first post-KS exchange-correlation functional is the local density approximation (LDA), the first rung in Jacob's ladder to the DFT heaven according to Perdew and Schmidt's categorization[24],

$$E_{\mathrm{XC}}^{\mathrm{LDA}} = \int d\mathbf{r} \epsilon_{\mathrm{XC}}^{\mathrm{LDA}}(\rho(\mathbf{r})), \tag{1.101}$$

where $\epsilon_{\mathrm{XC}}^{\mathrm{LDA}}(n)$ is the exchange-correlation energy per particle in homogeneous electron gas of density $n$. There are two popular versions of parametrization of LDA, i.e. VWN5[25] and PZ81[26], both from fitting homogeneous electron gas QMC calculations[27]. The results of these two implementations are very similar. The

thermochemistry behavior of LDA is never satisfactory to the chemistry community. The second rung of approximations are to add density gradient information to the exchange correlation functional, i.e. generalized gradient approximation (GGA)

$$E_{\mathrm{XC}}^{\mathrm{GGA}} = \int d\mathbf{r} \epsilon_{\mathrm{XC}}^{\mathrm{GGA}}(\rho(\mathbf{r}), |\nabla\rho(\mathbf{r})|). \tag{1.102}$$

Compared to the simple unique idea in LDA construction, the form and the philosophy to build GGA varies a lot. Lee-Yang-Parr[28] correlation functional was derived through fitting data from a helium atom, while Perdew-Burke-Ernzerhof[29] exchange-correlation functional was built based on some exact conditions of $E_{\mathrm{XC}}$. The third rung of approximations are meta-GGA which has density Laplacian and kinetic energy density as ingredients,

$$E_{\mathrm{XC}}^{\text{meta-GGA}} = \int d\mathbf{r} \epsilon_{\mathrm{XC}}^{\mathrm{GGA}}(\rho(\mathbf{r}), |\nabla\rho(\mathbf{r})|, \nabla^2\rho(\mathbf{r}), \tau(\mathbf{r})), \tag{1.103}$$

where the kinetic energy density is

$$\tau(\mathbf{r}) = \sum_i -\frac{1}{2}|\nabla\phi_i(\mathbf{r})|^2. \tag{1.104}$$

The fourth rung of the ladder can utilize occupied orbitals in $E_{\mathrm{XC}}$. Hybrid functionals which include some HF exchange energy is of the fourth rung of the ladder. The most successful functional, B3LYP[28, 30, 31] contains 20% of HF exchange, which becomes a synonym of DFT in the computational organic chemistry community. With the concept of hybrid functionals, the HF approximation can also be considered as a functional. The fifth rung of functional makes use of unoccupied orbitals, which includes MP2 correlation energies, random phase approximation (RPA) correlation energies, etc. in $E_{\mathrm{XC}}$. However, including unoccupied orbitals simply makes FCI a fifth rung functional, which is useless for practical use. As the components of $E_{\mathrm{XC}}$ go far beyond pure density dependent, criticism has posed on DFT for its arbitrariness[32].

### *1.3.5 Challenges of DFT*

Historically, DFT has gained its reputation for its low computational scaling and fair accuracy. DFT does perform well for a variety of range of systems. However, DFT still has difficulty describing molecule dissociation, charge-transfer excitations, van der Waals interactions, transition states, band gaps, etc. There is an expedient fix for the van der Waals interactions by explicit inclusion of terms with $C6$ coefficients[33], which corrects the total energy well but has no effect on the electronic structure. The rest of the errors can be understood as fractional charge errors and fractional spin errors[34]. There are two important exact conditions for the density functionals: the linearity condition and the constancy condition[35, 36]. The linearity condition states that the ground state energy of a system with a fractional number of electrons should be a linear interpolation of the energies of the two adjacent integer points, and the constancy condition requires that the ground state energy of a system with a fixed number of total electrons but a fractional number of $\alpha$ electrons should be constant. The violations of the linearity and the constancy conditions are the fractional charge and fractional spin errors respectively.

Fig 1.1 is the famous example to demonstrate the fractional spin and fractional charge errors with systems with no more than two electrons, adopted from Ref. [34]. Fig 1.1a illustrates the fractional charge errors in $H_2^+$ dissociation. The left pane of Fig 1.1a is the binding curve of $H_2^+$, while the right pane is the energy of a hydrogen atom with a fractional number of electrons. In this case, $E_{\text{ref}}$ is the energy of a neutral hydrogen atom for the corresponding functional, which is the correct limit of $H_2^+$ dissociation. HF is exact for any one electron system, thus the binding curve of HF functional is exact. It is clearly shown that LDA and B3LYP are qualitatively wrong for $R > 3$ Å. In the right pane, the fractional charge error is defined as

$$e_{\text{fc}}[N] = E[N, 0] - N \cdot E[1, 0], \quad 0 \leqslant N \leqslant 1, \tag{1.105}$$

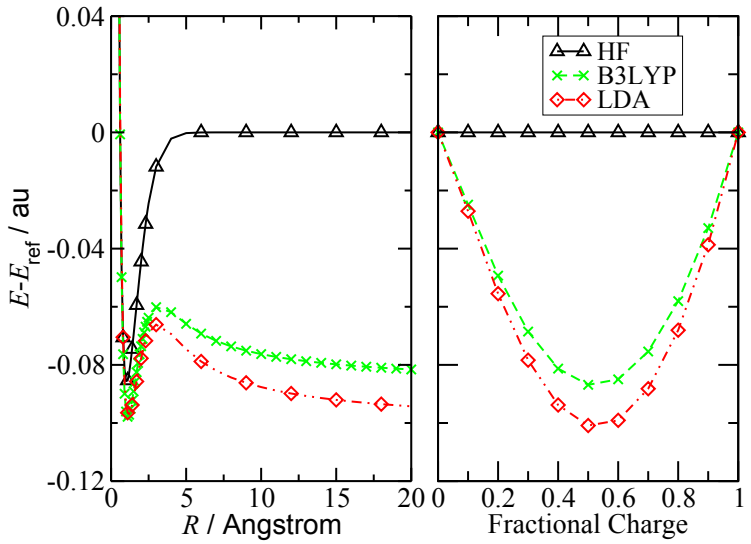


(a) Fractional charge errors in $H_2^+$

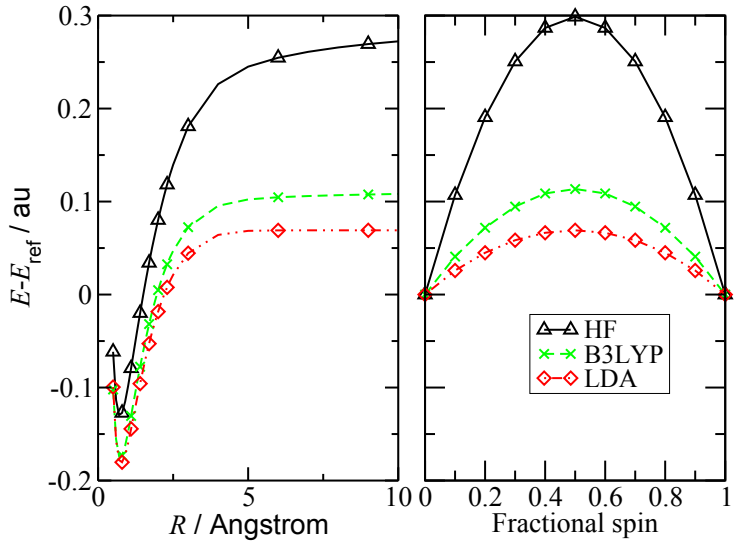


(b) Fractional spin errors in $H_2$

FIGURE 1.1: Fractional charge and spin errors illustrated by $H_2^+$ and $H_2$. PES calculations are done in Gaussian 09[8], while fractional charge and fractional spin calculations are done in QM4D[37]. Basis sets are all 6-31G. $H_2$ binding curves are calculated with restricted orbitals.

where $E[N_\alpha, N_\beta]$ is the energy of a hydrogen atom with $N_\alpha$ $\alpha$ electrons and $N_\beta$ $\beta$ electrons. The exact energy of $E[N, 0]$ $(0 \leqslant N \leqslant 1)$ should be the linear interpolation of $E[0, 0]$ and $E[1, 0]$, while $E[0, 0] = 0$ since no electron is present. The deviation from the linearity condition is the fractional charge error as depicted in the right pane. The right pane shows that B3LYP and LDA have very large fractional charge error at $N = 0.5$, while HF has no fractional charge error for this system at all. It is also striking that the dissociation limits on the left pane match the fractional charge errors at $N = 0.5$. Although $H_2^+$ always has one electron in total for any $R$, each atom has effectively half an electron as the molecule is stretched. Thus the error in the binding curve of $H_2^+$ is interpreted as an error induced by the fractional charge error. The simple illustration in Fig 1.1a provides a vivid example of how fractional charge error affects charged molecule dissociation. Fractional charge errors are also the culprit underestimating band gaps in semiconductors.

Similarly, Fig 1.1b illustrates the fractional spin errors in $H_2$ dissociation. The left pane of Fig 1.1b is the binding curve of $H_2$, while the right pane is the energy of a hydrogen atom with $N_\alpha$ $\alpha$ electrons and $N_\beta = 1 - N_\alpha$ $\beta$ electrons. In this case, $E_{\text{ref}}$ is twice the energy of a neutral hydrogen atom for the corresponding functional, which is the correct limit of $H_2$ dissociation. The correct binding curve should reach zero at the dissociation limit, while all functionals significantly deviate from the correct limit. The fractional spin error is defined as the difference between the energy of a functional for a fractional spin system and the correct energy from the constancy condition,

$$e_{\text{fs}}[N] = E[N, 1 - N] - E[1, 0], \quad 0 \leqslant N \leqslant 1. \tag{1.106}$$

Note that $e_{\text{fs}}$ is symmetric, i.e. $e_{\text{fs}}[N] = e_{\text{fs}}[1 - N]$, while the fractional charge error is not. All functionals have maximal fractional spin errors at $N = 0.5$. It is also observed that the dissociation limits of $H_2$ match the maximal fractional spin errors for

the corresponding functional. Thus the wrong dissociation behavior of $H_2$ is considered as being induced by the fractional spin error. Fractional spin errors are related to static correlation energies which are essential for strongly correlated systems. It is also interesting to see that the order of fractional spin errors HF>B3LYP>LDA, is contrary to the order of the fractional charge errors LDA>B3LYP$\gg$HF.

Fractional charge and fractional spin errors, which are fundamental errors to a functional, are considered to be the source of many errors in DFT applications, such as band gap prediction, transition state calculations, etc[34–36, 38, 39]. The linearity condition and the constancy condition can be combined to form the flat-plane condition[40]. Many efforts have been invested to reduce these errors, including MCY functionals[41, 42], scaled modified functionals[43, 44], and BNL functionals[45, 46], and B03/B05 functionals[47, 48]. However, these functionals usually solve one problem by creating others. No satisfactory solution is accepted in general.

### *1.3.6 Remarks on DFT*

In most cases, DFT has moderate accuracy with a relative low scaling. However, DFT skids on many systems such as molecule dissociation, charge-transfer excitations, van der Waals interactions, etc. These pathological issues are always haunting when we try to apply DFT outside its comfort zone. On the other hand, in the *ab initio* world, HF has very small fractional charge errors for cations, MC-SCF can qualitatively treat molecule dissociation, and MP2 captures van der Waals interactions well. In some sense, the approximations in DFT that make the computation handy sacrifice some performance.

There are still ongoing development in DFT trying to eliminates those annoying errors. No one knows whether there will be one satisfactory functional in the future. In my perspective, the sole in DFT lies on approximations. Although it has not been proved (to the best of my knowledge), FCI is very likely to be NP-complete

(nondeterministic polynomial time) and does not have a solution in polynomial time. Therefore, an $E_{\mathrm{XC}}$ that produces FCI exchange-correlation energies will also be NP-complete, and thus useless. Only through proper approximations can DFT (and also *ab initio* methods) be improved.

## 1.4 Response calculations

Most of the methods introduced in the previous sections are used to calculate static ground state properties, such as ground state energies, densities, etc. Many properties of a system are actually related to the response. For example, the UV-Vis spectrum of a molecule is the response to external periodic electromagnetic fields.

Response calculations can be categorized into two different types: static response and dynamic response, depending on whether the perturbative field is time-dependent or not. Static responses include static polarizability, forces on atoms, Hessian matrices, etc. Especially, force calculations are essential for geometry optimization, which is usually the first step to study a system. Dynamic responses include density-density response function, quasi-particle energies and such. Usually, the poles of the dynamic response functions are the excitation energies. Therefore, most excited state studies are done through dynamic response calculations.

The quantum theory to describe the response to external fields is perturbation theory[49]. Static response and dynamic response are results from time-independent and time-dependent perturbation theory, respectively. These two responses, nonetheless, are not totally distinguishable. For example, employing a time-dependent perturbation of two-electron interaction can derive the correlation energies of the ground state[19]. Subsection 1.4.1 describes the theory of static response and time-independent perturbation theory. Then in Subsection 1.4.2, we present a very powerful method called time-dependent density-functional theory to calculate excited states in DFT framework. In Subsection 1.4.3, we will introduce equation-of-motion

method applied dominantly to *ab initio* reference, which is also closely related to the Green's function methods. A summary is drawn in Subsection 1.4.4 to discuss some of the underlying connections between different methods.

### *1.4.1 Static response*

Static response is relatively easy to derive. In fact, static response is the zero-frequency limit of the dynamic response. The basic technique for static response derivation is time-independent perturbation theory. For details of the theory, readers can refer to Ref. [49] and [17]. The basic concepts of perturbation theory for nondegenerate systems is sketched in this subsection. For each different quantum chemistry methods, the detailed derivations would look very distinct. The perturbation theory in the correlation energy method, MPx in Subsection 1.2.4, is a special case of this more general perturbation theory.

Suppose we have a system governed by a Hamiltonian $H_0$ whose spectra is known,

$$H_0|\phi_i^{(0)}\rangle = \epsilon_i^{(0)}|\phi_i^{(0)}\rangle \tag{1.107}$$

Now there is a small perturbation $H_1$ that applies to the system. With time-independent perturbation theory, we can study the new system without actually solving the Schrodinger equation with the Hamiltonian $H_0 + H_1$. Defining a Hamiltonian of an intermediate interaction with $0 \leqslant \lambda \leqslant 1$,

$$H(\lambda) = H_0 + \lambda H_1, \tag{1.108}$$

we have a Schrodinger equation for each intermediate interaction

$$H(\lambda)|\phi_i(\lambda)\rangle = \epsilon_i(\lambda)|\phi_i(\lambda)\rangle. \tag{1.109}$$

Next we will do Taylor expansions to all quantities in Eq. (1.109). The Taylor expansion of the Hamiltonian is just Eq. (1.108). The Taylor expansions of the

wavefunction and the eigenvalue can be expressed as

$$|\phi_i(\lambda)\rangle = |\phi_i^{(0)}\rangle + \lambda|\phi_i^{(1)}\rangle + \frac{\lambda^2}{2!}|\phi_i^{(2)}\rangle \cdots \tag{1.110}$$

and

$$\epsilon_i(\lambda) = \epsilon_i^{(0)} + \lambda\epsilon_i^{(1)} + \frac{\lambda^2}{2!}\epsilon_i^{(2)} \cdots \tag{1.111}$$

Note that almost all textbooks use an expansion that the factor $1/n!$ is absorbed in $|\phi_i^{(n)}\rangle$ and $\epsilon_i^{(n)}$[17, 49]. Such convention does simplify some derivations for just one perturbative field. However, the coefficients with this convention become less appreciated when extended to perturbation theory with multiple perturbative fields, as in Section 2.4. Therefore, we use Taylor expansions throughout in this Dissertation. Note also that we use an intermediate normalization such that

$$\langle\epsilon_i^{(0)}|\epsilon_i(\lambda)\rangle = 1. \tag{1.112}$$

Eq. (1.109) is solved order by order with respect to $\lambda$. The zeroth order of Eq. (1.109) is Eq. (1.107), which has already been solved regardless of the perturbation. The first order of Eq. (1.109) is

$$H_1|\phi_i^{(0)}\rangle + H_0|\phi_i^{(1)}\rangle = \epsilon_i^{(0)}|\phi_i^{(1)}\rangle + \epsilon_i^{(1)}|\phi_i^{(0)}\rangle. \tag{1.113}$$

Multiplying $\langle\epsilon_j^{(0)}|$ to the left of Eq. (1.113), using Eq. (1.107), we have

$$\langle\phi_j^{(0)}|H_1|\phi_i^{(0)}\rangle = (\epsilon_i^{(0)} - \epsilon_j^{(0)})\langle\phi_j^{(0)}|\phi_i^{(1)}\rangle + \delta_{ij}\epsilon_i^{(1)}. \tag{1.114}$$

If $i = j$, we have the first order eigenvalue

$$\epsilon_i^{(1)} = \langle\phi_i^{(0)}|H_1|\phi_i^{(0)}\rangle. \tag{1.115}$$

If $i \neq j$, given that $i$ has no degenerate levels, we have

$$\langle\phi_j^{(0)}|\phi_i^{(1)}\rangle = \frac{\langle\phi_j^{(0)}|H_1|\phi_i^{(0)}\rangle}{\epsilon_i^{(0)} - \epsilon_j^{(0)}}. \tag{1.116}$$

Thus, the first order wavefunction can be expressed as

$$|\phi_i^{(1)}\rangle = \sum_{j \neq i} \frac{\langle \phi_j^{(0)} | H_1 | \phi_i^{(0)} \rangle}{\epsilon_i^{(0)} - \epsilon_j^{(0)}} |\phi_j^{(0)}\rangle, \tag{1.117}$$

with no $|\phi_i^{(0)}\rangle$ contribution due to the intermediate normalization.

With the wavefunction, we can calculate the first order property change of an observable $A$

$$\Delta A \approx \langle \phi_i^{(0)} | A | \phi_i^{(1)} \rangle + \langle \phi_i^{(1)} | A | \phi_i^{(0)} \rangle \tag{1.118}$$

Higher order results can be solved accordingly.

### *1.4.2 Time-dependent density-functional theory*

Time-dependent density-functional theory (TDDFT) studies the response of a system exposed to a time dependent external potential. The time-dependent version of Hohenberg-Kohn theorems have been proven and set the fundamentals of TDDFT[50, 51]. This subsection only discusses adiabatic linear-response TDDFT[52], which has become a standard method to calculate linear electronic spectra.

Suppose a stationary system is perturbed by a time-dependent external field (such as a laser beam), the external field changes

$$v_{\text{ext}}(\mathbf{r}, t) = v_{\text{ext}}^0(\mathbf{r}) + v_{\text{ext}}^1(\mathbf{r}, t). \tag{1.119}$$

Due to the perturbation, the orbitals, the density and the effective potential are all affected. Expanding up to the first order, the perturbed system becomes

$$\varphi_{i\sigma}(\mathbf{r}, t) = \varphi_{i\sigma}^0(\mathbf{r}, t) + \varphi_{i\sigma}^1(\mathbf{r}, t), \tag{1.120}$$

$$\rho_\sigma(\mathbf{r}, t) = \rho_\sigma^0(\mathbf{r}) + \rho_\sigma^1(\mathbf{r}, t). \tag{1.121}$$

and

$$H_{s,\sigma}(\mathbf{r}, t) = H_{s,\sigma}^0(\mathbf{r}) + H_{s,\sigma}^1(\mathbf{r}, t). \tag{1.122}$$

We have explicitly separated the spin from spatial coordinates for clear presentations.

The time-dependent SCF equation is

$$H_{s,\sigma}(\mathbf{r},t)\varphi_{i\sigma}(\mathbf{r},t) = i\frac{\partial\varphi_{i\sigma}(\mathbf{r},t)}{\partial t}, \tag{1.123}$$

with the orthonormalization

$$\int d\mathbf{r}\varphi^*_{p\sigma}(\mathbf{r},t)\varphi_{q\sigma}(\mathbf{r},t) = \delta_{pq}. \tag{1.124}$$

These equations are solved order by order to achieve the response to the order of our interest. The derivation below is actually part of time-dependent coupled-perturbed SCF (CP-SCF) equations[53].

The zeroth order solution of Eq. (1.123) is trivial,

$$\varphi^0_{i\sigma}(\mathbf{r},t) = \phi_{i\sigma}(\mathbf{r})e^{-i\epsilon_{i\sigma}t}, \tag{1.125}$$

where $\phi_{i\sigma}(\mathbf{r})$ is the unperturbed orbital.

The first order of Eq. (1.123) is

$$H^0_{s,\sigma}(\mathbf{r})\varphi^1_{i\sigma}(\mathbf{r},t) + H^1_{s,\sigma}(\mathbf{r},t)\varphi^0_{i\sigma}(\mathbf{r},t) = i\frac{\partial\varphi^1_{i\sigma}(\mathbf{r},t)}{\partial t}. \tag{1.126}$$

Multiplying $\varphi^{0*}_{p\sigma}(\mathbf{r},t)$ from the left of Eq. (1.126), we have

$$\begin{aligned}&\varphi^{0*}_{p\sigma}(\mathbf{r},t)H^0_{s,\sigma}(\mathbf{r})\varphi^1_{i\sigma}(\mathbf{r},t) + \varphi^{0*}_{p\sigma}(\mathbf{r},t)H^1_{s,\sigma}(\mathbf{r},t)\varphi^0_{i\sigma}(\mathbf{r},t)\\ =&i\frac{\partial\varphi^{0*}_{p\sigma}(\mathbf{r},t)\varphi^1_{i\sigma}(\mathbf{r},t)}{\partial t} - i\frac{\partial\varphi^{0*}_{p\sigma}(\mathbf{r},t)}{\partial t}\varphi^1_{i\sigma}(\mathbf{r},t).\end{aligned} \tag{1.127}$$

Using the complex conjugate of the zeroth order of Eq. (1.123) and integrating over $\mathbf{r}$, we have

$$e^{i(\epsilon_{p\sigma}-\epsilon_{i\sigma})t}\langle\phi_{p\sigma}|\hat{H}^1_{s,\sigma}(t)|\phi_{i\sigma}\rangle = i\frac{\partial\langle\varphi^0_{p\sigma}(t)|\varphi^1_{i\sigma}(t)\rangle}{\partial t}. \tag{1.128}$$

Thus

$$i(\langle\varphi^0_{p\sigma}(t)|\varphi^1_{i\sigma}(t)\rangle - \langle\varphi^0_{p\sigma}(-\infty)|\varphi^1_{i\sigma}(-\infty)\rangle) = \int_{-\infty}^{t} d\tau e^{i(\epsilon_{p\sigma}-\epsilon_{i\sigma})\tau}\langle\phi^0_{p\sigma}|\hat{H}^1_{s,\sigma}(\tau)|\phi_{i\sigma}\rangle. \tag{1.129}$$

With an adiabatic slowly-switching-on field, the perturbation is zero at time $t \to -\infty$, and thus $|\varphi^1_{i\sigma}(-\infty)\rangle = 0$. The RHS of Eq. (1.129) in an abstracted form can be simplified by Fourier transformation

$$\int_{-\infty}^{t} d\tau e^{i\epsilon\tau} f(\tau) \tag{1.130}$$

$$= \int_{-\infty}^{\infty} d\tau \theta(t-\tau) e^{i\epsilon\tau} f(\tau) \tag{1.131}$$

$$= \int_{-\infty}^{\infty} d\tau \theta(t-\tau) e^{i\epsilon\tau} \int_{-\infty}^{\infty} d\omega \frac{e^{-i\omega\tau}}{2\pi} f(\omega) \tag{1.132}$$

$$= \int_{-\infty}^{\infty} d\omega \frac{1}{2\pi} f(\omega) \int_{-\infty}^{\infty} d\tau \theta(t-\tau) e^{i(\epsilon-\omega)\tau} \tag{1.133}$$

$$= \int_{-\infty}^{\infty} d\omega \frac{e^{-i(\omega-\epsilon)t}}{2\pi} f(\omega) \int_{-\infty}^{\infty} d\tau \theta(t-\tau) e^{i(\omega-\epsilon)(t-\tau)} \tag{1.134}$$

$$= e^{i\epsilon t} \int_{-\infty}^{\infty} d\omega \frac{e^{-i\omega t}}{2\pi} f(\omega) \int_{-\infty}^{\infty} d\tau \theta(\tau) e^{i(\omega-\epsilon)\tau} \tag{1.135}$$

$$= -e^{i\epsilon t} \int_{-\infty}^{\infty} d\omega \frac{e^{-i\omega t}}{2\pi} \frac{f(\omega)}{i(\omega-\epsilon)-\eta}, \tag{1.136}$$

where $f(\omega)$ is the Fourier transformation of $f(t)$, and $\eta$ is an infinitesimal positive number to ensure the convergence of the integral. Therefore, Eq. (1.129) becomes

$$e^{-i(\epsilon_{p\sigma}-\epsilon_{i\sigma})t}\langle\varphi^0_{p\sigma}(t)|\varphi^1_{i\sigma}(t)\rangle = \int_{-\infty}^{\infty} d\omega \frac{e^{-i\omega t}}{2\pi} \frac{\langle\phi_p|H^1_{s,\sigma}(\omega)|\phi_i\rangle}{\omega-(\epsilon_p-\epsilon_i)+i\eta}. \tag{1.137}$$

Note that RHS of Eq. (1.137) is an inverse Fourier transformation.

On the other hand, the first order density is

$$\rho^1_\sigma(\mathbf{r},t) = \sum_i [\varphi^{0*}_{i\sigma}(\mathbf{r},t)\varphi^1_{i\sigma}(\mathbf{r},t) + \varphi^{1*}_{i\sigma}(\mathbf{r},t)\varphi^0_{i\sigma}(\mathbf{r},t)] \tag{1.138}$$

$$= \sum_{ip} [\varphi^{0*}_{i\sigma}(\mathbf{r},t)\varphi^0_{p\sigma}(\mathbf{r},t)\langle\varphi^0_{p\sigma}(t)|\varphi^1_{i\sigma}(t)\rangle + \langle\varphi^1_{i\sigma}(t)|\varphi^0_{p\sigma}(t)\rangle\varphi^{0*}_{p\sigma}(\mathbf{r},t)\varphi^0_{i\sigma}(\mathbf{r},t)] \tag{1.139}$$

$$= \sum_{ia} [\varphi^{0*}_{i\sigma}(\mathbf{r},t)\varphi^0_{a\sigma}(\mathbf{r},t)\langle\varphi^0_{a\sigma}(t)|\varphi^1_{i\sigma}(t)\rangle + \langle\varphi^1_{i\sigma}(t)|\varphi^0_{a\sigma}(t)\rangle\varphi^{0*}_{a\sigma}(\mathbf{r},t)\varphi^0_{i\sigma}(\mathbf{r},t)] \tag{1.140}$$

$$= \sum_{ia} [\phi^*_{i\sigma}(\mathbf{r})\phi_{a\sigma}(\mathbf{r})e^{-i(\epsilon_a-\epsilon_i)t}\langle\varphi^0_{a\sigma}(t)|\varphi^1_{i\sigma}(t)\rangle$$

$$+ e^{i(\epsilon_a-\epsilon_i)t}\langle\varphi^1_{i\sigma}(t)|\varphi^0_{a\sigma}(t)\rangle\phi^*_{a\sigma}(\mathbf{r})\phi_{i\sigma}(\mathbf{r})] \tag{1.141}$$

where any occupied $p$ in the summation is zero since

$$\sum_{ij} [\varphi^{0*}_{i\sigma}(\mathbf{r},t)\varphi^0_{j\sigma}(\mathbf{r},t)\langle\varphi^0_{j\sigma}(t)|\varphi^1_{i\sigma}(t)\rangle + \langle\varphi^1_{i\sigma}(t)|\varphi^0_{j\sigma}(t)\rangle\varphi^{0*}_{j\sigma}(\mathbf{r},t)\varphi^0_{i\sigma}(\mathbf{r},t)] \tag{1.142}$$

$$= \sum_{ij} \varphi^{0*}_{i\sigma}(\mathbf{r},t)\varphi^0_{j\sigma}(\mathbf{r},t)[\langle\varphi^0_{j\sigma}(t)|\varphi^1_{i\sigma}(t)\rangle + \langle\varphi^1_{j\sigma}(t)|\varphi^0_{i\sigma}(t)\rangle] \tag{1.143}$$

$$= 0, \tag{1.144}$$

where we have used the first order orthonormalization condition

$$\langle\varphi^0_{j\sigma}(t)|\varphi^1_{i\sigma}(t)\rangle + \langle\varphi^1_{j\sigma}(t)|\varphi^0_{i\sigma}(t)\rangle = 0. \tag{1.145}$$

Using the stationary basis $\phi$, the first order density matrix with Fourier transformation is

$$P^1_{ai\sigma}(\omega) = \frac{\langle\phi_a|H^1_{s,\sigma}(\omega)|\phi_i\rangle}{\omega - (\epsilon_a - \epsilon_i) + i\eta}, \tag{1.146}$$

and

$$P^1_{ia\sigma}(\omega) = \frac{\langle\phi_i|H^1_{s,\sigma}(\omega)|\phi_a\rangle}{-\omega - (\epsilon_a - \epsilon_i) - i\eta}. \tag{1.147}$$

From now on, we will drop the infinitesimal $\eta$ as it does not affect the derivations hereafter.

The first order effective potential $H^1_{s,\sigma}(\omega)$ contains external perturbation $v^1_{\rm ext}(\omega)$ and density response of $v^1_J$ and $v^1_{\rm XC}$. Thus, we have

$$[\omega - (\epsilon_a - \epsilon_i)]P^1_{ai\sigma}(\omega) = v^1_{{\rm ext},ai\sigma}(\omega) + v^1_{J,ai\sigma}(\omega) + v^1_{{\rm XC},ai\sigma}(\omega), \tag{1.148}$$

$$[-\omega - (\epsilon_a - \epsilon_i)]P^1_{ia\sigma}(\omega) = v^1_{{\rm ext},ia\sigma}(\omega) + v^1_{J,ia\sigma}(\omega) + v^1_{{\rm XC},ia\sigma}(\omega). \tag{1.149}$$

The exchange-correlation response could have memory effect due to the electron-electron interaction. In the adiabatic approximation, we ignore all memory effect of exchange-correlation potentials. Defining the adiabatic kernel $K$ such that

$$K_{pq\sigma,rs\tau} = \frac{\delta(v_J + v_{\rm XC})_{pq\sigma}}{\delta P_{rs\tau}} \tag{1.150}$$

$$= (pq|sr) + \int\int d\mathbf{r}d\mathbf{r}'\phi^*_{p\sigma}(\mathbf{r})\phi_{q\sigma}(\mathbf{r})f^{\sigma\tau}_{\rm XC}(\mathbf{r},\mathbf{r}')\phi^*_s(\mathbf{r}')\phi_r(\mathbf{r}'), \tag{1.151}$$

where

$$f^{\sigma\tau}_{\rm XC}(\mathbf{r},\mathbf{r}') = \frac{\delta^2 E_{\rm XC}[\rho]}{\delta\rho_\sigma(\mathbf{r})\delta\rho_\tau(\mathbf{r}')}, \tag{1.152}$$

we have

$$(v_J(\omega) + v_{\rm XC}(\omega))^1_{pq\sigma} = \sum_{rs\tau} K_{pq\sigma,rs\tau}P^1_{rs\tau}(\omega). \tag{1.153}$$

Note that the adiabatic kernel has the symmetry

$$K_{pq\sigma,rs\tau} = K^*_{qp\sigma,sr\tau} = K_{rs\tau,pq\sigma} = K^*_{sr\tau,qp\sigma}. \tag{1.154}$$

Consequently, Eqs. (1.148) and (1.149) become

$$[\omega - (\epsilon_a - \epsilon_i)]P^1_{ai\sigma}(\omega) = v^1_{{\rm ext},ai\sigma}(\omega) + \sum_{jb\tau}(K_{ai\sigma,jb\tau}P^1_{jb\tau}(\omega) + K_{ai\sigma,bj\tau}P^1_{bj\tau}(\omega)), \tag{1.155}$$

$$[-\omega - (\epsilon_a - \epsilon_i)]P^1_{ia\sigma}(\omega) = v^1_{{\rm ext},ia\sigma}(\omega) + \sum_{jb\tau}(K_{ia\sigma,jb\tau}P^1_{jb\tau}(\omega) + K_{ia\sigma,bj\tau}P^1_{bj\tau}(\omega)). \tag{1.156}$$

Finally, we have

$$\sum_{jb\tau} A_{ia\sigma,jb\tau} P^1_{jb\tau}(\omega) + \sum_{jb\tau} B_{ia\sigma,jb\tau} P^1_{bj\tau}(\omega) = \omega P^1_{ia\sigma}(\omega) - v^1_{\mathrm{ext},ia\sigma}(\omega) \tag{1.157}$$

$$\sum_{jb\tau} B^*_{jb\sigma,ia\tau} P^1_{jb\tau}(\omega) + \sum_{jb\tau} A^*_{ia\sigma,jb\tau} P^1_{bj\tau}(\omega) = -\omega P^1_{ai\sigma}(\omega) - v^1_{\mathrm{ext},ai\sigma}(\omega), \tag{1.158}$$

where

$$A_{ia\sigma,jb\tau} = \delta_{\sigma\tau}\delta_{ij}\delta_{ab}(\epsilon_{a\sigma} - \epsilon_{i\sigma}) + K_{ia\sigma,jb\tau}, \tag{1.159}$$

and

$$B_{ia\sigma,jb\tau} = K_{ia\sigma,bj\tau}. \tag{1.160}$$

For the zero field limit, Eqs. (1.157) and (1.158) describe the eigenmode of the electronic system. The resulting generalized eigenvalue equation becomes

$$\begin{bmatrix} \mathbf{A} & \mathbf{B} \\ \mathbf{B}^\dagger & \mathbf{A}^* \end{bmatrix} \begin{bmatrix} \mathbf{X} \\ \mathbf{Y} \end{bmatrix} = \omega \begin{bmatrix} \mathbf{I} & \mathbf{0} \\ \mathbf{0} & -\mathbf{I} \end{bmatrix} \begin{bmatrix} \mathbf{X} \\ \mathbf{Y} \end{bmatrix}, \tag{1.161}$$

where $X_{ia\sigma} = P_{ia\sigma}(\omega)$ and $Y_{ia\sigma} = P_{ai\sigma}(\omega)$. Setting $f_{\mathrm{XC}} = 0$ in TDDFT makes the random phase approximation (RPA) in Green's function method. There is also an approximation called Tamm-Dancoff approximation (TDA) which sets $B$ zero. Eq. (1.161) is the working equation for adiabatic linear-response TDDFT. Using Davidson's algorithm, TDDFT can be solved in a time complexity of $O(L^4)$. TDDFT can capture valence single excitations well. However, due to the dimension mismatch and the adiabatic kernel, TDDFT does not contain information about excitations of double or above. Additionally, TDDFT fails to get the correct $1/R$ trend of charge-transfer excitations[54].

Eq. (1.161) is a very typical form for dynamic response calculations. Using a HF reference and HF functional, Eq. (1.161) is then the TDHF equation, which can also be derived from equation-of-motion framework.

### *1.4.3 Equation-of-motion methods*

In the *ab initio* framework, the standard way to calculate dynamic response is equation-of-motion (EOM) methods. The equations in EOM methods usually are very similar to those in Green's function methods; sometimes they are even identical. Green's function methods are a composite of techniques backed by many-body perturbation theories to study various responses. It has connections with both *ab initio* methods and DFT. Currently Green's function methods are more popular in solid state physics than in chemistry, probably due to its solid-state origin. This subsection focuses the EOM formalism. The reader is encouraged to investigate Green's function methods in standard textbooks[19, 55, 56].

Rowe's EOM formalism[2, 57] starts from an electronic Hamiltonian $\hat{H}$ with its exact spectra:

$$\hat{H}|M\rangle = E_M|M\rangle. \tag{1.162}$$

Note that $\hat{H}$ is expressed in second quantization and $|M\rangle$ 's do not have to have the same number of electrons. Suppose we have an initial state $|0\rangle$ whose excitation spectra we want to study. For an excitation $|0\rangle \rightarrow |F\rangle$ and $F \neq 0$, defining an excitation operator

$$\hat{O}_F^\dagger = |F\rangle\langle 0|, \tag{1.163}$$

we have

$$\hat{O}_F^\dagger|0\rangle = |F\rangle, \tag{1.164}$$

and

$$\hat{O}_F|0\rangle = 0. \tag{1.165}$$

The excitation energy $\omega_F = E_F - E_I$ can then be expressed as

$$\omega_F = \frac{\langle 0|[\hat{O}_F, \hat{H}, \hat{O}_F^\dagger]|0\rangle}{\langle 0|[\hat{O}_F, \hat{O}_F^\dagger]|0\rangle}, \tag{1.166}$$

where the double commutator is

$$[\hat{A},\hat{B},\hat{C}] = \frac{1}{2}[\hat{A},[\hat{B},\hat{C}]] + \frac{1}{2}[[\hat{A},\hat{B}],\hat{C}], \tag{1.167}$$

for Bosonic excitation operators (operators as products of even number of electron creation and/or annihilation operators), or

$$[\hat{A},\hat{B},\hat{C}] = \frac{1}{2}\{\hat{A},[\hat{B},\hat{C}]\} + \frac{1}{2}\{[\hat{A},\hat{B}],\hat{C}\}. \tag{1.168}$$

for Fermionic excitation operators (operators as products of odd number of electron creation and/or annihilation operators)[2, 58].

By approximating the initial state $|0\rangle$ and the excitation operator $\hat{O}_F^\dagger$ , we can obtain an eigenvalue equation derived from Eq. (1.166). Expanding $\hat{O}_F^\dagger$ as a linear combination of some operators,

$$\hat{O}_F^\dagger = \sum_I X_{IF}\hat{Q}_I^\dagger - \sum_I Y_{IF}\hat{Q}_I, \tag{1.169}$$

the resulting generalized eigenvalue equation is

$$\begin{bmatrix} \mathbf{A} & \mathbf{B} \\ \mathbf{B}^\dagger & \mathbf{A}^* \end{bmatrix} \begin{bmatrix} \mathbf{X}_F \\ \mathbf{Y}_F \end{bmatrix} = \omega_F \begin{bmatrix} \mathbf{C} & \mathbf{D} \\ \mathbf{D}^\dagger & -\mathbf{C}^* \end{bmatrix} \begin{bmatrix} \mathbf{X}_F \\ \mathbf{Y}_F \end{bmatrix}, \tag{1.170}$$

where

$$A_{IJ} = \langle 0|[\hat{Q}_I,\hat{H},\hat{Q}_J^\dagger]|0\rangle, \tag{1.171}$$

$$B_{IJ} = -\langle 0|[\hat{Q}_I,\hat{H},\hat{Q}_J]|0\rangle, \tag{1.172}$$

$$C_{IJ} = \langle 0|[\hat{Q}_I,\hat{Q}_J^\dagger]|0\rangle, \tag{1.173}$$

and

$$D_{IJ} = -\langle 0|[\hat{Q}_I,\hat{Q}_J]|0\rangle. \tag{1.174}$$

As an example, we will derive the TDHF equation. The TDHF equation is achieved by approximating $|0\rangle$ as a HF Slater determinant $|\Phi_{\mathrm{HF}}\rangle$, and the excitation operator as a linear combination of particle-hole excitations and its deexcitations

$$\hat{O}_F^\dagger = \sum_{ia} X_{ia,F}\{a^\dagger i\} - \sum_{ia} Y_{ia,F}\{i^\dagger a\}. \tag{1.175}$$

The resulting EOM eigenvalue equation is the same equation as in TDDFT (Eq. (1.161))

$$\begin{bmatrix} \mathbf{A} & \mathbf{B} \\ \mathbf{B}^\dagger & \mathbf{A}^* \end{bmatrix} \begin{bmatrix} \mathbf{X} \\ \mathbf{Y} \end{bmatrix} = \omega \begin{bmatrix} \mathbf{I} & \mathbf{0} \\ \mathbf{0} & -\mathbf{I} \end{bmatrix} \begin{bmatrix} \mathbf{X} \\ \mathbf{Y} \end{bmatrix} \tag{1.176}$$

except for the matrix elements for $A$ and $B$ are

$$A_{ia,jb} = \delta_{ij}\delta_{ab}(\epsilon_a - \epsilon_i) + \langle ia||bj\rangle, \tag{1.177}$$

and

$$B_{ia,jb} = \langle ia||jb\rangle. \tag{1.178}$$

The TDA of Eq. (1.176) simply becomes the CIS equation in Eq. (1.31).

### *1.4.4 Summary of response calculations*

Response calculations are the pivoting point to connect *ab initio*, DFT and Green's function methods. TDHF from EOM, TDDFT from DFT and RPA from Green's function methods actually result in very similar working equations. Some dynamic response properties can even aid correlation energy calculations, such as RPA correlation energies. Although to the first order these working equations share similar pattern, they become quite different going beyond the first order approximation. For example, EE-EOM-CC equations in the *ab initio* framework will be very different from the GW-BSE[59] equation from DFT and Green's function method. However, in terms of studying response properties we hope we can gain deeper insight into the mechanism behind the veils of the equations.

## 1.5 Concluding remarks of the review

It is always inspiring to read quantum chemistry literature. Despite great success over the past 80 years, there are still many urgent problems to be solved. The correlation energies and the response are still the central of the topics.

# 2

# Fukui function and response function for nonlocal and fractional systems

## 2.1 Introduction

Conceptual DFT, alternatively named density-functional reactivity theory, has been a powerful tool to perceive chemical problems[4, 60], with quantitative indexes of chemical reactivity traced back to electron densities based on Hohenberg-Kohn theorems [20]. Many important quantities, including, but not limited to, the chemical potential (the negative of the electronegativity), the chemical hardness, the softness, and the Fukui functions, were proposed to understand the mechanism of chemistry. All indexes of chemical reactivity in conceptual DFT are deduced from the energy derivatives in a general form[61]

$$\frac{\delta^{p+q}E}{\delta N^p \delta v^q}. \tag{2.1}$$

Many researchers have devoted to rationalizing chemistry in the framework of conceptual DFT and achieved fruitful accomplishment.[61–73]

Besides providing insight into chemistry, conceptual DFT also introduces a perspective to study density-functional approximations (DFAs) in terms of derivatives in

Eq. (2.1). It is well-known that common DFAs still bear systematic errors highlighted as fractional charge errors and fractional spin errors[34, 35, 38, 40], despite their great success for many chemical systems. With the extension to fractional systems[74–77], the linearity and constancy conditions for exact functionals are revealed. The linearity condition states that the energy for a fractional system should be the energy interpolating the two adjacent integer points, restricting the chemical potential to be a constant, which is violated by most of DFAs. Enforcing the energetic linearity condition leads to some recent breakthroughs of density functional development, such as Mori-Sanchez-Cohen-Yang series functionals[41, 42], the scaled-modified local density approximation[43, 44], and Baer-Neuhauser-Livshits functional[45, 46, 78, 79]. These functionals tend to perform better in aspects of band gaps, charge-transfer states, and etc. Their encouraging results suggest that fulfilling the exact conditions is a promising route to tackle the functional problem.

While the linearity condition for the energies of fractional charge systems is a global condition, independent of the real space coordinate $\mathbf{r}$, using the energy derivatives of Eq. (2.1) within the linearity condition allows one to explore the same condition for (infinitely) many different external potential variations, as demonstrated in the Fukui conditions derived previously[80]. Since the linearity of the energy functional is general for any local external potential, it remains valid for a system with perturbed external potentials. Each distinct perturbation will generate a new linearity condition, resulting in numerous new conditions. Therefore, one single energetic linearity condition is transformed to infinitely many exact conditions. Such local conditions for a given physical system are satisfied at every real space point $\mathbf{r}$ and thus offers very rich and detailed information on the exact energy functional. Presently, we plan to develop more exact conditions which can be useful for functional development.

It is the perturbed energies, or in other words, the energy derivatives, that link

exact density functional conditions to the conceptual DFT. We recently developed the analytical expressions of $p+q=2$ derivatives (i.e. the linear-response functions, the Fukui functions, and the chemical hardness)[80], enabling us to study functionals in the space of $\mathbf{r}$ (the Fukui function $f(\mathbf{r})$) and even in the space of $(\mathbf{r},\mathbf{r}')$ (the linear-response function $\chi(\mathbf{r},\mathbf{r}')$). Since these real spaces have richer information of the functional, they will provide more guidance in functional study than just the global indexes. In order to fully explore the functionals, it is necessary to extend the expressions from integer to fractional systems, and also to higher order. In this work, we extend the analytical expressions of $p+q=2$ derivatives to fractional systems, and also systems with nonlocal potential. The analytical expressions of $p+q=3$ derivatives at integer points are also developed. These expressions link the exact conditions of linearity conditions for fractional charges and constancy conditions for fractional spins to equations in the real space. This approach can also be extended to express constancy conditions for fractional spins in real space.

The Chapter is organized as follows. Section 2.2 introduces the energy functional $E[N,v]$ and its derivatives containing important chemical information in conceptual DFT. Section 2.3 connects the derivatives of $E[N,v]$ with the linearity condition. The analytical expressions of derivatives are then derived in Section 2.4. Section 2.5 discusses the extensions of $E[N,v]$ to systems with a nonlocal potential. The constancy condition in terms of derivatives is covered in Section 2.6. Finally, Section 2.7 concludes this work.

## 2.2 $E[N,v]$ and its derivatives

Within Born-Oppenheimer approximation, the ground state chemistry is mainly governed by the time-independent Schrodinger equation of the electrons

$$\hat{H}\Phi = E\Phi, \tag{2.2}$$

with $\hat{H}$ being the nonrelativistic electronic Hamiltonian with an external potential $v(\mathbf{r})$. According to the variational principle, the ground state energy for a pure state with an integer number of electrons is

$$E_{\text{pure state}}[N, v] = \min_{\Phi \to N} \frac{\langle \Phi | \hat{H} | \Phi \rangle}{\langle \Phi | \Phi \rangle}, \tag{2.3}$$

where $N$ is the number of electrons in the system, which is an integer for a pure state. In ensemble theory, the system is described by the density matrix $\Gamma$ rather than the wavefunction $\Phi$, and the total number of electrons $N$ is continuous and not necessarily an integer. Then the ground-state energy functional $E[N, v]$ is defined through an energy minimization,

$$E[N, v] = \min_{\Gamma \to N} \text{Tr}(\Gamma \hat{H}), \tag{2.4}$$

where $\Gamma$ is a density matrix of a zero-temperature grand-canonical ensemble[76]. We now make the Taylor expansion of the functional $E[N, v]$ as

$$\begin{aligned}
&\delta E[N, v] \\
=&\frac{\delta E}{\delta N}\delta N + \int d\mathbf{r} \frac{\delta E}{\delta v(\mathbf{r})}\delta v(\mathbf{r}) + \int d\mathbf{r} \frac{\delta^2 E}{\delta N \delta v(\mathbf{r})}\delta v(\mathbf{r}) \times \delta N + \frac{1}{2}\frac{\delta^2 E}{\delta N^2}(\delta N)^2 \\
&+ \frac{1}{2}\int d\mathbf{r} d\mathbf{r}' \frac{\delta^2 E}{\delta v(\mathbf{r}) \delta v(\mathbf{r}')}\delta v(\mathbf{r})\delta v(\mathbf{r}') + \frac{1}{6}\frac{\delta^3 E}{\delta N^3}(\delta N)^3 \\
&+ \frac{1}{6}\int d\mathbf{r} d\mathbf{r}' d\mathbf{r}'' \frac{\delta^3 E}{\delta v(\mathbf{r}) \delta v(\mathbf{r}') \delta v(\mathbf{r}'')}\delta v(\mathbf{r})\delta v(\mathbf{r}')\delta v(\mathbf{r}'') \\
&+ \frac{1}{2}\int d\mathbf{r} \frac{\delta^3 E}{\delta N^2 \delta v(\mathbf{r})}\delta v(\mathbf{r}) \times (\delta N)^2 + \frac{1}{2}\int d\mathbf{r} d\mathbf{r}' \frac{\delta^3 E}{\delta N \delta v(\mathbf{r})} + \sum_{p+q=4} O((\delta N)^p (\delta v)^q)
\end{aligned} \tag{2.5}$$

Note that all derivatives with respect to $N$ when $N$ is an integer need to be taken at either the left or right limit of the derivatives, because of the energy derivative discontinuity at integer $N$ [76] (to be discussed in Section 2.3). To simplify the

expressions, throughout this Chapter, we have not indicated the variables that are held fixed in the partial differentiations, as they are clear from the context. Some derivatives are well-known chemical reactivity indexes, such as the chemical potential (the Fermi energy)[81]

$$\frac{\delta E}{\delta N} = \mu, \tag{2.6}$$

the electron density

$$\frac{\delta E}{\delta v(\mathbf{r})} = \rho(\mathbf{r}), \tag{2.7}$$

the Fukui function[62]

$$\frac{\delta^2 E}{\delta N \delta v(\mathbf{r})} = \frac{\partial \rho(\mathbf{r})}{\partial N} = f(\mathbf{r}), \tag{2.8}$$

the chemical hardness[82]

$$\frac{\delta^2 E}{\delta N^2} = \eta, \tag{2.9}$$

the linear-response function

$$\frac{\delta^2 E}{\delta v(\mathbf{r}) \delta v(\mathbf{r}')} = \frac{\delta \rho(\mathbf{r})}{\delta v(\mathbf{r}')} = \chi(\mathbf{r}, \mathbf{r}'), \tag{2.10}$$

the chemical hyperhardness[61]

$$\frac{\delta^3 E}{\delta N^3} = \gamma, \tag{2.11}$$

the dual descriptor[83]

$$\frac{\delta^3 E}{\delta N^2 \delta v(\mathbf{r})} = f^{(2)}(\mathbf{r}), \tag{2.12}$$

the Fukui response function[84, 85]

$$\frac{\delta^3 E}{\delta N \delta v(\mathbf{r}) \delta v(\mathbf{r}')} = g(\mathbf{r}, \mathbf{r}'), \tag{2.13}$$

Table 2.1: $\delta^{p+q}E/\delta N^p \delta v^q$ in the Taylor expansion of $E[N, v]$ up to the order of $p + q = 3$. See the text for the meaning of each derivative.

| $p$ \ $q$ | 0 | 1 | 2 | 3 |
|---|---|---|---|---|
| 0 | $E$ | $\rho(\mathbf{r})$ | $\chi(\mathbf{r}, \mathbf{r}')$ | $\chi^{(2)}(\mathbf{r}, \mathbf{r}', \mathbf{r}'')$ |
| 1 | $\mu$ | $f(\mathbf{r})$ | $g(\mathbf{r}, \mathbf{r}')$ | - |
| 2 | $\eta$ | $f^{(2)}(\mathbf{r})$ | - | - |
| 3 | $\gamma$ | - | - | - |

and the second-order response function

$$\frac{\delta^3 E}{\delta v(\mathbf{r})\delta v(\mathbf{r}')\delta v(\mathbf{r}')} = \chi^{(2)}(\mathbf{r}, \mathbf{r}', \mathbf{r}''). \tag{2.14}$$

Table 2.1 summarizes Eqs. (2.6)-(2.14).

Since the derivatives with respect to $N = N_0$ at integers have to specify a direction, we have

$$\left(\frac{\delta E}{\delta N}\right)_{N_0^-} = \mu^- = -I = E_{N_0} - E_{N_0-1}, \tag{2.15}$$

$$\left(\frac{\delta E}{\delta N}\right)_{N_0^+} = \mu^+ = -A = E_{N_0+1} - E_{N_0}, \tag{2.16}$$

$$\left(\frac{\partial \rho(\mathbf{r})}{\partial N}\right)_{N_0^-} = f^-(\mathbf{r}) = \rho_{N_0}(\mathbf{r}) - \rho_{N_0-1}(\mathbf{r}), \tag{2.17}$$

$$\left(\frac{\partial \rho(\mathbf{r})}{\partial N}\right)_{N_0^+} = f^+(\mathbf{r}) = \rho_{N_0+1}(\mathbf{r}) - \rho_{N_0}(\mathbf{r}) \tag{2.18}$$

and so forth, using the energy linearity conditions [76, 86]. It is worth noting that some derivatives with respect to $N$ in this context are different from those in traditional conceptual DFT. For instance, the hardness $\eta$ in conceptual DFT is half of the band gap, i.e. $\eta_{\text{CDFT}} = (I - A)/2 = (\mu^+ - \mu^-)/2$. Nonetheless, since all $N$ derivatives are taken in one direction here, due to the linearity of the functional $E[N, v]$, $\eta$ is uniformly zero in this definition for all $N$. Similar discrepancies exist

for $f^{(2)}(\mathbf{r})$ and $\gamma$. Note also that some derivatives may not be uniquely defined due to spatial degeneracy. For example, in a neutral carbon atom, the nonrelativistic ground state is a $^3P$ state of 9-fold degeneracy, with three degrees of freedom in spatial symmetry ($L_z = 1,\ 0,\ -1$) and spin symmetry ($S_z = 1,\ 0,\ -1$) respectively. Since in nonrelativistic limit, the spin-orbit coupling does not lift the degeneracy, the system can be well described in the uncoupled picture specified by quantum numbers $L_z$ and $S_z$. In the $^3P$ carbon atom, the global derivatives such as $\mu$ and $\eta$ still exist with well-defined values. However, all the derivatives with respect to $v(\mathbf{r})$ could be problematic. First, there is no unique $\rho(\mathbf{r})$ for this carbon atom, since different $L_z$'s render distinct total densities. Second, $\chi(\mathbf{r}, \mathbf{r}')$ is ill-defined, as some infinitesimal $\delta v(\mathbf{r}')$ could lead to finite change of the density $\rho(\mathbf{r})$. However, note that this indeterminacy can be dealt with if one focuses on a specific system from the collections of degenerate states. In order to avoid the difficulty, no degeneracy resulting from spatial symmetry is discussed throughout this Chapter. Spin degeneracy is still compatible with this spinless $E - N$ theory when only the total density is concerned. The total density $\rho(\mathbf{r})$ is in fact an expectation value of a spin-free operator and thus is independent of the value of $S_z$. For instance, the ground state of carbene $CH_2$ being $^3B_1$, choices of $S_z$ do not influence the total density.

Overall, under the premises that the system bears no spatial degeneracy and that all the derivatives with respect to $N$ at integer $N$ specify a direction, $E[N, v]$ could have all the derivatives in Eq. (2.5) well defined.

## 2.3 The linearity condition and its extensions

Assuming the energy convexity, i.e.

$$E_v(N_0 + 1) + E_v(N_0 - 1) \geqslant 2E_v(N_0), \tag{2.19}$$

where $N_0$ is an integer, and $E_v(N_0+1)$, $E_v(N_0-1)$, and $E_v(N_0)$ are ground state energies of a physical system with an external potential $v(\mathbf{r})$ with $N_0+1$, $N_0-1$, and $N_0$ electrons respectively, the energy functional $E[N,v]$ at a fractional system is [76]

$$E[N_0+\lambda,v] = (1-\lambda)E[N_0,v] + \lambda E[N_0+1,v], \tag{2.20}$$

with $0 \leqslant \lambda \leqslant 1$. In other words, $E[N,v]$ at a fractional $N$ is a linear interpolation of the two neighboring integer points $E[\lfloor N \rfloor, v]$ and $E[\lfloor N \rfloor + 1, v]$, where $\lfloor N \rfloor$ is the floor function[87] that returns the largest integer less than or equal to $N$. Thus

$$E[N,v] = (\lfloor N \rfloor + 1 - N)E[\lfloor N \rfloor, v] + (N - \lfloor N \rfloor)E[\lfloor N \rfloor + 1, v]. \tag{2.21}$$

Eq. (2.20), as a consequence of both ensemble[76] and pure state theories[77], reveals an exact condition for a fractional system, namely the linearity condition. The violation of Eq. (2.20) in commonly used density functional approximations is the delocalization error, which accounts for the tendency of approximate functionals to give much too low energies for delocalized charge distributions, such as in the wrong dissociation limit for charged molecules, and etc[39].

The linearity condition as of a global condition for density functionals has inspired fruitful functional development[41–46, 79]. As shown in Eq. (2.5), the variation of the energy functional actually contains much more information. Taking derivatives of both sides in Eq. (2.20) with respect to $\lambda$ and/or $v(\mathbf{r})$, we have, up to first order, the chemical potential condition [80]

$$\mu_{N_0+\lambda} = E[N_0+1,v] - E[N_0,v], \tag{2.22}$$

and the electron density condition

$$\rho_{N_0+\lambda}(\mathbf{r}) = (1-\lambda)\rho_{N_0}(\mathbf{r}) + \lambda\rho_{N_0+1}(\mathbf{r}). \tag{2.23}$$

Going beyond the first order, we can further explore the linearity condition by taking higher order derivatives of Eq. (2.20). Up to the second order, we have the hardness condition [80]

$$\eta_{N_0+\lambda} = 0, \tag{2.24}$$

the Fukui function condition[80]

$$f_{N_0+\lambda}(\mathbf{r}) = \rho_{N_0+1}(\mathbf{r}) - \rho_{N_0}(\mathbf{r}), \tag{2.25}$$

and the linear-response function condition

$$\chi_{N_0+\lambda}(\mathbf{r}, \mathbf{r}') = (1-\lambda)\chi_{N_0}(\mathbf{r}, \mathbf{r}') + \lambda\chi_{N_0+1}(\mathbf{r}, \mathbf{r}'). \tag{2.26}$$

New in this Chapter, we developed the exact conditions up to the third order, as the hyperhardness condition

$$\left(\frac{\delta^3 E}{\delta N^3}\right)_{N=N_0+\lambda} = 0, \tag{2.27}$$

the dual descriptor condition

$$\left(\frac{\delta^3 E}{\delta N^2 \delta v(\mathbf{r})}\right)_{N=N_0+\lambda} = 0, \tag{2.28}$$

the Fukui response function condition

$$\left(\frac{\delta^3 E}{\delta N \delta v(\mathbf{r}) \delta v(\mathbf{r}')}\right)_{N=N_0+\lambda} = \chi_{N_0+1}(\mathbf{r}, \mathbf{r}') - \chi_{N_0}(\mathbf{r}, \mathbf{r}'), \tag{2.29}$$

and the second-order response function condition

$$\begin{aligned}\left(\frac{\delta^3 E}{\delta v(\mathbf{r}) \delta v(\mathbf{r}') \delta v(\mathbf{r}'')}\right)_{N=N_0+\lambda} &= (1-\lambda)\left(\frac{\delta^3 E}{\delta v(\mathbf{r}) \delta v(\mathbf{r}') \delta v(\mathbf{r}'')}\right)_{N=N_0} \\ &\quad + \lambda\left(\frac{\delta^3 E}{\delta v(\mathbf{r}) \delta v(\mathbf{r}') \delta v(\mathbf{r}'')}\right)_{N=N_0+1}.\end{aligned} \tag{2.30}$$

Eqs. (2.22)-(2.30) are all exact conditions derived from the linearity condition, yet they contain richer information as the conditions are satisfied at each $\mathbf{r}$, $(\mathbf{r}, \mathbf{r}')$, or even $(\mathbf{r}, \mathbf{r}', \mathbf{r}'')$ point. The linearity condition of the density Eq. (2.23) was derived in the original work of Perdew, Parr, Levy, and Balduz[76], where the more general result on the linearity condition of $(N_0 + \lambda)$ density matrix was also given. As a consequence of the linearity of the density matrix condition, other properties such as expectation values of the density matrix, also have the linearity conditions. This was pointed out by Ayers as the "linear mixing rule" which also led to Eqs. (2.25) and (2.26).[88] These local conditions in conjunction with the analytical expressions for the derivatives, developed in the next section, should be more powerful than the global condition of Eq. (2.20) alone in providing guidance for density-functional development.

## 2.4 Analytical expressions for derivatives in Kohn-Sham and generalized Kohn-Sham framework

Kohn-Sham (KS)[21] and generalized Kohn-Sham (GKS)[89] formalisms decompose the total electronic energy into kinetic energy $T_s$ of a noninteracting system with identical electron density, external potential, classical Coulomb repulsion $J$, and exchange-correlation energy $E_{\mathrm{XC}}$ which accounts for all the missing quantum effect in the previous terms,

$$E[\rho] = T_s + \int v(\mathbf{r})\rho(\mathbf{r})d\mathbf{r} + J[\rho] + E_{\mathrm{XC}}. \tag{2.31}$$

The main difference between KS and GKS is that $E_{\mathrm{XC}}$ of a KS system is an explicit functional of the density $\rho(\mathbf{r})$ while $E_{\mathrm{XC}}$ of GKS is an explicit functional of the noninteracting density matrix $\rho_s(\mathbf{r}, \mathbf{r}')$. The minimization of the total energy with respect to the one-electron orbitals of the reference non-interacting system lead to a set of one electron equations with a local potential in the case of KS and a nonlocal

potential in the case of GKS. In a fractional system, all orbitals have an occupation number $n_{u\tau} \in [0, 1]$, and the non-interacting kinetic energy and the density matrix are expressed as

$$T_s = \sum_{i\tau} n_{i\tau} \langle \phi_{i\tau} | - \frac{1}{2} \nabla^2 | \phi_{i\tau} \rangle , \tag{2.32}$$

and

$$\rho_s(\mathbf{r}, \mathbf{r}') = \sum_{i\tau} n_{i\tau} \phi_{i\tau}(\mathbf{r}) \phi^*_{i\tau}(\mathbf{r}'). \tag{2.33}$$

In this Chapter, we use the index convention stated in Page 9 except that $f$ and $\sigma$ are exclusively used as the orbital and spin indexes of the frontier orbital. Within the framework of KS/GKS formalism, analytical expressions for all $p + q = 1$ derivatives are well established. The total density is just the diagonal element of the KS density matrix in Eq. (2.33), while the chemical potential is related to the KS/GKS frontier orbital eigenvalues

$$\mu = \epsilon_{f\sigma} = \langle \phi_{f\sigma} | \hat{H}_\sigma | \phi_{f\sigma} \rangle , \tag{2.34}$$

as established by Cohen *et al.*[36, 90]. Among higher derivatives, the linear-response function (also called density-density response function ) was the earliest to be studied. Casida offered solutions to frequency-dependent linear-response problems, from which the static linear-response function could be deduced[52]. Handy and coworkers obtained analytical expressions for both frequency-dependent and static polarizability and hyperpolarizability, which contain all essential ingredients for the linear and second-order response functions[53, 91, 92]. Flores-Moreno *et al.* developed analytical expressions for the linear-response function and the Fukui function within the framework of auxiliary DFT[93, 94]. Baer and coworkers also developed an iterative expression for chemical hardness in view of energetic curvature[95, 96]. Recently, the analytical expressions of all three $p + q = 2$ derivatives at integer limit have been

systematically developed by Yang and coworkers.[80]. This Chapter will extend the derivation to fractional systems and derivatives of higher order.

All the derivatives can be viewed as results of perturbation based on the self-consistent field equations,

$$\hat{H}_\tau|\phi_{i\tau}\rangle = \epsilon_{i\tau}|\phi_{i\tau}\rangle, \tag{2.35}$$

subject to the orthonormalization

$$\langle\phi_{i\tau}|\phi_{u\tau}\rangle = \delta_{iu\tau}, \tag{2.36}$$

where $\hat{H}_\tau = -1/2\nabla^2 + \hat{v}_{\text{ext}} + \hat{v}_J + \hat{v}_{\text{XC}}$ is the noninteracting effective Hamiltonian. Eqs. (2.33), (2.35) and (2.36) should be solved self-consistently as $\hat{H}_\tau$ depends on $\rho_s(\mathbf{r}, \mathbf{r}')$ or $\rho(\mathbf{r})$. These equations under perturbations are called coupled-perturbed self-consistent field (CP-SCF) equations, by solving which all derivatives could be obtained. For a system of an integer number of electrons, a unitary transformation within the occupied orbitals (or within the unoccupied orbitals) will not change the total energy or the total density. This enables a special choice of unitary transformation to simplify derivations in various previous works on response theories[53, 91, 97, 98], viz. using $\hat{H}_\tau|\phi_{i\tau}\rangle = \sum_j \epsilon_{ji\tau}|\phi_{j\tau}\rangle$ rather than Eq. (2.35). However, when a system has fractional occupations, the orbitals have to be canonical to define clearly occupation numbers. Even for $p + q = 3$ derivatives at integer, we still have to use canonical orbitals because of their potentially fractional connections. Therefore, throughout this Chapter, all orbitals are canonical orbitals as in Eq. (2.35).

### *2.4.1 $p + q = 2$ derivatives of a system with a fractional number of electrons*

To solve the CP-SCF equations, perturbations of external potentials or occupation numbers will be introduced, then Eqs. (2.33), (2.35) and (2.36) will be solved order by order. In the problem of $p + q = 2$ derivatives, perturbations $\lambda_A\delta(\mathbf{r} - \mathbf{R}_A)$ and

$\lambda_B\delta(\mathbf{r}-\mathbf{R}_B)$ are introduced. The SCF system is then perturbed, with the orbital variation

$$|\phi_{i\tau}\rangle = |\phi^0_{i\tau}\rangle + \lambda_A|\phi^A_{i\tau}\rangle + \lambda_B|\phi^B_{i\tau}\rangle + \lambda_A\lambda_B|\phi^{AB}_{i\tau}\rangle\cdots, \tag{2.37}$$

the noninteracting effective Hamiltonian variation

$$\hat{H}_\tau = \hat{H}^0_\tau + \lambda_A\hat{H}^B_\tau + \lambda_B\hat{H}^B_\tau + \lambda_A\lambda_B\hat{H}^{AB}_\tau + \cdots, \tag{2.38}$$

the eigenvalue variation

$$\epsilon_{i\tau} = \epsilon^0_{i\tau} + \lambda_A\epsilon^A_{i\tau} + \lambda_B\epsilon^B_{i\tau} + \lambda_A\lambda_B\epsilon^{AB}_{i\tau} + \cdots, \tag{2.39}$$

and the density matrix variation

$$\rho_{s,\tau} = \rho^0_{s,\tau} + \lambda_A\rho^A_{s,\tau} + \lambda_B\rho^B_{s,\tau} + \lambda_A\lambda_B\rho^{AB}_{s,\tau} + \cdots. \tag{2.40}$$

Note that $\hat{H}_\tau$ is the noninteracting effective Hamiltonian and thus contains a non-vanishing cross derivative $\hat{H}^{AB}_\tau$. In fact, one single perturbative field is sufficient to deduce all the $p+q=2$ derivatives, as demonstrated in our previous publication[80]. Nonetheless, the second perturbative field will be necessary to establish $\delta^3E/\delta v^3$ and $\delta^3E/\delta N\delta v^2$ in the later stage. The zeroth order CP-SCF equations are just the normal SCF equations with trivial unperturbed solutions. For the first order, the CP-SCF equations are,

$$\hat{H}^X_\tau|\phi_{i\tau}\rangle + \hat{H}_\tau|\phi^X_{i\tau}\rangle = \epsilon^X_{i\tau}|\phi_{i\tau}\rangle + \epsilon_{i\tau}|\phi^X_{i\tau}\rangle, \tag{2.41}$$

$$\langle\phi^X_{u\tau}|\phi_{i\tau}\rangle + \langle\phi_{u\tau}|\phi^X_{i\tau}\rangle = 0, \tag{2.42}$$

and

$$\rho^X_{s,\tau}(\mathbf{r},\mathbf{r}') = \sum_i n_i[\phi_{i\tau}(\mathbf{r})\phi^X_{i\tau}(\mathbf{r}') + \phi^X_{i\tau}(\mathbf{r})\phi_{i\tau}(\mathbf{r}')], \tag{2.43}$$

where the superscript "0" is omitted when no confusion is caused, and a generic superscript $X$ represents either $A$ or $B$ for the first order response. Additionally, all orbitals are taken to be real because there is no magnetic field in our study.

$\rho^X_{s,\tau}(\mathbf{r},\mathbf{r}')$ can be further simplified as

$$\begin{aligned}
\rho^X_{s,\tau}(\mathbf{r},\mathbf{r}') &= \sum_{i,u} n_{i\tau} \langle \phi^X_{i\tau} | \phi_{u\tau} \rangle \left[ \phi_{i\tau}(\mathbf{r}) \phi_{u\tau}(\mathbf{r}') + \phi_{u\tau}(\mathbf{r}) \phi_{i\tau}(\mathbf{r}') \right] \\
&= \sum_{i,u} n_{i\tau}(1 - n_{u\tau}) \langle \phi^X_{i\tau} | \phi_{u\tau} \rangle \left[ \phi_{i\tau}(\mathbf{r}) \phi_{u\tau}(\mathbf{r}') + \phi_{u\tau}(\mathbf{r}) \phi_{i\tau}(\mathbf{r}') \right] \\
&\quad + \sum_{i,u} n_{i\tau} n_{u\tau} \langle \phi^X_{i\tau} | \phi_{u\tau} \rangle \left[ \phi_{i\tau}(\mathbf{r}) \phi_{u\tau}(\mathbf{r}') + \phi_{u\tau}(\mathbf{r}) \phi_{i\tau}(\mathbf{r}') \right] \\
&= \sum_{ia} n_{i\tau}(1 - n_{a\tau}) \langle \phi^X_{i\tau} | \phi_{a\tau} \rangle \left[ \phi_{i\tau}(\mathbf{r}) \phi_{a\tau}(\mathbf{r}') + \phi_{a\tau}(\mathbf{r}) \phi_{i\tau}(\mathbf{r}') \right],
\end{aligned}$$

where Eq. (2.42) is applied to eliminate the occupied-occupied block. Applying $\langle \phi_{a\tau}|$ to the both sides of Eq. (2.41) results in

$$\langle \phi_{a\tau} | \hat{H}^X_\tau | \phi_{i\tau} \rangle + \epsilon_{a\tau} \langle \phi_{a\tau} | \phi^X_{i\tau} \rangle = \delta_{ia} \epsilon^X_{i\tau} + \epsilon_{i\tau} \langle \phi_{a\tau} | \phi^X_{i\tau} \rangle.$$

Defining the occupation-scaled orbitals[99, 100]

$$\tilde{\phi}_{i\tau} = \sqrt{n_{i\tau}} \phi_{i\tau}, \;\; \tilde{\phi}_{a\tau} = \sqrt{1 - n_{a\tau}} \phi_{a\tau}, \tag{2.44}$$

and the occupation-scaled first-order density matrix,

$$\tilde{P}^X_{ia\tau} = \tilde{P}^X_{ai\tau} = \sqrt{n_{i\tau}(1 - n_{a\tau})} \langle \phi_{a\tau} | \phi^X_{i\tau} \rangle, \tag{2.45}$$

then

$$\rho^X_{s,\tau}(\mathbf{r},\mathbf{r}') = \sum_{ia} \tilde{P}^X_{ia\tau} [\tilde{\phi}_{i\tau}(\mathbf{r}) \tilde{\phi}_{a\tau}(\mathbf{r}') + \tilde{\phi}_{a\tau}(\mathbf{r}) \tilde{\phi}_{i\tau}(\mathbf{r}')], \tag{2.46}$$

and for $a \neq i$

$$\begin{aligned}
-(\epsilon_{a\tau} - \epsilon_{i\tau}) \tilde{P}^X_{ia\tau} &= \langle \tilde{\phi}_{a\tau} | \hat{H}^X_\tau | \tilde{\phi}_{i\tau} \rangle \\
&= \tilde{\phi}_{i\tau}(\mathbf{R}_X) \tilde{\phi}_{a\tau}(\mathbf{R}_X) + \sum_{jb\zeta} (\tilde{K}_{ia\tau,jb\zeta} + \tilde{K}_{ia\tau,bj\zeta}) \delta \tilde{P}^X_{jb\zeta},
\end{aligned} \tag{2.47}$$

where, the kernel is, for a KS system,

$$K_{uv\tau,st\zeta} = \int d\mathbf{r} d\mathbf{r}' \phi_{u\tau}(\mathbf{r}) \phi_{v\tau}(\mathbf{r}) \left[ \frac{1}{|\mathbf{r} - \mathbf{r}'|} + \frac{\delta^2 E_{\mathrm{XC}}}{\delta \rho_\tau(\mathbf{r}) \delta \rho_\zeta(\mathbf{r}')} \right] \phi_{t\zeta}(\mathbf{r}') \phi_{s\zeta}(\mathbf{r}'), \tag{2.48}$$

and for a GKS system,

$$K_{uv\tau,st\zeta} = \int d\mathbf{r}_1 d\mathbf{r}'_1 d\mathbf{r}_2 d\mathbf{r}'_2 \phi_{u\tau}(\mathbf{r}'_1)\phi_{v\tau}(\mathbf{r}_1)\phi_{t\zeta}(\mathbf{r}_2)\phi_{s\zeta}(\mathbf{r}'_2)$$
$$\times \left[ \frac{\delta(\mathbf{r}_1 - \mathbf{r}'_1)\delta(\mathbf{r}_2 - \mathbf{r}'_2)}{|\mathbf{r}_1 - \mathbf{r}'_2|} + \frac{\delta^2 E_{\mathrm{XC}}}{\delta\rho_\tau(\mathbf{r}_1, \mathbf{r}'_1)\delta\rho_\zeta(\mathbf{r}_2, \mathbf{r}'_2)} \right], \tag{2.49}$$

while the occupation-scaled kernel $\tilde{K}$ is $K$ evaluated with occupation-scaled orbitals. Eq. (2.47) then becomes

$$\sum_{jb\zeta} \tilde{M}_{ia\tau,jb\zeta} \tilde{P}^X_{jb\zeta} = -\tilde{\phi}_{i\tau}(\mathbf{R}_X)\tilde{\phi}_{a\tau}(\mathbf{R}_X), \tag{2.50}$$

where

$$\tilde{M}_{ia\tau,jb\zeta} = \tilde{A}_{ia\tau,jb\zeta} + \tilde{B}_{ia\tau,jb\zeta}, \tag{2.51}$$

$$\tilde{A}_{ia\tau,jb\zeta} = \delta_{\tau\zeta}\delta_{ij}\delta_{ab}(\epsilon_{a\tau} - \epsilon_{i\tau}) + \tilde{K}_{ia\tau,jb\zeta}, \tag{2.52}$$

and

$$\tilde{B}_{ia\tau,jb\zeta} = \tilde{K}_{ia\tau,bj\zeta}. \tag{2.53}$$

The matrix $\tilde{M}$ is not directly invertible for a fractional system, as it contains singular values due to the existence of zero excitation energies. To eliminate the zero excitations, a singular value decomposition is carried out,

$$\tilde{\mathbf{A}} - \tilde{\mathbf{B}} = \mathbf{D}\boldsymbol{\Sigma}\mathbf{V}^\dagger = \mathbf{D}\boldsymbol{\Sigma}[\mathbf{V}_\varnothing \ \mathbf{V}_0]^\dagger, \tag{2.54}$$

where the submatrices $\mathbf{V}_\varnothing$ and $\mathbf{V}_0$ are the non-singular and singular space, respectively. The justification for projecting out the singular values of the matrix $\tilde{\mathbf{A}} - \tilde{\mathbf{B}}$ rather than $\tilde{\mathbf{A}} + \tilde{\mathbf{B}}$ comes from linear-response time-dependent DFT equation[52], i.e.

$$(\tilde{\mathbf{A}} - \tilde{\mathbf{B}})^{1/2}(\tilde{\mathbf{A}} + \tilde{\mathbf{B}})(\tilde{\mathbf{A}} - \tilde{\mathbf{B}})^{1/2}\mathbf{Z} = \omega^2\mathbf{Z}, \tag{2.55}$$

with $\omega$ the excitation energies. Then the solution of Eq. (2.50) is

$$\tilde{P}^X_{ia\tau} = -\sum_{jb\zeta}\{\mathbf{V}_{\varnothing}[\mathbf{V}^{\dagger}_{\varnothing}(\tilde{\mathbf{A}}+\tilde{\mathbf{B}})\mathbf{V}_{\varnothing}]^{-1}\mathbf{V}^{\dagger}_{\varnothing}\}_{ia\tau,jb\zeta}\tilde{\phi}_{j\zeta}(\mathbf{R}_X)\tilde{\phi}_{b\zeta}(\mathbf{R}_X). \tag{2.56}$$

We will denote the projected inversion in Eq. (2.56) as $\tilde{\mathbf{M}}^{-1}$ from now on for simplicity, but note that the formal $\tilde{\mathbf{M}}^{-1}$ is actually carried out in the way of Eq. (2.56).

Through the relation $\chi = \sum_\tau \rho^X_\tau$, we have the analytical expression for the linear-response function

$$\chi(\mathbf{r},\mathbf{r}') = -2\sum_{ia\tau,jb\zeta}(\tilde{\mathbf{M}}^{-1})_{ia\tau,jb\zeta}\tilde{\phi}_{i\tau}(\mathbf{r})\tilde{\phi}_{a\tau}(\mathbf{r})\tilde{\phi}_{j\zeta}(\mathbf{r}')\tilde{\phi}_{b\zeta}(\mathbf{r}'). \tag{2.57}$$

The Fukui function $f(\mathbf{r})$ is readily available through the relation $f(\mathbf{R}_X) = \epsilon^X_{f\sigma} = \langle\phi_{f\sigma}|\hat{H}^X_\sigma|\phi_{f\sigma}\rangle$,

$$f(\mathbf{r}) = |\phi_{f\sigma}(\mathbf{r})|^2 - 2\sum_{ia\tau,jb\zeta}K_{ff\sigma,ia\tau}G_{ia\tau,jb\zeta}\phi_{j\zeta}(\mathbf{r})\phi_{b\zeta}(\mathbf{r}), \tag{2.58}$$

with the matrix $\mathbf{G}$ defined as

$$\mathbf{G} = \mathbf{C}\tilde{\mathbf{M}}^{-1}\mathbf{C},$$

and $C_{ia\tau,jb\zeta} = \delta_{\tau\zeta}\delta_{ij}\delta_{ab}\sqrt{n_{i\tau}(1-n_{a\tau})}$. Accordingly, the chemical hardness $\eta$ can be derived via Hellmann-Feynman theorem,

$$\begin{aligned}\eta = \frac{\partial\mu}{\partial N} &= \frac{\partial\langle\phi_{f\sigma}|\hat{H}_\sigma|\phi_{f\sigma}\rangle}{\partial N} = \langle\phi_{f\sigma}|\frac{\partial\hat{H}_\sigma}{\partial N}|\phi_{f\sigma}\rangle \\ &= \int d\mathbf{r}'\langle\phi_{f\sigma}|\frac{\delta(\hat{v}_J+\hat{v}^\sigma_{\mathrm{XC}})}{\delta\rho_\tau(\mathbf{r}')}\frac{\partial\rho_\tau(\mathbf{r}')}{\partial N}|\phi_{f\sigma}\rangle \\ &= K_{ff\sigma,ff\sigma} - 2\sum_{ia\tau,jb\zeta}K_{ff\sigma,ia\tau}G_{ia\tau,jb\zeta}K_{ff\sigma,jb\zeta}.\end{aligned} \tag{2.59}$$

Eqs. (2.57)-(2.59) are generalization of the previous work on Fukui functions at fractional systems. All these expressions reduce to previous results at integer limit[80].

### *2.4.2 $\delta^3E/\delta v^3$ and $\delta^3E/\delta N\delta v^2$ for a system with an integer number of electrons*

Geerlings and De Proft summarized the chemical significance of $p+q=3$ derivatives in their recent extensive review on conceptual DFT[61]. The lack of practical implementations of analytical derivatives hindered the study of these derivatives. Among all four $p+q=3$ derivatives, the analytical expression for $\delta^3E/\delta v^3$ was actually derived for frequency-dependent hyperpolarizability by Rice *et al.*[53, 91, 97], and for static hyperpolarizability by Cowell *et al.*[92], yet they are not widely known by the conceptual DFT community. They utilized non-canonical orbitals during the derivation to simplify the solution of the CP-SCF equations. In this work, as we are dealing with a system with possible fractional occupations, only canonical orbitals can be used to define the occupation numbers clearly. Therefore, all derivations in this work remain in the form of canonical orbitals, and the derivative $\delta^3E/\delta v^3$ will be re-derived based on canonical orbitals, which proves to be equivalent with the approach using non-canonical orbitals by previous workers.

$\delta^3E/\delta v^3$ and $\delta^3E/\delta N\delta v^2$ could be perceived as cross derivatives in the second order response with the above-mentioned perturbations, $\lambda_A\delta(\mathbf{r}-\mathbf{R}_A)$ and $\lambda_B\delta(\mathbf{r}-\mathbf{R}_B)$. Specifically, $\sum_\tau \rho^{AB}_\tau = \delta^3E/\delta v^3$ and $\epsilon^{AB}_{f\sigma} = \delta^3E/\delta N\delta v^2$. The second order CP-SCF equations for a fractional system become very complicated, thus all $p+q=3$ derivatives are studied only for integer systems. Defining

$$P^1_{jb\zeta}(\mathbf{r}) = -\sum_{kc\theta}(\mathbf{M}^{-1})_{jb\zeta,kc\theta}\phi_{k\theta}(\mathbf{r})\phi_{c\theta}(\mathbf{r}), \tag{2.60}$$

$$H^1_{uv\tau}(\mathbf{r}) = \langle\phi_{u\tau}|\delta\hat{H}_\tau/\delta v(\mathbf{r})|\phi_{v\tau}\rangle = \phi_{u\tau}(\mathbf{r})\phi_{v\tau}(\mathbf{r}) + \sum_{jb\zeta}(K_{uv\tau,jb\zeta}+K_{uv\tau,bj\zeta})P^1_{jb\zeta}(\mathbf{r}), \tag{2.61}$$

$$Q_{ab\tau}(\mathbf{r},\mathbf{r}') = \sum_i[P^1_{ia\tau}(\mathbf{r})P^1_{ib\tau}(\mathbf{r}') + P^1_{ia\tau}(\mathbf{r}')P^1_{ib\tau}(\mathbf{r})], \tag{2.62}$$

$$Q_{ij\tau}(\mathbf{r},\mathbf{r}') = \sum_a[P^1_{ia\tau}(\mathbf{r})P^1_{ja\tau}(\mathbf{r}') + P^1_{ia\tau}(\mathbf{r}')P^1_{ja\tau}(\mathbf{r})], \tag{2.63}$$

$$F_{uv\tau,st\zeta,xy\theta} = \int d\mathbf{r}d\mathbf{r}'d\mathbf{r}''\phi_{u\tau}(\mathbf{r})\phi_{v\tau}(\mathbf{r})\phi_{s\zeta}(\mathbf{r}')\phi_{t\zeta}(\mathbf{r}')\phi_{x\theta}(\mathbf{r}'')\phi_{y\theta}(\mathbf{r}'')\frac{\delta^3 E_{\rm XC}}{\delta\rho_\tau(\mathbf{r})\delta\rho_\zeta(\mathbf{r}')\delta\rho_\theta(\mathbf{r}'')}, \tag{2.64}$$

$$\begin{aligned} W_{ia\tau}(\mathbf{r},\mathbf{r}') = &\sum_j [P^1_{ja\tau}(\mathbf{r})H^1_{ji\tau}(\mathbf{r}') + P^1_{ja\tau}(\mathbf{r}')H^1_{ji\tau}(\mathbf{r})] \\ &- \sum_b [H^1_{ab\tau}(\mathbf{r})P^1_{ib\tau}(\mathbf{r}') + H^1_{ab\tau}(\mathbf{r}')P^1_{ib\tau}(\mathbf{r})] \\ &- \sum_{bc\zeta} K_{ia\tau,bc\zeta}Q_{bc\zeta}(\mathbf{r},\mathbf{r}') + \sum_{jk\zeta} K_{ia\tau,jk\zeta}Q_{jk\zeta}(\mathbf{r},\mathbf{r}') \\ &- 4\sum_{jb\zeta,kc\theta} F_{ai\tau,jb\zeta,kc\theta}P^1_{jb\zeta}(\mathbf{r})P^1_{kc\theta}(\mathbf{r}'), \end{aligned} \tag{2.65}$$

and

$$Z_{ia\tau}(\mathbf{r},\mathbf{r}') = \sum_{jb\zeta}(\mathbf{M}^{-1})_{ia\tau,jb\zeta}W_{ia\tau}(\mathbf{r},\mathbf{r}'), \tag{2.66}$$

where we have used the $\mathbf{M}$ matrix in Eq. (2.51) with standard normalized orbitals , we achieve the solutions of the CP-SCF equations,

$$\begin{aligned} \chi^{(2)}(\mathbf{r},\mathbf{r}',\mathbf{r}'') &= \frac{\delta^3 E}{\delta v(\mathbf{r})\delta v(\mathbf{r}')\delta v(\mathbf{r}'')} = \frac{\delta^2\rho(\mathbf{r})}{\delta v(\mathbf{r}')\delta v(\mathbf{r}'')} \\ &= 2\sum_{ia\tau}\phi_{i\tau}(\mathbf{r})\phi_{a\tau}(\mathbf{r})Z_{ia\tau}(\mathbf{r}',\mathbf{r}'') + \sum_{ab\tau}\phi_{a\tau}(\mathbf{r})\phi_{b\tau}(\mathbf{r})Q_{ab\tau}(\mathbf{r}',\mathbf{r}'') \\ &\quad - \sum_{ij\tau}\phi_{i\tau}(\mathbf{r})\phi_{j\tau}(\mathbf{r})Q_{ij\tau}(\mathbf{r}',\mathbf{r}''), \end{aligned} \tag{2.67}$$

and

$$\begin{aligned} g(\mathbf{r},\mathbf{r}') &= \frac{\delta^3 E}{\delta N\delta v(\mathbf{r})\delta v(\mathbf{r}')} = \frac{\delta^2\epsilon_{f\sigma}}{\delta v(\mathbf{r})\delta v(\mathbf{r}')} \\ &= 2{\sum_u}' \frac{H^1_{fu\sigma}(\mathbf{r})H^1_{fu\sigma}(\mathbf{r}')}{\epsilon_{f\sigma}-\epsilon_{u\sigma}} + 4\sum_{ia\tau,jb\zeta} F_{ff\sigma,ia\tau,jb\zeta}P^1_{ia\tau}(\mathbf{r})P^1_{jb\zeta}(\mathbf{r}') \\ &\quad + 2\sum_{ia\tau} K_{ff\sigma,ia\tau}Z_{ia\tau}(\mathbf{r},\mathbf{r}') + \sum_{ab\tau} K_{ff\sigma,ab\tau}Q_{ab\tau}(\mathbf{r},\mathbf{r}') - \sum_{ij\tau} K_{ff\sigma,ij\tau}Q_{ij\tau}(\mathbf{r},\mathbf{r}'). \end{aligned} \tag{2.68}$$

where the summation $\sum'$ excludes all orbitals degenerate to $\phi_{f\sigma}$. The second-order response function $\chi^{(2)}$ is compatible with the static hyperpolarizability expression using non-canonical orbitals[92]. See the Appendix A for details of the derivation.

### *2.4.3 $\delta^3E/\delta N^2\delta v$ and $\delta^3E/\delta N^3$ for a system with an integer number of electrons*

The derivations of $\delta^3E/\delta N^2\delta v$ and $\delta^3E/\delta N^3$ share the same CP-SCF equations with the "perturbation" of $\delta N$. Parallel to the approach in Subsection 2.4.1, all essential elements in CP-SCF equations are expanded according to orders of $\delta N$ in Taylor series. Under the perturbation, the orbitals become,

$$|\bar{\phi}_{i\tau}\rangle = |\bar{\phi}^0_{i\tau}\rangle + (\delta N)|\bar{\phi}^1_{i\tau}\rangle + \frac{1}{2}(\delta N)^2|\bar{\phi}^2_{i\tau}\rangle + \cdots , \tag{2.69}$$

the noninteracting effective Hamiltonian becomes

$$\hat{\bar{H}}_\tau = \hat{\bar{H}}^0_\tau + (\delta N)\hat{\bar{H}}^1_\tau + \frac{1}{2}(\delta N)^2\hat{\bar{H}}^2_\tau + \cdots , \tag{2.70}$$

the eigenvalues become

$$\bar{\epsilon}_{i\tau} = \bar{\epsilon}^0_{i\tau} + (\delta N)\bar{\epsilon}^1_{i\tau} + \frac{1}{2}(\delta N)^2\bar{\epsilon}^2_{i\tau} + \cdots , \tag{2.71}$$

and the density matrix becomes

$$\bar{\rho}_{s,\tau} = \bar{\rho}^0_{s,\tau} + (\delta N)\bar{\rho}^1_{s,\tau} + \frac{1}{2}(\delta N)^2\bar{\rho}^2_{s,\tau} + \cdots . \tag{2.72}$$

For simplicity, only integer systems will be studied for these two derivatives. As usual, the superscript "0" will be omitted when no confusion is caused. The extra bars for the variables are added to distinguish perturbative variables in this subsection with those in the previous subsection. Then $\sum_\tau \bar{\rho}^2_\tau = \delta^3E/\delta N^2\delta v$ and $\bar{\epsilon}^2_{f\sigma} = \delta^3E/\delta N^3$. Defining,

$$\bar{P}^1_{ia\tau} = -\sum_{jb\zeta} K_{ff\sigma,jb\zeta}(\mathbf{M}^{-1})_{ia\tau,jb\zeta}, \tag{2.73}$$

$$\bar{H}^1_{uv\tau} = \langle \phi_{u\tau} | \hat{\bar{H}}^1_\tau | \phi_{v\tau} \rangle = K_{uv\tau,ff\sigma} + \sum_{jb\zeta} (K_{uv\tau,jb\zeta} + K_{uv\tau,bj\zeta}) \bar{P}^1_{jb\zeta}, \tag{2.74}$$

$$\bar{Q}_{ij\tau} = \sum_a \bar{P}^1_{ia\tau} \bar{P}^1_{ja\tau}, \tag{2.75}$$

$$\bar{Q}_{ab\tau} = \sum_i \bar{P}^1_{ia\tau} \bar{P}^1_{ib\tau}, \tag{2.76}$$

$$f_{uv\zeta} = \delta_{\sigma\zeta}\delta_{uf}\delta_{vf} + \sum_{jb\zeta} \bar{P}^1_{jb\theta} (\delta_{uj}\delta_{bv} + \delta_{ub}\delta_{vj}), \tag{2.77}$$

$$\begin{aligned} \bar{W}_{ia\tau} = {} & 2\sum_{jk\zeta} K_{ia\tau,jk\zeta} \bar{Q}_{jk\zeta} - 2\sum_{bc\zeta} K_{ia\tau,bc\zeta} \bar{Q}_{bc\zeta} - 2{\sum_u}' \frac{(K_{ia\tau,fu\sigma} + K_{ia\tau,uf\sigma}) \bar{H}^1_{fu\sigma}}{\epsilon_{f\sigma} - \epsilon_{u\sigma}} \\ & - 2\sum_b \bar{H}^1_{ab\tau} \bar{P}^1_{ib\tau} + 2\sum_j \bar{P}^1_{ja\tau} \bar{H}^1_{ji\tau} - \sum_{uv\zeta,st\theta} F_{ia\tau,uv\zeta,st\theta} f_{uv\zeta} f_{st\theta}, \end{aligned} \tag{2.78}$$

and

$$\bar{Z}_{ia\tau} = \sum_{jb\zeta} (\mathbf{M}^{-1})_{ia\tau,jb\zeta} \bar{W}_{jb\zeta}, \tag{2.79}$$

where the summation $\sum'$ excludes all orbitals degenerate to $\phi_{f\sigma}$, and the definitions of $\mathbf{M}$ and $F_{uv\tau,st\zeta,xy\theta}$ remain the same as in the previous subsection, thus

$$\begin{aligned} f^{(2)}(\mathbf{r}) = \frac{\delta^3 E}{\delta N^2 \delta v(\mathbf{r})} = {} & 2\sum_{ia\tau} \phi_{i\tau}(\mathbf{r}) \phi_{a\tau}(\mathbf{r}) \bar{Z}_{ia\tau} + 2\sum_{ab\tau} \phi_{a\tau}(\mathbf{r}) \phi_{b\tau}(\mathbf{r}) \bar{Q}_{ab\tau} \\ & - 2\sum_{ij\tau} \phi_{i\tau}(\mathbf{r}) \phi_{j\tau}(\mathbf{r}) \bar{Q}_{ij\tau} + 4{\sum_u}' \phi_{f\sigma}(\mathbf{r}) \phi_{u\sigma}(\mathbf{r}) \frac{\bar{H}^1_{fu\sigma}}{\epsilon_{f\sigma} - \epsilon_{u\sigma}} \end{aligned} \tag{2.80}$$

and

$$\begin{aligned} \gamma = \frac{\delta^3 E}{\delta N^3} = {} & 2\sum_{ia\tau} K_{ff\sigma,ia\tau} \bar{Z}_{ia\tau} + 2\sum_{ab\tau} K_{ff\sigma,ab\tau} \bar{Q}_{ab\tau} - 2\sum_{ij\tau} K_{ff\sigma,ij\tau} \bar{Q}_{ij\tau} \\ & + 4{\sum_u}' \frac{K_{ff\sigma,fu\sigma} \bar{H}^1_{fu\sigma}}{\epsilon_{f\sigma} - \epsilon_{u\sigma}} + \sum_{uv\zeta,st\theta} F_{ff\sigma,uv\zeta,st\theta} f_{uv\zeta} f_{st\theta} + 2{\sum_u}' \frac{|\bar{H}^1_{fu\sigma}|^2}{\epsilon_{f\sigma} - \epsilon_{u\sigma}}. \end{aligned} \tag{2.81}$$

Detailed derivations are given in the Appendix B.

### *2.4.4 Numerical verification*

The analytical expressions of fractional $p+q=2$ derivatives and integer $p+q=3$ derivatives are implemented in QM4D[37]. All the derivatives in this section has been numerically tested.

Fig 2.1 shows the analytical and numerical linear-response function and Fukui function for fractional systems, using Becke three-parameter exchange functional[30] and Lee-Yang-Parr correlation functional[28] (B3LYP) with 6-31G(d) basis sets. In Fig 2.1a, the fractional linear-response function of a lithium atom centered at origin with 1.8 $\alpha$ electrons and 1.0 $\beta$ electron is calculated. The numerical $\chi(\mathbf{r}', \mathbf{R})$ is obtained by introducing a potential of a Dirac delta function at $\mathbf{R}$,

$$\chi(\mathbf{r}', \mathbf{R}) \sim \frac{\rho[v(\mathbf{r}) + \lambda\delta(\mathbf{r}-\mathbf{R})](\mathbf{r}') - \rho[v(\mathbf{r}) - \lambda\delta(\mathbf{r}-\mathbf{R})](\mathbf{r}')}{2\lambda}.$$

The delta potential can be implemented exactly by adding the delta potential matrix elements into the KS/GKS Fock matrix,

$$v^{\delta}_{uv} = \int d\mathbf{r}\phi_u(\mathbf{r})\delta(\mathbf{r}-\mathbf{R})\phi_v(\mathbf{r}) = \phi_u(\mathbf{R})\phi_v(\mathbf{R}),$$

which barely increases any computation efforts. The Fukui function of a lithium atom with 1.8 $\alpha$ electrons and 1.2 $\beta$ electrons is shown in Fig 2.1b. The analytical and numerical derivatives agree well in these figures.

Two $p+q=3$ derivatives, $\delta^3 E/\delta N \delta v^2$ and $\delta^3 E/\delta N^2 \delta v$, are also evaluated for a neutral CO molecule, as illustrated in Fig 2.2. The VWN5[25] parametrization of the local-density functional approximation (LDA) is used, in conjunction with the basis set 6-31G(d). The numerical derivatives related to $N$ will inevitably require $p+q=2$ derivatives at fractional systems. To avoid the possible issue of unbounded anions, only the electron removal direction ($\delta N < 0$) is considered. All numerical and analytical derivatives overlap in Fig 2.2.

These numerical calculations verified that the analytical expressions for the derivatives are correct.

## 2.5 Extensions to nonlocal Fukui functions and linear-response functions

In the previous sections an analytical function $E[N, v]$ and its derivatives with a local potential $v(\mathbf{r})$ are discussed. We now extend the local potential $v(\mathbf{r})$ to a special nonlocal potential $w(\mathbf{r}, \mathbf{r}')$ which is coupled with the KS/GKS density matrix $\rho_s(\mathbf{r}, \mathbf{r}')$,

$$E[N, w(\mathbf{r}, \mathbf{r}')] = T_s[\rho_s] + \int w(\mathbf{r}, \mathbf{r}')\rho_s(\mathbf{r}', \mathbf{r})d\mathbf{r}d\mathbf{r}' + J[\rho_s] + E_{\mathrm{XC}}[\rho_s], \tag{2.82}$$

where $\rho_s(\mathbf{r}', \mathbf{r})$ is the KS/GKS density matrix defined in Eq. (2.33) rather than the one-body reduced density matrix (1-RDM) of the interacting system,

$$\gamma_1(\mathbf{r}, \mathbf{r}') = \langle \Psi_g | \psi^\dagger(\mathbf{r})\psi(\mathbf{r}') | \Psi_g \rangle, \tag{2.83}$$

with $|\Psi_g\rangle$ being the ground state wavefunction of the interacting system. For simplicity, we have only used the spinless nonlocal potential $w(\mathbf{r}, \mathbf{r}')$ here, but the extension to spin nonlocal potential $w(\mathbf{x}, \mathbf{x}')$ is straightforward. Such external nonlocal potentials $w(\mathbf{r}, \mathbf{r}')$ are nonphysical; nonetheless, effective nonlocal potential has been widely used in quantum mechanics, such as Hartree-Fock (HF) potential and pseudopotential representing core electrons.

The external nonlocal potential $w(\mathbf{r}, \mathbf{r}')$ is dual to the KS/GKS 1-RDM $\rho_s(\mathbf{r}', \mathbf{r})$ in the interacting system, as the local potential is dual to the electron density[101]. The dual to $\rho_s(\mathbf{r}', \mathbf{r})$ in a GKS noninteracting system is the optimized effective nonlocal

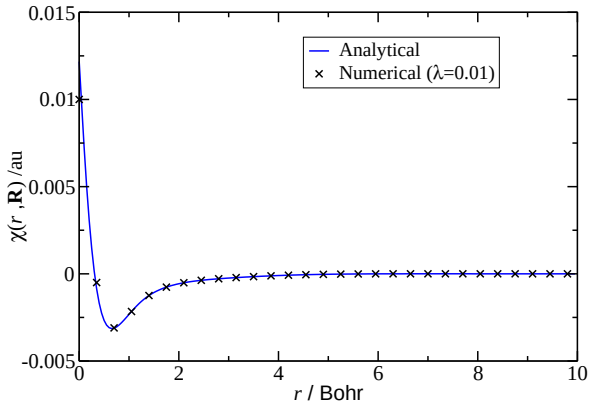


(a) Numerical and analytical $\chi(\mathbf{r}, \mathbf{R})$ for $\mathrm{Li}^{0.2+}$ with $\mathbf{R} = (0.0, 0.0, 1.0)$

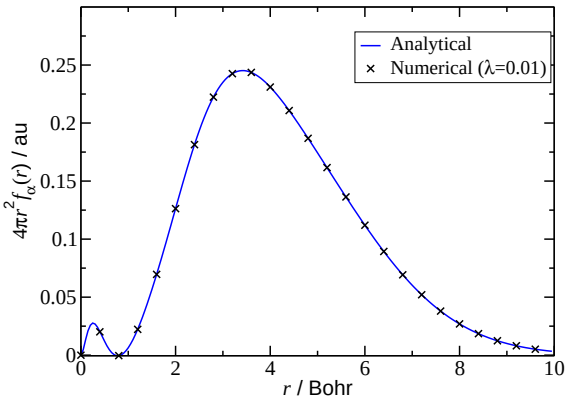


(b) Numerical and analytical $f_\alpha(\mathbf{r})$ of a Li atom with $N_\alpha = 1.8$ and $N_\beta = 1.2$

FIGURE 2.1: Numerical calculations of the linear-response functions and the Fukui functions of a fractional system. All calculations are performed in the level B3LYP/6-31G(d) in QM4D package[37]. $\lambda$'s in subfigures (a) and (b) indicate the stepsize for the numerical derivatives. The path of the plot is along the $z$-axis for both subfigures. (a) The linear-response function of $\mathrm{Li}^{0.2+}$ with $N_\alpha = 1.8$ and $N_\beta = 1.0$. A $\delta$ potential at $\mathbf{R} = (0.0, 0.0, 1.0)$ au is set to evaluate the numerical derivative. (b) The $\alpha$-spin Fukui function $f_\alpha(\mathbf{r}) = \partial\rho(\mathbf{r})/\partial N_\alpha$ of a special lithium atom with 1.8 $\alpha$ electrons and 1.2 $\beta$ electrons.

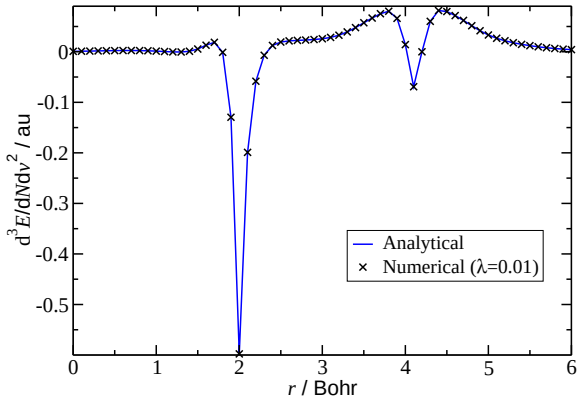


(a) Numerical and analytical Fukui response functions $g(\mathbf{r}, \mathbf{R})$ with $\mathbf{R} = (0.0,\ 0.0\ , 1.0)$

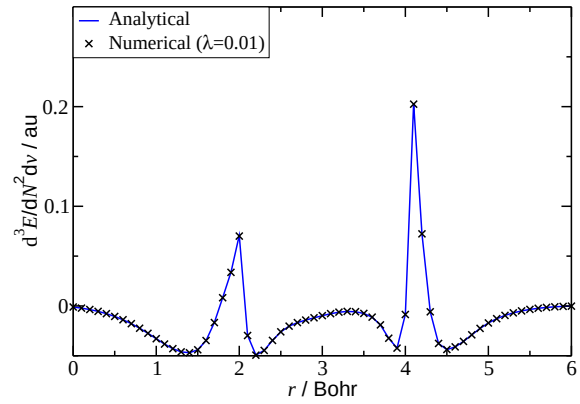


(b) Numerical and analytical dual descriptor $f^{(2)}(\mathbf{r})$

FIGURE 2.2: Numerical and analytical $p + q = 3$ derivatives for CO molecule at the level of LDA/6-31G(d). The plot path is along the $z$-axis. The coordinates of the carbon and the oxygen atoms are (0.0, 0.0, 2.0) and (0.0, 0.0, 4.104777) au, respectively. $\lambda$ indicates the stepsize of the numerical derivatives for all cases. When $N$ derivative is concerned, only electron removal direction is considered.

potential $v_s(\mathbf{r}, \mathbf{r}')$[102]. In potential functional point of view, the introduction of the external nonlocal potential $w(\mathbf{r}, \mathbf{r}')$ is a natural consequence of the potential functional theory for GKS systems. The external nonlocal potential is the sum of the normal local potential and the additive pure nonlocal potential; the real physical system resides in the regime where the pure nonlocal potential vanishes. Yet the nonlocal part of the external potential enables the study of special features such as nonlocal response. The use of external nonlocal potential is very similar to the use of spin specific local potential in spin DFT. To incorporate spin densities into DFT, a fictitious magnetic field coupled only with spin densities is introduced (see, for example, Page 169 of Ref.[4]), leading to spin specific local potentials. In that case, the spin density and the spin specific local potential are dual to each other. In the dual picture, the extensions to nonlocal systems provide a clear understanding of the GKS systems.

Parallel to the functional $E[N, v]$, the derivatives of $E[N, w]$ are defined as the chemical potential with an external nonlocal potential

$$\mu = \frac{\delta E}{\delta N}, \tag{2.84}$$

the density matrix,

$$\rho_s(\mathbf{r}', \mathbf{r}) = \frac{\delta E}{\delta w(\mathbf{r}, \mathbf{r}')}, \tag{2.85}$$

the chemical hardness with an external nonlocal potential,

$$\eta = \frac{\delta^2 E}{\delta N^2}, \tag{2.86}$$

the nonlocal Fukui function

$$f_w(\mathbf{r}, \mathbf{r}') = \frac{\delta^2 E}{\delta N \delta w(\mathbf{r}', \mathbf{r})} = \frac{\delta \rho_s(\mathbf{r}, \mathbf{r}')}{\delta N}, \tag{2.87}$$

and the nonlocal linear-response function

$$\chi_w(\mathbf{r}_1,\mathbf{r}_2;\mathbf{r}'_1,\mathbf{r}'_2) = \frac{\delta^2 E}{\delta w(\mathbf{r}'_1,\mathbf{r}_1)\delta w(\mathbf{r}_2,\mathbf{r}'_2)} = \frac{\delta \rho_s(\mathbf{r}_1,\mathbf{r}'_1)}{\delta w(\mathbf{r}_2,\mathbf{r}'_2)}. \tag{2.88}$$

Note that the nonlocal Fukui function $f_w(\mathbf{r},\mathbf{r}')$ is different from the object called the Fukui matrix in Ref. [103], where the Fukui matrix was defined with the physical 1-RDM.

With a general external nonlocal potential $w(\mathbf{r},\mathbf{r}')$, the $E$ vs $N$ curve is not necessarily piecewise linear, as the proof of the linearity condition cannot be easily extended to systems with an external nonlocal potential $w(\mathbf{r},\mathbf{r}')$[76, 77, 86]. Nevertheless, at the limit $w(\mathbf{r},\mathbf{r}') \to v(\mathbf{r})\delta(\mathbf{r}-\mathbf{r}')$, the feature of the $E$ vs $N$ curve for a local potential $v(\mathbf{r})$ preserves. At the local potential limit, we can obtain the analytical expressions for the nonlocal Fukui function

$$f_w(\mathbf{r},\mathbf{r}') = \phi_{f\sigma}(\mathbf{r})\phi_{f\sigma}(\mathbf{r}') - \sum_{jb\zeta,kc\theta} K_{ff\sigma,jb\zeta} G_{jb\zeta,kc\theta}[\phi_{k\theta}(\mathbf{r})\phi_{c\theta}(\mathbf{r}') + \phi_{k\theta}(\mathbf{r}')\phi_{c\theta}(\mathbf{r})], \tag{2.89}$$

and nonlocal linear-response function

$$\begin{aligned}\chi_w(\mathbf{r}_1,\mathbf{r}_2;\mathbf{r}'_1,\mathbf{r}'_2) = -\sum_{ia\tau,jb\zeta} G_{ia\tau,jb\zeta}[&\phi_{i\tau}(\mathbf{r}_1)\phi_{a\tau}(\mathbf{r}'_1)\phi_{j\zeta}(\mathbf{r}'_2)\phi_{b\zeta}(\mathbf{r}_2) \\ &+ \phi_{i\tau}(\mathbf{r}'_1)\phi_{a\tau}(\mathbf{r}_1)\phi_{j\zeta}(\mathbf{r}_2)\phi_{b\zeta}(\mathbf{r}'_2)].\end{aligned} \tag{2.90}$$

Although the total energy and the total density is linear with respect to $N$ at the local potential limit, $\rho_s(\mathbf{r},\mathbf{r}')$ and $\chi_w(\mathbf{r}_1,\mathbf{r}_2;\mathbf{r}'_1,\mathbf{r}'_2)$ may not be linear . Since $\rho(\mathbf{r}) = \rho_s(\mathbf{r},\mathbf{r})$ and $\chi(\mathbf{r},\mathbf{r}') = \chi_w(\mathbf{r},\mathbf{r}';\mathbf{r},\mathbf{r}')$, the diagonal elements are still linear at the local potential limit. This information is also useful as an exact condition of the functional. Combining Eqs. (2.87) and (2.89), we have

$$\frac{\delta\rho_s(\mathbf{r},\mathbf{r}')}{\delta N} = \phi_{f\sigma}(\mathbf{r})\phi_{f\sigma}(\mathbf{r}') - \sum_{jb\zeta,kc\theta} K_{ff\sigma,jb\zeta}G_{jb\zeta,kc\theta}[\phi_{k\theta}(\mathbf{r})\phi_{c\theta}(\mathbf{r}') + \phi_{k\theta}(\mathbf{r}')\phi_{c\theta}(\mathbf{r})]. \tag{2.91}$$

$\rho(\mathbf{r})$ at a fractional system can be obtained by a linear interpolation between two adjacent integer electron densities, then $\rho_s(\mathbf{r},\mathbf{r}')$ for the fractional system can be calculated via Wu-Yang optimized-effective-potential method[104]. For the exact functional, a finite difference derivative of $\rho_s(\mathbf{r},\mathbf{r}')$ with respect to $N$, i.e. the left-hand side, should be equal to the analytical expression in the right-hand side in Eq. (2.91). This two-point nonlocal Fukui function is more favorable than the local Fukui function in terms of density functional study, because it is more convenient to work on a matrix ($\langle\phi_u|f_w|\phi_v\rangle$) than a real-space function.

The nonlocal linear-response function $\chi_w$ in general has no direct physical meaning, as it is not connected to the 1-RDM of the real interacting system in nature. However, it is a quantity essential in understanding linear-response time-dependent GKS method[52], e.g. linear-response time-dependent HF or linear-response time-dependent hybid functionals such as B3LYP. The TD-GKS equation of these systems in terms of time-dependent nonlocal linear-response function is

$$\begin{aligned}\chi_w(\mathbf{1},\mathbf{2};\mathbf{1}',\mathbf{2}') = \chi_s(\mathbf{1},\mathbf{2};\mathbf{1}',\mathbf{2}') + \int d\mathbf{3}d\mathbf{3}'d\mathbf{4}d\mathbf{4}'\chi_s(\mathbf{1},\mathbf{3};\mathbf{1}',\mathbf{3}';\omega) \\ \times f_{\mathrm{HXC}}(\mathbf{3}',\mathbf{4}';\mathbf{3},\mathbf{4})\chi_w(\mathbf{4},\mathbf{2};\mathbf{4}',\mathbf{2}'),\end{aligned} \tag{2.92}$$

where $\mathbf{k}$ is a compact notation of $(\mathbf{r}_k,\sigma_k,t_k)$ and $f_{\mathrm{HXC}}$ is the kernel in the Eq. (2.49), which is a four-point function for GKS. $\chi_s$ in Eq. (2.92) is the GKS noninteracting nonlocal linear-response function, also a four-point function. The TD-GKS equation can be understood clearly via the use of the nonlocal linear-response function $\chi_w(\mathbf{1},\mathbf{2};\mathbf{1}',\mathbf{2}')$. In TDDFT calculation, the Fourier transformation of Eq. (2.92) is

the well-known Dyson-like equation for TDDFT in frequency domain,

$$\chi_w(\mathbf{x}_1,\mathbf{x}_2;\mathbf{x}_1',\mathbf{x}_2';\omega) = \chi_s(\mathbf{x}_1,\mathbf{x}_2;\mathbf{x}_1',\mathbf{x}_2';\omega) + \int d\mathbf{x}_3 d\mathbf{x}_3' d\mathbf{x}_4 d\mathbf{x}_4' \chi_s(\mathbf{x}_1,\mathbf{x}_3;\mathbf{x}_1',\mathbf{x}_3';\omega) \times f_{\mathrm{HXC}}(\mathbf{x}_3',\mathbf{x}_4';\mathbf{x}_3,\mathbf{x}_4;\omega)\chi_w(\mathbf{x}_4,\mathbf{x}_2;\mathbf{x}_4',\mathbf{x}_2';\omega). \tag{2.93}$$

On the other hand, in many-body Green function theory, the Bethe-Salpeter equation[105] (BSE) is an accurate method to calculate optical properties. Refer to Ref. [106] for a recent review on this topic. BSE can be expressed in another Dyson equation,

$$L(\mathbf{1},\mathbf{2};\mathbf{1}',\mathbf{2}') = L_0(\mathbf{1},\mathbf{2};\mathbf{1}',\mathbf{2}') + \int d\mathbf{3} d\mathbf{3}' d\mathbf{4} d\mathbf{4}' L_0(\mathbf{1},\mathbf{3};\mathbf{1}',\mathbf{3}')\Xi(\mathbf{3}',\mathbf{4}';\mathbf{3},\mathbf{4})L(\mathbf{4},\mathbf{2};\mathbf{4}',\mathbf{2}'), \tag{2.94}$$

where $L$ is the two-body correlation function, $L_0$ is the noninteracting part of the two-body correlation function, and $\Xi$ represents an effective two-body interaction. Although sharing a similar form, Eqs. (2.92) and (2.94) contains distinct the physical contents. Based on the definition, $L$ is the response of the one-body Green function with respect to the external nonlocal potential,

$$L(\mathbf{x}_1 t_1, \mathbf{x}_2 t_2; \mathbf{x}_1' t_1', \mathbf{x}_2' t_2^+) = -i\frac{\delta G_1(\mathbf{x}_1 t_1, \mathbf{x}_1' t_1')}{\delta U(\mathbf{x}_2, \mathbf{x}_2', t_2)}, \tag{2.95}$$

where $U(\mathbf{x}_2, \mathbf{x}_2', t_2)$ is the nonlocal potential coupled with 1-RDM. Therefore, $L$ actually can represent the interacting 1-RDM response, since one-body Green function is related to the 1-RDM through

$$\langle \Psi_g | \psi^\dagger(\mathbf{r}t)\psi(\mathbf{r}'t)|\Psi_g\rangle = -i\sum_\sigma G_1(\mathbf{r}\sigma t, \mathbf{r}'\sigma t^+). \tag{2.96}$$

$\chi_w$, on the other hand, measures the KS/GKS 1-RDM response with respect to the external nonlocal potential coupled with the KS/GKS 1-RDM, as shown in Eq.

(2.88). TD-GKS of Eq. (2.92) not only resembles BSE of Eq. (2.94) in the appearance, they also contain some identical physical significance, i.e.

$$\chi_w(\mathbf{x}_1 t_1, \mathbf{x}_2 t_2; \mathbf{x}_1 t_1, \mathbf{x}_2 t_2) = L(\mathbf{x}_1 t_1, \mathbf{x}_2 t_2; \mathbf{x}_1 t_1^+, \mathbf{x}_2 t_2^+) = \chi(\mathbf{x}_1, \mathbf{x}_2; t_1 - t_2) \qquad (2.97)$$

at $t_1 > t_2$, where $\chi(\mathbf{x}_1, \mathbf{x}_2; t_1 - t_2)$ is the density-density response function of the system. Note that although $\chi_w(\mathbf{x}_1 t_1, \mathbf{x}_2 t_2; \mathbf{x}_1 t_1, \mathbf{x}_2 t_2)$ and $L(\mathbf{x}_1 t_1, \mathbf{x}_2 t_2; \mathbf{x}_1 t_1^+, \mathbf{x}_2 t_2^+)$ share precisely the same diagonal elements and excitation spectrum, they have distinct off diagonal elements. It is both the similarity and the distinction that make the comparison of these two theories interesting.

## 2.6 The constancy condition and its extensions

In the common application of DFT, the term density-functional theory actually refers to spin-density-functional theory, especially when treating open-shell species. The original Hohenberg-Kohn theorem[20] was spin free; spin was introduced in a later stage[107, 108]. As an intrinsic property of electrons, spin plays a very important part in atoms and molecules. The inclusion of spin improves numerical accuracy of most DFAs, while complicating the theory with the fractional-spin error[35]. It was recently reported that the fractional-spin error can account for singlet-triplet spin gaps[16, 109], making its nature more abstruse. See Ref. [110] for a recent review on spin-DFT.

When spin is involved, the energy functional of $E[N, v]$ is extended to $E[N_\alpha, N_\beta, v]$ such that

$$E[N_\alpha, N_\beta, v] = \min_{\Gamma \to N_\alpha, N_\beta} \mathrm{Tr}(\Gamma \hat{H}). \qquad (2.98)$$

These two functionals are related through

$$E[N, v] = \min_{N_\alpha + N_\beta = N} E[N_\alpha, N_\beta, v]. \qquad (2.99)$$

When the ground state has spin degeneracy, there exist a series of $\Gamma$ fulfilling the minimization of Eq. (2.98). Therefore, we have the constancy condition [35]

$$E[N/2-\kappa, N/2+\kappa, v] = E[N/2+\bar{S}, N/2-\bar{S}, v], \tag{2.100}$$

where $\kappa \in [-\bar{S},\ \bar{S}]$ is the index of spin polarization of the system, and $\bar{S} = (\lfloor N \rceil + 1 - N)S_{\lfloor N \rceil} + (N - \lfloor N \rceil)S_{\lfloor N \rceil + 1}$ is the possible maximal spin polarization for $\kappa$, with $S_M$ the spin quantum number of the system with number of electrons $M$. The state on the right-hand side of Eq. (2.100) is the maximal spin-polarized state, while the state on the left-hand side of Eq. (2.100) is a state between the two opposite maximal spin-polarized states. The ground state is free from spin degeneracy only when $N$ is an even integer and the ground state is singlet, i.e. $\bar{S} = S_N = 0$. The violation of the constancy condition is also common in most DFAs, attributed to the failure of dissociation limit of homonuclear molecules and the incorrect description of Mott insulators. Combination of the linearity condition of Eq. (2.20) and the constancy condition of Eq. (2.100) results in the flat-plan condition, as shown by Mori-Sánchez, Cohen, and Yang[40].

Parallel to Eq. (2.5), given no spatial degeneracy, assuming the derivatives with respect to $N_\alpha$ or $N_\beta$ have a specific direction when $N_\alpha + N_\beta$ is an integer, $E[N_\alpha, N_\beta, v]$ can also be expanded in Taylor series,

$$\begin{aligned}
\delta E[N_\alpha, N_\beta, v] = {} & \mu_\alpha \times \delta N_\alpha + \mu_\beta \times \delta N_\beta + \int d\mathbf{r}\rho(\mathbf{r})\delta v(\mathbf{r}) \\
& + \frac{1}{2}\eta_{\alpha\alpha} \times (\delta N_\alpha)^2 + \eta_{\alpha\beta} \times \delta N_\alpha \delta N_\beta + \frac{1}{2}\eta_{\beta\beta} \times (\delta N_\beta)^2 \\
& + \int d\mathbf{r} f_\alpha(\mathbf{r})\delta v(\mathbf{r}) \times \delta N_\alpha + \int d\mathbf{r} f_\beta(\mathbf{r})\delta v(\mathbf{r}) \times \delta N_\beta \\
& + \frac{1}{2}\int d\mathbf{r} d\mathbf{r}' \chi(\mathbf{r}, \mathbf{r}')\delta v(\mathbf{r})\delta v(\mathbf{r}') + \sum_{p+q+r=3} O((\delta N_\alpha)^p (\delta N_\beta)^q (\delta v)^r),
\end{aligned} \tag{2.101}$$

where the spin chemical potential is

$$\mu_\tau = \frac{\delta E}{\delta N_\tau}, \tag{2.102}$$

the spin chemical hardness is

$$\eta_{\tau\zeta} = \frac{\delta^2 E}{\delta N_\tau \delta N_\zeta}, \tag{2.103}$$

and the spin Fukui function is

$$f_\tau(\mathbf{r}) = \frac{\delta^2 E}{\delta N_\tau \delta v(\mathbf{r})}. \tag{2.104}$$

Taking derivatives of both sides in Eq. (2.100) with respect to the spin polarization index $\kappa$ and the external potential $v(\mathbf{r})$, we have the spin chemical potential condition,

$$\mu_\alpha - \mu_\beta = 0, \tag{2.105}$$

the spin density condition,

$$\rho[N/2+\kappa, N/2-\kappa](\mathbf{r}) = \rho[N/2+\bar{S}, N/2-\bar{S}](\mathbf{r}), \tag{2.106}$$

the spin Fukui function condition,

$$f_\alpha(\mathbf{r}) - f_\beta(\mathbf{r}) = 0, \tag{2.107}$$

the spin hardness condition,

$$\eta_{\alpha\alpha} - 2\eta_{\alpha\beta} + \eta_{\beta\beta} = 0, \tag{2.108}$$

the condition on the linear-response function

$$\chi[N/2+\kappa, N/2-\kappa](\mathbf{r}, \mathbf{r}') = \chi[N/2+\bar{S}, N/2-\bar{S}](\mathbf{r}, \mathbf{r}'), \tag{2.109}$$

$$\frac{\partial \chi(\mathbf{r}, \mathbf{r}')}{\partial N_\alpha} - \frac{\partial \chi(\mathbf{r}, \mathbf{r}')}{\partial N_\beta} = 0, \tag{2.110}$$

and other higher-order derivatives. Eq. (2.105) is recently obtained through the constancy condition by Yang *et al.*[90].

The evaluations of these derivatives are straight forward, with the knowledge of the analytical derivatives in Section 2.4. $f_\tau(\mathbf{r})$ and $\partial\chi(\mathbf{r},\mathbf{r}')/\partial N_\tau$ could be obtained replacing $\phi_{f\sigma}$ with $\phi_{f\tau}$ in Eq. (2.58) and Eq. (2.68). The expression of $\eta_{\tau\zeta}$ is similar to that in Eq. (2.59),

$$\eta_{\tau\zeta} = K_{ff\tau,ff\zeta} - 2\sum_{jb\theta,kc\xi} K_{ff\tau,jb\theta} G_{jb\theta,kc\xi} K_{ff\zeta,kc\xi}. \tag{2.111}$$

Eqs. (2.105)-(2.110) form a new set of exact conditions for functionals derived from the constancy conditions, some of which contain richer information in $\mathbf{r}$ and even $(\mathbf{r},\mathbf{r}')$ space.

## 2.7 Conclusions

In this work, analytical expressions of the energy derivatives $\delta^{p+q}E/\delta N^p \delta v^q$ are explored. These derivatives are obtained from CP-SCF equations for a KS or GKS formalism. All $p+q=2$ derivatives, namely the linear-response function, the Fukui function, and the chemical hardness, for a system with a fractional number of electrons, and all $p+q=3$ derivatives, namely the second-order response function, the Fukui response function, the dual descriptor, and the hyperhardness, for a system with an integer number of electrons, can be evaluated analytically. All analytical derivatives are verified by finite difference numerical derivatives.

Besides the significance of these analytical expressions in conceptual DFT, the analytical derivatives enable a series of derived exact conditions as Eqs. (2.24)-(2.30) based on the linearity condition, and Eqs. (2.105)-(2.110) based on the constancy condition. Many of these conditions contains local information, establishing exact conditions at $\mathbf{r}$, $(\mathbf{r},\mathbf{r}')$, and even $(\mathbf{r},\mathbf{r}',\mathbf{r}'')$ space. These local conditions will be more powerful in future functional development.

The Fukui function and the linear-response function are also extended to systems

with a special external nonlocal potential. This extension enables another exact condition based on the nonlocal Fukui function. Additionally, the nonlocal potential is essential to understand the underlying theory of the linear-response time-dependent density-functional theory with generalized Kohn-Sham functionals.

# 3

# Linear-response time-dependent density-functional theory with pairing fields

## 3.1 Introduction

Particle-particle random phase approximation[57, 111–116] (pp-RPA) has been a widely-known method in nuclear physics and textbook material[55, 117] to describe pairing vibrations in nuclei. Recent introduction of pp-RPA[118] to quantum chemistry demonstrated a very interesting perspective. Pp-RPA is the first density-functional approximation (DFA) to satisfy the flat-plane condition exactly[40, 118], and outperforms traditional direct particle-hole random phase approximation in many aspects[119]. Theoretical analysis reveals that the correlation energy from pp-RPA with Hartree-Fock references is equivalent to ladder-coupled-cluster doubles[15, 120]. Additionally, the $N \pm 2$ excitation energies from pp-RPA can be used to capture valence, double, charge transfer, and Rydberg excitations with a potential $O(L^4)$ scaling[121]. Viewed as an approximation to the pairing-matrix-pairing matrix (pp) response function, in this Chapter we establish the connection of the pp-RPA formalism to the time-dependent density-functional theory (TDDFT) for

superconductors[122, 123] as a special case for non-superconducting system.

Density-functional theory[4, 20, 21] (DFT) has been a robust ground state electronic structure theory by treating the electronic density,

$$\rho(\mathbf{r}) = \sum_{\sigma} \langle \Phi | \hat{\psi}^{\dagger}(\mathbf{x}) \hat{\psi}(\mathbf{x}) | \Phi \rangle, \tag{3.1}$$

instead of the wavefunction, as the basic variable. In Eq. (3.1), $\mathbf{x}$ is the generalized coordinate that includes both spatial coordinate $\mathbf{r}$ and spin coordinate $\sigma$, while $\hat{\psi}^{\dagger}$ and $\hat{\psi}$ are field creation and annihilation operators in the second quantized form. The time dependent extension of DFT, i.e. TDDFT [50–52], further enables us to explore the physics and chemistry of excited states. The adiabatic linear-response formalism of TDDFT[52] has been a routine method to study particle-hole excitations for various systems with moderate complexity and accuracy.[124–129]

In superconducting systems, due to the non-vanishing pairing matrix,

$$\kappa(\mathbf{x}, \mathbf{x}') = \langle \Phi | \hat{\psi}(\mathbf{x}') \hat{\psi}(\mathbf{x}) | \Phi \rangle, \tag{3.2}$$

the density $\rho(\mathbf{r})$ alone does not contain all the properties of the system. Accordingly, the Hohenberg-Kohn theorem[20] for superconductors in equilibrium at finite temperature was established for singlet[130] and triplet[131] pairing interactions, using $\rho(\mathbf{r})$ and $\kappa(\mathbf{x}, \mathbf{x}')$ as basic variables. The corresponding Kohn-Sham model[21] is also proposed by mapping $\rho(\mathbf{r})$ and $\kappa(\mathbf{x}, \mathbf{x}')$ to those of a non-interacting system with non-vanishing pairing fields. As for the time-dependent extension, Wacker, Kümmel, and Gross[132] (WKG) further proved a Runge-Gross-like theorem[50] for superconductors, which states that the time evolution of the density ($\rho(\mathbf{r}, t)$), the diagonal component of the singlet pairing matrix ($\kappa(\mathbf{r}\uparrow, \mathbf{r}\downarrow; t)$), and the current density ($\mathbf{j}(\mathbf{r}, t)$) uniquely determine the scalar potential ($v(\mathbf{r}, t)$), the diagonal component of the singlet pairing field ($D(\mathbf{r}\uparrow, \mathbf{r}\downarrow; t)$), and the vector potential ($\mathbf{A}(\mathbf{r}, t)$),

up to a gauge transformation. Unfortunately, the Runge-Gross-like theorem involving the general pairing matrix of Eq. (3.2) has not been proven, probably due to the difficulty resulting from the non-locality of $\kappa(\mathbf{x}, \mathbf{x}')$. In fact, the TDDFT formalism for superconductors of Ref. [122] and [123] was built on the adiabatic linear response of singlet pairing matrix of a Kohn-Sham-like system, where the WKG theorem is not applicable. A kernel of the local-density approximation (LDA) which accounts only singlet effects was also proposed as a screened Coulomb potential[123, 133], with numerical results presented in Ref. [134].

For normal non-superconducting systems such as atoms and molecules, the pairing matrix $\kappa$ is identically zero in the absence of external pairing fields. However, the fluctuation of the pairing matrix, i.e. the pp response function, is non-vanishing, even for a normal system[118]. Such fluctuation is related to $N \pm 2$ excitation energies, where double ionization and double electron attachment processes are involved. The mean-field description of this pairing matrix fluctuation, i.e. pp-RPA[55, 117], has been used to calculate the Auger spectroscopy[135–138]. Recently, Yang *et al.[121]* developed a scheme to calculate neutral excitations based on pp-RPA, demonstrating promising results. To capture the effect beyond the mean-field approximation, one can resort to *ab initio* wavefunction techniques, which utilize correlated ground state wavefunctions and include higher order excitation operators. Double-ionization-potential/double-electron-attachment equation-of-motion coupled-cluster singles and doubles (DIP/DEA-EOM-CC)[139, 140] are examples of such approaches.

However, because of the steep scaling of the *ab initio* wavefunction method, we are interested in the DFT formalism of the pp response function. In previous works, the kernel in the pp-RPA equation is always the bare Coulomb, where the potential of other approximate functionals with pairing matrix dependence has never been explored. The TDDFT method for superconductors is a closely related theory; however, triplet excitations are totally absent, and the pp response function on normal

systems has not been inferred. In this Chapter, we establish the linear-response time-dependent density-functional theory with pairing fields (TDDFT-P) to tackle the $N \pm 2$ excitation problem of non-superconducting systems, with its connection to and extension of the TDDFT for superconductors. Both the adiabatic and non-adibatic versions of linear-response TDDFT-P are explored. Especially, the adiabatic TDDFT-P justified the practice of utilizing orbitals and eigenvalues of common DFAs in pp-RPA equations[118, 119, 121]. Such an extension enables us to capture effects beyond mean-field approximations in $N \pm 2$ excitations, and would also make it possible to capture neutral excitations better by suitable approaches[121, 141].

This article is organized as follows. Section 3.2 reviews the counterparts of the Hohenberg-Kohn theorem and the Kohn-Sham model in superconducting systems. Section 3.3 establishes the adiabatic linear-response TDDFT-P for systems in the non-superconducting limit. Section 3.4 further extends the theory to include frequency-dependent particle-particle kernels. Section 3.5 concludes this article.

## 3.2 DFT with pairing interactions

In this section the theory of time-independent DFT with pairing interactions is reviewed for completeness. The theory is mainly based on the work of Ref. [130] and [131]. We also extend the definition of the functionals involved.

We consider a general Hamiltonian including a pairing potential (in atomic units),

$$\hat{H} = \hat{T} + \hat{V} + \hat{D} + \hat{W}, \tag{3.3}$$

where $\hat{T}$ is the kinetic energy operator,

$$\hat{T} = -\frac{1}{2}\int d\mathbf{x}\hat{\psi}^{\dagger}(\mathbf{x})\nabla^2\hat{\psi}(\mathbf{x}), \tag{3.4}$$

$\hat{V}$ is the normal external potential,

$$\hat{V} = \int d\mathbf{x} v(\mathbf{r}) \hat{\psi}^\dagger(\mathbf{x}) \hat{\psi}(\mathbf{x}), \tag{3.5}$$

$\hat{D}$ is the external pairing field,

$$\hat{D} = \frac{1}{2} \int d\mathbf{x} d\mathbf{x}' [D^*(\mathbf{x}, \mathbf{x}') \hat{\psi}(\mathbf{x}') \hat{\psi}(\mathbf{x}) + h.c.], \tag{3.6}$$

and $\hat{W}$ is the two electron interaction

$$\hat{W} = \frac{1}{2} \int d\mathbf{x}_1 d\mathbf{x}_1' d\mathbf{x}_2 d\mathbf{x}_2' w(\mathbf{x}_1, \mathbf{x}_2, \mathbf{x}_2', \mathbf{x}_1') \hat{\psi}^\dagger(\mathbf{x}_1) \hat{\psi}^\dagger(\mathbf{x}_2) \hat{\psi}(\mathbf{x}_2') \hat{\psi}(\mathbf{x}_1'). \tag{3.7}$$

In Eq. (3.6), *h.c.* represents the Hermitian conjugate of the previous term. For a superconducting system, $w$ in Eq. (3.7) includes the phonon – or other medium, such as antiferromagnetic correlation in high temperature superconductors – mediated electron-electron interaction[130, 131], while for a non-superconducting system, $w$ is just the Coulomb potential as the only electron-electron interaction in atoms and molecules in quantum chemistry,

$$w_{\mathrm{NS}}(\mathbf{x}_1, \mathbf{x}_2, \mathbf{x}_2', \mathbf{x}_1') = \delta(\mathbf{x}_2, \mathbf{x}_2') \delta(\mathbf{x}_1, \mathbf{x}_1') \frac{1}{|\mathbf{r}_1 - \mathbf{r}_2|}, \tag{3.8}$$

where NS stands for non-superconducting. Refer to Ref. [130] and [131] for different models of $w$'s in a superconducting system. A physical external pairing field $D$ only exists when the system is juxtaposed to a superconducting material. Here it is just used as a mathematical tool to establish the theory, and we will take the external pairing field at zero limit in the end[130, 131, 142]. Since $[\hat{D}, \hat{N}] \neq 0$, where $\hat{N}$ is the number operator, the system is not electron number conserving. We will introduce the chemical potential $\mu$ to control the electron number, such that the expectation value of $\hat{H}' = \hat{H} - \mu \hat{N}$, i.e. the grand potential $\Omega$ , rather than the total energy, is

minimized. A generalized ensemble density matrix $\hat{\Gamma}$ could be defined as

$$\hat{\Gamma} = \sum_I \gamma_I |\Phi_I\rangle\langle\Phi_I|, \tag{3.9}$$

where $\gamma_I$'s are non-negative weights that sum to unity, and $|\Phi_I\rangle$'s are vectors in the Fock space which are linear combinations of vectors in Hilbert spaces associated with different particle numbers. Note that although DFT of superconductors normally treats systems at finite temperature[130, 131], we focus on the zero-temperature formalism as we are interested in its connection to quantum chemistry. Thus $\hat{\Gamma}$ in Eq. (3.9) is a zero-temperature ensemble rather than a finite-temperature ensemble. Then the density and the pairing matrix of an ensemble $\hat{\Gamma}$ can be expressed as $\rho(\mathbf{r}) = \mathrm{Tr}[\hat{\Gamma}\hat{\rho}(\mathbf{r})]$ and

$$\kappa(\mathbf{x}, \mathbf{x}') = \mathrm{Tr}[\hat{\Gamma}\hat{\psi}(\mathbf{x}')\hat{\psi}(\mathbf{x})]. \tag{3.10}$$

The zero-temperature ground state grand potential is then the following minimum:

$$\Omega_0[v(\mathbf{r}) - \mu, D(\mathbf{x}, \mathbf{x}')] = \min_{\hat{\Gamma}} \mathrm{Tr}(\hat{\Gamma}\hat{H}'). \tag{3.11}$$

Apart from the normal density $\rho(\mathbf{r})$, the pairing matrix $\kappa(\mathbf{x}, \mathbf{x}')$ is also important in the presence of an internal pairing interaction from $\hat{W}$ or an external pairing interaction from $\hat{D}$. The pairing matrix has also been called the pairing tensor[117], the anomalous density[122, 123], or the non-local gap function[130] in different context. Due to the anticommutation relations of Fermionic field operators, the pairing matrix is always antisymmetric,

$$\kappa(\mathbf{x}, \mathbf{x}') = -\kappa(\mathbf{x}', \mathbf{x}). \tag{3.12}$$

As a consequence, only the antisymmetric part of the pairing field $D(\mathbf{x}, \mathbf{x}')$ will have nonzero contribution to the total energy. We therefore require that the pairing field should also be antisymmetric,

$$D(\mathbf{x}, \mathbf{x}') = -D(\mathbf{x}', \mathbf{x}). \tag{3.13}$$

Capelle *et al.*[131] presented the Hohenberg-Kohn theorem of this system, stating that there exists a one-to-one mapping between the ground state densities ($\rho(\mathbf{r})$ and $\kappa(\mathbf{x},\mathbf{x}')$) and the ensemble operator for the system. So there is a density functional $\Omega_{\rm HK}[\rho(\mathbf{r}),\kappa(\mathbf{x},\mathbf{x}')]$ that maps the ensemble representable density and pairing matrix to its ground state grand potential. The density and pairing matrix are said to be $v\&D$ ensemble representable if they can come from an ensemble of *ground state* wavefunction(s) of some external potential $v$ and external pairing potential $D$.

We now further generalize this functional to Fock space $\bar{N}$ representable density and pairing matrices using the Levy constrained search definition[22],

$$\Omega[\rho(\mathbf{r}),\kappa(\mathbf{x},\mathbf{x}')]$$

$$= \inf_{\hat{\Gamma}\to(\rho,\kappa)} {\rm Tr}(\hat{\Gamma}\hat{H}') \tag{3.14}$$

$$= \inf_{\hat{\Gamma}\to(\rho,\kappa)} \left\{ {\rm Tr}[\hat{\Gamma}(\hat{T}+\hat{W})] + \int d\mathbf{r}(v(\mathbf{r})-\mu)\rho(\mathbf{r}) - \frac{1}{2}\int d\mathbf{x}d\mathbf{x}'[D^*(\mathbf{x},\mathbf{x}')\kappa(\mathbf{x}',\mathbf{x}) + h.c.] \right\} \tag{3.15}$$

$$= F_{\rm Levy}[\rho,\kappa] + \int d\mathbf{r}(v(\mathbf{r})-\mu)\rho(\mathbf{r}) - \frac{1}{2}\int d\mathbf{x}d\mathbf{x}'[D^*(\mathbf{x},\mathbf{x}')\kappa(\mathbf{x}',\mathbf{x}) + h.c.]. \tag{3.16}$$

Note that Fock space $\bar{N}$ representability is different from the fractional-$\bar{N}$ representability in Ref. [143]. The Fock space $\bar{N}$ representable density and pairing matrix in Eqs. (3.14)-(3.16) are only required to come from a Fermionic ensemble density matrix (not necessarily of a ground state), a much less constrained condition than the $v\&D$ ensemble representability. The Fock space $\bar{N}$ representability and the $v\&D$ representability are the superconducting counterpart of $N$ representability and $v$ representability in conventional DFT[4]. The universal functional $F_{\rm Levy}[\rho(\mathbf{r}),\kappa(\mathbf{x},\mathbf{x}')]$ thus contains the kinetic and two-body interaction energy. Alternatively, we can use the Lieb-type definition for this universal functional[144]:

$$F_{\rm Lieb}[\rho(\mathbf{r}),\kappa(\mathbf{x},\mathbf{x}')] = \sup_{v,D}\{\Omega_0[v(\mathbf{r})-\mu, D(\mathbf{x},\mathbf{x}')] - \int d\mathbf{r}(v(\mathbf{r})-\mu)\rho(\mathbf{r}) + \frac{1}{2}\int d\mathbf{x}d\mathbf{x}'[D^*(\mathbf{x},\mathbf{x}')\kappa(\mathbf{x}',\mathbf{x}) + h.c.]\}, \quad (3.17)$$

with $\Omega_0$ defined in Eq. (3.11).

Now we assume the non-interacting $v\&D$ ensemble representability of Fock space $\bar{N}$ representable densities and pairing matrices, in which the density and the pairing matrix of an interacting ground state system ($w \neq 0$) can be represented by a density and a pairing matrix of a non-interacting system ($w = 0$). In other words, for $\rho(\mathbf{r})$ and $\kappa(\mathbf{x},\mathbf{x}')$ of an interacting ground state, there is always $\rho_s(\mathbf{r})$ and $\kappa_s(\mathbf{x},\mathbf{x}')$ from a non-interacting system with normal potential $v_s(\mathbf{r})$ and and pairing potential $D_s(\mathbf{x},\mathbf{x}')$ such that

$$\rho(\mathbf{r}) = \rho_s(\mathbf{r}), \quad (3.18)$$

and

$$\kappa(\mathbf{x},\mathbf{x}') = \kappa_s(\mathbf{x},\mathbf{x}'). \quad (3.19)$$

Then we can have the grand potential decomposition,[123, 130, 131, 133, 142]

$$\Omega[\rho,\kappa] = V[\rho] - \mu N + G[\kappa] + F_{\rm Levy}[\rho,\kappa] \quad (3.20)$$

$$= T_s[\rho,\kappa] + V[\rho] + G[\kappa] + J[\rho] + R[\kappa] + E_{\rm XC}[\rho,\kappa] - \mu N, \quad (3.21)$$

where $T_s[\rho,\kappa]$ is the kinetic energy of the hypothetical non-interacting system with the same density and the pairing matrix, $V[\rho] = {\rm Tr}(\hat{\Gamma}\hat{V})$, $G[\kappa] = {\rm Tr}(\hat{\Gamma}\hat{D})$, $J[\rho]$ is the mean-field energy of the particle-hole channel (usually called the Hartree term in DFT),

$$J[\rho] = \frac{1}{2}\int \frac{\rho(\mathbf{r})\rho(\mathbf{r}')}{|\mathbf{r}-\mathbf{r}'|} d\mathbf{r}d\mathbf{r}', \quad (3.22)$$

and $R[\kappa]$ is the mean-field energy of the particle-particle channel

$$R[\kappa] = \frac{1}{2}\int \frac{\kappa(\mathbf{x},\mathbf{x}')\kappa^*(\mathbf{x},\mathbf{x}')}{|\mathbf{r}-\mathbf{r}'|}d\mathbf{x}d\mathbf{x}'. \tag{3.23}$$

$E_{\mathrm{XC}}[\rho,\kappa]$ includes all the quantum effects that are absent in the other energy terms,

$$\begin{aligned} E_{\mathrm{XC}}[\rho,\kappa] &= F_{\mathrm{Levy}}[\rho,\kappa] - T_s[\rho,\kappa] - J[\rho] - R[\kappa] \\ &= T[\rho,\kappa] + W[\rho,\kappa] - T_s[\rho,\kappa] - J[\rho] - R[\kappa]. \end{aligned} \tag{3.24}$$

The corresponding Kohn-Sham-like non-interacting system is governed by the non-interacting Hamiltonian

$$\hat{H}_s = \int d\mathbf{x}\hat{\psi}^\dagger(\mathbf{x})[-\frac{1}{2}\nabla^2+v_s(\mathbf{r})]\hat{\psi}(\mathbf{x})+\frac{1}{2}\int d\mathbf{x}d\mathbf{x}'[D_s(\mathbf{x},\mathbf{x}')\hat{\psi}^\dagger(\mathbf{x})\hat{\psi}^\dagger(\mathbf{x}')+h.c.], \tag{3.25}$$

with the non-interacting normal potential

$$v_s(\mathbf{r}) = v(\mathbf{r}) + \int \frac{\rho(\mathbf{r}')}{|\mathbf{r}-\mathbf{r}'|}d\mathbf{r}' + \left(\frac{\delta E_{\mathrm{XC}}[\rho,\kappa]}{\delta\rho(\mathbf{r})}\right)_\kappa, \tag{3.26}$$

and the non-interacting pairing potential

$$D_s(\mathbf{x},\mathbf{x}') = D(\mathbf{x},\mathbf{x}') + D_R(\mathbf{x},\mathbf{x}') + D_{\mathrm{XC}}(\mathbf{x},\mathbf{x}'), \tag{3.27}$$

where

$$D_R(\mathbf{x},\mathbf{x}') = \frac{\kappa(\mathbf{x},\mathbf{x}')}{|\mathbf{r}-\mathbf{r}'|}, \tag{3.28}$$

and

$$D_{\mathrm{XC}}(\mathbf{x},\mathbf{x}') = \left(\frac{\delta E_{\mathrm{XC}}[\rho,\kappa]}{\delta\kappa^*(\mathbf{x},\mathbf{x}')}\right)_\rho. \tag{3.29}$$

The resulting self-consistent equation for this non-interacting system is the well-known Kohn-Sham Bogoliubov-de Gennes (KS-BdG) equation[123, 134, 145], or the Hartree-Fock-Bogoliubov equation for the Hartree-Fock approximate functional[117,

146]. The KS-BdG equation and its solution are not necessary to establish the linear response theory in Section 3.3 and 3.4, and are thus not addressed here. Refer to standard textbooks such as Ref. [55] and [117] for details of the equation and its solution.

## 3.3 Adiabatic linear-response TDDFT-P for non-superconducting systems

We now establish the theory for adiabatic linear-response TDDFT with pairing fields (TDDFT-P) for non-superconducting systems. This generalizes the previous TDDFT for superconductors with singlet-only excitations[122, 123] to include triplet excitations. The adiabatic linear-response TDDFT-P provides a theoretical foundation for using adiabatic DFAs in the pp-RPA equation. Especially, it justifies the application of orbitals and eigenvalues from common DFAs in the pp-RPA equation.

Suppose we perturb the interacting non-superconducting system with a small paring field

$$\delta D(\mathbf{x},\mathbf{x}';t)=\sum_{pq}\delta D_{pq}(t)\varphi_p(\mathbf{x})\varphi_q(\mathbf{x}'). \tag{3.30}$$

In this Chapter we will use the same index convention as in Page 9. For simplicity, we only discuss non-degenerate ground states which can be represented as vectors in the Hilbert space for non-superconducting systems. According to the linear response theory[55, 118], the linear response of the pairing matrix is related to the pairing field by a pp response function,

$$K(\mathbf{x},\mathbf{x}';\mathbf{y},\mathbf{y}';t)=-i\theta(t)\langle\Phi^{\mathrm{gs}}|[\hat{\psi}_H(\mathbf{x}'t)\hat{\psi}_H(\mathbf{x}t),\hat{\psi}^\dagger(\mathbf{y})\hat{\psi}^\dagger(\mathbf{y}')]|\Phi^{\mathrm{gs}}\rangle, \tag{3.31}$$

such that

$$\delta\kappa(\mathbf{x},\mathbf{x}';t)=\int d\tau d\mathbf{y}d\mathbf{y}'K(\mathbf{x},\mathbf{x}';\mathbf{y},\mathbf{y}';t-\tau)\delta D(\mathbf{y},\mathbf{y}';\tau), \tag{3.32}$$

with $\hat{\psi}_H(\mathbf{x}t) = e^{i\hat{H}'t}\hat{\psi}(\mathbf{x})e^{-i\hat{H}'t}$ the interacting field operator in the Heisenberg picture and $\theta(t)$ the Heaviside step function. Expressed in a one-particle basis and transferred to the frequency domain, Eq. (3.32) becomes

$$\delta\kappa_{pq}(\omega) = \sum_{rs} K_{pq,rs}(\omega)\delta D_{rs}(\omega),$$

with

$$K_{pq,rs}(\omega) = \int dt e^{i\omega t} d\mathbf{x} d\mathbf{x}' d\mathbf{y} d\mathbf{y}' K(\mathbf{x},\mathbf{x}';\mathbf{y},\mathbf{y}';t)\varphi_p^*(\mathbf{x})\varphi_q^*(\mathbf{x}')\varphi_r(\mathbf{y})\varphi_s(\mathbf{y}'). \tag{3.33}$$

The pp response function is related to the correlation energy and $N \pm 2$ excitation energies.[118, 121] Specifically, if we perturb the corresponding KS-BdG system with a small pairing field $\delta D_s(\mathbf{x},\mathbf{x}';t) = \sum_{pq}\delta D_{pq}^s(t)\varphi_p(\mathbf{x})\varphi_q(\mathbf{x}')$, the pp response function is

$$K_0(\mathbf{x},\mathbf{x}';\mathbf{y},\mathbf{y}';t) = -i\theta(t)\langle\Phi_s^{\mathrm{gs}}|[\hat{\psi}_{H_s}(\mathbf{x}'t)\hat{\psi}_{H_s}(\mathbf{x}t),\hat{\psi}^\dagger(\mathbf{y})\hat{\psi}^\dagger(\mathbf{y}')]|\Phi_s^{\mathrm{gs}}\rangle, \tag{3.34}$$

with $\hat{\psi}_{H_s}(\mathbf{x}t) = e^{i\hat{H}_s't}\hat{\psi}(\mathbf{x})e^{-i\hat{H}_s't}$ the non-interacting field operator in the interacting picture. The corresponding first order pairing matrix variation is,

$$\delta\kappa_s(\mathbf{x},\mathbf{x}';t) = \int d\tau d\mathbf{y} d\mathbf{y}' K_0(\mathbf{x},\mathbf{x}';\mathbf{y},\mathbf{y}';t-\tau)\delta D_s(\mathbf{y},\mathbf{y}';\tau). \tag{3.35}$$

For a non-interacting non-superconducting system, $K_{pq,rs}^0(\omega)$ is trivial[55, 118],

$$K_{pq,rs}^0(\omega) = (\delta_{pr}\delta_{qs} - \delta_{qr}\delta_{ps})\frac{\theta(p-F)\theta(q-F) - \theta(F-p)\theta(F-q)}{\omega - (\epsilon_p + \epsilon_q - 2\mu) + i\eta}, \tag{3.36}$$

where $F$ represents the Fermi level such that $p - F > 0$ if $p$ is an unoccupied orbital and $p - F < 0$ if $p$ is an occupied orbital. Accordingly, we can express the linear response of the pairing matrix as,

$$\delta\kappa_{ij}^s(\omega) = -\frac{\delta D_{ij}^s(\omega)}{\omega - (\epsilon_i + \epsilon_j - 2\mu) + i\eta}, \tag{3.37}$$

$$\delta\kappa^s_{ab}(\omega) = \frac{\delta D^s_{ab}(\omega)}{\omega - (\epsilon_a + \epsilon_b - 2\mu) + i\eta}, \tag{3.38}$$

and $\delta\kappa^s_{ia}(\omega) = \delta\kappa^s_{ai}(\omega) = 0$. $\eta$ is an infinitesimal positive number to ensure the convergence of the Fourier transformation. For the derivations below, we will drop $\eta$ as it does not affect the resulting equation.

To establish the adiabatic linear-response TDDFT-P, we assume that a) the first order interacting pairing matrix variation $\delta\kappa(\mathbf{x}, \mathbf{x}'; \omega)$ can be represented by the first order non-interacting pairing matrix variation $\delta\kappa_s(\mathbf{x}, \mathbf{x}'; \omega)$, and that b) the response of $\delta D_s(\mathbf{x}, \mathbf{x}'; \omega)$ to $\delta\kappa(\mathbf{y}, \mathbf{y}'; \omega)$ is adiabatic. The representability assumption enables us to study a many-body interacting system in terms of its non-interacting KS-BdG system. From now on we will drop the subscript or superscript of $\kappa$ as $\delta\kappa_s = \delta\kappa$. Approximation a) is made in analogy to the assumption in conventional TDDFT where the first order density change in the KS system also represents the first order density change in the interacting system, viz $\delta\rho_s = \delta\rho$.The conditions under which this assumption is valid are perhaps more restrictive than in DFT, and we consider this an *ad hoc* assumption that enables us to formulate a linear-response TDDFT-P. Under an external pairing field perturbation of Eq. (3.30), using Eqs. (3.37)-(3.38), we have

$$\begin{aligned} -[\omega - (\epsilon_i + \epsilon_j - 2\mu)]\delta\kappa_{ij}(\omega) &= \delta D^s_{ij}(\omega) \\ &= \delta D_{ij}(\omega) + \delta D^R_{ij}(\omega) + \delta D^{\mathrm{XC}}_{ij}(\omega) \\ &= \delta D_{ij}(\omega) + \sum_{k>l} L_{ij,kl}\delta\kappa_{kl}(\omega) + \sum_{c>d} L_{ij,cd}\delta\kappa_{cd}(\omega), \end{aligned} \tag{3.39}$$

and

$$[\omega - (\epsilon_a + \epsilon_b - 2\mu)]\delta\kappa_{ab}(\omega) = \delta D_{ab}(\omega) + \sum_{k>l} L_{ab,kl}\delta\kappa_{kl}(\omega) + \sum_{c>d} L_{ab,cd}\delta\kappa_{cd}(\omega), \tag{3.40}$$

where the adiabatic pp response kernel is

$$L_{pq,rs} = \langle pq||rs\rangle + 2\int d\mathbf{x}_1 d\mathbf{x}_2 d\mathbf{x}_1' d\mathbf{x}_2' \varphi_p^*(\mathbf{x}_1)\varphi_q^*(\mathbf{x}_1') \times \left(\frac{\delta^2 E_{\mathrm{XC}}[\rho,\kappa]}{\delta\kappa^*(\mathbf{x}_1,\mathbf{x}_1')\delta\kappa(\mathbf{x}_2,\mathbf{x}_2')}\right)_\rho \varphi_r(\mathbf{x}_2)\varphi_s(\mathbf{x}_2'), \tag{3.41}$$

with $\langle pq||rs\rangle$ defined in Eq. (1.7). The adiabatic pp response kernel has the same symmetry as the antisymmetrized two-electron integral

$$L_{pq,rs} = -L_{pq,sr} = -L_{qp,rs} = L_{qp,sr} = L_{rs,pq}^*. \tag{3.42}$$

Then we rearrange Eqs. (3.39) and (3.40) using a compact matrix notation,

$$\begin{bmatrix} \mathbf{A} & \mathbf{B} \\ \mathbf{B}^\dagger & \mathbf{C} \end{bmatrix}\begin{bmatrix} \mathbf{X} \\ \mathbf{Y} \end{bmatrix} - \omega\begin{bmatrix} \mathbf{I} & \mathbf{0} \\ \mathbf{0} & -\mathbf{I} \end{bmatrix}\begin{bmatrix} \mathbf{X} \\ \mathbf{Y} \end{bmatrix} = -\begin{bmatrix} \delta\mathbf{D}^{pp} \\ \delta\mathbf{D}^{hh} \end{bmatrix}, \tag{3.43}$$

where

$$A_{ab,cd} = (\epsilon_a + \epsilon_b - 2\mu)\delta_{ac}\delta_{bd} + L_{ab,cd}, \tag{3.44}$$

$$B_{ab,ij} = L_{ab,ij}, \tag{3.45}$$

$$C_{ij,kl} = -(\epsilon_i + \epsilon_j - 2\mu)\delta_{ik}\delta_{jl} + L_{ij,kl}, \tag{3.46}$$

$$X_{ab} = \delta\kappa_{ab}(\omega), \tag{3.47}$$

$$Y_{ij} = \delta\kappa_{ij}(\omega), \tag{3.48}$$

$$[\delta\mathbf{D}^{pp}]_{ab} = \delta D_{ab}(\omega), \tag{3.49}$$

and

$$\left[\delta\mathbf{D}^{hh}\right]_{ij} = \delta D_{ij}(\omega). \tag{3.50}$$

Note that all matrix indexes require $a > b$ or $i > j$ to eliminate the redundancy and that the two identity matrices $\mathbf{I}$'s have different dimensions. With Eq. (3.43), the

pp response function in real-space representation can be expressed as

$$K(\mathbf{x}_1,\mathbf{x}_1';\mathbf{x}_2,\mathbf{x}_2';\omega) = -\sum_{a>b,c>d}[\mathbf{M}(\omega)^{-1}]_{ab,cd}\Psi_{ab,cd}(\mathbf{x}_1,\mathbf{x}_1',\mathbf{x}_2,\mathbf{x}_2') - \sum_{i>j,k>l}[\mathbf{M}(\omega)^{-1}]_{ij,kl}\Psi_{ij,kl}(\mathbf{x}_1,\mathbf{x}_1',\mathbf{x}_2,\mathbf{x}_2'), \tag{3.51}$$

where

$$\mathbf{M}(\omega) = \begin{bmatrix} \mathbf{A} & \mathbf{B} \\ \mathbf{B}^\dagger & \mathbf{C} \end{bmatrix} - \omega \begin{bmatrix} \mathbf{I} & \mathbf{0} \\ \mathbf{0} & -\mathbf{I} \end{bmatrix}, \tag{3.52}$$

and

$$\Psi_{pq,rs}(\mathbf{x}_1,\mathbf{x}_1',\mathbf{x}_2,\mathbf{x}_2') = \varphi_p(\mathbf{x}_1)\varphi_q(\mathbf{x}_1')\varphi_r^*(\mathbf{x}_2)\varphi_s^*(\mathbf{x}_2') - \varphi_p(\mathbf{x}_1)\varphi_q(\mathbf{x}_1')\varphi_s^*(\mathbf{x}_2)\varphi_r^*(\mathbf{x}_2') - \varphi_q(\mathbf{x}_1)\varphi_p(\mathbf{x}_1')\varphi_r^*(\mathbf{x}_2)\varphi_s^*(\mathbf{x}_2') + \varphi_q(\mathbf{x}_1)\varphi_p(\mathbf{x}_1')\varphi_s^*(\mathbf{x}_2)\varphi_r^*(\mathbf{x}_2'). \tag{3.53}$$

Eq. (3.43) describes the response of the pairing matrix with respect to the pairing field perturbation, similar to a driven harmonic oscillator. Alternatively, we can study the eigenmode of the system by eliminating the driving force $\delta D$. The resulting eigenvalue equation is

$$\begin{bmatrix} \mathbf{A} & \mathbf{B} \\ \mathbf{B}^\dagger & \mathbf{C} \end{bmatrix} \begin{bmatrix} \mathbf{X} \\ \mathbf{Y} \end{bmatrix} = \omega \begin{bmatrix} \mathbf{I} & \mathbf{0} \\ \mathbf{0} & -\mathbf{I} \end{bmatrix} \begin{bmatrix} \mathbf{X} \\ \mathbf{Y} \end{bmatrix}, \tag{3.54}$$

with the eigenvalues $N+2$ excitation energies

$$\omega_n^{N+2} = \Omega_n^{N+2} - \Omega_0^N = E_n^{N+2} - E_0^N - 2\mu, \tag{3.55}$$

and $N-2$ excitation energies

$$\omega_n^{N-2} = \Omega_0^N - \Omega_n^{N-2} = E_0^N - E_n^{N-2} - 2\mu. \tag{3.56}$$

These eigenvalues are also the poles of the pp response function in Eq. (3.51). Eq. (3.54) can be solved for every interacting strength so the correlation energy can also

be covered in the adiabatic-connection fluctuation-dissipation approach, similar to the correlation energy beyond ph-RPA.[147–149]

The accuracy of Eq. (3.54) relies on how physical the approximation of Eq. (3.41) is. For a non-superconducting system, both $\kappa$ and $\delta E_{\mathrm{XC}}[\rho,\kappa]/\delta\kappa^*$ are zero, thus the only explicit contribution of $E_{\mathrm{XC}}$ to $L$ is

$$\lim_{\kappa\to 0}\frac{\delta^2 E_{\mathrm{XC}}[\rho,\kappa]}{\delta\kappa^*\delta\kappa}. \tag{3.57}$$

The dependency of $E_{\mathrm{XC}}$ with respect to $\kappa$ is non-trivial and not well understood as the exchange-correlation functional in traditional DFT. The simplest approximation to $E_{\mathrm{XC}}[\rho,\kappa]$ is to neglect the pairing matrix dependence,

$$E_{\mathrm{XC}}^{\mathrm{DFA}}[\rho,\kappa] \equiv E_{\mathrm{XC}}^{\mathrm{DFA}}[\rho,\kappa=0] = E_{\mathrm{XC}}^{\mathrm{DFA}}[\rho], \tag{3.58}$$

where $E_{\mathrm{XC}}^{\mathrm{DFA}}[\rho]$ is the common exchange-correlation energy functionals in DFT. When the approximation of Eq. (3.58) is adopted, $E_{\mathrm{XC}}$ has zero contribution to $L$ and the resulting pp kernel is

$$L_{pq,rs}^{\mathrm{DFA}} = \langle pq||rs\rangle, \tag{3.59}$$

identical to the kernel in pp-RPA[55, 117]. The use of Eq. (3.59) has been a natural consequence of the mean-field approximation in pp-RPA when a Hartree-Fock reference is deployed. Now in view of TDDFT-P, Eq. (3.59) can be interpreted as a kernel under the approximation of Eq. (3.58) for any pairing matrix free DFAs. More importantly, the TDDFT-P perspective rationalizes the practice of using orbitals and eigenvalues from common DFAs (such as B3LYP or PBE) in the pp-RPA equation[118, 119, 121]. If the pp-RPA equation is derived through the equation-of-motion ansatz, since the KS orbitals are not eigenvectors of the Fock matrix, thus the resulting matrix elements will contains the non-diagonal Fock matrix elements in Eqs. (3.44) and (3.46). It is clear now that the pp-RPA equation can utilize DFT

reference according to the approximation of Eq. (3.58), which is a main result of this Chapter.

In the aforementioned approximation, $E_{\rm XC}$ has zero contribution to $L$. Ref. [133] and [123] presented an LDA functional for the pp interaction with non-zero $E_{\rm XC}$ contribution to $L$, which in principle could be used to calculate $N \pm 2$ excitation energies. However, their LDA is just a Coulomb with screening counting only singlet interactions, which is not the true LDA. The true LDA should include the energies of homogeneous electron gas at different pairing fields, like that in the local-spin-density approximation. Unfortunately, to the best of our knowledge, no quantum Monte Carlo calculations for the homogeneous electron gas were performed under pairing fields. Thus, a true LDA functional accounts for both singlet and triplet interactions is still in need.

In summary, adiabatic linear-response TDDFT-P justifies the use of common pairing matrix independent DFAs in the pp-RPA equation by the approximation of Eq. (3.58). This approximation leads to the working equation of pp-RPA using common DFAs as practiced in Ref. [118, 119, 121]. Additionally, TDDFT-P allows other pairing matrix dependent functionals $E_{\rm XC}[\rho, \kappa]$ to be used to calculate $N \pm 2$ excitations in the pp-RPA equation.

## 3.4 Linear-response TDDFT-P with frequency-dependent pp kernels

Section 3.3 establishes the theory of adiabatic linear-response TDDFT-P. We demonstrate in this section that the extension beyond the adiabatic approximation can also be formulated by just adopting the same representability approximation as that in Section 3.3.

WKG[132] proved that there is a one-to-one mapping between the time evolution of $(\rho(\mathbf{r};t), \kappa(\mathbf{r}\uparrow, \mathbf{r}\downarrow;t), \mathbf{j}(\mathbf{r};t))$ and the field $(v(\mathbf{r};t), D(\mathbf{r}\uparrow, \mathbf{r}\downarrow;t), \mathbf{A}(\mathbf{r};t))$, except for a gauge transformation. However, the one-to-one mapping involving the general

pairing matrix $\kappa(\mathbf{x},\mathbf{x}';t)$ and the general pairing field $D(\mathbf{x},\mathbf{x}';t)$ has not been proved, and the existence of this one-to-one mapping is still unknown. In fact, the linear-response TDDFT for superconductors[122, 123] was built on an approximation of the kernel rather than on the WKG one-to-one mapping.

Due to the absence of the proof of the one-to-one mapping between densities $(\rho(\mathbf{r},t),\kappa(\mathbf{r},\mathbf{r}';t))$ and potentials $(v(\mathbf{r}t),D(\mathbf{x},\mathbf{x}';t))$, it is not straightforward to present the Dyson-like equation of TDDFT-P. If one follows the usual TDDFT derivation, the density-density response function can be expressed as[128]

$$\chi(\mathbf{r}_1t_1;\mathbf{r}_2t_2)=\frac{\delta\rho(\mathbf{r}_1t_1)}{\delta v(\mathbf{r}_2t_2)} \tag{3.60}$$

$$=\int d\mathbf{r}_3dt_3\frac{\delta\rho_s(\mathbf{r}_1t_1)}{\delta v_s(\mathbf{r}_3t_3)}\frac{\delta v_s(\mathbf{r}_3t_3)}{\delta v(\mathbf{r}_2t_2)} \tag{3.61}$$

$$=\int d\mathbf{r}_3dt_3\frac{\delta\rho_s(\mathbf{r}_1t_1)}{\delta v_s(\mathbf{r}_3t_3)}\left(\frac{\delta v(\mathbf{r}_3t_3)}{\delta v(\mathbf{r}_2t_2)}+\frac{\delta(v_s(\mathbf{r}_3t_3)-v(\mathbf{r}_3t_3))}{\delta v(\mathbf{r}_2t_2)}\right) \tag{3.62}$$

$$\begin{aligned}=&\int d\mathbf{r}_3dt_3\frac{\delta\rho_s(\mathbf{r}_1t_1)}{\delta v_s(\mathbf{r}_3t_3)}\\&\times\left(\delta(\mathbf{r}_3t_3,\mathbf{r}_2t_2)+\int d\mathbf{r}_4dt_4\frac{\delta(v_s(\mathbf{r}_3t_3)-v(\mathbf{r}_3t_3))}{\delta\rho(\mathbf{r}_4t_4)}\frac{\delta\rho(\mathbf{r}_4t_4)}{\delta v(\mathbf{r}_2t_2)}\right)\end{aligned} \tag{3.63}$$

$$=\chi_s(\mathbf{r}_1t_1;\mathbf{r}_2t_2)+\int d\mathbf{r}_3dt_3d\mathbf{r}_4dt_4\chi_s(\mathbf{r}_1t_1;\mathbf{r}_3t_3)f_{\mathrm{MB}}(\mathbf{r}_3t_3;\mathbf{r}_4t_4)\chi(\mathbf{r}_4t_4;\mathbf{r}_2t_2), \tag{3.64}$$

where the non-adiabatic kernel representing the many-body (MB) memory effect is

$$f_{\mathrm{MB}}(\mathbf{r}_3t_3;\mathbf{r}_4t_4)=\frac{\delta(v_s(\mathbf{r}_3t_3)-v(\mathbf{r}_3t_3))}{\delta\rho(\mathbf{r}_4t_4)}. \tag{3.65}$$

The existence of the derivatives of $v_s(\mathbf{r}_3t_3)$ and $v(\mathbf{r}_3t_3)$ with respect to $\rho(\mathbf{r}_4t_4)$ is guaranteed by the Runge-Gross theorem[50]: there is a one-to-one mapping between $v(\mathbf{r}_3t_3)$ $(v_s(\mathbf{r}_3t_3))$ and $\rho(\mathbf{r}_4t_4)$ up to an additive merely time-dependent function in the potential. However, in deriving the pp response function $\delta\kappa_s(\mathbf{x}_1,\mathbf{x}_1';t_1)/\delta D(\mathbf{x}_2,\mathbf{x}_2';t_2)$

following Eqs. (3.60)-(3.64), the difficulty lies in the use of the chain rule in Eq. (3.63): due to the lack of the proof of the particle-particle counterpart of the Runge-Gross theorem, it is unknown whether the map $D \rightarrow \kappa$ ($D_s \rightarrow \kappa$) is invertible and thus the corresponding derivative $\delta(D_s - D)/\delta\kappa$ may not be rigorously defined. Therefore, a frequency dependent pp kernel for TDDFT-PF is not as straightforward as that in TDDFT.

We bypass the difficulty of the lack of the proof of the one-to-one mapping by adopting Assumption a) in Section 3.3 and introducing a special probe of $\delta\tilde{D}$ that is bijectively mapped to $\delta\tilde{\kappa}$. The pp response function so defined is thus invertible and contains the same spectrum of the original pp response function. The final Dyson-like equation is then

$$\tilde{\mathbf{K}}(\omega) = \tilde{\mathbf{K}}_s(\omega) + \tilde{\mathbf{K}}_s(\omega)\tilde{\mathbf{L}}(\omega)\tilde{\mathbf{K}}(\omega), \tag{3.66}$$

where we have expressed the equation in frequency domain and used matrix multiplication to denote integration, and the frequency dependent pp kernel is

$$\tilde{\mathbf{L}}(\omega) = \frac{\delta(\tilde{\mathbf{D}}_s(\omega) - \tilde{\mathbf{D}}(\omega))}{\delta\tilde{\boldsymbol{\kappa}}(\omega)}, \tag{3.67}$$

and the projected interacting and non-interacting linear-response pp response functions are defined

$$\tilde{\mathbf{K}}(\omega) = \frac{\delta\tilde{\boldsymbol{\kappa}}(\omega)}{\delta\tilde{\mathbf{D}}(\omega)},$$

and

$$\tilde{\mathbf{K}}_s(\omega) = \frac{\delta\tilde{\boldsymbol{\kappa}}(\omega)}{\delta\tilde{\mathbf{D}}_s(\omega)}.$$

Refer to Appendix **??** for mathematical details.

Similar to non-adiabatic linear-response TDDFT where double and higher-rank excitations could be included, with a frequency dependent pp kernel of $\tilde{\mathbf{L}}(\omega)$, the dynamic effects of particle-particle (hole-hole) excitations could be accounted, while

in DIP/DAE-EOM-CC methods such effects must come from higher-rank excitations such as 3-particle-1-hole and 4-particle-2-hole excitation operators[141, 150]. The Dyson-like equation of Eq. (3.64) justifies the use of frequency dependent pp kernel in the pp-RPA equation of Eq. (3.43). Additionally, if we cast the adiabatic approximation in $\tilde{\mathbf{L}}(\omega)$, i.e. using Eq. (3.41), we recover exactly the same results as in Section 3.3.

## 3.5 Conclusions

We establish the linear response time-dependent density-functional theory with pairing fields (TDDFT-P) for non-superconducting systems, for pairing fields of general spins including both singlet and triplet interactions. Although the pairing density is identically zero for a non-superconducting system, its linear response is non-zero and contains important information of $N \pm 2$ excitation energies as well as the correlation energy of the $N-$electron system. Due to the lack of a one-to-one mapping proof of the $(\rho(\mathbf{r}t), \kappa(\mathbf{x}, \mathbf{x}'; t))$ and $(v(\mathbf{r}t) - \mu, D(\mathbf{x}, \mathbf{x}'; t))$, the time dependent response theory is not a straightforward generalization of the normal TDDFT. By assuming that any linear-response pairing matrix generated from a pairing field perturbation of an interacting non-superconducting system can be reproduced by the linear-response pairing matrix generated from some pairing field perturbation of a non-interacting non-superconducting system, the Dyson-like equation for the pp response function is obtained, with a frequency dependent pp kernel. We also present the adiabatic linear-response theory in which the kernel is derived from the second order derivatives of the exchange-correlation energy with respect to the pairing matrix. The adiabatic theory is an extension of the previous TDDFT for superconductors to include triplet excitations[123], and applies to non-superconducting systems like atoms and molecules. TDDFT-P can be a useful theory to capture $N \pm 2$ excitations and correlation energies[121], going beyond the simplest pp-RPA.

Furthermore, TDDFT-P rationalizes the use of orbitals and eigenvalues directly from DFAs in the pp-RPA equation. The singlet-only LDA functional for superconductors in Ref. [133] and [123] could be used for TDDFT-PF calculations, but this functional does not include triplet state information and will probably not be that useful for this purpose. With better approximation of the pp kernel, one can have more accurate $N \pm 2$ excitation energies and ground state correlation energies, and even important neutral excitation energies.

# 4

# Ladder-Coupled-Cluster Doubles and its equivalence to particle-particle random phase approximation

## 4.1 Introduction

The random phase approximation (RPA) was originally proposed in the 1950s by Pine and Bohm[151, 152] to treat the homogeneous electron gas. Since then, the idea of RPA has spawned the studies of excitation energies, linear-response functions and correlation energies in solid state physics[153–156], nuclear physics[55, 117, 157–160], and quantum chemistry[161–164]. In the recent decade, there has been a renaissance of interest in the RPA correlation energy in quantum chemistry because of its good description of van der Waals interaction[164], the correct dissociation limit of $H_2$[165] and, through the adiabatic connection its link to density-functional theory (DFT)[164]. These features have motivated the development of efficient implementations, leading to relatively low scaling algorithms ($O(L^4 \log L)$ by Eshuis *et al.*[166] and $O(L^4)$ by Ren *et al.*[167] with $L$ the number of basis functions) and going beyond RPA is an active field of research that achieves exciting results[99, 147–149, 168–170].

Recently, van Aggelen *et al.*[118] established an adiabatic connection for the exchange-correlation energy in terms of the dynamic pairing matrix fluctuation, parallel to the adiabatic connection fluctuation dissipation (ACFD) theorem in terms of the density fluctuation[155, 171]. Like the ACFD theorem, this adiabatic connection is in principle exact, but requires the particle-particle propagator as a function of the interaction strength. The particle-particle channel of random phase approximation (pp-RPA) is the first-order approximation to the paring matrix fluctuation. The first applications of the pp-RPA correlation energies to molecular systems provide promising results in describing systems with both fractional charge and fractional spin.[118] The RPA usually applied in quantum chemistry describes exclusively the particle-hole channel of correlations. To distinguish the two RPAs of different channels, we will, hereafter, refer to the conventional particle-hole RPA as ph-RPA. In nuclear physics, pp-RPA[55, 57, 111–117, 172, 173], also known as Brueckner's theory[174–177], is also widely discussed. In chemistry, however, pp-RPA has only been used in computational study of Auger spectroscopy which involves double ionization of molecules[135, 137], before van Aggelen *et al.*[118].

In the diagrammatic language extensively used in many-body perturbation-theory (MBPT), the ph-RPA correlation energy is the sum of all ring diagrams[55, 178]. Based on the same diagrammatic arguments, already in the seminal work of Čížek[179], ph-RPA has been identified as a subset of the coupled-cluster doubles (CCD) equations, i.e. accounting only for the ring summation terms. The ph-RPA wavefunction being of an exponential form is textbook knowledge[117]. Despite the well-known equivalence between the ph-RPA correlation energy and summation of all ring diagrams in direct ring-CCD, the mathematical connection between the linear ph-RPA equation and the quadratic equation in direct ring-CCD has only recently been presented by Scuseria *et al.*[180], while ideas can be traced back to work done forty years before.[181] In the particle-particle channel, the pp-RPA correlation energy

can be interpreted as the sum of all ladder diagrams[55]. As the sum of all ladder diagrams, methods like pp-RPA have also been closely related to the "ladder approximation" in the literature[182]. Again, considering the diagrams involved, Čížek identified the sum of all ladder diagrams as a subset of CCD, which might be called ladder-CCD[179] and the exponential form of the pp-RPA wavefunction is also textbook knowledge[117]. However, we are not aware of any explicit demonstration of the equivalence of the linear form of the pp-RPA equation and the quadratic ladder-CCD equation. The purpose of this paper is, following Ref. [180], to establish this connection between the two sets of seemingly distinct equations. Since pp-RPA is a straightforward approximation in Green's function theory[118], the establishment of this connection might shed light on the relationship between Green's function based methods and coupled-cluster theory, a perspective from which both fields could benefit. Furthermore, it is our hope that the insight gained from linking Green's functions, coupled-cluster theory and DFT provides new stimulus to develop novel density functional approximations. Moreover, the coupled-cluster connection opens up a direct way to obtain molecular properties from a virtual orbital dependent density functional and the pp-RPA based excited states can straightforwardly be obtained via equation-of-motion coupled-cluster[12, 139, 183, 184] or, linear-response coupled-cluster theory[185, 186].

## 4.2 The pp-RPA equation and its stability

The pp-RPA equation can be derived from the two-particle Green's function, the equation-of-motion ansatz, or the time-dependent Hartree-Fock-Bogoliubov approximation (TDHFB)[55, 57, 117, 118]. The resulting generalized eigenvalue equation is very similar to the ph-RPA equation (see, for example, Ref. [55, 117, 164, 180] for

the ph-RPA equation),

$$\begin{bmatrix} \mathbf{A} & \mathbf{B} \\ \mathbf{B}^\dagger & \mathbf{C} \end{bmatrix} \begin{bmatrix} \mathbf{x}_n \\ \mathbf{y}_n \end{bmatrix} = \omega_n \begin{bmatrix} \mathbf{I} & \mathbf{0} \\ \mathbf{0} & -\mathbf{I} \end{bmatrix} \begin{bmatrix} \mathbf{x}_n \\ \mathbf{y}_n \end{bmatrix}, \tag{4.1}$$

where

$$A_{ab,cd} = (\epsilon_c + \epsilon_d - 2\nu)\delta_{ac}\delta_{bd} + \langle ab||cd\rangle, \tag{4.2}$$

$$C_{ij,kl} = -(\epsilon_k + \epsilon_l - 2\nu)\delta_{ki}\delta_{jl} + \langle ij||kl\rangle, \tag{4.3}$$

and

$$B_{ab,ij} = \langle ab||ij\rangle. \tag{4.4}$$

We use the index convention stated in Page 9 except that $m$, $n$ are used to denote eigenvector and eigenvalue indexes. Additionally, $\epsilon_u$ is the molecular orbital eigenvalue, and $\langle uv||st\rangle$ is the antisymmetrized two-electron integral defined in Eq. (1.7). The chemical potential $\nu$ is not an necessity in the equation-of-motion[57, 117] or the two-particle Green's function derivation[118]; while during the derivation from the the TDHFB[55], $\nu$ is used to ensure that the ground state has the desired number of electrons $N$. In practice, it is usually approximated to be half of HOMO (highest occupied molecular orbital) and LUMO (lowest unoccupied molecular orbital) eigenvalues[118]. We will later show that the exact choice of the chemical potential is unimportant within a certain range as long as the pp-RPA equation is stable.

The indexes of the matrix are either hole pairs or particle pairs. These indexes have only $i > j$ for hole pairs and $a > b$ for particle pairs to eliminate the redundancy. The number of particle (hole) pairs is

$$N_{pp(hh)} = \frac{1}{2} N_{\mathrm{vir(occ)}}(N_{\mathrm{vir(occ)}} - 1), \tag{4.5}$$

where $N_{\mathrm{vir(occ)}}$ is the number of virtual (occupied) orbitals. In general, $N_{pp}$ is much larger than $N_{hh}$. The the upper left (lower right) identity matrix in Eq. (4.1) has

the same dimension as $\mathbf{A}$ ($\mathbf{C}$). Throughout the paper, the dimensions of identity matrices will be omitted as they are clear from the context. The difference of the dimensions of $\mathbf{A}$ and $\mathbf{C}$ makes the solution of the pp-RPA equation quite different from that of the usual ph-RPA equation or the linear-response time-dependent DFT equation[52]. Nevertheless, Eq. (4.1) and the ph-RPA equation share conceptually similar properties as discussed in Ref. [158].

For simplicity, we use a compact matrix notation

$$\mathbf{M}\mathbf{z}_n = \omega_n \mathbf{W}\mathbf{z}_n, \tag{4.6}$$

to denote Eq. (4.1), where $\mathbf{M}$ is the Hermitian matrix on the left hand side

$$\mathbf{M} = \begin{bmatrix} \mathbf{A} & \mathbf{B} \\ \mathbf{B}^\dagger & \mathbf{C} \end{bmatrix}, \tag{4.7}$$

$\mathbf{W}$ is the non-positive definite metric

$$\mathbf{W} = \begin{bmatrix} \mathbf{I} & \mathbf{0} \\ \mathbf{0} & -\mathbf{I} \end{bmatrix}, \tag{4.8}$$

and $\mathbf{z}_n$ is the full eigenvector

$$\mathbf{z}_n = \begin{bmatrix} \mathbf{x}_n \\ \mathbf{y}_n \end{bmatrix}, \tag{4.9}$$

with its eigenvalue $\omega_n$. Due to the non-positive definite metric $\mathbf{W}$, Eq. (4.1) is not guaranteed to have all real eigenvalues. We call $\mathbf{z}_n^\dagger \mathbf{W}\mathbf{z}_n$ the signature of an eigenvector $\mathbf{z}_n$. The signature can be positive, zero, or negative. The zero signature coincides with an imaginary eigenvalue (see Appendix D.1), while positive and negative signatures are associated with real eigenvalues. We categorize the eigenvectors according to their signature, where eigenvectors with positive signatures are called $N+2$ excitations and eigenvectors with negative signatures are called $N-2$ excitations. For a diagonalizable pp-RPA equation with all real eigenvalues, according to Subsection

D.2 in the Appendix, the orthonormalization of the eigenvectors can be written as,

$$\mathbf{Z}^\dagger \mathbf{W} \mathbf{Z} = \mathbf{W}, \tag{4.10}$$

with all $N+2$ eigenvectors to the left of all $N-2$ eigenvectors in $\mathbf{Z}$. This special arrangement will be kept all through the paper.

When all the eigenvalues of a diagonalizable pp-RPA equation are real, the pp-RPA equation is defined to be stable if all the $N+2$ excitation eigenvalues are positive and $N-2$ excitation eigenvalues are negative, i.e. $\min_n \omega_n^{N+2} > 0 > \max_m \omega_m^{N-2}$. With the eigenvector arrangement according to signatures, the stability condition can be expressed in a concise equation,

$$\text{sign}(\boldsymbol{\omega}) = \mathbf{W}, \tag{4.11}$$

where $\text{sign}(\boldsymbol{\omega})$ is the sign function[187] of the eigenvalue matrix $\boldsymbol{\omega}$, which gives $[\text{sign}(\boldsymbol{\omega})]_{nm} = \delta_{nm}\text{sign}(\omega_n)$ since $\boldsymbol{\omega}$ is diagonal. Note that Eq. (4.10) is a necessary but not sufficient condition for the stability of Eq. (4.11).

These eigenvalues are interpreted as the double ionization and double electron attachment energies in a molecular system, i.e.

$$\omega_n^{N+2} = E_n^{N+2} - E_0^N - 2\nu, \tag{4.12}$$

are the $N+2$ excitation energies, and

$$\omega_n^{N-2} = E_0^N - E_n^{N-2} - 2\nu, \tag{4.13}$$

the $N-2$ excitation energies. With the eigenvalue interpretation of Eqs. (4.12)-(4.13), an unstable pp-RPA equation violates the energy convexity condition[4]. It has not been proved that such stability is intrinsic for a self-consistent solution of a Hartree-Fock or Kohn-Sham/generalized Kohn-Sham molecular system, but in practice unstable solutions have never been encountered for molecular systems so

far in Ref.[118] and in present work, as compared to the notorious instability issue of ph-RPA with exchange, namely the Hartree-Fock instability[158, 188, 189].

The stability condition of the pp-RPA equation is equivalent to the positive definiteness of the matrix $\mathbf{M}$ (see Appendix D.3 and Ref. [55] for further details).

With the whole spectrum of a stable pp-RPA equation, the pp-RPA correlation energy can be expressed in several equivalent ways[118]

$$E_{\mathrm{c}}^{\text{pp-RPA}} = \sum_m \omega_m^{N+2} - \mathrm{Tr}\mathbf{A} = -\sum_n \omega_n^{N-2} - \mathrm{Tr}\mathbf{C} = \frac{1}{2}\sum_n |\omega_n| - \frac{1}{2}\mathrm{Tr}\mathbf{M}. \tag{4.14}$$

The precise value of $\nu$ is irrelevant for the correlation energy since it cancels out in the expression, Eq. (4.14), as long as

$$\min_m(E_m^{N+2} - E_0^N) > 2\nu > \max_n(E_0^N - E_n^{N-2}),$$

such that the $N+2$ eigenvalues are positive and the $N-2$ eigenvalues are negative. A proper chemical potential also categorizes $\mathbf{M}$ to be positive definite, equivalent to the stability condition (see Subsection D.3 in the Appendix for details).

## 4.3 Proof of the equivalence of pp-RPA and ladder-CCD

The CCD ansatz, the simplest method in the coupled cluster family, expresses the wavefunction as

$$|\mathrm{CCD}\rangle = e^{\hat{T}_2}|\Phi_0\rangle, \tag{4.15}$$

where $|\Phi_0\rangle$ is a single Slater determinant, and $\hat{T}_2$ is the two-body cluster operator

$$\hat{T}_2 = \frac{1}{(2!)^2}\sum_{ijab} t_{ij}^{ab}\hat{a}^\dagger\hat{i}\hat{b}^\dagger\hat{j} = \sum_{ijab}^{i>j,a>b} t_{ij}^{ab}\hat{a}^\dagger\hat{i}\hat{b}^\dagger\hat{j}, \tag{4.16}$$

where $\hat{a}^\dagger, \hat{i}$ are the creation and annihilation operators for spin orbital $a$ and $i$, respectively and $t_{ij}^{ab}$ is the double excitation amplitude, having the symmetry

$$t_{ij}^{ab} = -t_{ji}^{ab} = -t_{ij}^{ba} = t_{ji}^{ba}. \tag{4.17}$$

The correlation energy is expressed in terms of the amplitudes through the energy equation

$$E_{\rm c}^{\rm CCD} = \sum_{ijab}^{i>j,a>b} \langle ij||ab\rangle t_{ij}^{ab}, \tag{4.18}$$

while the amplitudes $t_{ij}^{ab}$ are solved for by the CCD amplitude equation (see Ref. [12] for extensive discussions),

$$\begin{aligned}\epsilon_{ij}^{ab} t_{ij}^{ab} = &\langle ab||ij\rangle + \frac{1}{2}\sum_{cd}\langle ab||cd\rangle t_{ij}^{cd} + \frac{1}{2}\sum_{kl}\langle ij||kl\rangle t_{kl}^{ab} \\ &- \sum_{kc}(\langle bk||cj\rangle t_{ik}^{ac} - \langle bk||ci\rangle t_{jk}^{ac} - \langle ak||cj\rangle t_{ik}^{bc} + \langle ak||ci\rangle t_{jk}^{bc}) \\ &+ \sum_{klcd}\langle kl||cd\rangle [\frac{1}{4} t_{ij}^{cd} t_{kl}^{ab} - \frac{1}{2}(t_{ij}^{ac} t_{kl}^{bd} + t_{ij}^{bd} t_{kl}^{ac}) - \frac{1}{2}(t_{ik}^{ab} t_{jl}^{cd} + t_{ik}^{cd} t_{jl}^{ab}) + (t_{ik}^{ac} t_{jl}^{bd} + t_{ik}^{bd} t_{jl}^{ac})].\end{aligned} \tag{4.19}$$

By allowing only particle-hole summations in Eq. (4.19), Scuseria *et al.*[180] have shown that the amplitude equation reduces to the ph-RPA equation with exchange, i.e., the time-dependent Hartree-Fock (TDHF) equation. Further eliminating the exchange terms in the two-electron integrals yields the conventional direct ph-RPA. Similarly, if we allow only summations of particle pairs and hole pairs, Eq. (4.19) becomes

$$\begin{aligned}&\sum_{kl}(\epsilon_k + \epsilon_l) t_{kl}^{ab} \delta_{ki}\delta_{jl} - \sum_{cd}(\epsilon_c + \epsilon_d) t_{ij}^{cd}\delta_{ac}\delta_{bd} \\ =&\langle ab||ij\rangle + \frac{1}{2}\sum_{cd}\langle ab||cd\rangle t_{ij}^{cd} + \frac{1}{2}\sum_{kl}\langle ij||kl\rangle t_{kl}^{ab} + \frac{1}{4}\sum_{kl,cd} t_{kl}^{ab}\langle kl||cd\rangle t_{ij}^{cd}.\end{aligned} \tag{4.20}$$

We refer to this truncated CCD as ladder-CCD, due to its restriction to ladder diagrams included in the correlation energy[179]. The exponential wavefunction of Eq. (4.15) with exponent of Eq. (4.25) has been proposed in Ref. [117], together with a similar form for ph-RPA, however without exploring their connection to the form

of truncated CCD, a question worth while investigating, considering that the there are several possibilities to evaluate the energy of an exponential wavefunction[190]. By utilizing the antisymmetry of the two-electron integrals $\langle uv||st\rangle = -\langle uv||ts\rangle$, Eq. (4.20) can be rearranged as

$$\sum_{cd}^{c>d} A_{ab,cd} t_{ij}^{cd} + \sum_{kl}^{k>l} C_{ij,kl} t_{kl}^{ab} + B_{ab,ij} + \sum_{kl,cd}^{k>l,c>d} t_{kl}^{ab} B_{cd,kl}^{*} t_{ij}^{cd} = 0, \tag{4.21}$$

with $A$, $B$, and $C$ defined in Eqs. (4.2)-(4.4). Denoting the amplitude as a matrix $T_{ab,ij} = t_{ij}^{ab}$, Eq. (4.21) results in an algebraic matrix equation

$$\mathbf{AT} + \mathbf{TC} + \mathbf{B} + \mathbf{TB}^{\dagger}\mathbf{T} = 0. \tag{4.22}$$

Now, we will show that the pp-RPA equation of Eq. (4.1) is equivalent to the ladder-CCD amplitude equation under the assumption that the pp-RPA equation is stable.

The pp-RPA equation for only the $N+2$ excitations reads,

$$\begin{bmatrix} \mathbf{A} & \mathbf{B} \\ \mathbf{B}^{\dagger} & \mathbf{C} \end{bmatrix} \begin{bmatrix} \mathbf{X} \\ \mathbf{Y} \end{bmatrix} = \begin{bmatrix} \mathbf{I} & \mathbf{0} \\ \mathbf{0} & -\mathbf{I} \end{bmatrix} \begin{bmatrix} \mathbf{X} \\ \mathbf{Y} \end{bmatrix} \boldsymbol{\omega}^{N+2}, \tag{4.23}$$

where $\dim \mathbf{X} = N_p \times N_p$, $\dim \mathbf{Y} = N_h \times N_p$, and $\dim \boldsymbol{\omega}^{N+2} = N_p \times N_p$. Multiplying $\mathbf{X}^{-1}$ from the right on Eq. (4.23) gives

$$\begin{bmatrix} \mathbf{A} & \mathbf{B} \\ \mathbf{B}^{\dagger} & \mathbf{C} \end{bmatrix} \begin{bmatrix} \mathbf{I} \\ \tilde{\mathbf{T}}^{\dagger} \end{bmatrix} = \begin{bmatrix} \mathbf{I} & \mathbf{0} \\ \mathbf{0} & -\mathbf{I} \end{bmatrix} \begin{bmatrix} \mathbf{I} \\ \tilde{\mathbf{T}}^{\dagger} \end{bmatrix} \mathbf{R}, \tag{4.24}$$

where

$$\tilde{\mathbf{T}} = (\mathbf{Y}\mathbf{X}^{-1})^{\dagger}, \tag{4.25}$$

and

$$\mathbf{R} = \mathbf{X}\boldsymbol{\omega}^{N+2}\mathbf{X}^{-1}. \tag{4.26}$$

The invertibility of $\mathbf{X}$ is guaranteed by a stable pp-RPA equation (see Subsection D.4 in the Appendix for the detailed proof). Multiplying $[\tilde{\mathbf{T}}^{\dagger}\ \mathbf{1}]$ from the left Eq.

(4.24) becomes

$$\tilde{\mathbf{T}}^{\dagger}\mathbf{A} + \tilde{\mathbf{T}}^{\dagger}\mathbf{B}\tilde{\mathbf{T}}^{\dagger} + \mathbf{B}^{\dagger} + \mathbf{C}\tilde{\mathbf{T}}^{\dagger} = 0. \tag{4.27}$$

Comparing Eq. (4.22) and Eq. (4.27), we infer that $\mathbf{T} = \tilde{\mathbf{T}}$.

The particle-particle block of Eq. (4.24) gives

$$\mathbf{A} + \mathbf{B}\mathbf{T}^{\dagger} = \mathbf{R}. \tag{4.28}$$

Then, the ladder-CCD correlation energy of Eq. (4.18) can be expressed as

$$E_{\mathbf{c}}^{\mathbf{ladder-CCD}} = \mathrm{Tr}(\mathbf{B}^{\dagger}\mathbf{T}) = [\mathrm{Tr}(\mathbf{R} - \mathbf{A})]^{*} = \sum_{m} \omega_{m}^{N+2} - \mathrm{Tr}\mathbf{A}, \tag{4.29}$$

which is identical to the pp-RPA correlation energy in Eq. (4.14). From Eqs. (4.20)-(4.22), it is also clear that the chemical potential has no contribution because they cancel each other in the CCD equations through $\mathbf{AT} + \mathbf{TC}$.

Alternatively, one can also derive the equivalence using the $N - 2$ excitation eigenvectors with similar techniques. The resulting amplitude will be the same, while the correlation energy expression will be the second equation in Eq. (4.14). An alternative proof of equivalence can also be formulated using a Schur decomposition in analogy to Appendix 5 in Ref. [180].

In conclusion, the correlation energy from pp-RPA is equivalent to that of ladder-CCD, assuming that the pp-RPA equation is stable. The equivalence raises the question if the nonlinear ladder-CCD equations always converge to the unique solution of the linear pp-RPA equation system.

## 4.4 Numerical demonstrations

All coupled cluster and second-order Møller–Plesset perturbation theory (MP2) computations reported herein are performed in a locally modified version of CFOUR[191], while pp-RPA is performed with QM4D[37].

Concerning the algorithm, truncating the CCD equations to include only the ladder diagrams (Eq. (4.20)) can be seen as a small modification of the CCD equations or a small extension of the linearized CCD, also known as CEPA(0) or D-MBPT($\infty$)[12], amplitude equations. Note that the computationally most expensive term of coupled-cluster singles and doubles (CCSD), scaling as $N_{\mathrm{occ}}^2 N_{\mathrm{vir}}^4$, is the major part of the term quadratic in the amplitudes of Eq. (4.20). In terms of efficiency, the matrix multiplications necessary for solving the non-linear system of equations in standard coupled cluster algorithms are traded against the diagonalization in the pp-RPA algorithm, which, at the non-optimized stage of the code,[37] is significantly slower than solving the non-linear equations. However, the diagonalization has the indisputable advantage that the solution is unique, whereas the non-linear coupled cluster equations have multiple minima (most of them lacking any physical meaning), without an *a priori* guarantee or check that the "correct" solution is found.[12]

All computations are carried out in the unrestricted Hartree-Fock (UHF) framework, but without breaking spatial symmetry. The correlation consistent basis sets of Dunning and coworkers[192, 193] have been applied with cartesian d- and f- atomic-orbitals. The ladder-CCD amplitudes are found to converge essentially as fast (or with a couple of iterations less) than the corresponding CCSD equations.

All total energies of ladder-CCD and pp-RPA (see Table 4.2) agree exceedingly well, the largest difference being $10^{-5}$ Hartree, which is on the same order of magnitude as the difference in nuclear repulsion energy between the two programs and can have its origin in, e.g., integral screening (SCF and CC iteration convergence has been checked carefully). In terms of correlation energy, ladder-CCD captures between 43% (Be) to 80% (Ne) of CCSD, while the full CCD energy recovers about 99%. Note that MP2 has min and max values of 70% and 99% for the same systems. Furthermore, changing to a DFT reference leads to an increased (in absolute terms) correlation energy, with min/max values reaching 51(54)% and 92 (95)% for

B3LYP[28, 30] (PBE[29]) orbitals. It is important to point out that the present pp-RPA@DFT is not equivalent to ladder-CCD with a DFT reference when following the usual practice in the coupled cluster community[194, 195]: for pp-RPA@DFT, the molecular orbital energies are the eigenvalues of the Kohn-Sham Hamiltonian. However, the use of DFT orbitals in coupled cluster computations is considered as a "non-HF" reference wavefunction, for which the one-particle Hamiltonian is not diagonal and the corresponding terms can be accounted for, yielding results that are much closer to HF based computations.[196, 197]

As a graphical illustration, Fig 4.1a shows the case of a dissociating cationic dimer ($Ne_2^+$), a typical probe for (de)localization error. We are using a spatial symmetry ($D_{\infty h}$) preserving unrestricted HF reference wavefunction for $Ne_2^+$ which corresponds to the $^2\Sigma_g$ ground state, as compared to $F_2^+$ the ground state of which is $^2\Pi_g$[198]. Again, the total energies of ladder-CCD and pp-RPA are identical to numerical precision (considering the two very different algorithms and programs), but not in very good agreement with CCSD. To further investigate the (de)localization error[39], Fig 4.1b shows the binding energy with respect to the separated fragments. The binding energy of ladder-CCD is in fairly good agreement with CCSD and only a small "bump" is observed somewhere between 3 and 4 Å, revealing that the missing absolute correlation energies in ladder-CCD compared to CCSD are almost irrelevant for the binding energy. The localization error of HF is over-corrected by MP2, but increasing the correlation treatment to the coupled cluster level improves the dissociation limit further, leading to the previously reported[118] negligible fractional charge error.

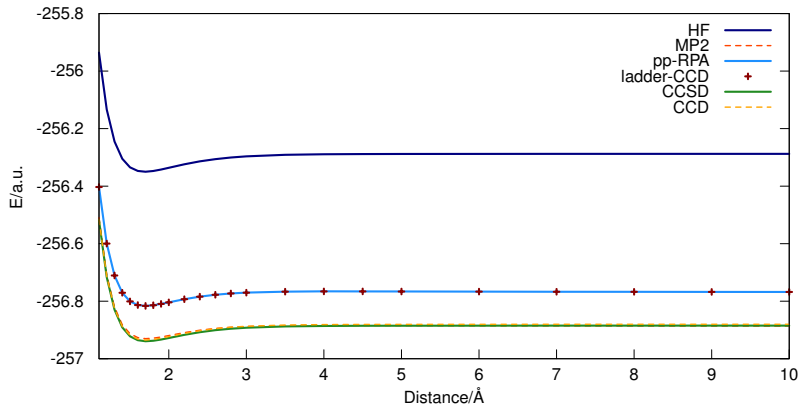


(a) The potential energy surface of $Ne_2^+$

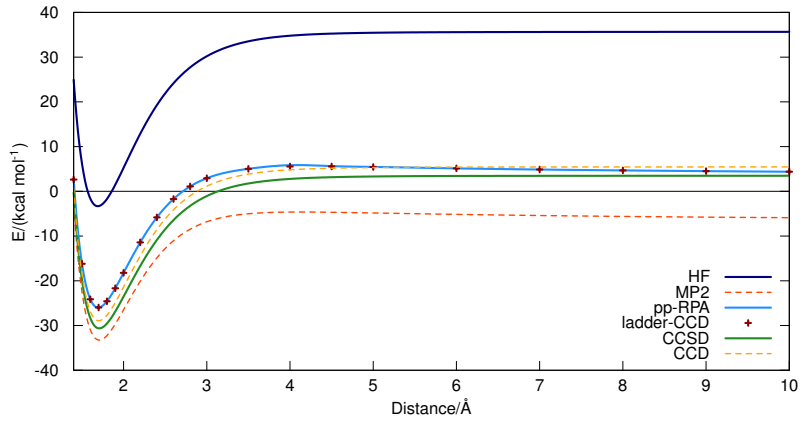


(b) The binding curve of $Ne_2^+$ (with respect to Ne and $Ne^+$)

FIGURE 4.1: The potential energy surface (a) and the binding curve (b) of $Ne_2^+$ of various methods with the aug-cc-pVTZ basis set. The total energies of pp-RPA are substantially in error (a), since the correlation energy of the ladder diagrams is not very well balanced (MP2 total energies are, on the scale of the figure, indistinguishable from CCD, and pp-RPA is correct through second order[118]). However, the binding energy (b) reveals that the missing correlation energy cancels almost perfectly out, yielding a pp-RPA binding energy curve very close to CCD, while MP2 deviates from CCSD in the other direction (overbinding).

Table 4.1: Atomization energies (in kcal $mol^{-1}$) of various methods. Geometries are taken from the G3 set[199, 200]. Experimental atomization energies are taken from Ref. [201–204]. The basis set is cc-pVTZ. The mean absolute deviation (MAD) is with respect to experimental data.

| | $CH_4$ | $H_2O$ | $NH_3$ | $CH_2O$ | MAD |
|---|---|---|---|---|---|
| HF | 327.9 | 153.8 | 199.3 | 255.5 | 96.5 |
| pp-RPA@HF | 392.8 | 208.7 | 264.9 | 343.5 | 28.2 |
| ladder-CCD | 392.8 | 208.7 | 264.9 | 343.5 | 28.2 |
| pp-RPA@PBE | 410.7 | 225.8 | 284.5 | 373.5 | 7.0 |
| pp-RPA@B3LYP | 406.4 | 221.7 | 279.8 | 366.8 | 12 |
| MP2 | 416.3 | 230.3 | 290.2 | 378.1 | 4.2 |
| CCD | 416.4 | 223.2 | 287.7 | 359.7 | 8.9 |
| CCSD | 416.6 | 223.6 | 288.1 | 361.6 | 8.2 |
| Exp. | 419.2 | 232.2 | 297.5 | 373.6 | – |

Table 4.2: Total energies of lCCD and related methods. Geometries are taken from the G3 set[199, 200]. The basis set is cc-pVTZ. All energies are in Hartree.

| | HF | pp-RPA@HF | ladder-CCD | pp-RPA@PBE | pp-RPA@B3LYP | MP2 | CCD | CCSD |
|---|---|---|---|---|---|---|---|---|
| He | -2.861154 | -2.885608 | -2.885608 | -2.889343 | -2.888504 | -2.894441 | -2.900328 | -2.900351 |
| Li | -7.432706 | -7.443903 | -7.443903 | -7.444664 | -7.444450 | -7.446781 | -7.449184 | -7.449243 |
| Be | -14.572875 | -14.598923 | -14.598923 | -14.605231 | -14.603533 | -14.614751 | -14.632242 | -14.632817 |
| B | -24.532104 | -24.566435 | -24.566436 | -24.575674 | -24.573063 | -24.584950 | -24.604746 | -24.605490 |
| C | -37.691663 | -37.746778 | -37.746778 | -37.760145 | -37.756583 | -37.769564 | -37.789208 | -37.789809 |
| N | -54.400883 | -54.482916 | -54.482916 | -54.500883 | -54.496235 | -54.509992 | -54.525553 | -54.525893 |
| O | -74.811910 | -74.933839 | -74.933839 | -74.959853 | -74.953384 | -74.969918 | -74.985506 | -74.986128 |
| F | -99.405657 | -99.576884 | -99.576884 | -99.611587 | -99.603292 | -99.622736 | -99.633484 | -99.634177 |
| Ne | -128.532010 | -128.760771 | -128.760771 | -128.804849 | -128.794546 | -128.816523 | -128.817814 | -128.818536 |
| $CH_4$ | -40.213408 | -40.372051 | -40.372054 | -40.411910 | -40.402169 | -40.432266 | -40.452031 | -40.452991 |
| $H_2O$ | -76.056687 | -76.266046 | -76.266049 | -76.318304 | -76.305731 | -76.336459 | -76.340863 | -76.342084 |
| $NH_3$ | -56.217964 | -56.404439 | -56.404440 | -56.452289 | -56.440556 | -56.471921 | -56.483441 | -56.484474 |
| $CH_2O$ | -113.910280 | -114.227562 | -114.227552 | -114.313824 | -114.293495 | -114.341669 | -114.347547 | -114.351726 |

Similarly to the binding energy of $Ne_2^+$, the atomization energies (Table 4.1) illustrate that the correlation energy missing in ladder-CCD largely cancels out when computing reaction energies. For the four molecules considered, ladder-CCD provides 77% on of the correction between the HF and CCSD atomization energies on average. This is to be compared with MP2 which recovers on average 107%. However, the mean absolute deviation for pp-RPA@PBE compared to the experimental values is substantially better, having the same level of accuracy as CCSD. In summary, the numerical analysis shows that ladder-CCD and pp-RPA are equivalent and that pp-RPA covers a substantial amount of correlation energy that is relevant for atomization energies of typical small molecules in Table 4.1. An efficient pp-RPA implementation has, therefore, the potential to become a valuable electronic structure theory.

## 4.5 Conclusions

The connection between the linear pp-RPA equation and the quadratic ladder-CCD equation has been established and numerically verified. The numerical assessment suggests that pp-RPA is fairly accurate for some reaction energies, despite its incomplete diagram summation. This mathematical connection is helpful in understanding the relationship between Green's function theory and coupled-cluster methods. The ladder-CCD perspective of pp-RPA makes the study of its ground and excited state properties straightforward.

# 5

# Second random phase approximations

## 5.1 Introduction

The particle-hole random phase approximation (ph-RPA)[151, 152] has been a convenient method to study particle-hole excitations and correlation energies for nuclei[55, 58, 117, 157–159], molecules[161–164] and solids[154–156]. The ph-RPA can be viewed as a response in time-dependent Hartree theory where exchange correlation contribution is omitted in time-dependent density-functional theory (TDDFT)[52], as the correlation energies of all ring diagrams[55], or alternatively as a ring approximation in coupled-cluster doubles[180]. Viewed as a correlation energy functional from adiabatic connection in density-functional theory[164], there is a renaissance of the ph-RPA in the quantum chemistry community due to its good description of van der Waals interaction[164] and the correct dissociation limit of $H_2$[165]. These features have incentivized developments of fast algorithms for ph-RPA correlation energies[161, 167]. Nonetheless, the ph-RPA exhibits formidable fractional charge errors which prohibit the applications of the ph-RPA to many systems.[99]

On the other hand, the particle-particle random phase approximation (pp-RPA)[57,

111–113, 172, 173], also known as Brueckner's theory[174–176], has been a textbook method in nuclear physics to study pairing vibrations[55, 117]. The pp-RPA can be interpreted as the time-dependent Hartree-Fock-Bogoliubov approximation[55], as linear-response time-dependent density-functional theory with pairing fields at the zero pairing field limit[14], as the adiabatic connection of the pairing matrix fluctuation[118], as the sum of all ladder diagrams[55], or as a ladder approximation in coupled-cluster doubles[15, 179]. Recent applications of the pp-RPA in molecular systems reveal that the pp-RPA satisfies the flat-plane condition[40, 118] and has better thermochemistry behavior than ph-RPA[119]. The pp-RPA can also capture double excitations from an $N-2$ reference, which is impossible for adiabatic linear-response TDDFT[121]. However, due to the limitation of the $N-2$ reference construction, single excitations from non-highest occupied molecular orbitals (HOMO) are absent in the pp-RPA. In this Chapter, we develop the restricted second particle-hole random-phase approximation and the restricted second particle-particle random phase approximation that can capture the full single excitation spectrum and some double excitations.

The second particle-hole random phase approximation (2ph-RPA)[58, 205–208] is a natural extension of ph-RPA or time-dependent Hartree-Fock (TDHF) in the equation-of-motion (EOM)[57] framework, where the the excitation operators include both single and double excitations. 2ph-RPA has been used in nuclear physics[206, 207] and metal clusters[208] to study double excitations, but not in chemistry in general. Parallel to the 2ph-RPA, we devise here the second particle-particle random phase approximation (2pp-RPA) that supplements the pp-RPA excitation operators with three-particle-one-hole (3p1h) and one-particle-three-hole (1p3h) operators. From an $N-2$ reference, 2pp-RPA has all critical double excitations in the pp-RPA, plus all single excitations and some triple excitations. The computational scaling of the 2ph-RPA and the 2pp-RPA can be reduced by placing

some rational restrictions on the excitation operators, leading to formal scaling of $O(L^4)$, the same scaling of TDDFT and the pp-RPA. The philosophy behind the 2ph-RPA and the 2pp-RPA is very similar to including 3p1h/1p3h operators and above in double-ionization-potential/double-electron-affinity equation-of-motion coupled-cluster (DIP/DEA-EOM-CC) methods[141, 150].

This Chapter is organized as follows. The theories of the 2ph-RPA and the 2pp-RPA and their restrictions are described in Section 5.2. Section 5.3 presents the implementation and calculation details for these methods. Results are shown in Section 5.4 with discussions. Finally, Section 5.5 concludes this Chapter.

## 5.2 Theory

### *5.2.1 2ph-RPA formalism*

The second particle-hole random phase approximation (2ph-RPA) is the EOM with $|0\rangle$ using HF wavefunction and $\hat{Q}_I^\dagger$ including all single and double particle-hole excitation operators, i.e. operators of $\{a^\dagger i\}$ and $\{a^\dagger i b^\dagger j\}$. $\{\cdots\}$ indicates the operator is normal ordered with respect to the Fermi sea.[12] The resulting eigenvalue equation is[58, 205–208]

$$\begin{bmatrix} \mathbf{A}_{SS} & \mathbf{A}_{SD} & \mathbf{B}_{SS} & \mathbf{0} \\ \mathbf{A}_{SD}^\dagger & \mathbf{A}_{DD} & \mathbf{0} & \mathbf{0} \\ \mathbf{B}_{SS}^\dagger & \mathbf{0} & \mathbf{A}_{SS}^* & \mathbf{A}_{SD}^* \\ \mathbf{0} & \mathbf{0} & \mathbf{A}_{SD}^T & \mathbf{A}_{DD}^* \end{bmatrix} \begin{bmatrix} \mathbf{X}_S \\ \mathbf{X}_D \\ \mathbf{Y}_S \\ \mathbf{Y}_D \end{bmatrix} = \omega \begin{bmatrix} \mathbf{I}_{SS} & \mathbf{0} & \mathbf{0} & \mathbf{0} \\ \mathbf{0} & \mathbf{I}_{DD} & \mathbf{0} & \mathbf{0} \\ \mathbf{0} & \mathbf{0} & -\mathbf{I}_{SS} & \mathbf{0} \\ \mathbf{0} & \mathbf{0} & \mathbf{0} & -\mathbf{I}_{DD} \end{bmatrix} \begin{bmatrix} \mathbf{X}_S \\ \mathbf{X}_D \\ \mathbf{Y}_S \\ \mathbf{Y}_D \end{bmatrix}, \tag{5.1}$$

where subscripts $S$ and $D$ denote the single and double excitation blocks respectively, and $\mathbf{I}$ is an identity matrix. The matrix elements are

$$A_{ia,jb} = \delta_{ij} F_{ab} - \delta_{ab} F_{ji} + \langle aj||ib\rangle, \tag{5.2}$$

$$A_{ia,kcld} = U(kl)[\delta_{ik}\langle al||cd\rangle] - U(cd)[\delta_{ac}\langle kl||id\rangle], \tag{5.3}$$

$$A_{iajb,kcld} = U(ab)U(ij)[U(cd)\delta_{jl}\delta_{ik}\delta_{bd}F_{ac} - U(kl)\delta_{bd}\delta_{ac}\delta_{jl}F_{ki}] + U(ab)[\delta_{ac}\delta_{bd}\langle kl||ij\rangle] \tag{5.4}$$

$$+ U(ij)[\delta_{ik}\delta_{jl}\langle ab||cd\rangle] + U(ij)U(ab)U(kl)U(cd)[\delta_{ik}\delta_{ac}\langle bl||jd\rangle], \tag{5.5}$$

and

$$B_{ia,jb} = \langle ij||ab\rangle, \tag{5.6}$$

where $F_{pq}$ is the Fock matrix element, $\langle pq||rs\rangle$ is an antisymmetrized two-electron integral defined in Eq. (1.7), and $U(pq)$ is an operator that antisymmetrizes the term with respect to $p$ and $q$,

$$U(pq)f(p,q) = f(p,q) - f(q,p). \tag{5.7}$$

Note that only the single-single block of the $\mathbf{B}$ matrix is nonzero. For a HF reference, $F_{pq} = \delta_{pq}\epsilon_p$ where $\epsilon_p$ is the molecular orbital eigenvalue.

It is interesting to compare Eq. (5.1) and the CISD equation in Eq. (1.32)

$$\begin{bmatrix} \mathbf{0} & \mathbf{0} & \mathbf{A}_{0D} \\ \mathbf{0} & \mathbf{A}_{SS} & \mathbf{A}_{SD} \\ \mathbf{A}_{0D}^\dagger & \mathbf{A}_{SD}^\dagger & \mathbf{A}_{DD} \end{bmatrix} \begin{bmatrix} \mathbf{X}_0 \\ \mathbf{X}_S \\ \mathbf{X}_D \end{bmatrix} = \mathcal{E} \begin{bmatrix} \mathbf{X}_0 \\ \mathbf{X}_S \\ \mathbf{X}_D \end{bmatrix}, \tag{5.8}$$

where

$$A_{0,iajb} = \langle ij||ab\rangle = B_{ia,jb}, \tag{5.9}$$

and $\mathbf{A}_{SS}$, $\mathbf{A}_{SD}$ and $\mathbf{A}_{DD}$ are defined the same as those in 2ph-RPA. Therefore, the CISD matrix and the 2ph-RPA matrix contain exactly the same amount of information. However, the rearrangement of matrix elements makes CISD and 2ph-RPA dramatically different.

It is also noted that the matrix in the time-dependent Hartree-Fock (TDHF) equation in Eq. (1.176) is a submatrix of the 2ph-RPA matrix. It is well-known that TDHF suffers from HF instability issues for many systems. Therefore, any instability in TDHF leads to instability in 2ph-RPA. TDA is the approximation to set the $\mathbf{B}$

matrix zero, which could ameliorate some instability issues and improve the result. The second particle-hole Tamm-Dancoff approximation (2ph-TDA) is then

$$\begin{bmatrix} \mathbf{A}_{SS} & \mathbf{A}_{SD} \\ \mathbf{A}_{SD}^{\dagger} & \mathbf{A}_{DD} \end{bmatrix} \begin{bmatrix} \mathbf{X}_S \\ \mathbf{X}_D \end{bmatrix} = \omega \begin{bmatrix} \mathbf{X}_S \\ \mathbf{X}_D \end{bmatrix}. \tag{5.10}$$

### *5.2.2 2pp-RPA formalism*

Parallel to the 2ph-RPA, by complementing the three-particle one-hole $\{a^{\dagger}b^{\dagger}c^{\dagger}i\}$ and one-particle three-hole $\{a^{\dagger}ijk\}$ operators in the pp-RPA equation, we derive the 2pp-RPA equation using Wick's theorem contraction[12],

$$\begin{aligned} &\begin{bmatrix} \mathbf{A}_{2p,2p} & \mathbf{A}_{2p,3p1h} & \mathbf{B}_{2p,2h} & \mathbf{0} \\ \mathbf{A}_{2p,3p1h}^{\dagger} & \mathbf{A}_{3p1h,3p1h} & \mathbf{0} & \mathbf{0} \\ \mathbf{B}_{2p,2h}^{\dagger} & \mathbf{0} & \mathbf{C}_{2h,2h} & \mathbf{C}_{2h,1p3h} \\ \mathbf{0} & \mathbf{0} & \mathbf{C}_{2h,1p3h}^{\dagger} & \mathbf{C}_{3p1h,3p1h} \end{bmatrix} \begin{bmatrix} \mathbf{X}_{2p} \\ \mathbf{X}_{3p1h} \\ \mathbf{Y}_{2h} \\ \mathbf{Y}_{1p3h} \end{bmatrix} \\ =&\omega \begin{bmatrix} \mathbf{I}_{2p,2p} & \mathbf{0} & \mathbf{0} & \mathbf{0} \\ \mathbf{0} & \mathbf{I}_{3p1h,3p1h} & \mathbf{0} & \mathbf{0} \\ \mathbf{0} & \mathbf{0} & -\mathbf{I}_{2h,2h} & \mathbf{0} \\ \mathbf{0} & \mathbf{0} & \mathbf{0} & -\mathbf{I}_{3p1h,3p1h} \end{bmatrix} \begin{bmatrix} \mathbf{X}_{2p} \\ \mathbf{X}_{3p1h} \\ \mathbf{Y}_{2h} \\ \mathbf{Y}_{1p3h} \end{bmatrix}, \end{aligned} \tag{5.11}$$

with

$$A_{ab,de} = U(ab)U(de)[\delta_{be}F_{ad}] + \langle ab||de\rangle, \tag{5.12}$$

$$A_{ab,defl} = \frac{1}{2}U(ab)U(def)[\delta_{ad}\langle bl||ef\rangle], \tag{5.13}$$

$$\begin{aligned} A_{abci,defl} = &\frac{1}{2}\delta_{il}U(abc)U(def)[F_{ad}\delta_{be}\delta_{cf}] - F_{li}U(abc)[\delta_{ad}\delta_{be}\delta_{cf}] \\ &- \frac{1}{2}U(abc)U(def)[\delta_{ad}\delta_{be}\langle cl||fi\rangle] + \frac{1}{4}U(abc)U(def)[\delta_{il}\delta_{cf}\langle ab||de\rangle], \end{aligned} \tag{5.14}$$

$$B_{ab,lm} = \langle ab||lm\rangle, \tag{5.15}$$

$$C_{ij,lm} = -U(ij)U(lm)[\delta_{jm}F_{il}] + \langle ij||lm\rangle, \tag{5.16}$$

$$C_{ij,dlmn} = \frac{1}{2}U(ij)U(lmn)[\delta_{jn}\langle di||lm\rangle], \tag{5.17}$$

and

$$C_{aijk,dlmn} = F_{da}U(ijk)[\delta_{il}\delta_{jm}\delta_{kn}] - \frac{1}{2}\delta_{ad}U(ijk)U(lmn)[F_{il}\delta_{jm}\delta_{kn}]$$
$$- \frac{1}{2}U(ijk)U(lmn)[\delta_{jm}\delta_{kn}\langle di||al\rangle] + \frac{1}{4}U(ijk)U(lmn)[\delta_{ad}\delta_{kn}\langle ij||lm\rangle]. \tag{5.18}$$

Again, only the 2p-2h block of the **B** matrix is nonzero.

Similarly, we can obtain 2pp-TDA by setting **B** zero,

$$\begin{bmatrix} \mathbf{A}_{2p,2p} & \mathbf{A}_{2p,3p1h} \\ \mathbf{A}^{\dagger}_{2p,3p1h} & \mathbf{A}_{3p1h,3p1h} \end{bmatrix} \begin{bmatrix} \mathbf{X}_{2p} \\ \mathbf{X}_{3p1h} \end{bmatrix} = \omega \begin{bmatrix} \mathbf{X}_{2p} \\ \mathbf{X}_{3p1h} \end{bmatrix}. \tag{5.19}$$

### *5.2.3 Excited state properties*

In EOM, since there is no explicit excited state wavefunction, properties of excited states such as density matrices and $S^2$ expectation values are not directly available. The motivation for excited state property calculations comes from the need to distinguish spin states in the results for an unrestricted calculation. There were a few discussions on this topic in the literature. The original proposal for excited state properties by Rowe is[1]

$$\langle F|\hat{W}|F\rangle_{\text{Rowe}} = \langle 0|\hat{W}|0\rangle + \frac{\langle 0|[\hat{O}_F, \hat{W}, \hat{O}^{\dagger}_F]|0\rangle}{\langle 0|[\hat{O}_F, \hat{O}^{\dagger}_F]0\rangle}. \tag{5.20}$$

Alternatively, we can use the expression

$$\langle F|\hat{W}|F\rangle_{\text{Rowe}} = \langle 0|\hat{W}|0\rangle + \frac{\begin{bmatrix} \mathbf{X}_F \\ \mathbf{Y}_F \end{bmatrix}^{\dagger} \begin{bmatrix} \mathbf{A}(W) & \mathbf{B}(W) \\ \mathbf{B}(W)^{\dagger} & \mathbf{A}(W)^{*} \end{bmatrix} \begin{bmatrix} \mathbf{X}_F \\ \mathbf{Y}_F \end{bmatrix}}{\begin{bmatrix} \mathbf{X}_F \\ \mathbf{Y}_F \end{bmatrix}^{\dagger} \begin{bmatrix} \mathbf{C} & \mathbf{D} \\ \mathbf{D}^{\dagger} & -\mathbf{C}^{*} \end{bmatrix} \begin{bmatrix} \mathbf{X}_F \\ \mathbf{Y}_F \end{bmatrix}}, \tag{5.21}$$

with $\mathbf{A}(W)$ and $\mathbf{B}(W)$ defined as in Eqs. (4.2) and (4.4) but replacing $\hat{H}$ with $\hat{W}$. Ref. [209, 210] proposed other formulas, however, due to the complexity of their

[1] Note that in Ref. [58] the denominator $\langle 0|[\hat{O}_F, \hat{O}^{\dagger}_F]0\rangle$ is absent, probably they assume to study the excited state and not the deexcited state and the normalization is one by default.

expressions, Eq. (5.20) is the most used expressions. Eq. (5.20) does not always produce reasonably values. For example, for triplet excited states from a closed-shell singlet reference in TDDFT[211],

$$\langle F|\hat{S}^2|F\rangle_{\text{Rowe}} = \frac{2(\mathbf{X}_F^\dagger \mathbf{X}_F + \mathbf{Y}_F^\dagger \mathbf{Y}_F)}{\mathbf{X}_F^\dagger \mathbf{X}_F - \mathbf{Y}_F^\dagger \mathbf{Y}_F}, \tag{5.22}$$

which is normally larger than 2. On the other hand, Casida explicitly assigned the excited state wavefunction $|F\rangle$ in TDDFT[52],

$$|F\rangle_{\text{Casida}} = \sum_{ia} \sqrt{\frac{\epsilon_a - \epsilon_i}{\omega_F}} Z_{ia,F}\{a^\dagger i\}|0\rangle, \tag{5.23}$$

where $\mathbf{Z}_F$ is the orthonormal eigenvector of a transformed TDDFT equation,

$$[(\mathbf{A}-\mathbf{B})^{1/2}(\mathbf{A}+\mathbf{B})(\mathbf{A}-\mathbf{B})^{1/2}]\mathbf{Z}_F = \omega_F^2 \mathbf{Z}_F. \tag{5.24}$$

In TDDFT, $\mathbf{Z}_F$ is related to $\mathbf{X}_F$ and $\mathbf{Y}_F$,

$$\mathbf{Z}_F = (\mathbf{A}-\mathbf{B})^{-1/2}(\mathbf{X}_F + \mathbf{Y}_F). \tag{5.25}$$

Casida's explicit construction of the wavefunction enables the calculation of excited state expectation values. In this way, Casida's expectation value is equivalent to

$$\langle F|\hat{W}|F\rangle_{\text{Casida}} = \langle 0|\hat{W}|0\rangle + \frac{1}{\omega_F}\mathbf{Z}_F^\dagger(\Delta\boldsymbol{\epsilon})^{1/2}\mathbf{A}(W)(\Delta\boldsymbol{\epsilon})^{1/2}\mathbf{Z}_F, \tag{5.26}$$

with $\Delta\epsilon_{ia,jb} = \delta_{ij}\delta_{ab}(\epsilon_a - \epsilon_i)$. Ipatov *et al.*[211] also proposed another expectation value formula

$$\langle F|\hat{W}|F\rangle_{\text{Ipatov}} = \langle 0|\hat{W}|0\rangle + \mathbf{Z}_F^\dagger \mathbf{A}(W)\mathbf{Z}_F. \tag{5.27}$$

Eqs. (5.26) and (5.27) are preferable for delivering exact $\langle F|\hat{S}^2|F\rangle$ for closed-shell triplet excitations. In this subsection, we will discuss some other possible expressions for excited state properties.

Eqs. (5.26) and (5.27) actually resembles the expectation value expressions in TDA,

$$\langle F|\hat{W}|F\rangle_{\mathrm{TDA}} = \langle 0|\hat{W}|0\rangle + \frac{\mathbf{X}_F^\dagger \mathbf{A}(W)\mathbf{X}_F}{\mathbf{X}_F^\dagger \mathbf{X}_F}. \tag{5.28}$$

Therefore, we deem that $\mathbf{B}(W)$ and $\mathbf{Y}_F$ may not be useful in expectation evaluation, and propose to use Eq. (5.28) for general EOM solutions. Note that for hole-hole excitations in pp-RPA/2pp-RPA solutions, Eq. (5.28) should be slightly modified,

$$\langle F|\hat{W}|F\rangle_{\mathrm{TDA(hh)}} = \langle 0|\hat{W}|0\rangle - \frac{\mathbf{Y}_F^\dagger \mathbf{C}(W)\mathbf{Y}_F}{\mathbf{Y}_F^\dagger \mathbf{Y}_F}. \tag{5.29}$$

Note also that in EOM the normalization requires that

$$\mathbf{X}_F^\dagger \mathbf{X}_F - \mathbf{Y}_F^\dagger \mathbf{Y}_F = \mathrm{sign}(\mathbf{X}_F^\dagger \mathbf{X}_F - \mathbf{Y}_F^\dagger \mathbf{Y}_F),$$

therefore the normalization factors in Eqs. (5.28) and (5.29) are required. Alternatively, Eq. (5.22) delivers an intuition that reversing the sign of the $\mathbf{Y}_F^\dagger \mathbf{Y}_F$ term may be a good way to calculate expectation values. Thus we have a revised expression

$$\begin{aligned}\langle F|\hat{W}|F\rangle_{\mathrm{Rev}} = {} & \langle 0|\hat{W}|0\rangle \\ & + \frac{\mathbf{X}_F^\dagger \mathbf{A}(W)\mathbf{X}_F + \mathbf{X}_F^\dagger \mathbf{B}(W)\mathbf{Y}_F + \mathbf{Y}_F^\dagger \mathbf{B}(W)^\dagger \mathbf{X}_F + \mathbf{Y}_F^\dagger \mathbf{G}(W)\mathbf{Y}_F}{\mathbf{X}_F^\dagger \mathbf{X}_F + \mathbf{Y}_F^\dagger \mathbf{Y}_F}\end{aligned} \tag{5.30}$$

where $\mathbf{G}(W) = \mathbf{A}(W)^*$ for particle-hole excitations and $\mathbf{G}(W) = \mathbf{C}(W)$ for particle-particle or hole-hole excitations. Note that for $\hat{W} = \hat{H}$, Eq. (5.30) could produce excitation energies quite different from the eigenvalues from the original EOM equations. The performance of expressions above will be discussed in Section 5.3.

Before we conclude this subsection, we have a brief description of obtaining the matrix elements of $\mathbf{A}(W)$, $\mathbf{B}(W)$, and $\mathbf{C}(W)$ for $\hat{S}^2$. The $\hat{S}^2$ operator can be expressed as

$$\hat{S}^2 = \hat{S}_+ \hat{S}_- + \hat{S}_z^2 - \hat{S}_z. \tag{5.31}$$

Since both the reference and excited states are $\hat{S}_z$ eigenvectors from construction, the operator we need to study is

$$\hat{\Sigma} = \hat{S}_+ \hat{S}_-. \tag{5.32}$$

Using normal order techniques, $\hat{\Sigma}$ can be partitioned into a constant, a one-body operator, and a two-body operator,

$$\begin{aligned}
\hat{\Sigma} &= \sum_{pqrs} \langle p|\hat{S}_+|q\rangle\langle r|\hat{S}_-|s\rangle p^\dagger q r^\dagger s \\
&= \sum_{ia} \langle i|\hat{S}_+|a\rangle\langle a|\hat{S}_-|i\rangle + \sum_{psa} \langle p|\hat{S}_+|a\rangle\langle a|\hat{S}_-|s\rangle\{p^\dagger s\} + \sum_{qri} \langle i|\hat{S}_+|q\rangle\langle r|\hat{S}_-|i\rangle\{q r^\dagger\} \\
&\quad + \sum_{pqrs} \langle p|\hat{S}_+|q\rangle\langle r|\hat{S}_-|s\rangle\{p^\dagger q r^\dagger s\} \\
&= \sum_{ia} \langle i|\hat{S}_+|a\rangle\langle a|\hat{S}_-|i\rangle + \sum_{pq}(\sum_a \langle p|\hat{S}_+|a\rangle\langle a|\hat{S}_-|q\rangle - \sum_i \langle i|\hat{S}_+|q\rangle\langle p|\hat{S}_-|i\rangle)\{p^\dagger q\} \\
&\quad - \frac{1}{4}\sum_{pqrs}[U(pq)U(rs)\langle p|\hat{S}_+|r\rangle\langle q|\hat{S}_-|s\rangle]\{p^\dagger q^\dagger r s\},
\end{aligned} \tag{5.33}$$

where we have assumed that all orbitals are either $\alpha$ or $\beta$ orbitals. Therefore, the normal ordered matrix elements of $\hat{\Sigma}$ are

$$(\Sigma_N^1)_{pq} = \sum_a \langle p|\hat{S}_+|a\rangle\langle a|\hat{S}_-|q\rangle - \sum_i \langle i|\hat{S}_+|q\rangle\langle p|\hat{S}_-|i\rangle, \tag{5.34}$$

and

$$(\Sigma_N^2)_{pq,rs} = -U(pq)U(rs)\langle p|\hat{S}_+|r\rangle\langle q|\hat{S}_-|s\rangle. \tag{5.35}$$

All these matrix elements can be expressed via the spatial overlap matrix between $\alpha$ and $\beta$ orbitals. Then the resulting matrix elements of $\mathbf{A}(\Sigma)$, $\mathbf{B}(\Sigma)$ and $\mathbf{C}(\Sigma)$ are the same as those in $\mathbf{A}$, $\mathbf{B}$ and $\mathbf{C}$ except that $F_{pq}$ is replaced by $(\Sigma_N^1)_{pq}$ and that $\langle pq||rs\rangle$ is replaced by $(\Sigma_N^2)_{pq,rs}$.

### *5.2.4 Orbital restrictions*

Those eigenvalue problems in 2RPAs (i.e. the 2ph-RPA, the 2ph-TDA, the 2pp-RPA, and the 2pp-TDA) stated above are still too time-consuming to be solved, with scaling of $O(L^6)$ even employing Davidson's algorithm[212]. Our goal for utilizing these extended models is to capture all single excitations and the most important – low-lying – double excitations that remedies the lack of double excitations in the RPA or the missing of non-HOMO single excitations in the pp-RPA. Therefore, for the 2ph-RPA and the 2ph-TDA, we will restrict the double excitation tensors to include only double excitations from HOMOs. The resulting models are thus named the restricted second random phase approximation (r2ph-RPA) and the restricted second Tamm-Dancoff approximation (r2ph-TDA). Depending on the degeneracy of frontier orbitals, HOMOs may include multiple spatial orbitals. The resulting excitation operator for the r2ph-TDA is then

$$\hat{O}_F^\dagger = \sum_{ia} X_{ia}\{a^\dagger i\} + \frac{1}{4}\sum_{ijab}^{i,j\in\text{HOMOs}} X_{iajb}\{a^\dagger i b^\dagger j\}, \tag{5.36}$$

and similar for the r2ph-RPA.

On the other hand, for the 2pp-TDA, we limit the 3p1h excitation operator to include only those excitations that place two electrons back to HOMOs of the $N$-electron state (the LUMOs of the $(N-2)$-electron state). Then the resulting r2pp-TDA operator is

$$\hat{O}_F^\dagger = \sum_{ab} X_{ab}\{a^\dagger b^\dagger\} + \frac{1}{6}\sum_{abci}^{b,c\in\text{HOMOs}} X_{abci}\{a^\dagger b^\dagger c^\dagger i\}. \tag{5.37}$$

Note that the HOMOs in Eqs. (5.36) and (5.37) are both HOMOs for $N$-electron states. If the $N$-electron state has degenerate HOMOs (e.g. HOMOs of benzene have two-fold degenerate), the self-consistent $(N-2)$-electron state is likely to break

the spatial symmetry which could cause problems for excitation energy calculations. Therefore, HOMOs in 2pp-TDA usually contains one spatial orbital (two spin orbitals). Due to the asymmetry of 3p1h operators and 1p3h operators, restricting 3p1h operators but not 1p3h operators seems unbalanced for the 2pp-RPA. Therefore the restricted 2pp-RPA will not be discussed.

With these orbital restrictions, the scaling of the r2ph-RPA, the r2ph-TDA, and the r2pp-TDA can be reduced to $O(L^4)$ with Davidson's diagonalization[212].

## 5.3 Computation details

All the methods described above are implemented in QM4D[37], except for the unbalanced restricted 2pp-RPA. For testing purposes, all excitations have $\Delta S_z = 0$, and only closed-shell systems are tested. At the current stage, we only implemented direct diagonalization which scales as $O(L^6)$ even for restricted 2RPAs. All calculations in QM4D, except for FCI results in GAMESS[9]. By default, neutral excitation energies for electron number conserving EOMs are calculated at an $N-$electron reference, while DIP/DEA-EOM excitations are calculated at an $(N-2)$-electron reference, with the excitation energies expressed as differences of double electron affinities of an $N$-electron state with the lowest $N$-electron state. All calculations use HF references unless noted otherwise.

## 5.4 Results

### *5.4.1 $\hat{S}^2$ expression tests*

We first study the behavior of various $\langle \hat{S}^2 \rangle$ formulas for CO with 6-31G basis set as an example for the triplet excited states $a'^3\Sigma^+$ ($\pi \rightarrow \pi^*$). It is noted that results from Rowe's formula deviate from the exact value (2) very much, especially for pp-RPA and 2pp-RPA. Both TDA and Rev formulas deliver the exact value for all RPAs. They expectation values from the TDA and the Rev formula give no difference for

Table 5.1: $\hat{S}^2$ expectation values for different formulas. The state to study is the $a'^3\Sigma^+(\pi \rightarrow \pi^*)$ state of CO, with the basis set 6-31G. Rowe, TDA and Rev refers to Eqs. (5.20), (5.28) and (5.30) respectively.

| Formula | Rowe | TDA | Rev |
|---|---|---|---|
| TDHF | 2.133 | 2.000 | 2.000 |
| 2ph-RPA | 2.215 | 2.000 | 2.000 |
| pp-RPA | 2.003 | 2.000 | 2.000 |
| 2pp-RPA | 2.004 | 2.000 | 2.000 |

all examples in this study. The $\langle \hat{S}^2 \rangle$ assignments for the rest of the calculations in this Chapter use the TDA formula by default.

### *5.4.2 $H_2O$*

$H_2O$ is used as a test case for all methods with a relatively small basis set 6-31G. Since the basis set is small enough, all 2RPAs without restrictions can be tested. All data are listed in Table 5.2, with FCI calculations in the same basis set as a reference. CIS, TDHF and TDDFT-B3LYP[28, 30, 31] are most practiced methods to calculate single excitations, with the average errors of 0.5-1.0 eV. As a general trend, the 2ph-RPA/2ph-TDA and the r2ph-RPA/r2ph-TDA systematically pull down excitations from CIS and TDHF. The 2ph-RPA and the 2ph-TDA correct CIS and TDHF excitation energies in the correct direction, but underestimate the excitation energies by more than 1.5 eV. This is probably caused by the unbalanced treatment between the excited and ground states. Interestingly, with hole restrictions, the r2ph-RPA and the r2ph-TDA produce much better results, with errors below 0.5 eV. Pp-RPA and pp-TDA substantially underestimate the excitation energies, probably due to its HF reference, as the same calculations with a B3LYP reference reduce the error to about 1.0 eV. At this time, the 2pp-RPA and the 2pp-TDA produce better results while the the r2pp-TDA overestimate most excitations. The pp-RPA and the pp-TDA fails to capture single excitations from non-HOMO level, such as $^3A_1$ and $^1A_1$ in Table 5.2. The 2pp-RPA, the 2pp-TDA and the r2pp-TDA are all cable of

Table 5.2: $H_2O$ excitation spectra with different methods using a small basis set 6-31G. All calculations are done in QM4D[37], except for FCI in Gamess[9]. Unit: eV.

| State | $^3B_1$ | $^1B_1$ | $^3A_1$ | $^3A_2$ | $^1A_2$ | $^1A_1$ | MSE[b] |
|---|---|---|---|---|---|---|---|
| FCI | 7.63 | 8.37 | 9.85 | 10.07 | 10.58 | 10.93 | - |
| CIS | 8.33 | 9.3 | 10.12 | 10.55 | 11.2 | 11.77 | 0.64 |
| TDHF | 8.20 | 9.24 | 9.8 | 10.42 | 11.13 | 11.69 | 0.51 |
| TDDFT[a] | 6.92 | 7.72 | 8.66 | 9.24 | 9.83 | 9.88 | -0.87 |
| 2ph-RPA | 5.83 | 6.61 | 7.89 | 8.27 | 8.79 | 9.11 | -1.82 |
| 2ph-TDA | 5.95 | 6.67 | 8.15 | 8.38 | 8.86 | 9.19 | -1.71 |
| r2ph-RPA | 7.68 | 8.75 | 9.8 | 9.98 | 10.7 | 11.68 | 0.19 |
| r2ph-TDA | 7.8 | 8.8 | 10.11 | 10.1 | 10.77 | 11.77 | 0.32 |
| pp-RPA | 3.09 | 3.60 | NA | 5.49 | 5.76 | NA | -4.68 |
| pp-TDA | 2.98 | 3.49 | NA | 5.38 | 5.65 | NA | -4.79 |
| 2pp-RPA | 7.58 | 8.34 | 12.65 | 9.98 | 10.49 | 13.65 | 0.87 |
| 2pp-TDA | 7.46 | 8.22 | 12.53 | 9.86 | 10.37 | 13.53 | 0.75 |
| r2pp-TDA | 11.25 | 11.79 | 12.56 | 13.67 | 13.95 | 13.53 | 3.22 |

[a]: TDDFT with B3LYP functional.
[b]: mean signed error. For pp-RPA and pp-TDA, $^3A_1$ and $^1A_1$ states are excluded.

producing these non-HOMO excitations. Note that for all states studied here, no double excitations are involved.

We also tested the use of B3LYP references in the 2ph-RPA and the 2pp-RPA, where we use the eigenvalues and orbitals from B3LYP instead of HF in Eqs. (5.2)-(5.6) and (5.12)-(5.17). Neither the 2ph-RPA nor the 2pp-RPA based on B3LYP reference achieve reasonable excitation energies: the 2ph-RPA has many imaginary and negative excitations, while the 2pp-RPA predicts many low-lying double excitations. The bad performance of B3LYP reference is probably because the KS reference cannot response properly to the two-body interaction.

### *5.4.3 Be*

Be is a small atom with low-lying double excitations. Table 5.3 shows excitation energies of various methods with the basis set aug-cc-pVTZ with no f functions. Note that HF reference of the Be atom suffers from instability. Therefore, TDHF, the 2ph-

RPA, and the r2ph-RPA have imaginary eigenvalues. These eigenvalues are labeled explicitly imaginary rather than negative in some package[8] and literature[211]. At this case, pp-series methods are very accurate, since there are only two valence electrons in the system. CIS, TDHF and TDDFT cannot capture double excitations as expected. Among methods based on $N$-electron reference, r2ph-TDA is the best as it is free from stability issues and capable of describing double excitations while keeping the MSE relatively low. In fact, r2ph-TDA systematically underestimates the excitation energies, showing that there seems to be a missing ground state correlation energies. We think this is related to the HF instability issue where this $\sim$1 eV correlation energy comes from. The example of BH also confirms this hypothesis.

### *5.4.4 BH*

The BH molecule has both low-lying double excitations and non-HOMO single excitations. Table 5.4 lists some lowest excitations. The ground state configuration for BH is $(1\sigma)^2(2\sigma)^2(3\sigma)^2$, where $1\sigma$ is the $1s$ orbital of the B atom, while the two lowest virtual orbitals are $1\pi$ and $4\sigma$. CIS, TDHF and B3LYP miss quite a few double excitations from $3\sigma$ to $1\pi$. The 2ph-TDA captures all these double excitations, while the r2ph-RPA, the r2ph-TDA, the pp-RPA, the pp-TDA and the r2pp-TDA fail to capture the quintet $^5\Sigma$. Such a quintet state may not be of chemical interest as it probably has little coupling with the ground and other low-lying excited states due to its special high spin angular momentum. Again, a systematic downshift of r2ph-TDA excitation energies is observed, probably related to the HF instability. The pp-RPA and the pp-TDA could not describe single excitations from non-HOMO orbitals, such as the two transitions of $2\sigma \rightarrow 1\pi$. R2pp-TDA remedies this issue with qualitative descriptions on these transitions. Overall, the best method in Table 5.4 that capture most of the important excited states and with good quantitative results is r2ph-TDA.

Table 5.3: Be excitation spectra with different methods using the basis set aug-cc-pVTZ with no f functions. All calculations are done in QM4D[37], except for FCI in Gamess[9]. Unit: eV.

| Configuration | $1s^2 2s2p$ | $1s^2 2s2p$ | $1s^2 2s3s$ | $1s^2 2s3s$ | $1s^2 2p^2$ | $1s^2 2s3p$ | $1s^2 2p^2$ | MSE[c] |
|---|---|---|---|---|---|---|---|---|
| Term | $^3$P | $^1$P | $^3$S | $^1$S | $^1$D | $^3$P | $^3$P | - |
| Exp.[a] | 2.73 | 5.28 | 6.46 | 6.78 | 7.05 | 7.3 | 7.46 | - |
| FCI | 2.72 | 5.33 | 6.43 | 6.77 | 7.16 | 7.42 | 7.4 | 0.03 |
| CIS | 1.70 | 5.10 | 5.53 | 6.17 | NA | 6.56 | NA | -0.65 |
| TDHF[d] | -0.96$i$ | 4.84 | 5.49 | 6.16 | NA | 6.55 | NA | -1.64 |
| TDDFT[b] | 2.10 | 4.90 | 5.69 | 5.97 | NA | 6.08 | NA | -0.65 |
| 2ph-RPA[d] | -1.27$i$ | 3.74 | 5.12 | 5.45 | 5.92 | 6.15 | 6.19 | -1.76 |
| 2ph-TDA | 1.45 | 4.07 | 5.16 | 5.47 | 5.92 | 6.16 | 6.19 | -1.22 |
| r2ph-RPA[d] | -1.22$i$ | 3.77 | 5.15 | 5.47 | 5.94 | 6.17 | 6.21 | -1.73 |
| r2ph-TDA | 1.49 | 4.10 | 5.19 | 5.49 | 5.94 | 6.18 | 6.21 | -1.19 |
| pp-RPA | 2.73 | 5.36 | 6.44 | 6.77 | 7.18 | 7.43 | 7.46 | 0.06 |
| pp-TDA | 2.73 | 5.36 | 6.44 | 6.77 | 7.18 | 7.42 | 7.45 | 0.06 |
| r2pp-TDA | 2.73 | 5.34 | 6.44 | 6.77 | 7.18 | 7.43 | 7.46 | 0.06 |

[a]: Experimental values from NIST.
[b]: TDDFT with B3LYP functional.
[c]: MSE stands for mean signed error. The weights from spatial degeneracy are accounted. For CIS, TDHF and TDDFT, double excitations are excluded.
[d]: HF reference of the Be atom suffers from instability problem. The first "negative" triplet excitation energies are actually imaginary.

Table 5.4: BH excitation spectra with different methods using the basis set cc-pVTZ with no f functions. All calculations are done in QM4D[37], except for FCI in Gamess[9]. Unit: eV.

| Term | Transition | FCI | CIS | TDHF | B3LYP | 2ph-TDA | r2ph-RPA | r2ph-TDA | pp-RPA | pp-TDA | r2pp-TDA |
|---|---|---|---|---|---|---|---|---|---|---|---|
| $^3\Pi$ | $3\sigma \rightarrow 1\pi$ | 1.36 | 0.54 | -1.63$i$ | -0.44$i$ | -0.35 | -1.63$i$ | 0.24 | 1.64 | 1.61 | 2.40 |
| $^1\Pi$ | $3\sigma \rightarrow 1\pi$ | 3.01 | 2.87 | 2.66 | 2.71 | 1.25 | 1.84 | 2.11 | 3.25 | 3.22 | 4.26 |
| $^3\Sigma$ | $3\sigma^2 \rightarrow 1\pi^2$ | 4.79 | NA | NA | NA | 3.47 | 4.42 | 4.42 | 5.51 | 5.48 | 6.57 |
| $^1\Delta$ | $3\sigma^2 \rightarrow 1\pi^2$ | 6.00 | NA | NA | NA | 4.65 | 5.15 | 5.15 | 6.24 | 6.20 | 7.29 |
| $^1\Sigma$ | $3\sigma^2 \rightarrow 1\pi^2$ | 7.13 | NA | NA | NA | 5.43 | 5.97 | 5.97 | 7.08 | 7.09 | 8.16 |
| $^5\Sigma$ | $2\sigma 3\sigma \rightarrow 1\pi^2$ | 7.74 | NA | NA | NA | 5.86 | NA | NA | NA | NA | NA |
| $^3\Sigma$ | $3\sigma \rightarrow 4\sigma$ | 7.74 | 7.38 | 7.23 | 7.09 | 6.10 | 6.74 | 6.87 | 7.07 | 7.04 | 8.02 |
| $^3\Pi$ | $2\sigma \rightarrow 1\pi$ | 8.17 | 8.16 | 7.82 | 7.56 | 6.54 | 7.59 | 7.91 | NA | NA | 10.61 |
| $^1\Sigma$ | $3\sigma \rightarrow 4\sigma$ | 8.35 | 8.31 | 8.29 | 7.72 | 6.67 | 7.39 | 7.41 | 7.64 | 7.61 | 8.58 |
| $^1\Pi$ | $2\sigma \rightarrow 1\pi$ | 10.20 | 10.92 | 10.89 | 9.88 | 8.50 | 10.55 | 10.65 | NA | NA | 12.09 |
| MSE | - | - | -0.09 | -0.65 | -0.73 | -1.63 | -1.00 | -0.62 | 0.08 | 0.05 | 1.37 |

[a]: For all excitations studied here,

### *5.4.5 CO*

Various methods are tested on the CO molecule with results tabulated in Table 5.5. No double excitations are involved in the range of spectra of interest. The pp-TDA fails to capture single excitations from non-HOMO orbitals, such as $\pi \rightarrow \pi^*$ transitions. The r2pp-TDA qualitatively captures these states, however, systematically overestimating all excitation energies. For this system, HF reference is stable, and r2ph-TDA has the same level of error of CIS, TDHF and TDDFT, with relatively low average errors.

### *5.4.6 Correlation energy offsets*

Fig 5.1 plots the r2ph-TDA excitation energies with respect to the reference excitation energies for $H_2O$, Be, BH, and CO. The figure shows that the r2ph-TDA underestimates most of the excitation energies of Be, BH, and CO, especially those low-lying excitations. We speculate that this is due to some ground state correlation energy offsets caused by the uncorrelated HF reference. In fact, Be and BH suffer from HF instability and CO has a triple bond, all demonstrating some strong correlation. As a reference, the CISD correlation energies are -0.35 eV for $H_2O$, -1.24 eV for Be, -2.56 eV for BH, and -0.86 eV for CO, calculated from Gaussian 03[8]. Although these correlation energies do not match the offset in Fig 5.1, these numbers suggest that the correlation energies are correlated to the systematic underestimation of r2ph-TDA excitation energies.

## 5.5 Conclusions

2RPAs are tested to study molecular excitations. Based on orbital restrictions, the r2ph-RPA, the r2ph-TDA and the r2pp-TDA can describe all single excitations, and double excitations from HOMOs, with formal scaling of $O(L^4)$. Since the r2ph-RPA inherits all instability issues from TDHF, we suggest that the r2ph-TDA is preferable

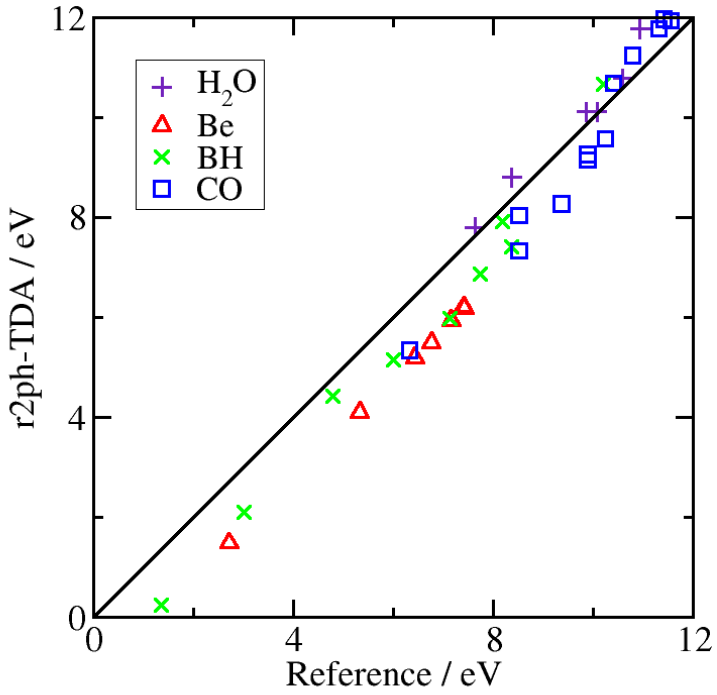


FIGURE 5.1: R2ph-TDA vs. reference excitation energies for $H_2O$, Be, BH, and CO. Basis sets are all aug-cc-pVTZ without f functions except that $H_2O$ uses 6-31G. The reference values for Be and CO are experimental values, while $H_2O$ and BH use FCI excitation energies from the same basis sets.

compared to the r2ph-RPA. The r2ph-TDA could systematically underestimates the excitation energies for systems with strong correlations, specially for systems with HF instability, probably due to the loss of ground state correlations. In theory, the r2pp-TDA is capable to describe what the r2ph-TDA can capture. However, the r2pp-TDA usually overestimates the excitation energies. Additionally, because the $N-2$ reference may be degenerate and the SCF result could deteriorate the symmetry, the r2pp-TDA is not advisable in general. Non-HF references are also tested for 2RPAs, yet the resulting excitation energies do not seem reasonable probably due to the incompetence of KS systems in responding two-body interactions. In conclusion, the

r2ph-TDA is recommended to study systems with both single and double excitations. Beyond the excitation energy tests, we also propose some expressions on property evaluations that are at least suitable for $\langle \hat{S}^2 \rangle$ calculations.

Table 5.5: CO excitation spectra with different methods using the basis set cc-pVTZ with no f functions. All calculations are done in QM4D[37], except for FCI in Gamess[9]. Unit: eV.

| State | Transition | Exp | CIS | TDHF | TDDFT | r2ph-TDA | pp-TDA | r2pp-TDA |
|---|---|---|---|---|---|---|---|---|
| $a^3\Pi$ | $\sigma \rightarrow \pi^*$ | 6.32 | 5.67 | 5.07 | 5.69 | 5.34 | 5.55 | 9.12 |
| $a'^3\Sigma^+$ | $\pi \rightarrow \pi^*$ | 8.51 | 7.34 | 5.79 | 7.51 | 7.33 | NA | 12.85 |
| $A^1\Pi$ | $\sigma \rightarrow \pi^*$ | 8.51 | 8.84 | 8.55 | 8.21 | 8.04 | 7.83 | 11.54 |
| $d^3\Delta$ | $\pi \rightarrow \pi^*$ | 9.36 | 8.28 | 7.37 | 8.23 | 8.27 | NA | 13.90 |
| $e^3\Sigma^-$ | $\pi \rightarrow \pi^*$ | 9.88 | 9.27 | 8.89 | 9.30 | 9.15 | NA | 14.82 |
| $I^1\Sigma^-$ | $\pi \rightarrow \pi^*$ | 9.88 | 9.27 | 8.89 | 9.30 | 9.26 | NA | 15.03 |
| $D^1\Delta$ | $\pi \rightarrow \pi^*$ | 10.23 | 9.69 | 9.49 | 9.63 | 9.57 | NA | 15.35 |
| $b^3\Sigma^+$ | $\sigma \rightarrow 3s$ | 10.40 | 11.20 | 11.10 | 9.89 | 10.68 | 8.88 | 12.50 |
| $B^1\Sigma^+$ | $\sigma \rightarrow 3s$ | 10.78 | 12.18 | 12.14 | 10.37 | 11.23 | 9.34 | 12.88 |
| $j^3\Sigma^+$ | $\sigma \rightarrow 3p\sigma$ | 11.30 | 12.44 | 12.42 | 10.62 | 11.77 | 9.68 | 13.28 |
| $C^1\Sigma^+$ | $\sigma \rightarrow 3p\sigma$ | 11.40 | 12.78 | 12.76 | 10.77 | 11.96 | 9.94 | 13.46 |
| $c^3\Pi$ | $\sigma \rightarrow 3p\pi$ | 11.55 | 12.57 | 12.39 | 10.87 | 11.93 | 9.98 | 13.59 |
| $E^1\Pi$ | $\sigma \rightarrow 3p\pi$ | 11.53 | 12.89 | 12.88 | 10.98 | 12.08 | 10.12 | 13.76 |
| MSE | - | - | 0.17 | -0.19 | -0.64 | -0.28 | -1.24 | 2.37 |

# 6

# Variational fractional spin density-functional theory for diradicals

## 6.1 Introduction

Diradicals are chemical species that have two electrons occupying two degenerate, or nearly-degenerate, frontier molecular orbitals[213]. Diradicals can exist as fleeting reactive intermediates in chemical reactions[214–217] or as stable structures used in molecular magnets[218–221] and other molecular electronic devices[222, 223]. Diradicals typically have low lying singlet and triplet states and the energy gap between these states ($\Delta E_{\mathrm{ST}} = E_{\mathrm{Singlet}} - E_{\mathrm{Triplet}}$) can be used as a predictive tool of their electronic properties and reactivity. Accurate predictions of the singlet-triplet energy gaps remains a challenge for conventional density-functional theory because of the multireference nature of the singlet state[224, 225]. Therefore, most computational studies involving singlet diradicals utilize *ab initio* multireference methods, such as CASSCF[226–228], CASPT2[229, 230], or multireference CC theory[231, 232]. Unfortunately, all these multireference *ab initio* methods are extremely computationally demanding.

This work is an extension to the previous work of fractional-spin density-functional theory (DFT) approaches to compute the ST gaps of diradicals[109]. Direct application of DFT usually takes the form of unrestricted calculations and is complicated with spin contamination that leads to overstabilization of singlet states similar to unrestricted Hartree-Fock calculations [226, 227, 233, 234]. Many efforts have been devoted to understanding and correcting spin contamination.[42, 227, 235–237] , and a factor-of-2 correction is normally needed to account for spin contamination[238]. One can also use spin-projection to improve the accuracy of unrestricted methods for calculating ST gaps [233, 239–241], but it is not a self-consistent approach and does not provide satisfactory densities. Despite the difficulty in describing singlet diradicals, DFT calculations of the high-spin triplet states ($M_s = 1$) are stable and reliable [242]. Thus several methods have been developed to address the singlet states of diradicals based on the electronic structure obtained from triplet-state computations. For instance, various spin-flip approaches treat the high-spin triplet state ($M_s = 1$) as the ground state and obtain the ST gaps using one-electron excitations involving a spin-flip process [243–247].

Recently, fractional-spin DFT (FS-DFT)[109] was proposed to calculate of singlet-triplet energy gaps for diradicals. FS-DFT is a special case of DFT with fractional orbital occupations[36, 75, 76, 86]. The fractional spin concept was originally proposed to illustrate current limitations of conventional functionals[35, 40]. In using FS-DFT for calculation of singlet diradical states, degenerate energy levels are assigned fractional occupancy with zero net spin by assigning equal fractional-spin occupancies (0.5 $\alpha$-spin and 0.5 $\beta$-spin) for each of the degenerate (or nearly-degenerate) frontier molecular orbitals.

In this Chapter, FS-DFT is extended to a variational fractional-spin density-functional theory (VFS-DFT) with optimization of the fractional occupation numbers. The paper is organized as follows. In Secction 6.2, we show how VFS-DFT

can be formulated by analogy to configuration interaction. We further present computational results for several diradicals to illustrate fractional-spin optimization of the singlet diradical energy in Section 6.3, with emphasis on the interesting case of $C_{2v}$ diradicals, for which FS-DFT and VFS-DFT can capture different singlet states. VFS-DFT reduces to FS-DFT for diradicals where the frontier orbitals belong to the same multidimensional irreducible representation. For diradicals in which the frontier orbitals can be confined to disjoint sets of atoms, neither FS-DFT nor VFS-DFT can predict correct gaps due to previously-identified fractional-spin (non-dynamical correlation, or static correlation) errors in conventional density functionals[35, 36, 40]. We conclude our work in Section 6.4.

## 6.2 Methods

### *6.2.1 Density-functional theory with fractional occupation numbers*

Kohn-Sham DFT [20, 21] (KS-DFT) maps a real interacting system onto a fictitious non-interacting system with the same electron density via

$$E_v[\rho] = T_S[\rho] + \int v(\mathbf{r})\rho(\mathbf{r})d\mathbf{r} + J[\rho] + E_{\mathrm{XC}}[\rho], \tag{6.1}$$

where $T_S$ is the kinetic energy of the non-interacting system with the same electron density $\rho$ as the interacting system, $v$ is the external potential, $J$ is the electron-electron Coulomb interaction, and all other energy contributions constitute the exchange correlation energy $E_{\mathrm{XC}}$. The approximation of $E_{\mathrm{XC}}$ is key to the accuracy of DFT since there is no clear route to the exact functional for all chemical systems.

DFT can be extended to densities obtained with fractional orbital occupations[36, 75–77, 86],

$$\rho^\sigma(\mathbf{r}) = \sum_i n_i^\sigma |\phi_i^\sigma|^2, \tag{6.2}$$

where $\sigma$ denotes different spins and $n_i^\sigma$ is the occupation number of orbital $\phi_i^\sigma$, which

can be any number between 0 and 1. The energy expression in Eq. (6.1) then becomes,

$$E_v[\rho] = \sum_{\sigma}\sum_{i} n_i^{\sigma} \langle \phi_i^{\sigma} | -\frac{1}{2}\nabla^2 | \phi_i^{\sigma} \rangle + J[\rho] + \int v(\mathbf{r})\rho(\mathbf{r}) d\mathbf{r} + E_{\mathrm{XC}}[\rho]. \tag{6.3}$$

The fractional occupation numbers introduced in Eq. (6.3) form the basis for two important exact conditions in DFT: the fractional-charge linearity condition and the fractional-spin constancy condition[35, 36, 40, 86], which are commonly violated by all density functional approximations. These two conditions have guided development of many novel functionals[42, 43, 46, 248]. The concept of fractional number of electrons has also been utilized to calculate redox potentials[249, 250]. In this work, we employ DFT with fractional occupation numbers to calculate singlet-triplet energy gaps of diradical systems.

### *6.2.2 Variational-fractional-spin DFT for diradicals*

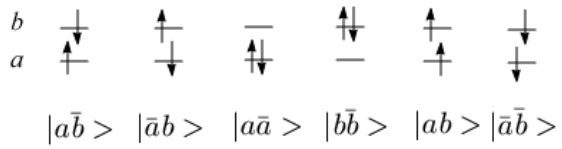


FIGURE 6.1: All six configurations in a two-level diradical model

Diradicals can be described by two electrons occupying two (nearly) degenerate frontier orbitals $a$ and $b$. This system contains six configurations as enumerated in Fig 6.1 using Szabo and Ostlund's notation[1]. Note that configurations $|a\bar{a}\rangle$ and $|b\bar{b}\rangle$ were not considered in our previous FS-DFT work[109]. The minimal building

blocks of spin-adapted singlet and triplet wavefunctions are

$$ {}_{O}\Phi_0^1 = 1/\sqrt{2}(|a\bar{b}\rangle - |\bar{a}b\rangle), \tag{6.4} $$

$$ {}_{A}\Phi_0^1 = |a\bar{a}\rangle, \tag{6.5} $$

$$ {}_{B}\Phi_0^1 = |b\bar{b}\rangle, \tag{6.6} $$

$$ \Phi_{-1}^3 = |\bar{a}\bar{b}\rangle, \tag{6.7} $$

$$ \Phi_0^3 = 1/\sqrt{2}(|a\bar{b}\rangle + |\bar{a}b\rangle), \tag{6.8} $$

$$ \Phi_1^3 = |ab\rangle, \tag{6.9} $$

where the superscript denotes the multiplicity (1 for singlet and 3 for triplet) and the subscript indicates the eigenvalues of $S_z$ (i.e., the spin operator in the $z$ direction). The left subscripts $A$, $B$, and $O$ are used to distinguish between three different singlet states (i.e., ${}_{O}\Phi_0^1$, ${}_{A}\Phi_0^1$, and ${}_{B}\Phi_0^1$). The wavefunction of ${}_{O}\Phi_0^1$ is sometimes referred as the "open-shell singlet".

In FS-DFT, an ensemble density can be constructed to obtain the same density described by ${}_{O}\Phi_0^1$,

$$ \rho_{\text{FS-DFT}} = \rho[{}_{O}\Phi_0^1] = 1/2\rho[|a\bar{a}\rangle] + 1/2\rho[|b\bar{b}\rangle]. \tag{6.10} $$

An algebraic analysis of the occupation numbers in $\rho_{\text{FS-DFT}}$ reveals that

$$ n_a^\alpha = n_a^\beta = n_b^\alpha = n_b^\beta = 1/2. $$

This ensemble density is constructed from the restricted spin orbitals and does not contain spin contamination. However, when full configuration interaction (FCI) is considered within the subspace in Fig 6.1, ${}_{A}\Phi_0^1$ and ${}_{B}\Phi_0^1$ can interact with ${}_{O}\Phi_0^1$ and thus the complete singlet state wave function is

$$ \Psi_0^1 = c_1({}_{O}\Phi_0^1) + c_2\,|a\bar{a}\rangle + c_3\,|b\bar{b}\rangle, \tag{6.11} $$

where $c_1$, $c_2$, and $c_3$ are FCI coefficients with the normalization constraint $c_1^2+c_2^2+c_3^2 = 1$.

Therefore, assuming real orbitals, the density associated with the FCI singlet state in Eq. (6.11) is

$$\rho[\Psi_0^1] = \begin{bmatrix} \phi_a & \phi_b \end{bmatrix} \begin{bmatrix} c_1^2/2 + c_2^2 & (c_1c_2 + c_1c_3)/\sqrt{2} \\ (c_1c_2 + c_1c_3)/\sqrt{2} & c_1^2/2 + c_3^2 \end{bmatrix} \begin{bmatrix} \phi_a \\ \phi_b \end{bmatrix}. \tag{6.12}$$

To eliminate the cross terms $\phi_a\phi_b$, we consider instead the two natural orbitals $\psi_p$ and $\psi_q$, which diagonalize the coefficient matrix in Eq. (6.12). The corresponding eigenvalues are

$$c_p, c_q = \frac{1}{2} \pm \frac{1}{2}(c_2 + c_3)\sqrt{2 - (c_2 + c_3)^2},$$

where the normalization constraint has been applied. We then rewrite $\rho[\Psi_0^1]$ in terms of natural orbitals, which yields the variational-fractional-spin DFT (VFS-DFT) density in this work,

$$\rho_{\text{VFS-DFT}} = \rho[\Psi_0^1] = c_p\rho[|p\bar{p}\rangle] + c_q\rho[|q\bar{q}\rangle]. \tag{6.13}$$

The coefficients in Eq. (6.13) are related to the frontier orbital occupation numbers by

$$n_p^\alpha = n_p^\beta = c_p\,, \quad n_q^\alpha = n_q^\beta = 1 - c_p = c_q, \quad c_p,\ c_q \in [0,\ 1]. \tag{6.14}$$

The FS-DFT density in Eq. (6.10), corresponds to the special case with $c_p = c_q = 1/2$ and the natural orbitals are $a$ and $b$ in Eq. (6.13). In VFS-DFT, $c_p$ is optimized to minimize the singlet state energy. Such optimization can be viewed as a version of the occupation optimization approach proposed by Ayers and Yang[251] within the framework of KS-DFT, but with the constraint that the resulting electron density is consistent with a singlet state. The ensemble density constructed by VFS-DFT is more flexible to describe the density of the diradical ground-state singlet. The concept of occupation number variation was previously studied in the spin-restricted ensemble-referenced Kohn-Sham method by Filatov and Shaik[252–255] and by Wang and Schwarz[256], with different total energy expressions.

In VFS-DFT, the energy derivative with respect to $c_p$ for a singlet state can be readily derived using Janak's Theorem[75] (the general expression of this derivative in generalized Kohn-Sham calculations with nonlocal potential is given by Cohen, Mori-Sánchez, and Yang[36])

$$\frac{dE_{\mathrm{S}}(c_p)}{dc_p} = \frac{\partial E_{\mathrm{S}}}{\partial c_p} - \frac{\partial E_{\mathrm{S}}}{\partial c_p} = -2(\epsilon_q - \epsilon_p) = -2\Delta\epsilon_{\mathrm{gap}}. \tag{6.15}$$

Here $\epsilon_p$ and $\epsilon_q$ are eigenvalues of $\psi_p$ and $\psi_q$, while $\Delta\epsilon_{\mathrm{gap}} = \epsilon_q - \epsilon_p$ is the eigenvalue gap of the two frontier orbitals, which should not be confused with the ST gap, $\Delta E_{\mathrm{ST}}$. At the energy minimum with no constraints, $\psi_p$ and $\psi_q$ become degenerate, such that $\epsilon_p = \epsilon_q = \epsilon_F$, where $\epsilon_F$ denotes the frontier orbital level. This degeneracy can also be explained by the Aufbau principle. Assuming both $c_p$ and $c_q$ are fractional, $\epsilon_p \neq \epsilon_q$ would result in a hole in the system, which violates the Aufbau principle. The $c_p$ optimization to minimize the total energy can be performed efficiently with this derivative information in Eq. (6.15). Such degeneracy is also consistent with previous research[75, 81].

With the objective function of $E_{\mathrm{S}}(c_p)$, we propose an algorithm to optimize the occupation number of the frontier orbital $\phi_p$ as follows,

1. With an initial guess or updated occupation number for $c_p$, establish occupation patterns according to Eq. (6.14);

2. Do a restricted SCF calculation according to the density and energy expressions in Eq. (6.2) and Eq. (6.3);

3. If not converged, go to Step 1 with an updated $c_p$ according to Eq. (6.15).

Please note that occupation numbers are all 1 for orbitals below the frontier orbital level and all 0 for orbitals above the frontier orbital level. The only changeable occupation numbers are $c_p$ and $c_q$ of the frontier orbitals. Actually, for a typical

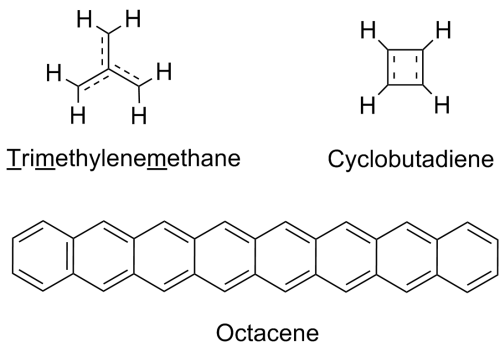


FIGURE 6.2: Structure of trimethylenemethane, cyclobutadiene, and octacene

diradical since it is just a one-dimensional problem, we carry out a scan of $E_S$ versus $c_p$ instead of an optimization.

### *6.2.3 Computational details*

VFS-DFT calculations were performed using the Amsterdam Density Functional (ADF) program[257] and the PBE[29] generalized-gradient approximation (GGA) functional in conjunction with the Slater-type TZP basis set. We have also used the VWN5 parametrization[25] of the local-density approximation (LDA) and the PBE functional implemented in the QM4D program [37] with the 6-311++G(2d,2p) Gaussian basis set. The use of PBE and LDA functionals were based on their better performance for fractional spin systems relative to hybrid functionals[36, 109]. The geometries used for NH, NF, $O_2$, $OH^+$, and trimethylenemethane (TMM) were adopted from our previous work[109]. Carbene-like molecule geometries were consistent with the calculations in Slipchenko and Krylov's work[244], where all geometries were summarized in Footnote/Ref. 86. The geometry of cyclobutadiene was taken from the work of Saito *et al*[258]. $\cdot CH_2CH_2CH_2\cdot$ and octacene geometries were optimized using UB3LYP/6-31G(d) with Gaussian 03[8] program. Fig 6.2 shows the structures of TMM, cyclobutadiene, and octacene.

Triplet-state energies were computed using unrestricted DFT. Since minimization of the VFS-DFT singlet-state energy with respect to $c_p$ is a one-dimensional problem, we performed scans over values between 0 and 1 rather than a complete optimization to analyze how variations in $c_p$ affect the energy.

## 6.3 Results and Discussion

### *6.3.1 Degenerate frontier orbitals*

Fig 6.3 shows the PBE/TZP VFS-DFT scan profiles of the singlet-triplet energy gaps ($\Delta E_{\mathrm{ST}}$) and the partially-occupied orbital-energy gaps ($\Delta\epsilon_{\mathrm{gap}}$) as a function of occupation number ($c_p$) for six representative diradicals: $O_2$, NF, NH, $OH^+$, TMM, and cyclobutadiene. Note that $\Delta E_{\mathrm{ST}}$ curves will have the same shape as $E_{\mathrm{S}}$ curves, because $E_{\mathrm{T}}$ is a constant, independent of $c_p$. The $\Delta\epsilon_{\mathrm{gap}}$ curves are shown as well, since $\Delta\epsilon_{\mathrm{gap}}$ is related to the derivative of $E_{\mathrm{S}}$ according to Eq. (6.15). As expected from symmetry arguments, all of these diradicals show a variational minimum and optimal occupation number $c_p = 1/2$, in that the two frontier orbitals belong to the same multidimensional irreducible representation. This situation is associated with exactly degenerate orbitals, such that $\Delta\epsilon_{\mathrm{gap}} = 0$ and VFS-DFT reduces to FS-DFT for these cases.

### *6.3.2 Non-degenerate frontier orbitals*

As another extreme, results for stretched $H_2$ and $\cdot CH_2CH_2CH_2\cdot$ in Fig 6.4 show that both $\Delta E_{\mathrm{ST}}$ and $\Delta\epsilon_{\mathrm{gap}}$ curves are almost flat. While the orbital-energy gap $\Delta\epsilon_{\mathrm{gap}}$ is quite small (ca. 1 kcal/mol for stretched $H_2$ and 3 kcal/mol for $\cdot CH_2CH_2CH_2\cdot$), it is non-zero for the entire range of $c_p$ values such that the two frontier orbitals never become degenerate. The $\sigma$-orbital is always lower in energy than the $\sigma^*$ and these orbitals would only become degenerate if the two H atoms or terminal $CH_2$ groups were infinitely separated. Both the orbital and singlet-triplet gaps are minimized with

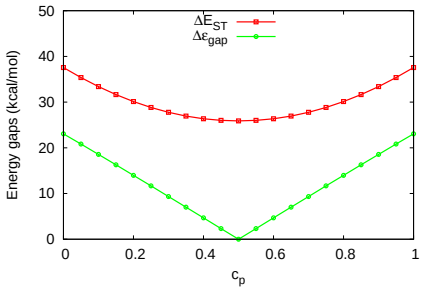


(a) $O_2$

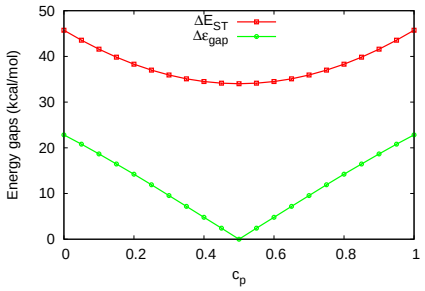


(b) NF

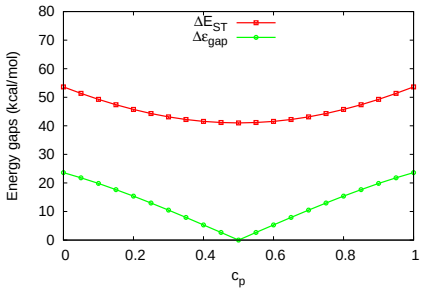


(c) NH

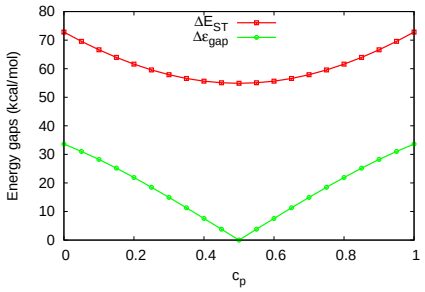


(d) $OH^+$

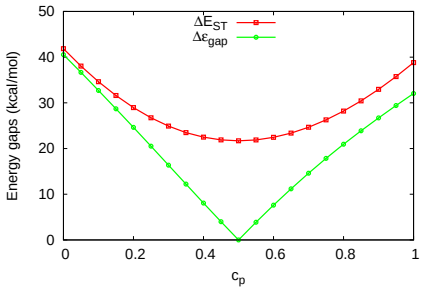


(e) TMM

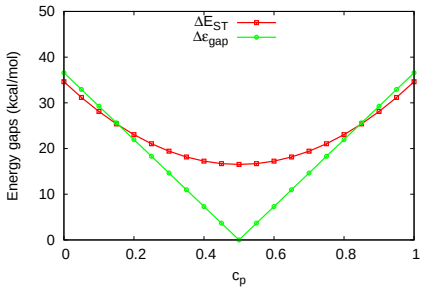


(f) Square cyclobutadiene

FIGURE 6.3: Plots of PBE singlet-triplet ($\Delta E_{\mathrm{ST}} = E_{\mathrm{S}}(c_p) - E_{\mathrm{T}}$) and orbital ($\Delta\epsilon_{\mathtt{gap}} = \epsilon_q - \epsilon_p$) energy gaps as functions of $c_p$ for six diradicals. The adiabatic $\Delta E_{\mathrm{ST}}$ is used for all cases, except cyclobutadiene, where the vertical $\Delta E_{\mathrm{ST}}$ is used. All data were calculated in ADF with the TZP basis set.

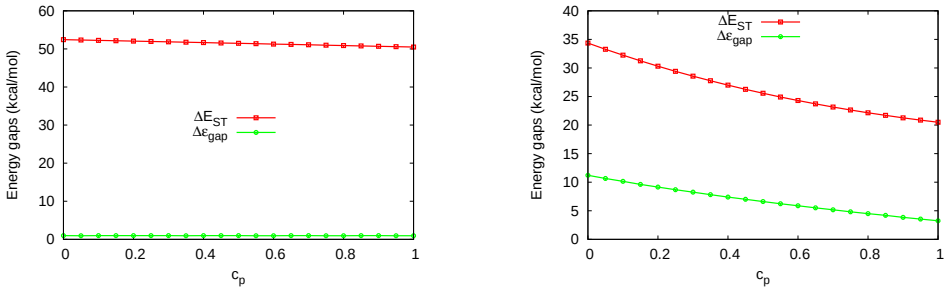


(a) $H_2$ (b) $CH_2CH_2CH_2$

FIGURE 6.4: Plots of PBE vertical singlet-triplet ($\Delta E_{\mathrm{ST}} = E_{\mathrm{S}}(c_p) - E_{\mathrm{T}}$) and orbital ($\Delta\epsilon_{\mathtt{gap}} = \epsilon_q - \epsilon_p$) energy gaps as functions of $c_p$ for stretched $H_2$ and the $\cdot CH_2CH_2CH_2\cdot$ diradical. All data were calculated in ADF with the TZP basis set.

$c_p = 1$ and the usual integer occupation numbers are obtained, which are identical to the solutions with a normal restricted KS-DFT calculation with the designated functionals. $\Delta\epsilon_{\mathrm{gap}}$ being non-zero does not violate the Aufbau principle, as the higher energetic orbital is fully unoccupied and the lower energetic orbital is fully occupied, with no hole below the frontier orbital level.

### *6.3.3 Two types of diradicals*

The LDA and PBE singlet-triplet energy gaps obtained from VFS-DFT for diradicals are present in Table 6.1. These diradicals are grouped into two blocks for reasons discussed below. As stated previously, VFS-DFT reduces to FS-DFT for the diradicals in the upper block and reasserts the validity of the FS-DFT approach. To the contrary, VFS-DFT always overestimates $\Delta E_{\mathrm{ST}}$ of diradicals in the lower block compared to the reference values, even predicting the wrong signs for stretched $H_2$ and cyclobutadiene. We observe that the reference $\Delta E_{\mathrm{ST}}$'s for diradicals in the lower block are fairly small compared to the values in the upper block.

Table 6.1: Singlet-triplet energy gaps (in kcal/mol) calculated with VFS-DFT using the LDA and PBE functionals with the 6-311++G(2d,2p) basis set calculated by QM4D. The numbers in the parentheses indicate the optimal occupation number, $c_p$.

| Molecules[a] | Ref. | VFS-LDA | VFS-PBE |
|---|---|---|---|
| NH | 35.9[c] | 35.9(0.50) | 41.1(0.50) |
| NF | 34.3[c] | 30.3(0.50) | 34.0(0.50) |
| $OH^+$ | 50.5[c] | 48.4(0.50) | 54.8(0.50) |
| $O_2$ | 22.6[c] | 23.6(0.50) | 26.2(0.50) |
| TMM[b] | 16.1[c] | 15.4(0.50) | 21.5(0.50) |
| Cyclobutadiene | -8.1[d] | 12.41(0.50) | 16.53(0.50) |
| $H_2$($R_{HH}$ =5 Å) | -0.002[e] | 40.3(1.00) | 50.5(1.00) |
| $\cdot CH_2CH_2CH_2\cdot$ | 1.8[e] | 12.8(1.00) | 20.4(1.00) |

[a] The geometries of the molecules in the upper block are adopted from our previous work[109]. The geometry of square cyclobutadiene is adopted from Ref. [241]. The $\cdot CH_2CH_2CH_2\cdot$ geometry is optimized with UB3LYP/6-31G(d) in Gaussian 03[8]. $\Delta E_{ST}$'s for NH, NF, $OH^+$, and $O_2$ are adiabatic gaps, while those for TMM, square cyclobutadiene, stretched $H_2$, and $\cdot CH_2CH_2CH_2\cdot$ are vertical gaps.
[b] Trimethylenemethane.
[c] Experimental values from Ref. [244] are used.
[d] CASSCF/MkCCSD values from Ref. [241].
[e] CASMP2 results were computed by Gaussian 03[8]. Specifically, CASMP2(2,4)/6-311++G(2d,2p) for $H_2$ and CASMP2(8,8)/6-311++G(2d,2p) for $\cdot CH_2CH_2CH_2\cdot$.

According to Borden and Davidson[259], diradicals can be divided into two groups based on whether their frontier orbitals are confined to different sets of atoms. Their argument was based on Hückel-theory analysis of conjugated hydrocarbon diradicals, which can be generalized to all diradical systems. If the frontier orbitals (FO) can be confined to separate sets of atoms (disjoint or FO-separable), the $\Delta E_{ST}$ is very small and the sign may be positive or negative; if the frontier orbitals cannot be confined to separate sets of atoms (FO-non-separable), the $\Delta E_{ST}$ is positive and usually considerable. TMM and cyclobutadiene were prototypes of FO-non-separable and FO-separable diradicals in Borden and Davidson's original work[259]. In Table 6.1, all diradicals in the upper block are FO-non-separable, while diradicals in the lower block are FO-separable. Our calculation suggests that VFS-DFT with LDA

or PBE gives much larger errors for FO-separable diradicals. Since by definition the FS-DFT gaps are always no smaller than VFS-DFT gaps, the FS-DFT gaps for FO-separable diradicals would be even worse.

The distinct behavior of two different kinds of diradicals brought our attention to fractional-spin error. The failure of common functionals to describe the stretched hydrogen molecule is well understood in terms of the "fractional-spin" or "non-dynamical correlation" error[35, 36]. However, current results indicate that fractional-spin error may be very different from case to case. Thus, we briefly review the concept of fractional-spin error below.

Yang, Zhang, and Ayers[77] proved that with the exact density functional, for an $N$-electron system with $g$ degenerate ground states, the energy of an arbitrary ensemble density of orthogonal ground state wavefunctions is constant.

$$E_v\left[\sum_{i=1}^{g} c_i\rho_i\right] = E_v[\rho_i] = E_v^0(N) \tag{6.16}$$

In this equation, $E_v$ is the energy functional, and $\rho_i$ is the electron density of one of the $g$ ground-state wavefunctions $\Psi_i$. The weighting factors $c_i$'s are all non-negative and sum to unity. The degeneracy could be generated from spin and or spatial symmetry. The violation of Eq. 6.16 is usually referred as fractional-spin error in the spin-degenerate case (however, such error could also originate from spatial symmetry). For example, Fig 6.5 is a partial reproduction of Fig 2 in Ref. [35], which describes the error as a spin-polarized carbon atom at $\xi = 0$ gradually becomes spin-compensated at $\xi = 1$. Fig 6.5 is essential to explain the wrong dissociation limit of $C_2$ molecule for common density functionals, with the dissociation error twice as the fractional spin error at $\xi = 1$. At the same time, the state at $\xi = 1$ is the very fractional-spin state where we obtain the singlet-triplet energy gap for a carbon atom, i.e. 31.5 kcal/mol for LDA and 34.1 kcal/mol for PBE, compared to the

experimental 29.1 kcal/mol. Following this logic, for fractional-spin-error-free functionals, the error at $\xi = 1$ will be zero, then the fractional-spin ansatz renders $\Delta E_{\mathrm{ST}}$ as zero, interpreting the FS-DFT density as an $M_s = 0$ triplet state rather than a singlet state. This contradiction lies in the definition of the functional. The exact ground-state (spin) density functional (defined in the Levy constrained search[22]) is free from fractional-spin error and symmetry-independent. However, the singlet-triplet energy gap involves an excited state in general, thus a spin-specific (or more generally, symmetry-specific)[260] density functional is needed. Unfortunately, current functionals are neither fractional-spin error free nor spin-specific. Commonly used ground-state functional approximations describe well the highest $M_s$ state of the lowest energy of each spin eigenstates, for example, the $M_s = 1$ state of the lowest energy triplet state. The lack of symmetry-specific functional complicates the challenge of the fractional spin error. Nevertheless, FS-DFT/VFS-DFT are still good ansatz to capture singlet states.

In the context of such symmetry non-specific functionals, fractional-spin errors are still very distinct from system to system. Previous study and our test calculations on a spherical carbon atom indicate that fractional-spin errors of systems with spatial degeneracy and localized orbitals tend to be much smaller in scale. The success of VFS-DFT in FO-non-separable diradicals may be rooted in similar reasoning. The details are still being studied.

### *6.3.4 Carbene-like diradicals*

We next consider the interesting case of the $XH_2$ diradical (X=C, N, Si, P), in which the frontier orbitals are of different symmetry ($A_1$ and $B_1$) and are therefore possibly, but not necessarily, degenerate. Hence, the optimal $c_p$ cannot be predicted *a priori*.

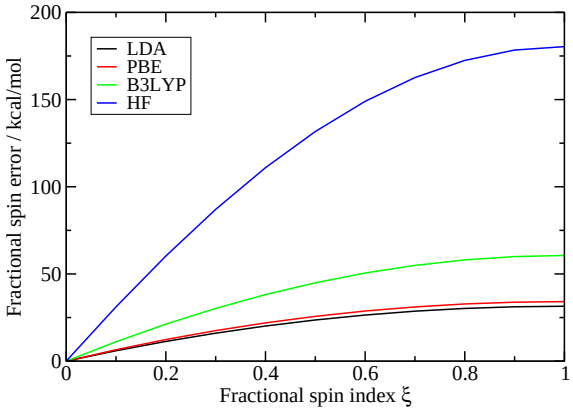


FIGURE 6.5: Fractional spin error of a carbon atom as the two electrons in $p$ shell become depolarized. The fractional spin error is defined as $e(\xi) = E_{\mathrm{DFA}}[(1-\xi/2)(\rho_{2p_x} + \rho_{2p_y}),\ \xi/2(\rho_{2p_x} + \rho_{2p_y})] - E_{\mathrm{DFA}}[\rho_{2p_x} + \rho_{2p_y},\ 0]$, with $1s$ and $2s$ doubly occupied. At $\xi = 0$, two electrons in $p$ shell are fully polarized, while at $\xi = 1$, two electrons in $p$ shell are fully spin-compensated. The energy at $\xi = 0$ is set zero for each functional. The calculations are performed with 6-311++G(2d,2p) basis set in a modified version of NWChem package[10].

The two low-lying singlet states in these molecules are $^1A_1$ and $^1B_1$ states,

$$\Phi(^1B_1) = 1/\sqrt{2}(|a_1\bar{b}_1\rangle - |\bar{a}_1 b_1\rangle), \tag{6.17}$$

$$\Phi(^1A_1) = 1/\sqrt{1+\lambda^2}(|a_1\bar{a}_1\rangle - \lambda\,|b_1\bar{b}_1\rangle). \tag{6.18}$$

Fig 6.6 presents fractional scan profiles for $CH_2$ at bond angles ranging from $90^\circ$ to $180^\circ$, with a fixed bond length of 1.1089 Å, which is the equilibrium bond length for the $^1A_1$ state[244]. As the bond angle increases from $90^\circ$ to $180^\circ$, the optimal $c_p$ decreases from 1.0 to 0.5. At the linear configuration, we find the optimal $c_p = 1/2$, and VFS-DFT reduces to FS-DFT, as expected from symmetry analysis. Davidson[261] has shown that when a $CH_2$-like $C_{2v}$ diradical is straightened, the $^1A_1$ state and the $^1B_1$ states become a set of twofold degenerate $^1\Delta_g$ states. This occurs because the $a_1$ and $b_1$ orbitals of $C_{2v}$ symmetry become a pair of degenerate $\pi_u$ orbitals of $D_{\infty h}$ symmetry. When the fixed bond length is changed from 1.1089 Å to 1.0748 Å, the equilibrium bond length of $^1B_1$ state, the energy differences are

usually less than 1 kcal/mol. Scan profiles of $NH_2^+$, $SiH_2$, and $PH_2^+$ all have very similar overall trends with increasing bond angle.

In this special symmetry of $C_{2v}$, $\Phi(^1B_1)$ and $\Phi(^1A_1)$ do not interact even in the configuration interaction picture owing to different symmetry. In other words, $c_1$, $c_2$ and $c_3$ in Eq. (6.11) cannot be nonzero at the same time. In case $c_1 = 0$, we will have $\Phi(^1A_1)$, with optimal $c_p = \lambda^2/(1+\lambda^2)$ (or $1/(1+\lambda^2)$, depending on the indexing of the orbital). On the other hand, in case $c_2 = c_3 = 0$, the full CI wavefunction is just $\Phi(^1B_1)$, with fixed optimal occupation number $c_p = 1/2$. If energies are assigned such that

$$E(^1B_1) = E_{\text{FS-DFT}} = E_{\text{S}}(c_p = 1/2),$$
$$E(^1A_1) = E_{\text{VFS-DFT}} = \min_{c_p} E_{\text{S}}(c_p),$$

then the potential-energy surfaces of the two singlet states for $CH_2$ and $NH_2^+$ can be obtained from the fractional scan profiles at each angle. These results are shown in Fig 6.6, and compared to reference high-level *ab initio* potential-energy surfaces[262–264]. It is clear from the potential-energy surfaces that the glancing intersection[265] that occurs at the linear configuration of $CH_2$ and $NH_2^+$ is captured by this combination of FS-DFT and VFS-DFT approaches. The equilibrium bond angles for the $^1B_1$ and $^1A_1$ states from PBE are qualitative close to the reference data, viz. 141.56° and 101.89° for $CH_2$, and 161.47° and 107.96° for $NH_2^+$[244]. While the FS/VFS-DFT potential-energy surfaces are qualitatively correct, the quantitative well depths are not accurately reproduced. This is nevertheless impressive considering that only the simple LDA and PBE functionals were used and it is possible that more advanced functionals could produce more accurate potential-energy surfaces.

We present the adiabatic $\Delta E_{\text{ST}}$'s of both $^1A_1$ and $^1B_1$ states for four $C_{2v}$ diradicals in Table 6.2. Note that for $SiH_2$ and $PH_2^+$ the ground states are $^1A_1$ state rather than triplet and the optimal occupation number is $c_p = 1$, indicating the solutions are

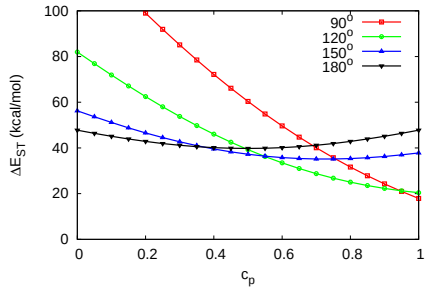


(a) $CH_2$ scan profiles

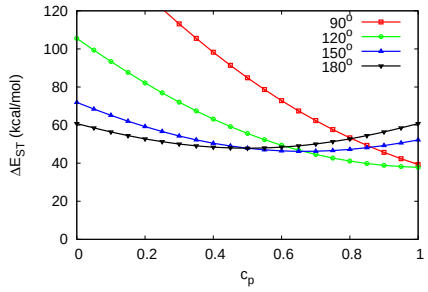


(b) $NH_2^+$ scan profiles

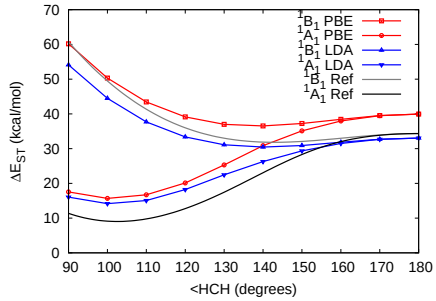


(c) $CH_2$ bending potential

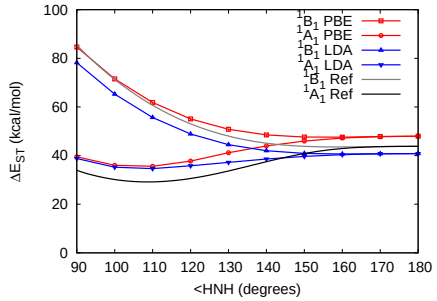


(d) $NH_2^+$ bending potential

FIGURE 6.6: PBE fractional scan profiles for selected bond angles for the $CH_2$ and $NH_2^+$ molecules by ADF. Potential-energy surfaces obtained with a combined FS-DFT and VFS-DFT approach are compared to literature MRCI data[262–264]. All calculations used fixed equilibrium bond lengths for the $^1A_1$ state, adopted from Footnote/Ref. 86 in Slipchenko and Krylov's work[244], which are 1.1089 Å and 1.0459 Å for $CH_2$ and $NH_2^+$, respectively. The $\Delta E_{\mathrm{ST}}$ is the adiabatic energy gap.

restored to the normal KS-DFT calculation with integer occupations. Results show that the $^1B_1$ reference values always fall between the FS-LDA and FS-PBE gaps. The error of both functionals is about 3 kcal/mol. For $^1A_1$ states, the differences between LDA and PBE functionals tend to be smaller, while both functionals systematically overestimate $\Delta E_{\mathrm{ST}}$ for about 3-5 kcal/mol.

In general, VFS-DFT will always reach the lowest-energy singlet state regardless of the symmetry. However, with special symmetry, the combination of FS-DFT and

Table 6.2: Adiabatic singlet-triplet energy gaps for $C_{2v}$ diradicals in kcal/mol by QM4D

| | | $CH_2$ | $NH_2^+$ | $SiH_2$ | $PH_2^+$ | MUE |
|---|---|---|---|---|---|---|
| | FS-LDA | 30.24 | 41.03 | 18.96 | 22.98 | -3.1 |
| $^1B_1$ | FS-PBE | 36.22 | 47.82 | 24.01 | 28.81 | 2.8 |
| | Ref. | 31.74[a] | 43.55[b] | 23.5±0.7[c] | 27.±1.[e] | |
| | VFS-LDA | 14.13(1.0) | 34.55(1.0) | -18.92(1.0) | -15.65(1.0) | 3.5 |
| $^1A_1$[f] | VFS-PBE | 15.66(1.0) | 35.45(1.0) | -16.09(1.0) | -12.75(1.0) | 5.5 |
| | Ref. | 9.03[a] | 29.16[b] | -21.0±0.7[d] | -17.±1.[e] | |

[a] Experimental values from Ref. [263].
[b] MRCI values from Ref. [262].
[c] Experimental values from Ref. [266].
[d] Experimental values from Ref. [267].
[e] Experimental values from Ref. [268].
[f] The values in the parentheses in $^1A_1$ series indicate the optimal occupation number $c_p$.

VFS-DFT can potentially capture more than just the lowest singlet state. Above is a vivid example that the lower-energy $^1A_1$ state is captured with VFS-DFT and the higher-energy $^1B_1$ state with FS-DFT in carbene-like diradicals. The treatment of the $^1B_1$ state in FS-DFT is very similar to the perspective of constrained-DFT[269] or block-localized-wavefunction DFT[270], in that the ground state with constraints generally corresponds to an excited state. The main difference is that the constraint imposed by FS-DFT is placed on the Kohn-Sham molecular orbital occupation number rather than spatial localization.

### *6.3.5 Octacene*

Polyacenes are potential semiconducting materials that can be used in development of field-effect transistors[271]. Prediction of their singlet-triplet energy gaps is of considerable interest and also challenging due to their comparatively large molecular sizes. We will consider the case of octacene as a prototypical large polyacene. The point group of octacene is $D_{2h}$, which is a direct product of the $C_{2v}$ and $C_i$

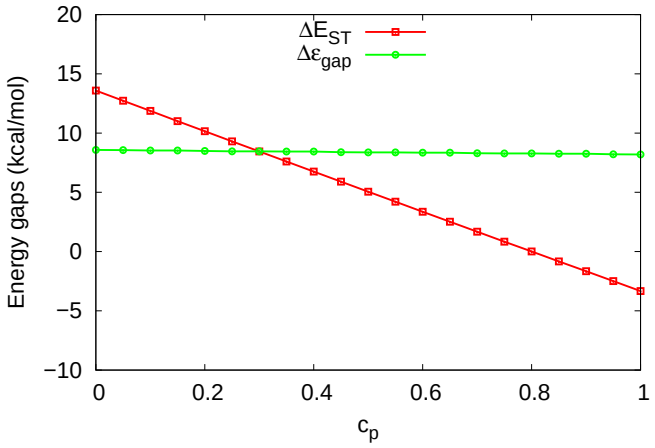


FIGURE 6.7: Plots of PBE vertical singlet-triplet ($\Delta E_{\mathrm{ST}} = E_{\mathrm{S}}(c_p) - E_{\mathrm{T}}$) and orbital ($\Delta\epsilon_{\mathrm{gap}} = \epsilon_q - \epsilon_p$) energy gaps as a function of $c_p$ for octacene. All data were calculated in ADF with the TZP basis set.

point groups. Similar to $C_{2v}$, $D_{2h}$ does not have a multidimensional irreducible representation. Therefore, we expect that FS-DFT and VFS-DFT can capture the ${}^1B_{3u}$ state (corresponding to ${}^1B_1$ state in $C_{2v}$ group) and the ${}^1A_g$ state (corresponding to ${}^1A_1$ state in $C_{2v}$ group) respectively. The PBE fractional spin scan profile of octacene is plotted in Fig 6.7. The resulting $\Delta E_{\mathrm{ST}}$ is -3.3 kcal/mol for ${}^1A_g$ state and 5.5 kcal/mol for ${}^1B_{3u}$ state. From the scan profile, the two frontier orbitals never become degenerate and the minimum $\Delta E_{\mathrm{ST}}$ occurs at $c_p = 1.0$. Therefore, VFS-DFT lowers the singlet energy (relative to FS-DFT), capturing ${}^1A_g$ state as the ground state. The conclusion in our previous work[109] that the triplet state was the ground state was biased by the inability to capture ${}^1A_g$ state within FS-DFT framework. The VFS-DFT result is comparable with the previous broken-symmetry unrestricted DFT calculations[272]. Quantitatively, the VFS-DFT gap is close to the previous studies, i.e. -5.8 kcal/mol for B3LYP/6-31G(d) and -2.9 kcal/mol BLYP/6-31G(d).[272] However, it should be noted that octacene is reported to have disjoint features[109, 272], like $\cdot CH_2CH_2CH_2\cdot$ and stretched $H_2$. Since conventional function-

als perform poorly for disjoint diradicals, due to fractional-spin error, our predictions of the gap are likely overestimated.

## 6.4 Conclusions

VFS-DFT was developed as an extension of our previous FS-DFT approach to compute singlet-triplet energy gaps of diradicals. For normal molecules with close-shell singlet ground states, the VFS-DFT approach reduces to normal KS-DFT calculations with integer occupations. VFS-DFT was applied to several types of diradicals and it was found that VFS-DFT reduces to FS-DFT if the frontier orbitals belong to the same multidimensional irreducible representation. In the case of carbene-like diradicals, the $^1A_1$ and $^1B_1$ states can be captured by VFS-DFT and FS-DFT, respectively. While VFS-DFT performs well for frontier-orbital non-separable diradicals, it drastically overestimates $\Delta E_{\mathrm{ST}}$ for frontier-orbital separable (disjoint) diradicals, because of fractional-spin error. Our calculations thus suggest that fractional-spin errors inherent in conventional density-functional approximations are much more significant for FO-separable diradicals. The detailed connection between FO-separability and the the magnitude of fractional-spin error requires further study. A brief review on the fractional-spin errors shows that the concept of spin-specific functional is needed for DFT to calculate $\Delta E_{\mathrm{ST}}$.

# Appendix A

## Second Quantization

### A.1 Operator and wavefunction representations

This Dissertation uses the same convention as in Shavitt and Bartlett[12]. The basic second quantization operators are the creation operator $a_u^\dagger$ which creates a particle of $\phi_u$, and its Hermitian conjugate, the annihilation operator $a_u$ which annihilates a particle of $\phi_u$. For simplicity, when there is no confusion, we use $u^\dagger$ and $u$ to represent $a_u^\dagger$ and $a_u$ respectively. We assume that the set of orbitals $\phi$'s are orthonormalized.

There is a vacuum state $|\text{vac}\rangle$ which contains no electrons. Any wavefunction can be generated by creating particles from the vacuum state. For example, a one-particle wavefunction ket of $\phi_u$ is

$$|\phi_u\rangle = |u\rangle = u^\dagger|\text{vac}\rangle, \tag{A.1}$$

while the annihilation of the same particle returns $|\phi_u\rangle$ to a vacuum

$$u|u\rangle = |\text{vac}\rangle. \tag{A.2}$$

Any annihilation operator acting on a vacuum state produces zero,

$$u|\text{vac}\rangle = 0. \tag{A.3}$$

For Fermions, the antisymmetrization of the particles require

$$\{u^\dagger, v\} \equiv u^\dagger v + v u^\dagger = \delta_{uv}, \tag{A.4}$$

$$\{u, v\} \equiv uv + vu = 0, \tag{A.5}$$

$$\{u^\dagger, v^\dagger\} \equiv u^\dagger v^\dagger + v^\dagger u^\dagger = 0, \tag{A.6}$$

where $\{\ ,\ \}$ is an anticommutator. Eqs. (A.4)-(A.6) are the most important basic equations used in the derivation.

A HF determinant in Eq. (1.3) can be expressed as

$$|\Phi_{\rm HF}\rangle = |\phi_1\phi_2\cdots\phi_N\rangle = a_1^\dagger a_2^\dagger \cdots a_N^\dagger |{\rm vac}\rangle = \prod_i i^\dagger |{\rm vac}\rangle. \tag{A.7}$$

A single excitation configuration can be expressed as $a^\dagger i|\Phi_{\rm HF}\rangle$, while a double excitation configuration can be expressed as $a^\dagger i b^\dagger j|\Phi_{\rm HF}\rangle$, etc.

A one-body operator can be expressed as

$$\hat{h} = \sum_{pq} |p\rangle\langle p|\hat{h}|q\rangle\langle q| = \sum_{pq} h_{pq} p^\dagger q, \tag{A.8}$$

while a two-body operator can be expressed as

$$\hat{G} = \sum_{pqrs} \frac{1}{2}|pq\rangle\langle pq|\hat{G}\frac{1}{2}|sr\rangle\langle sr| = \frac{1}{4}\sum_{pqrs}\langle pq|\hat{G}|sr\rangle p^\dagger q^\dagger r s. \tag{A.9}$$

If $\hat{G}$ is the two electron repulsion,

$$\begin{aligned}
\langle pq|\hat{G}|sr\rangle &= \int d\mathbf{x}_1 d\mathbf{x}_2 \frac{1}{\sqrt{2!}} \begin{vmatrix} \phi_p(\mathbf{x}_1) & \phi_p(\mathbf{x}_2) \\ \phi_q(\mathbf{x}_1) & \phi_q(\mathbf{x}_2) \end{vmatrix}^* \frac{1}{r_{12}} \frac{1}{\sqrt{2!}} \begin{vmatrix} \phi_s(\mathbf{x}_1) & \phi_s(\mathbf{x}_2) \\ \phi_r(\mathbf{x}_1) & \phi_r(\mathbf{x}_2) \end{vmatrix} \\
&= \frac{1}{2}\int d\mathbf{x}_1 d\mathbf{x}_2 (\phi_p(\mathbf{x}_1)\phi_q(\mathbf{x}_2) - \phi_q(\mathbf{x}_1)\phi_p(\mathbf{x}_2))^* \\
&\quad \times \frac{1}{r_{12}}(\phi_s(\mathbf{x}_1)\phi_r(\mathbf{x}_2) - \phi_r(\mathbf{x}_1)\phi_s(\mathbf{x}_2)) \\
&= \langle pq||sr\rangle
\end{aligned} \tag{A.10}$$

Thus the electronic Hamiltonian in second quantization is

$$\hat{H} = \sum_{pq} h_{pq} p^\dagger q + \frac{1}{4} \sum_{pqrs} \langle pq||sr\rangle p^\dagger q^\dagger rs. \tag{A.11}$$

## A.2 Normal order

Deriving second quantization formula is mainly based on Eqs. (A.4)-(A.6). However, the maths involved become very complicated when the number of operators increases. One way to simplify the derivation is to use normal order in Wick's theorem contraction[12].

An operator is referred as in normal order if all killer operators with respect to some reference is to the right of all non-killer operators. The reference we use will be the HF wavefunction in Eq. (A.7), and the killer operators are $a$ for all virtual orbitals and $i^\dagger$ for all occupied orbitals. We define a procedure to bring a string of operators to normal order by reorganizing the operators into normal order while multiplying the signature of the necessary permutation. This procedure is denoted by a pair of curly bracket. For example,

$$\{ab\} = ab = -ba, \tag{A.12}$$

$$\{ij\} = ij = -ji, \tag{A.13}$$

$$\{a^\dagger b^\dagger\} = a^\dagger b^\dagger = -b^\dagger a^\dagger, \tag{A.14}$$

$$\{i^\dagger j^\dagger\} = i^\dagger j^\dagger = -j^\dagger i^\dagger. \tag{A.15}$$

$$\{a^\dagger i\} = a^\dagger i = -i a^\dagger, \tag{A.16}$$

Note that there may be more than one way to reorganize the operators into normal order, but due to the factor of the signature of the necessary permutation, they are all equivalent. Here are some more examples where there is only one unique normal

ordered form for each of them,

$$\{a^\dagger b\} = a^\dagger b, \tag{A.17}$$

$$\{ab^\dagger\} = -b^\dagger a, \tag{A.18}$$

$$\{ij^\dagger\} = ij^\dagger, \tag{A.19}$$

$$\{i^\dagger j\} = -ji^\dagger. \tag{A.20}$$

A normal ordered contraction of a pair of operators is defined as

$$\overbrace{\hat{A}\hat{B}} = \hat{A}\hat{B} - \{\hat{A}\hat{B}\} \tag{A.21}$$

The only nonzero pair contractions are those that are not normal ordered, i.e.

$$\overbrace{i^\dagger j} = i^\dagger j - \{i^\dagger j\} = i^\dagger j + ji^\dagger = \delta_{ij}, \tag{A.22}$$

and

$$\overbrace{ab^\dagger} = ab^\dagger - \{ab^\dagger\} = ab^\dagger + ba^\dagger = \delta_{ab}. \tag{A.23}$$

Wick's theorem proved that a string of operators equals its normal ordered plus all possible pair contractions. For example, for a string of four creation and annihilation operators,

$$\begin{aligned}
\hat{A}\hat{B}\hat{C}\hat{D} = {} & \{\hat{A}\hat{B}\hat{C}\hat{D}\} + \{\overbrace{\hat{A}\hat{B}}\hat{C}\hat{D}\} + \{\hat{A}\overbrace{\hat{B}\hat{C}}\hat{D}\} + \{\hat{A}\hat{B}\overbrace{\hat{C}\hat{D}}\} + \{\overbrace{\hat{A}\hat{B}\hat{C}\hat{D}}\} \\
& + \{\overbrace{\hat{A}\hat{B}\hat{C}}\hat{D}\} + \{\hat{A}\overbrace{\hat{B}\hat{C}\hat{D}}\} + \{\overbrace{\hat{A}\overbrace{\hat{B}}\hat{C}}\hat{D}\} + \{\overbrace{\hat{A}\overbrace{\hat{B}\hat{C}}\hat{D}}\} + \{\overbrace{\hat{A}\hat{B}}\overbrace{\hat{C}\hat{D}}\} \qquad \text{(A.24)} \\
= {} & \{\hat{A}\hat{B}\hat{C}\hat{D}\} + \overbrace{\hat{A}\hat{B}}\{\hat{C}\hat{D}\} + \{\hat{A}\hat{B}\}\overbrace{\hat{C}\hat{D}} + \overbrace{\hat{B}\hat{C}}\{\hat{A}\hat{D}\} + \overbrace{\hat{A}\hat{D}}\{\hat{B}\hat{C}\} \\
& - \overbrace{\hat{A}\hat{C}}\{\hat{B}\hat{D}\} - \overbrace{\hat{B}\hat{D}}\{\hat{A}\hat{C}\} - \overbrace{\hat{B}\hat{D}}\overbrace{\hat{A}\hat{C}} + \overbrace{\hat{B}\hat{C}}\overbrace{\hat{A}\hat{D}} + \overbrace{\hat{A}\hat{B}}\overbrace{\hat{C}\hat{D}}. \qquad \text{(A.25)}
\end{aligned}$$

Details of the proof and the form of the contractions can be found in Ref. [12].

Now we will work though how to obtain a normal ordered electronic Hamiltonian. For the two body part, we have

$$\hat{G} = \frac{1}{4}\sum_{pqrs}\langle pq||sr\rangle p^\dagger q^\dagger rs \tag{A.26}$$

$$= \frac{1}{4}\sum_{pqrs}\langle pq||sr\rangle(\{p^\dagger q^\dagger rs\} + \overbrace{q^\dagger r}\{p^\dagger s\} + \overbrace{p^\dagger s}\{q^\dagger r\}$$

$$- \overbrace{p^\dagger r}\{q^\dagger s\} - \overbrace{q^\dagger s}\{p^\dagger r\} + \overbrace{p^\dagger \overbrace{q^\dagger r}s} + \overbrace{p^\dagger \overbrace{q^\dagger r}s}). \tag{A.27}$$

Since only $\overbrace{i^\dagger j} = \delta_{ij}$ is nonzero, the equation can be simplified as

$$\hat{G} = \frac{1}{4}\sum_{pqrs}\langle pq||sr\rangle\{p^\dagger q^\dagger rs\} + \sum_{ipq}\langle pi||qi\rangle\{p^\dagger q\} + \frac{1}{2}\sum_{ij}\langle ji||ji\rangle \tag{A.28}$$

$$= \frac{1}{4}\sum_{pqrs}\langle pq||sr\rangle\{p^\dagger q^\dagger rs\} + \sum_{pq}(J_{pq} - K_{pq})\{p^\dagger q\} + \frac{1}{2}\sum_{ij}\langle ji||ji\rangle, \tag{A.29}$$

where $J$ and $K$ are defined in Eqs. (1.20) and (1.21). The one body part of the Hamiltonian is,

$$\hat{h} = \sum_{pq} h_{pq} p^\dagger q \tag{A.30}$$

$$= \sum_{pq} h_{pq}(\{p^\dagger q\} + \overbrace{p^\dagger q}) \tag{A.31}$$

$$= \sum_{pq} h_{pq}\{p^\dagger q\} + \sum_i h_{ii}. \tag{A.32}$$

Therefore, we have

$$\hat{H} = \hat{h} + \hat{G} \tag{A.33}$$

$$= \sum_i h_{ii} + \frac{1}{2}\sum_{ij}\langle ji||ji\rangle + \sum_{pq}(h_{pq} + J_{pq} - K_{pq})\{p^\dagger q\} + \frac{1}{4}\sum_{pqrs}\langle pq||sr\rangle\{p^\dagger q^\dagger rs\} \tag{A.34}$$

$$= E_{\mathrm{HF}} + \sum_p \epsilon_p\{p^\dagger p\} + \frac{1}{4}\sum_{pqrs}\langle pq||sr\rangle\{p^\dagger q^\dagger rs\}, \tag{A.35}$$

where we have used Eqs. (1.18) and (1.6). Defining the normal ordered Fock operator

$$\hat{F}_N = \sum_p \epsilon_p \{p^\dagger p\}, \tag{A.36}$$

and the normal ordered two electron interaction operator

$$\hat{G}_N = \frac{1}{4} \sum_{pqrs} \langle pq||sr\rangle \{p^\dagger q^\dagger r s\}, \tag{A.37}$$

then the normal ordered Hamiltonian is

$$\hat{H}_N = \hat{F}_N + \hat{G}_N. \tag{A.38}$$

Normal ordered operators simplify the evaluation of integrals. For example, if we want to evaluate $\langle \Phi_{\rm HF}|\hat{X}\hat{Y}|\Phi_{\rm HF}\rangle$, we have

$$\langle \Phi_{\rm HF}|\hat{X}\hat{Y}|\Phi_{\rm HF}\rangle = \langle \Phi_{\rm HF}|(X_{\rm HF} + \hat{X}_N)(Y_{\rm HF} + \hat{Y}_N)|\Phi_{\rm HF}\rangle \tag{A.39}$$

$$= X_{\rm HF}Y_{\rm HF} + X_{\rm HF}\langle \Phi_{\rm HF}|\hat{Y}_N|\Phi_{\rm HF}\rangle + Y_{\rm HF}\langle \Phi_{\rm HF}|\hat{X}_N|\Phi_{\rm HF}\rangle + \langle \Phi_{\rm HF}|\hat{X}_N\hat{Y}_N|\Phi_{\rm HF}\rangle \tag{A.40}$$

$$= X_{\rm HF}Y_{\rm HF} + \overbrace{\hat{X}_N\hat{Y}_N}, \tag{A.41}$$

where the HF expectation value of a normal ordered operator is always zero since a normal ordered operator is a killer either to the left or to the right (or both), and $\overbrace{\hat{X}_N\hat{Y}_N}$ denotes the complete contraction between $\hat{X}_N$ and $\hat{Y}_N$ leaving no operators uncontracted. By using normal ordered operators, the integral evaluation is much simpler with Wick's theorem and directly leads to Feynman diagram representations.

# Appendix B

## Detailed derivations for Fukui and response functions

### B.1 Detailed derivations of $\delta^3 E/\delta v^3$ and $\delta^3 E/\delta N \delta v^2$

This section presents the detailed derivations in Subsection 2.4.2. Please note that all the notations in this section are inherited from Subsection 2.4.2, incompatible with those in Subsection 2.4.3. For an integer system, the CP-SCF equations for the order $\lambda_A \lambda_B$ are

$$\hat{H}_\tau^{AB}|\phi_{i\tau}\rangle + \hat{H}_\tau^{A}|\phi_{i\tau}^{B}\rangle + \hat{H}_\tau^{B}|\phi_{i\tau}^{A}\rangle + \hat{H}_\tau|\phi_{i\tau}^{AB}\rangle = \epsilon_{i\tau}^{AB}|\phi_{i\tau}\rangle + \epsilon_{i\tau}^{A}|\phi_{i\tau}^{B}\rangle + \epsilon_{i\tau}^{B}|\phi_{i\tau}^{A}\rangle + \epsilon_{i\tau}|\phi_{i\tau}^{AB}\rangle, \tag{B.1}$$

$$\langle\phi_{u\tau}^{AB}|\phi_{i\tau}\rangle + \langle\phi_{u\tau}^{A}|\phi_{i\tau}^{B}\rangle + \langle\phi_{u\tau}^{B}|\phi_{i\tau}^{A}\rangle + \langle\phi_{u\tau}|\phi_{i\tau}^{AB}\rangle = 0, \tag{B.2}$$

and

$$\rho_{s,\tau}^{AB}(\mathbf{r},\mathbf{r}') = \sum_i [\phi_{i\tau}^{AB}(\mathbf{r})\phi_{i\tau}(\mathbf{r}') + \phi_{i\tau}^{A}(\mathbf{r})\phi_{i\tau}^{B}(\mathbf{r}') + \phi_{i\tau}^{B}(\mathbf{r})\phi_{i\tau}^{A}(\mathbf{r}') + \phi_{i\tau}(\mathbf{r})\phi_{i\tau}^{AB}(\mathbf{r}')]. \tag{B.3}$$

As usual, the superscript "0" is omitted when no confusion is caused. By expanding $\phi_{i\tau}^{A}$, $\phi_{i\tau}^{B}$, and $\phi_{i\tau}^{AB}$ in the basis of unperturbed orbitals, and utilizing the orthonor-

malization of Eq. (B.2), $\rho^{AB}_{s,\tau}$ could be cast into

$$\rho^{AB}_{s,\tau}(\mathbf{r},\mathbf{r}') = \sum_{ia}[\phi_{i\tau}(\mathbf{r})\phi_{a\tau}(\mathbf{r}') + \phi_{a\tau}(\mathbf{r})\phi_{i\tau}(\mathbf{r}')][P^{AB}_{ia\tau} + Q_{ia\tau}(\mathbf{R}_A,\mathbf{R}_B)]$$
$$- \sum_{ij}\phi_{i\tau}(\mathbf{r})\phi_{j\tau}(\mathbf{r}')Q_{ij\tau}(\mathbf{R}_A,\mathbf{R}_B) + \sum_{ab}\phi_{a\tau}(\mathbf{r})\phi_{b\tau}(\mathbf{r}')Q_{ab\tau}(\mathbf{R}_A,\mathbf{R}_B), \tag{B.4}$$

where $Q_{ab\tau}(\mathbf{R}_A,\mathbf{R}_B)$ and $Q_{ij\tau}(\mathbf{R}_A,\mathbf{R}_B)$ are defined in Eqs. (2.62)-(2.63), and we have additionally

$$P^{AB}_{ia\tau} = \langle\phi_{a\tau}|\phi^{AB}_{i\tau}\rangle, \tag{B.5}$$

and

$$Q_{ia\tau}(\mathbf{R}_A,\mathbf{R}_B) = \sum_j(\langle\phi_{a\tau}|\phi^A_{j\tau}\rangle\langle\phi^B_{j\tau}|\phi_{i\tau}\rangle + \langle\phi_{a\tau}|\phi^B_{j\tau}\rangle\langle\phi^A_{j\tau}|\phi_{i\tau}\rangle). \tag{B.6}$$

In Eq. (B.4), it seems that only $P^{AB}_{ia\tau}$ is unknown so far, as all $Q$ matrices are just first order response. However, the definition of $Q_{ia\tau}$ involves $\langle\phi^X_{j\tau}|\phi_{i\tau}\rangle$, $X = A$ or $B$, which could be problematic when $\phi_{i\tau}$ and $\phi_{j\tau}$ are degenerate. This difficulty can be alleviated by utilizing a special choice of unitary transformation such that $\langle\phi^X_{j\tau}|\phi_{i\tau}\rangle = 0$, as was widely used to derive various response properties[53, 91, 97, 98]. For canonical orbitals, nonetheless, $\langle\phi^X_{j\tau}|\phi_{i\tau}\rangle$ is non-zero and will only be canceled out after combining other terms, as will be shown later.

Applying $\langle\phi_{a\tau}|$ to Eq. (B.1), we have

$$\langle\phi_{a\tau}|\hat{H}^{AB}_\tau|\phi_{i\tau}\rangle + (\epsilon_{a\tau} - \epsilon_{i\tau})P^{AB}_{ia\tau}$$
$$=\epsilon^A_{i\tau}\langle\phi_{a\tau}|\phi^B_{i\tau}\rangle + \epsilon^B_{i\tau}\langle\phi_{a\tau}|\phi^A_{i\tau}\rangle - (\langle\phi_{a\tau}|\hat{H}^A_\tau|\phi^B_{i\tau}\rangle + \langle\phi_{a\tau}|\hat{H}^B_\tau|\phi^A_{i\tau}\rangle), \tag{B.7}$$

where the term $\langle\phi_{a\tau}|\hat{H}^A_\tau|\phi^B_{i\tau}\rangle$ also has contribution from the troublesome $\langle\phi_{j\tau}|\phi^B_{i\tau}\rangle$. Whatsoever, the two terms in the parenthesis on the right hand side of Eq. (B.7)

can be simplified to

$$
\begin{aligned}
&\langle\phi_{a\tau}|\hat{H}^A_\tau|\phi^B_{i\tau}\rangle + \langle\phi_{a\tau}|\hat{H}^B_\tau|\phi^A_{i\tau}\rangle \\
=&\sum_u(\langle\phi_{a\tau}|\hat{H}^A_\tau|\phi_{u\tau}\rangle\langle\phi_{u\tau}|\phi^B_{i\tau}\rangle + \langle\phi_{a\tau}|\hat{H}^B_\tau|\phi_{u\tau}\rangle\langle\phi_{u\tau}|\phi^A_{i\tau}\rangle) \\
=&\sum_b[H^1_{ab\tau}(\mathbf{R}_A)P^1_{ib\tau}(\mathbf{R}_B) + H^1_{ab\tau}(\mathbf{R}_B)P^1_{ib\tau}(\mathbf{R}_A)] \\
&+\sum_j(\langle\phi_{a\tau}|\hat{H}^A_\tau|\phi_{j\tau}\rangle\langle\phi_{j\tau}|\phi^B_{i\tau}\rangle + \langle\phi_{a\tau}|\hat{H}^B_\tau|\phi_{j\tau}\rangle\langle\phi_{j\tau}|\phi^A_{i\tau}\rangle) \\
=&\sum_b[H^1_{ab\tau}(\mathbf{R}_A)P^1_{ib\tau}(\mathbf{R}_B) + H^1_{ab\tau}(\mathbf{R}_B)P^1_{ib\tau}(\mathbf{R}_A)] \\
&+\sum_j(\epsilon_{j\tau}-\epsilon_{a\tau})(P^1_{ja\tau}(\mathbf{R}_A)\langle\phi_{j\tau}|\phi^B_{i\tau}\rangle + P^1_{ja\tau}(\mathbf{R}_B)\langle\phi_{j\tau}|\phi^A_{i\tau}\rangle) \\
=&\sum_b[H^1_{ab\tau}(\mathbf{R}_A)P^1_{ib\tau}(\mathbf{R}_B) + H^1_{ab\tau}(\mathbf{R}_B)P^1_{ib\tau}(\mathbf{R}_A)] \\
&-\sum_j(\epsilon_{a\tau}-\epsilon_{i\tau})[P^1_{ja\tau}(\mathbf{R}_A)\langle\phi_{j\tau}|\phi^B_{i\tau}\rangle + P^1_{ja\tau}(\mathbf{R}_B)\langle\phi_{j\tau}|\phi^A_{i\tau}\rangle] \\
&-\sum_j(\epsilon_{i\tau}-\epsilon_{j\tau})[P^1_{ja\tau}(\mathbf{R}_A)\langle\phi_{j\tau}|\phi^B_{i\tau}\rangle + P^1_{ja\tau}(\mathbf{R}_B)\langle\phi_{j\tau}|\phi^A_{i\tau}\rangle] \\
=&\sum_b[H^1_{ab\tau}(\mathbf{R}_A)P^1_{ib\tau}(\mathbf{R}_B) + H^1_{ab\tau}(\mathbf{R}_B)P^1_{ib\tau}(\mathbf{R}_A)] \\
&+(\epsilon_{a\tau}-\epsilon_{i\tau})Q_{ia\tau}(\mathbf{R}_A,\mathbf{R}_B) - \sum_{j\neq i}[P^1_{ja\tau}(\mathbf{R}_A)H^1_{ji\tau}(\mathbf{R}_B) + P^1_{ja\tau}(\mathbf{R}_B)H^1_{ji\tau}(\mathbf{R}_A)], \quad \text{(B.8)}
\end{aligned}
$$

where $P^1$ and $H^1$ are defined in Eqs. (2.60) and (2.61). Apparently, according to

the definitions, $P^1_{ia\tau}(\mathbf{R}_X) = P^X_{ia\tau}$ and $H^1_{uv\tau}(\mathbf{R}_X) = H^X_{uv\tau}$. On the other hand,

$$\begin{aligned}
\langle\phi_{a\tau}|\hat{H}^{AB}_{\tau}|\phi_{i\tau}\rangle &= \langle\phi_{a\tau}|\frac{\partial^2\hat{H}_\tau}{\partial\lambda_A\partial\lambda_B}|\phi_{i\tau}\rangle \\
&= \langle\phi_{a\tau}|\frac{\partial^2(\hat{v}_J+\hat{v}^\tau_{\mathrm{XC}})}{\partial\lambda_A\partial\lambda_B}|\phi_{i\tau}\rangle \\
&= \sum_{\zeta,\theta}\int d\mathbf{r}d\mathbf{r}'\langle\phi_{a\tau}|\frac{\delta^2(\hat{v}_J+\hat{v}^\tau_{\mathrm{XC}})}{\delta\rho_\zeta(\mathbf{r})\delta\rho_\theta(\mathbf{r}')}|\phi_{i\tau}\rangle\rho^A_\zeta(\mathbf{r})\rho^B_\theta(\mathbf{r}') \\
&\quad + \sum_{\zeta}\int d\mathbf{r}\langle\phi_{a\tau}|\frac{\delta(\hat{v}_J+\hat{v}^\tau_{\mathrm{XC}})}{\delta\rho_\zeta(\mathbf{r})}|\phi_{i\tau}\rangle\rho^{AB}_\zeta(\mathbf{r}) \\
&= 4\sum_{jb\zeta,kc\theta}F_{ia\tau,jb\zeta,kc\theta}P^1_{jb\zeta}(\mathbf{R}_A)P^1_{kc\theta}(\mathbf{R}_B) + \sum_{bc\zeta}K_{ia\tau,bc\zeta}Q_{bc\zeta}(\mathbf{R}_A,\mathbf{R}_B) \\
&\quad + \sum_{jb\zeta}K_{ia\tau,jb\zeta}[P^{AB}_{jb\zeta}+Q_{jb\zeta}(\mathbf{R}_A,\mathbf{R}_B)] - \sum_{jk\zeta}K_{ia\tau,jk\zeta}Q_{jk\zeta}(\mathbf{R}_A,\mathbf{R}_B),
\end{aligned} \tag{B.9}$$

where Eqs. (B.4), (2.60), and (2.64) have been applied.

Combining Eqs. (B.7), (B.8), and (B.9), noting that $\epsilon^X_{i\tau} = H^X_{ii\tau}$, we have

$$\sum_{jb\zeta}M_{ia\tau,jb\zeta}[P^{AB}_{jb\zeta}+Q_{jb\zeta}(\mathbf{R}_A,\mathbf{R}_B)] = W_{ia\tau}(\mathbf{R}_A,\mathbf{R}_B), \tag{B.10}$$

where $M$ and $W$ are defined in Eqs. (2.51) (using conventional orbitals normalized to one) and (2.65), respectively. Now that $W_{ia\tau}$ contains only first order response independent of $\langle\phi_{i\tau}|\phi^X_{j\tau}\rangle$ elements, $P^{AB}_{jb\zeta} + Q_{jb\zeta}(\mathbf{R}_A,\mathbf{R}_B)$ are unambiguously defined as $Z_{jb\zeta}(\mathbf{R}_A,\mathbf{R}_B)$. Then the diagonal element in Eq. (B.4) becomes $\delta^3E/\delta v(\mathbf{r})\delta v(\mathbf{R}_A)\delta v(\mathbf{R}_B)$, as shown in Eq. (2.67). Since $Z_{jb\zeta}(\mathbf{R}_A,\mathbf{R}_B)$ as a whole enters $\rho^{AB}$, the final expression is robust regardless of the ill-defined $Q_{jb\zeta}$. Also, the final expression of Eq. (2.67) is compatible with the previous results using non-canonical orbital conventions $\langle\phi_{i\tau}|\phi^X_{j\tau}\rangle = 0$. Using definitions in Eqs. (2.60)-(2.66),Eq. (2.67)

can also be rewritten as

$$\begin{aligned}\chi^{(2)}(\mathbf{r},\mathbf{r}',\mathbf{r}'') = 8 &\sum_{ia\tau,jb\zeta,kc\theta} F_{ia\tau,jb\zeta,kc\theta} P^1_{ia\tau}(\mathbf{r}) P^1_{jb\zeta}(\mathbf{r}') P^1_{kc\theta}(\mathbf{r}'') \\ &+ \sum_{ab\tau} [H^1_{ab\tau}(\mathbf{r}'') Q_{ab\tau}(\mathbf{r},\mathbf{r}') + H^1_{ab\tau}(\mathbf{r}') Q_{ab\tau}(\mathbf{r},\mathbf{r}'') + H^1_{ab\tau}(\mathbf{r}) Q_{ab\tau}(\mathbf{r}',\mathbf{r}'')] \\ &- \sum_{ij\tau} [H^1_{ij\tau}(\mathbf{r}'') Q_{ij\tau}(\mathbf{r},\mathbf{r}') + H^1_{ij\tau}(\mathbf{r}') Q_{ij\tau}(\mathbf{r},\mathbf{r}') + H^1_{ij\tau}(\mathbf{r}) Q_{ij\tau}(\mathbf{r}',\mathbf{r}'')],\end{aligned} \tag{B.11}$$

which explicitly demonstrates the symmetry of $\chi^{(2)}$ and closely resembles the static hyperpolarizability expression in Ref [92].

Applying $\langle\phi_{i\tau}|$ to Eq. (B.7), and setting $\phi_{i\tau} = \phi_{f\sigma}$, we have $\epsilon^{AB}_{f\sigma} = \langle\phi_{f\sigma}|\hat{H}^{AB}_{\sigma}|\phi_{f\sigma}\rangle + \langle\phi_{f\sigma}|\hat{H}^{A}_{\sigma}|\phi^{B}_{f\sigma}\rangle + \langle\phi_{f\sigma}|\hat{H}^{B}_{\sigma}|\phi^{A}_{f\sigma}\rangle$. $\langle\phi_{f\sigma}|\hat{H}^{AB}_{\sigma}|\phi_{f\sigma}\rangle$ is readily available by applying $\delta^3 E/\delta v^3$ in Eq. (2.67) to Eq. (B.9). The first order terms in the expression are

$$\langle\phi_{f\sigma}|\hat{H}^{A}_{\sigma}|\phi^{B}_{f\sigma}\rangle + \langle\phi_{f\sigma}|\hat{H}^{B}_{\sigma}|\phi^{A}_{f\sigma}\rangle = \sum_{u} [\langle\phi_{f\sigma}|\hat{H}^{A}_{\sigma}|\phi_{u\sigma}\rangle\langle\phi_{u\sigma}|\phi^{B}_{f\sigma}\rangle + \langle\phi_{f\sigma}|\hat{H}^{B}_{\sigma}|\phi_{u\sigma}\rangle\langle\phi_{u\sigma}|\phi^{A}_{f\sigma}\rangle], \tag{B.12}$$

which could be unstable if there are more than one degenerate frontier orbitals. In fact, we have implicitly apply an perturbation of occupation number to establish $\epsilon_{f\sigma} = \mu$, thus the zeroth order orbital $\phi_{f\sigma}$ is set regardless of the perturbation $\hat{H}^X$. In other words, we are not interested with the real derivative $\delta^3 E/\delta N \delta v^2$ which could be ill-defined as the $N-1$ or $N+1$ state is degenerate when the frontier orbitals are degenerate; instead, we want to explore $\delta^3 E/\delta n_{f\sigma}\delta v^2$ with a specific chosen frontier orbital $\phi_{f\sigma}$. Replacing $\phi_{i\tau}$ with $\phi_{f\sigma}$ in Eq. (2.41) and applying another frontier orbital $\langle\phi_{f'\sigma}|$ to both sides, we have

$$\langle\phi_{f'\sigma}|\hat{H}^{X}_{\sigma}|\phi_{f\sigma}\rangle = \epsilon^{X}_{f\sigma}\delta_{f'f}, \tag{B.13}$$

where $\epsilon_{f\sigma} = \epsilon_{f'\sigma}$ is applied. Therefore, all frontier orbitals in the summation of Eq. (B.12) will be omitted, and we finally reach the expression of $\epsilon^{AB}_{f\sigma}$ in Eq. (2.80).

## B.2 Detailed derivations of $\delta^3 E/\delta N^2 \delta v$ and $\delta^3 E/\delta N^3$

Parallel to the previous section, this section shows the detailed derivations in Subsection 2.4.3. Please note that all the notations in this section are inherited from Subsection 2.4.3, incompatible from those in Subsection 2.4.2.

The first order equations are

$$\hat{H}_\tau|\bar{\phi}^1_{i\tau}\rangle + \hat{\bar{H}}^1_\tau|\phi_{i\tau}\rangle = \epsilon_{i\tau}|\bar{\phi}^1_{i\tau}\rangle + \bar{\epsilon}^1_{i\tau}|\phi_{i\tau}\rangle, \tag{B.14}$$

and

$$\langle\bar{\phi}^1_{u\tau}|\phi_{i\tau}\rangle + \langle\phi_{u\tau}|\bar{\phi}^1_{i\tau}\rangle = 0, \tag{B.15}$$

which are actually already solved by the analytical Fukui function, i.e.

$$\bar{\rho}^1_{s,\tau}(\mathbf{r},\mathbf{r}') = \delta_{\tau\sigma}\phi_{f\sigma}(\mathbf{r})\phi_{f\sigma}(\mathbf{r}') + \sum_{ia}\bar{P}^1_{ia\tau}[\phi_{i\tau}(\mathbf{r})\phi_{a\tau}(\mathbf{r}') + \phi_{a\tau}(\mathbf{r})\phi_{i\tau}(\mathbf{r}')], \tag{B.16}$$

and

$$f(\mathbf{r}) = \bar{\rho}^1(\mathbf{r}) = |\phi_{f\sigma}|^2 + 2\sum_{ia\tau}\bar{P}^1_{ia\tau}\phi_{i\tau}(\mathbf{r})\phi_{a\tau}(\mathbf{r}), \tag{B.17}$$

with $\bar{P}^1_{ia\tau}$ defined in Eq. (2.73). Eq. (B.16) is nothing but the nonlocal Fukui function in Eq. (2.89).

The second order equations are

$$\hat{\bar{H}}^2_\tau|\phi_{i\tau}\rangle + 2\hat{\bar{H}}^1_\tau|\bar{\phi}^1_{i\tau}\rangle + \hat{H}_\tau|\bar{\phi}^2_{i\tau}\rangle = \bar{\epsilon}^2_{i\tau}|\bar{\phi}_{i\tau}\rangle + 2\bar{\epsilon}^1_{i\tau}|\bar{\phi}^1_{i\tau}\rangle + \epsilon_{i\tau}|\bar{\phi}^2_{i\tau}\rangle, \tag{B.18}$$

and

$$\langle\bar{\phi}^2_{u\tau}|\phi_{i\tau}\rangle + 2\langle\bar{\phi}^1_{u\tau}|\bar{\phi}^1_{i\tau}\rangle + \langle\phi_{u\tau}|\bar{\phi}^2_{i\tau}\rangle = 0, \tag{B.19}$$

while the KS density matrix variation is

$$\begin{aligned}\bar{\rho}^2_{s,\tau}(\mathbf{r},\mathbf{r}') &= \sum_i [\bar{\phi}^2_{i\tau}(\mathbf{r})\phi_{i\tau}(\mathbf{r}') + 2\bar{\phi}^1_{i\tau}(\mathbf{r})\bar{\phi}^1_{i\tau}(\mathbf{r}') + \phi_{i\tau}(\mathbf{r})\bar{\phi}^2_{i\tau}(\mathbf{r}')] \\ &\quad + 2\bar{\phi}^1_{f\tau}(\mathbf{r})\phi_{f\tau}(\mathbf{r}') + 2\phi_{f\tau}(\mathbf{r})\bar{\phi}^1_{f\tau}(\mathbf{r}') \\ &= \sum_{ai}(\bar{P}^2_{ia\tau} + 2\bar{Q}_{ia\tau})[\phi_{a\tau}(\mathbf{r})\phi_{i\tau}(\mathbf{r}') + \phi_{i\tau}(\mathbf{r})\phi_{a\tau}(\mathbf{r}')] \\ &\quad + \sum_{ab}\phi_{a\tau}(\mathbf{r})\phi_{b\tau}(\mathbf{r}')2\bar{Q}_{ab\tau} - \sum_{ij}\phi_{i\tau}(\mathbf{r})\phi_{j\tau}(\mathbf{r}')2\bar{Q}_{ij\tau} \\ &\quad + \sum_u 2[\phi_{u\tau}(\mathbf{r})\phi_{f\tau}(\mathbf{r}') + \phi_{u\tau}(\mathbf{r}')\phi_{f\tau}(\mathbf{r})]\langle\phi_{u\tau}|\bar{\phi}^1_{f\tau}\rangle, \end{aligned} \tag{B.20}$$

where $\bar{Q}_{ab\tau}$ and $\bar{Q}_{ij\tau}$ are defined in Eqs. (2.76) and (2.75), and $\bar{P}^2_{ia\tau} = \langle\bar{\phi}^2_{i\tau}|\phi_{a\tau}\rangle$, $\bar{Q}_{ia\tau} = \sum_k\langle\bar{\phi}^1_{k\tau}|\phi_{i\tau}\rangle\bar{P}^1_{ka\tau}$. Similar to the perturbation of $dv^2$, terms as $\langle\bar{\phi}^1_{k\tau}|\phi_{i\tau}\rangle$ in $\bar{Q}_{ia\tau}$ could be troublesome. As for the frontier orbital perturbation, $\langle\phi_{u\tau}|\bar{\phi}^1_{f\tau}\rangle$ in Eq. (B.20) is well defined for $\epsilon_{u\tau} \neq \epsilon_{f\tau}$. When $u$ and $f$ are degenerate, i.e. both frontier orbitals, the perturbation $\delta N$ should actually be interpreted as $\delta n_{f\sigma}$, and the change of the occupation number will deteriorate the symmetry of the electron density and thus $\hat{H}_\tau$. Therefore, $\langle\phi_{f'\sigma}|\hat{\bar{H}}^n_\sigma|\phi_{f\sigma}\rangle = 0$ and $\langle\bar{\phi}^n_{f'\sigma}|\phi_{f\sigma}\rangle = 0$ for all orders of $n$ with arbitrary degenerate frontier orbitals $f' \neq f$ and $\epsilon_{f'\sigma} = \epsilon_{f\sigma}$. Hence the degenerate orbital contribution in the last term of Eq. (B.20) can be omitted and the summation can be replaced by $\sum'$.

Applying $\langle\phi_{a\tau}|$ to both sides of Eq. (B.18), we have

$$\langle\phi_{a\tau}|\hat{\bar{H}}^2_\tau|\phi_{i\tau}\rangle + (\epsilon_{a\tau} - \epsilon_{i\tau})\bar{P}^2_{ia\tau} = 2\bar{\epsilon}^1_{i\tau}\langle\phi_{a\tau}|\bar{\phi}^1_{i\tau}\rangle - 2\langle\phi_{a\tau}|\hat{\bar{H}}^1_\tau|\bar{\phi}^1_{i\tau}\rangle. \tag{B.21}$$

The second-order effective Hamiltonian can be expanded as

$$\begin{aligned}\langle\phi_{a\tau}|\hat{\bar{H}}^2_\tau|\phi_{i\tau}\rangle = &\sum_{jb\zeta}(K_{ai\tau,jb\zeta}+K_{ai\tau,bj\zeta})(\bar{P}^2_{jb\zeta}+2\bar{Q}_{jb\zeta})+2\sum_{bc\zeta}K_{ai\tau,bc\zeta}\bar{Q}_{bc\zeta}\\ &-2\sum_{jk\zeta}K_{ai\tau,jk\zeta}\bar{Q}_{jk\zeta}+2{\sum_u}'(K_{ai\tau,fu\sigma}+K_{ai\tau,uf\sigma})\langle\bar{\phi}^1_{f\sigma}|\phi_{u\sigma}\rangle\\ &+\sum_{uv\zeta,st\theta}F_{ai\tau,uv\zeta,st\theta}f_{uv\zeta}f_{st\theta},\end{aligned}\tag{B.22}$$

where $f_{uv\zeta}$ is the KS density matrix of the Fukui function, defined in Eq. (2.77). The last term on the right-hand side in Eq. (B.21) can also be expressed as

$$\begin{aligned}\langle\phi_{a\tau}|\hat{\bar{H}}^1_\tau|\bar{\phi}^1_{i\tau}\rangle &= \sum_b\langle\phi_{a\tau}|\hat{\bar{H}}^1_\tau|\phi_{b\tau}\rangle\langle\phi_{b\tau}|\bar{\phi}^1_{i\tau}\rangle+\sum_j\langle\phi_{a\tau}|\hat{\bar{H}}^1_\tau|\phi_{j\tau}\rangle\langle\phi_{j\tau}|\bar{\phi}^1_{i\tau}\rangle\\ &= \sum_b\bar{H}^1_{ab\tau}\bar{P}^1_{ib\tau}+\sum_j(\epsilon_{j\tau}-\epsilon_{a\tau})\bar{P}^1_{ja\tau}\langle\phi_{j\tau}|\bar{\phi}^1_{i\tau}\rangle\\ &= \sum_b\bar{H}^1_{ab\tau}\bar{P}^1_{ib\tau}-\sum_j(\epsilon_{a\tau}-\epsilon_{i\tau})\bar{P}^1_{ja\tau}\langle\phi_{j\tau}|\bar{\phi}^1_{i\tau}\rangle-\sum_j(\epsilon_{i\tau}-\epsilon_{j\tau})\bar{P}^1_{ja\tau}\langle\phi_{j\tau}|\bar{\phi}^1_{i\tau}\rangle\\ &= \sum_b\bar{H}^1_{ab\tau}\bar{P}^1_{ib\tau}+(\epsilon_{a\tau}-\epsilon_{i\tau})\bar{Q}_{ia\tau}-\sum_{j\neq i}\bar{P}^1_{ja\tau}\bar{H}^1_{ji\tau}.\end{aligned}\tag{B.23}$$

Combining Eqs. (B.21)-(B.23), we reach

$$\sum_{jb\zeta}M_{ia\tau,jb\zeta}[\bar{P}^2_{jb\zeta}+2\bar{Q}_{jb\zeta}]=\bar{W}_{ia\tau},\tag{B.24}$$

with $M_{ia\tau,jb\zeta}$ and $\bar{W}_{ia\tau}$ defined in Eqs. (2.51) (using conventional orbitals normalized to one) and (2.78). Again, $\bar{W}_{ia\tau}$ contains only first order response and free from degeneracy issue. Setting $\bar{Z}_{ia\tau}=\bar{P}^2_{ia\tau}+2\bar{Q}_{ia\tau}$, Eq. (B.24) is solved by Eq. (2.79). Then the diagonal element of Eq. (B.20) delivers the Fukui response function in Eq. (2.80).

Replacing $\phi_{i\tau}$ with the frontier orbital $\phi_{f\sigma}$ in Eq. (B.18), and applying $\langle\phi_{f\sigma}|$ to both sides, we have

$$\bar{\epsilon}^2_{f\sigma}=\langle\phi_{f\sigma}|\hat{\bar{H}}^2_\sigma|\phi_{f\sigma}\rangle+2\langle\phi_{f\sigma}|\hat{\bar{H}}^1_\sigma|\bar{\phi}^1_{f\sigma}\rangle,$$

in which the first term can be expressed from $\bar{\rho}^2_\tau$ and $\bar{\rho}^1_\tau$, while the second term from first order response. Therefore, we reach the hyperhardness in Eq. (2.81).

In summary, the second-order CP-SCF equations are solved for both the external potential perturbation and the occupation number perturbation. In the framework of canonical orbitals, terms like $\langle \phi_{j\tau} | \phi^X_{i\tau} \rangle$ ($X = A$, $B$, or 1) are seemingly troublesome during the derivations. The final expressions, however, are free from these undetermined terms. The numerical results verify that the techniques to get rid of these terms are valid.

# Appendix C

## Mathematical Details of Non-Adiabatic Linear-Response TDDFT-P

In absence of the proof of the time-dependent one-to-one mapping between the pairing matrix and the pairing field, the the inclusion of the frequency dependent effects can merely be introduced based on some assumption. We adopt Assumption a) in Section 3.3; i.e., we assume that at the zero pairing field limit, any first order pairing matrix of an interacting non-superconducting system induced by a pairing field can be reproduced by the first order pairing matrix induced by a pairing field in a non-interacting non-superconducting system. Concisely, it can be expressed as following: for every $\delta\mathbf{D}(\omega)$, there exists a $\delta\mathbf{D}_s(\omega)$ such that

$$\delta\boldsymbol{\kappa}(\omega) = \mathbf{K}(\omega)\delta\mathbf{D}(\omega) = \mathbf{K}_s(\omega)\delta\mathbf{D}_s(\omega), \tag{C.1}$$

where we have used matrix multiplication to represent integrals. In this way, $\delta\mathbf{D}_s(\omega)$, $\delta\mathbf{D}(\omega)$, and $\delta\boldsymbol{\kappa}(\omega)$ are vectors in the linear space $\mathcal{V}$ of general functions $g(\mathbf{x}, \mathbf{x}')$ of two points. Then $\mathbf{K}_s(\omega)$ and $\mathbf{K}(\omega)$ are linear operators on $\mathcal{V}$. In the language of linear algebra (see, for example, Ref. [274]), the aforementioned assumption is equivalent

to

$$\mathrm{Im}\mathbf{K}(\omega) \subseteq \mathrm{Im}\mathbf{K}_s(\omega), \tag{C.2}$$

where Im$\mathbf{S}$ is the image of a linear operator $\mathbf{S}$,

$$\mathrm{Im}\mathbf{S} = \{\mathbf{v} \in \mathcal{V} | \mathbf{v} = \mathbf{S}\mathbf{u}, \mathbf{u} \in \mathcal{V}\}. \tag{C.3}$$

This linear-response representability is less restrictive than the full representability, as the full representability of $\boldsymbol{\kappa}(\omega)$ requires response of all orders should equal. This is the only assumption necessary to establish the Dyson-like equation for non-adiabatic linear-response TDDFT-P. Note that the particle-hole blocks in $\mathbf{K}_s(\omega)$ and $\delta\boldsymbol{\kappa}(\omega)$ are zero, as indicated in Eq. (3.36). Therefore $\mathbf{K}_s(\omega)$ is rank deficient and not invertible, and so is $\mathbf{K}(\omega)$. The non-invertibility makes it difficult to derive the Dyson-like equation in the straightforward way as stated in Section 3.4, yet we can bypass such difficulty by restricting the perturbing field. Also note that although there is no particle-hole terms in $\delta\boldsymbol{\kappa}(\omega)$ due to the rank deficiency of $\mathbf{K}_s(\omega)$ in Eq. (C.1), the full response $\boldsymbol{\kappa}(\omega)$ could have a non-zero particle-hole block.

We perturb the interacting non-superconducting system with a specially designed pairing field $\delta\tilde{\mathbf{D}}(\omega)$ such that

$$\delta\tilde{\mathbf{D}}(\omega) \in \mathrm{Im}\mathbf{K}^{-}(\omega), \tag{C.4}$$

where $\mathbf{K}^{-}(\omega)$ is the Moore-Penrose pseudoinverse (see, for example, Ref. [275]) of matrix $\mathbf{K}(\omega)$. Such pairing perturbation will generate first order pairing matrix

$$\delta\tilde{\boldsymbol{\kappa}}(\omega) = \mathbf{K}(\omega)\delta\tilde{\mathbf{D}}(\omega). \tag{C.5}$$

According to Eq. (C.1), there are infinitely many $\delta\mathbf{D}_s(\omega)$'s to satisfy the conditions due to the rank deficiency of $\mathbf{K}_s(\omega)$ described above. However, we can choose a specific solution $\delta\tilde{\mathbf{D}}_s(\omega)$ that fulfills Eq. (C.1),

$$\delta\tilde{\mathbf{D}}_s(\omega) = \mathbf{K}_s^{-}(\omega)\delta\tilde{\boldsymbol{\kappa}}(\omega) = \mathbf{K}_s^{-}(\omega)\mathbf{K}(\omega)\delta\tilde{\mathbf{D}}(\omega), \tag{C.6}$$

without ambiguity. Owing to the constraint of Eq. (C.4), the pairing field can also be expressed by the first order pairing matrix perturbation

$$\delta\tilde{\mathbf{D}}(\omega) = \mathbf{K}^{-}(\omega)\delta\tilde{\boldsymbol{\kappa}}(\omega). \tag{C.7}$$

Now we introduce a projected linear-response functions

$$\tilde{\mathbf{K}}(\omega) = \frac{\delta\tilde{\boldsymbol{\kappa}}(\omega)}{\delta\tilde{\mathbf{D}}(\omega)}, \tag{C.8}$$

and

$$\tilde{\mathbf{K}}_s(\omega) = \frac{\delta\tilde{\boldsymbol{\kappa}}(\omega)}{\delta\tilde{\mathbf{D}}_s(\omega)}, \tag{C.9}$$

which only response to the selected fields $\delta\tilde{\mathbf{D}}(\omega)$ and $\delta\tilde{\mathbf{D}}_s(\omega)$. When acting on $\delta\tilde{\mathbf{D}}(\omega)$ ($\delta\tilde{\mathbf{D}}_s(\omega)$), $\tilde{\mathbf{K}}$ ($\tilde{\mathbf{K}}_s$) gives the same result as $\mathbf{K}(\omega)$ ($\mathbf{K}_s(\omega)$).

Defining $\delta\tilde{\mathbf{D}}_{\mathrm{MB}}(\omega) = \delta\tilde{\mathbf{D}}_s(\omega) - \delta\tilde{\mathbf{D}}(\omega)$, where the subscript MB denotes many-body effects, we have

$$\delta\tilde{\mathbf{D}}_{\mathrm{MB}}(\omega) = [\tilde{\mathbf{K}}_s^{-}(\omega) - \tilde{\mathbf{K}}^{-}(\omega)]\delta\tilde{\boldsymbol{\kappa}}(\omega), \tag{C.10}$$

which enables us to define the functional derivative

$$\tilde{\mathbf{L}}(\omega) = \frac{\delta(\tilde{\mathbf{D}}_s(\omega) - \tilde{\mathbf{D}}(\omega))}{\delta\tilde{\boldsymbol{\kappa}}(\omega)} = \frac{\delta\tilde{\mathbf{D}}_{\mathrm{MB}}(\omega)}{\delta\tilde{\boldsymbol{\kappa}}(\omega)} = \tilde{\mathbf{K}}_s^{-}(\omega) - \tilde{\mathbf{K}}^{-}(\omega) \tag{C.11}$$

as the general frequency-dependent pp response kernel. Then, we can express the Dyson-like equation

$$\tilde{\mathbf{K}}(\omega) = \frac{\delta\tilde{\boldsymbol{\kappa}}(\omega)}{\delta\tilde{\mathbf{D}}(\omega)} \tag{C.12}$$

$$= \frac{\delta\tilde{\boldsymbol{\kappa}}(\omega)}{\delta\tilde{\mathbf{D}}_s(\omega)}\frac{\delta\tilde{\mathbf{D}}_s(\omega)}{\delta\tilde{\mathbf{D}}(\omega)} \tag{C.13}$$

$$= \tilde{\mathbf{K}}_s(\mathbf{I} + \frac{\delta\tilde{\mathbf{D}}_{\mathrm{MB}}(\omega)}{\delta\tilde{\boldsymbol{\kappa}}(\omega)}\frac{\delta\tilde{\boldsymbol{\kappa}}(\omega)}{\delta\tilde{\mathbf{D}}(\omega)}) \tag{C.14}$$

$$= \tilde{\mathbf{K}}_s(\omega) + \tilde{\mathbf{K}}_s(\omega)\tilde{\mathbf{L}}(\omega)\tilde{\mathbf{K}}(\omega). \tag{C.15}$$

The multiplication by $\delta\tilde{D}_s$and its inverse in the second step are allowed because from Eqs. (C.2), (C.6) and (C.7) it follows that all quantities are in Im$\mathbf{K}^-(\omega)$. With only the assumption that the first order pairing matrix of an interacting system can be represented by a first order pairing matrix of some non-interacting system, we obtain the Dyson-like equation with a frequency-dependent pp kernel, which is not necessarily a second order derivative of some functional. Note that if the original $\delta\mathbf{D}_s(\omega)$ and $\delta\boldsymbol{\kappa}(\omega)$ were used, the derivative of Eq. (C.11) would be undefined since $\delta\mathbf{D}_s(\omega)$ and $\delta\mathbf{D}(\omega)$ are not necessarily a function of $\delta\boldsymbol{\kappa}(\omega)$.

It is essential to introduce $\delta\tilde{\mathbf{D}}(\omega)$ in the way expressed in Eq. (C.4). We bypass the difficulty of the absence of a one-to-one mapping in Eq. (C.1) by choosing a specific type of perturbation in Eq. (C.4). Although there is no one-to-one mapping between $\delta\mathbf{D}(\omega)$ and $\delta\boldsymbol{\kappa}(\omega)$, there is a one-to-one mapping between $\delta\tilde{\mathbf{D}}(\omega)$ and $\delta\tilde{\boldsymbol{\kappa}}(\omega)$ as shown in Eqs. (C.5) and (C.7). For every $\delta\tilde{\mathbf{D}}(\omega)$ that satisfies Eq. (C.5), any $\delta\tilde{\mathbf{D}}' = \mathbf{s} + \delta\tilde{\mathbf{D}}(\omega)$ with $\mathbf{s} \in$ Ker$\mathbf{K}(\omega)$ is also a solution of Eq. (C.5), where Ker$\mathbf{K}(\omega)$ is the kernel (or the null space)[274] of the linear operator $\mathbf{K}(\omega)$,

$$\text{Ker}\mathbf{K}(\omega) = \{\mathbf{x} \in \mathcal{V} | \mathbf{K}(\omega)\mathbf{x} = 0\}. \tag{C.16}$$

The constraint of Eq. (C.4) specifies the solution associated with $\mathbf{s} = 0$ so that the one-to-one mapping between $\delta\tilde{\mathbf{D}}(\omega)$ and $\delta\tilde{\boldsymbol{\kappa}}(\omega)$ can be established. Using the Hohenberg-Kohn[20] or Runge-Gross[50] language, we can say that $\delta\mathbf{D}(\omega)$ can be uniquely determined from $\delta\boldsymbol{\kappa}(\omega)$, up to an unimportant additive vector $\mathbf{s} \in$ Ker$\mathbf{K}(\omega)$. Fig C.1a illustrates the relationship of this mapping. Each distinct vector $\mathbf{s} \in$ Ker$\mathbf{K}(\omega)$ generates a unique coset (represented as an oval in Fig C.1a) of $\mathbf{s} +$ Im$\mathbf{K}^-(\omega) = \{\mathbf{s} + \mathbf{x} | \mathbf{x} \in \text{Im}\mathbf{K}^-(\omega)\}$, the image of which is exactly Im$\mathbf{K}(\omega)$ because

$$\begin{aligned} &\{\mathbf{y} \in \mathcal{V} | \mathbf{y} = \mathbf{K}(\omega)(\mathbf{s} + \mathbf{x}), \mathbf{x} \in \text{Im}\mathbf{K}^-(\omega), \mathbf{s} \in \text{Ker}\mathbf{K}(\omega)\} \\ =&\{\mathbf{y} \in \mathcal{V} | \mathbf{y} = \mathbf{K}(\omega)\mathbf{x}, \mathbf{x} \in \text{Im}\mathbf{K}^-(\omega)\} = \text{Im}\mathbf{K}(\omega). \end{aligned}$$

We design the perturbation $\delta\tilde{\mathbf{D}}(\omega)$ such that it belongs to the coset associated with

$\mathbf{s} = \mathbf{0}$, hence a one-to-one mapping (isomorphism) between $\delta\tilde{\mathbf{D}}(\omega)$ and $\delta\tilde{\boldsymbol{\kappa}}(\omega)$ can be established. Figure C.1b shows the density-density response function map, i.e. the linear order of the Runge-Gross map[50], as an analogy to the $\mathbf{K}(\omega)$ map in this paper. For the linear order of the Runge-Gross map, i.e.

$$\delta\boldsymbol{\rho}(\omega) = \boldsymbol{\chi}(\omega)\delta\mathbf{v}(\omega), \tag{C.17}$$

there is no one-to-one mapping between $\delta\boldsymbol{\rho}(\omega)$ and $\delta\mathbf{v}(\omega)$, since $\mathbf{c}(\omega) + \delta\mathbf{v}(\omega)$ with $\mathbf{c}(\omega)$ any spatial independent vector will not generate a new $\delta\boldsymbol{\rho}(\omega)$ which is generated by $\delta\mathbf{v}(\omega)$. Note that $\delta\boldsymbol{\rho}(\omega)$ and $\delta\mathbf{v}(\omega)$ now represent functions with one coordinate index $\delta\rho(\mathbf{r},\omega)$ and $\delta v(\mathbf{r},\omega)$ as they are both local, different from the non-local $\delta\boldsymbol{\kappa}(\omega)$ and $\delta\mathbf{D}(\omega)$ with two coordinate indexes. Nevertheless, we can achieve the one-to-one mapping between $\delta\tilde{\mathbf{v}}(\omega)$ and $\delta\tilde{\boldsymbol{\rho}}(\omega)$ by designing the perturbation $\delta\tilde{\mathbf{v}}(\omega)$ such that $\delta\tilde{\mathbf{v}}(\omega) \in \mathrm{Im}\boldsymbol{\chi}^{-}(\omega)$. Such a potential-centric perspective is an example of the potential functional in Ref. [101].

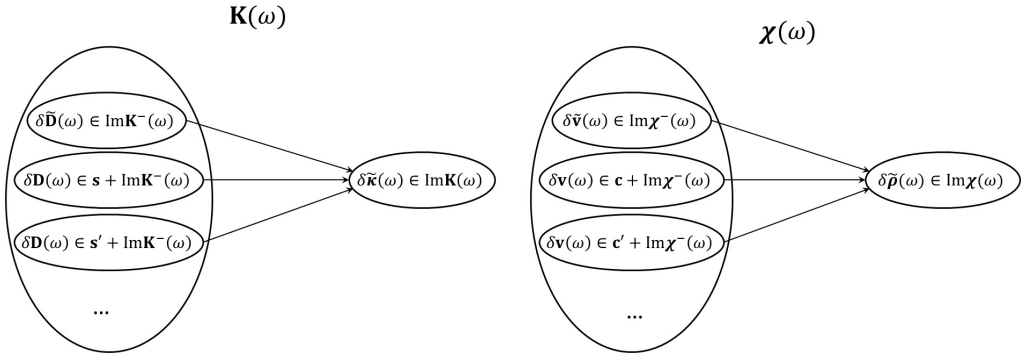


(a) The $\mathbf{K}(\omega)$ map (b) The $\boldsymbol{\chi}(\omega)$ map

FIGURE C.1: The illustration of the one-to-one mapping between (a) $\delta\tilde{\mathbf{D}}(\omega)$ and $\delta\tilde{\boldsymbol{\kappa}}(\omega)$, and (b) $\delta\tilde{\mathbf{v}}(\omega)$ and $\delta\tilde{\boldsymbol{\rho}}(\omega)$. In (a), $\mathbf{s}$ and $\mathbf{s}'$ are different vectors in $\mathrm{Ker}\mathbf{K}(\omega)$. The small ovals in the domain represents different cosets. A coset is defined as $\mathbf{s} + \mathrm{Im}\mathbf{K}^{-}(\omega) = \{\mathbf{s} + \mathbf{x} | \mathbf{x} \in \mathrm{Im}\mathbf{K}^{-}(\omega)\}$. The image of each coset is the full image $\mathrm{Im}\mathbf{K}(\omega)$. We design the perturbation such that $\delta\tilde{\mathbf{D}}(\omega)$ only resides in one single oval, thus there is a one-to-one mapping between $\delta\tilde{\mathbf{D}}(\omega)$ and $\delta\tilde{\boldsymbol{\kappa}}(\omega)$, despite the overall many-to-one mapping between $\delta\mathbf{D}(\omega)$ and $\delta\tilde{\boldsymbol{\kappa}}(\omega)$. An analogy is present in (b) for the $\boldsymbol{\chi}(\omega)$ map. In this case, $\mathbf{c}$ and $\mathbf{c}'$ are different vectors in $\mathrm{Ker}\boldsymbol{\chi}(\omega)$. Any spatial coordinate independent vector $\mathbf{c}$ belongs to $\mathrm{Ker}\boldsymbol{\chi}(\omega)$ and generates a coset $\mathbf{c} + \mathrm{Im}\boldsymbol{\chi}^{-}(\omega)$. The one-to-one mapping between $\delta\tilde{\mathbf{v}}(\omega)$ and $\delta\tilde{\boldsymbol{\rho}}(\omega)$ is fulfilled by designing the perturbation $\delta\tilde{\mathbf{v}}(\omega)$.

# Appendix D

## Mathematical analysis of the pp-RPA equation

The appendix discusses many mathematical properties of the pp-RPA equation. These properties are conceptually very similar to those of ph-RPA equation as shown in Ref. [158].

### D.1 The zero signature of an eigenvector with an imaginary eigenvalue

For an eigenvalue $\omega_n$ and eigenvector $\mathbf{z}_n$, we have

$$\mathbf{M}\mathbf{z}_n = \omega_n \mathbf{W}\mathbf{z}_n. \tag{D.1}$$

The Hermitian conjugate of Eq. (D.1) becomes

$$\mathbf{z}_n^\dagger \mathbf{M} = \omega_n^* \mathbf{z}_n^\dagger \mathbf{W}. \tag{D.2}$$

Multiplying $\mathbf{z}_n^\dagger$ to the left of Eq. (D.1) and $\mathbf{z}_n$ to the right of Eq. (D.2), we have

$$\mathbf{z}_n^\dagger \mathbf{M}\mathbf{z}_n = \omega_n \mathbf{z}_n^\dagger \mathbf{W}\mathbf{z}_n = \omega_n^* \mathbf{z}_n^\dagger \mathbf{W}\mathbf{z}_n.$$

Therefore

$$(\omega_n - \omega_n^*)(\mathbf{z}_n^\dagger \mathbf{W}\mathbf{z}_n) = 0. \tag{D.3}$$

For an imaginary eigenvalue $\omega_n \neq \omega_n^*$, the signature $\mathbf{z}_n^\dagger \mathbf{W} \mathbf{z}_n = 0$.

## D.2 The orthonormalization of eigenvectors with all real eigenvalues

Using the same approach in Subsection D.1 in the Appendix but with two different eigenvalues and eigenvectors, we have

$$\mathbf{z}_n^\dagger \mathbf{M} \mathbf{z}_m = \omega_m \mathbf{z}_n^\dagger \mathbf{W} \mathbf{z}_m = \omega_n^* \mathbf{z}_n^\dagger \mathbf{W} \mathbf{z}_m,$$

and

$$(\omega_m - \omega_n^*)(\mathbf{z}_n^\dagger \mathbf{W} \mathbf{z}_m) = 0. \tag{D.4}$$

Therefore, when two real eigenvalues are different ($\omega_m \neq \omega_n^*$), the two eigenvectors are orthogonal under the metric $\mathbf{W}$ ($\mathbf{z}_n^\dagger \mathbf{W} \mathbf{z}_m = 0$). Since linear combination of eigenvectors of a degenerate eigenvalue stays in the same eigenspace, we can choose the eigenvectors of a degenerate eigenvalue to orthogonal to each other within the eigenspace. When all eigenvalues are real, eigenvectors can, therefore, be chosen to be orthogonalized under the metric $\mathbf{W}$. For a diagonalizable pp-RPA equation with all real eigenvalues, $\mathbf{z}_n^\dagger \mathbf{W} \mathbf{z}_n$ should not be zero, otherwise we have $\mathbf{z}_n^\dagger \mathbf{W} \mathbf{Z} = 0$, which indicates the eigenvector matrix is rank-deficit, which contradicts with the diagonalizability assumption. Therefore, the signatures of eigenvectors are all nonzero for a diagonalizable pp-RPA equation with all real eigenvalues. The resulting orthonormalization can be written as

$$\mathbf{Z}^\dagger \mathbf{W} \mathbf{Z} = \Lambda, \tag{D.5}$$

where $\Lambda$ is a diagonal matrix with only $\pm 1$ diagonal elements. According to Sylvester's law of inertia[273], $\mathbf{W}$ and $\Lambda$ share the same number of $+1$'s and $-1$'s. In another word, there are $N_{pp}$ $N+2$ excitations and $N_{hh}$ $N-2$ excitations, according to the definition of $N \pm 2$ excitations in Sec. 4.2. We can further arrange the eigenvectors

such that eigenvectors with positive signatures stay in the left of $\mathbf{Z}$, then finally we reach the normalization condition

$$\mathbf{Z}^\dagger \mathbf{W} \mathbf{Z} = \mathbf{W}. \tag{D.6}$$

## D.3 The equivalence between stability and positive definiteness of $\mathbf{M}$

First we show that the stability condition of Eq. (4.11) leads to the positive definiteness of $\mathbf{M}$.

From the stability of the pp-RPA equation (Eq. (4.11)) and the normalization (Eq. (4.10)), we have

$$\begin{aligned}
\mathbf{c}^\dagger \mathbf{M} \mathbf{c} &= \sum_{mn} (\mathbf{z}_m c_m)^\dagger \mathbf{M} (\mathbf{z}_n c_n) \\
&= \sum_{mn} c_m^* \mathbf{z}_m^\dagger \omega_n \mathbf{W} \mathbf{z}_n c_n \\
&= \sum_{n} c_m^* \delta_{mn} W_{mn} \omega_n c_n \\
&= \sum_{mn} c_m^* |\omega_m| \delta_{mn} c_n \\
&= \sum_{m} |c_m|^2 |\omega_m| > 0,
\end{aligned}$$

with an arbitrary nonzero column vector $\mathbf{c}$. Thus, $\mathbf{M}$ is positive definite for a pp-RPA equation.

Next, we show that the reverse is also true.

Given that $\mathbf{M}$ is positive definite, the pp-RPA equation in the compact form reads

$$\mathbf{M} \mathbf{z}_n = \omega_n \mathbf{W} \mathbf{z}_n. \tag{D.7}$$

Since $\mathbf{M}$ is positive definite, Eq. (4.6) could be rewritten as

$$\mathbf{L}^\dagger \mathbf{z}_n = \omega_n \mathbf{L}^{-1} \mathbf{W} \left(\mathbf{L}^{-1}\right)^\dagger \mathbf{L}^\dagger \mathbf{z}_n,$$

where $\mathbf{M} = \mathbf{L}\mathbf{L}^\dagger$ is the Cholesky decomposition. With $\tilde{\mathbf{z}}_n = \mathbf{L}^\dagger \mathbf{z}_n$ and $\tilde{\mathbf{W}} = \mathbf{L}^{-1}\mathbf{W}\left(\mathbf{L}^{-1}\right)^\dagger$, then the eigenvalue problem

$$\tilde{\mathbf{W}}\tilde{\mathbf{z}}_n = \tilde{\omega}_n \tilde{\mathbf{z}}_n \tag{D.8}$$

is diagonalizable with all real eigenvalues, since $\tilde{\mathbf{W}}^\dagger = \tilde{\mathbf{W}}$ by definition. Additionally, all eigenvalues of $\tilde{\mathbf{W}}$, $\tilde{\omega}_n$'s, will be nonzero, since zero eigenvalue indicates $\det(\tilde{\mathbf{W}}) = 0$ which contradicts the definition of $\tilde{\mathbf{W}}$. With orthonormalization of the eigenvectors $\tilde{\mathbf{z}}_n^\dagger \tilde{\mathbf{z}}_m = \delta_{nm}|\tilde{\omega}_n|^{-1}$, Eq. (4.6) can be diagonalized with real eigenvalues

$$\omega_n = \tilde{\omega}_n^{-1}, \tag{D.9}$$

and eigenvector orthonormalization with the eigenvalue sign constraints (the eigenvectors are arranged in the same way as in Subsection D.2 in the Appendix),

$$\mathbf{z}_n^\dagger \mathbf{W} \mathbf{z}_m = \delta_{mn}\mathrm{sign}(\omega_m) = W_{nm}. \tag{D.10}$$

Eq. (D.10) guarantees that the $\min_n \omega_n^{N+2} > 0 > \max_m \omega_m^{N-2}$. Therefore, by definition, this pp-RPA equation is stable since all the eigenvalues are real and the $N+2$ and $N-2$ excitation spectra are nicely separated.

In summary, the stability condition of an pp-RPA equation is equivalent to the positive definiteness of $\mathbf{M}$.

## D.4 The invertibility of $\mathbf{X}$ for a stable pp-RPA equation

We now prove the invertibility of $\mathbf{X}$ in Sec. 4.3. According to Subsection D.2 in the Appendix, the eigenvalues of a stable pp-RPA equation are orthonormalized according to

$$\mathbf{Z}^\dagger \mathbf{W} \mathbf{Z} = \mathbf{W}. \tag{D.11}$$

For only $N+2$ excitation vectors,

$$\mathbf{Z}_{N+2}^\dagger \mathbf{W} \mathbf{Z}_{N+2} = \mathbf{I}, \tag{D.12}$$

where

$$\mathbf{Z}_{N+2} = \begin{bmatrix} \mathbf{X} \\ \mathbf{Y} \end{bmatrix},$$

with $\mathbf{X}$ and $\mathbf{Y}$ the particle-particle and hole-hole block of the $N + 2$ excitation eigenvector matrices. Expanding Eq. (D.12), we have

$$\mathbf{X}^\dagger\mathbf{X} - \mathbf{Y}^\dagger\mathbf{Y} = \mathbf{I}. \tag{D.13}$$

Therefore, $\mathbf{X}^\dagger\mathbf{X} = \mathbf{I} + \mathbf{Y}^\dagger\mathbf{Y}$ is positive definite, and $\mathbf{X}$ is invertible, otherwise $\mathbf{X}^\dagger\mathbf{X}$ will not be positive definite.

# Bibliography


[1] A. Szabo and N. Ostlund, *Modern Quantum Chemistry: Introduction to advanced Electronic Structure Theory* (Dover Publications, Inc., Mineola, 1989).

[2] R. McWeeny, *Methods of Molecular Quantum Mechanics*, 2nd ed., Theoretical Chemistry (Academic Press, 1992).

[3] P. Dirac, Proc. R. Soc. A **123**, 714 (1929).

[4] R. G. Parr and W. Yang, *Density-Functional Theory of Atoms And Molecules* (Oxford University Press, New York, 1989).

[5] A. Coleman and V. Yukalov, *Reduced Density Matrices: Coulson's Challenge*, Lecture Notes in Chemistry (Springer Berlin Heidelberg, 2000).

[6] B. Hammond, W. Lester, and P. Reynolds, *Monte Carlo Methods in Ab Initio Quantum Chemistry*, World Scientific Lecture and Course Notes in Chemistry; Vol. 1 (World Scientific, 1994).

[7] G. K.-L. Chan and S. Sharma, Annu. Rev. Phys. Chem. **62**, 465 (2011).

[8] M. J. Frisch, G. W. Trucks, H. B. Schlegel, G. E. Scuseria, M. A. Robb, J. R. Cheeseman, J. A. Montgomery, Jr., T. Vreven, K. N. Kudin, J. C. Burant, J. M. Millam, S. S. Iyengar, J. Tomasi, V. Barone, B. Mennucci, M. Cossi, G. Scalmani, N. Rega, G. A. Petersson, H. Nakatsuji, M. Hada, M. Ehara, K. Toyota, R. Fukuda, J. Hasegawa, M. Ishida, T. Nakajima, Y. Honda, O. Kitao, H. Nakai, M. Klene, X. Li, J. E. Knox, H. P. Hratchian, J. B. Cross, V. Bakken, C. Adamo, J. Jaramillo, R. Gomperts, R. E. Stratmann, O. Yazyev, A. J. Austin, R. Cammi, C. Pomelli, J. W. Ochterski, P. Y. Ayala, K. Morokuma, G. A. Voth, P. Salvador, J. J. Dannenberg, V. G. Zakrzewski, S. Dapprich, A. D. Daniels, M. C. Strain, O. Farkas, D. K. Malick, A. D. Rabuck, K. Raghavachari, J. B. Foresman, J. V. Ortiz, Q. Cui, A. G. Baboul, S. Clifford, J. Cioslowski, B. B. Stefanov, G. Liu, A. Liashenko, P. Piskorz, I. Komaromi, R. L. Martin, D. J. Fox, T. Keith, M. A. Al-Laham, C. Y. Peng, A. Nanayakkara, M. Challacombe, P. M. W. Gill, B. Johnson, W. Chen, M. W. Wong, C. Gonzalez, and J. A. Pople, Gaussian 03, Revision C.02, Gaussian, Inc., Wallingford, CT, 2004.

[9] J. R. Schmidt, N. Shenvi, and J. C. Tully, J. Chem. Phys. **129** (2008).

[10] M. Valiev, E. J. Bylaska, N. Govind, K. Kowalski, T. P. Straatsma, H. J. J. Van Dam, D. Wang, J. Nieplocha, E. Apra, T. L. Windus, and W. A. de Jong, Comput. Phys. Commun. **181**, 1477 (2010).

[11] D. Cook, *Handbook of Computational Quantum Chemistry*, Dover books on chemistry (Oxford University Press, Incorporated, 1998).

[12] I. Shavitt and R. J. Bartlett, *Many-Body Methods in Chemistry and Physics: MBPT and Coupled-Cluster Theory* (Cambridge University Press, 2009).

[13] D. Peng and W. Yang, J. Chem. Phys. **138**, 184108 (2013).

[14] D. Peng, H. van Aggelen, Y. Yang, and W. Yang, J. Chem. Phys. **140**, 18A522 (2014).

[15] D. Peng, S. N. Steinmann, H. van Aggelen, and W. Yang, J. Chem. Phys. **139**, 104112 (2013).

[16] D. Peng, X. Hu, D. Devarajan, D. H. Ess, E. R. Johnson, and W. Yang, J. Chem. Phys. **137**, 114112 (2012).

[17] I. Levine, *Quantum Chemistry*, Allyn and Bacon chemistry series (Allyn and Bacon, 1983).

[18] M. Reiher and A. Wolf, *Relativistic Quantum Chemistry: The Fundamental Theory of Molecular Science* (Wiley, Weinheim, 2009).

[19] E. K. U. Gross, E. Runge, and O. Heinonen, *Many-Particle Theory* (Adam Hilger, New York, 1991).

[20] P. Hohenberg and W. Kohn, Phys. Rev. **136**, B864 (1964).

[21] W. Kohn and L. Sham, Phys. Rev. **385**, A1133 (1965).

[22] M. Levy, Proc. Natl. Acad. Sci. USA **76**, 6062 (1979).

[23] V. Lignères and E. Carter, "An introduction to orbital-free density functional theory," in *Handbook of Materials Modeling*, edited by S. Yip (Springer Netherlands, 2005) pp. 137–148.

[24] J. P. Perdew and K. Schmidt, AIP Conf. Proc. **577**, 1 (2001).

[25] S. H. Vosko, L. Wilk, and M. Nusair, Can. J. Phys. **58**, 1200 (1980).

[26] J. P. Perdew and A. Zunger, Phys. Rev. B **23**, 5048 (1981).

[27] D. M. Ceperley and B. J. Alder, Phys. Rev. Lett. **45**, 566 (1980).

[28] C. T. Lee, W. Yang, and R. G. Parr, Phys. Rev. B **37**, 785 (1988).

[29] J. P. Perdew, K. Burke, and M. Ernzerhof, Phys. Rev. Lett. **77**, 3865 (1996).

[30] A. D. Becke, J. Chem. Phys. **98**, 5648 (1993).

[31] A. D. Becke, Phys. Rev. A **38**, 3098 (1988).

[32] P. M. W. Gill, Aust. J. Chem. **54** (2001).

[33] Q. Wu and W. Yang, J. Chem. Phys. **116**, 515 (2002).

[34] A. J. Cohen, P. Mori-Sánchez, and W. Yang, Science **321**, 792 (2008).

[35] A. J. Cohen, P. Mori-Sánchez, and W. Yang, J. Chem. Phys. **129**, 121104 (2008).

[36] A. J. Cohen, P. Mori-Sánchez, and W. Yang, Phys. Rev. B **77**, 115123 (2008).

[37] An in-house program for QM/MM simulations (http://www.qm4d.info) .

[38] A. J. Cohen, P. Mori-Sánchez, and W. Yang, Chem. Rev. **112**, 289 (2011).

[39] P. Mori-Sánchez, A. Cohen, and W. Yang, Phys. Rev. Lett. **100**, 146401 (2008).

[40] P. Mori-Sánchez, A. Cohen, and W. Yang, Phys. Rev. Lett. **102**, 066403 (2009).

[41] A. J. Cohen, P. Mori-Sánchez, and W. Yang, J. Chem. Phys. **127**, 034101 (2007).

[42] A. J. Cohen, P. Mori-Sánchez, and W. Yang, J. Chem. Phys. **126**, 191109 (2007).

[43] X. Zheng, A. J. Cohen, P. Mori-Sánchez, X. Q. Hu, and W. Yang, Phys. Rev. Lett. **107**, 026403 (2011).

[44] X. Zheng, T. Zhou, and W. Yang, J. Chem. Phys. **138**, 174105 (2013).

[45] R. Baer and D. Neuhauser, Phys. Rev. Lett. **94**, 043002 (2005).

[46] R. Baer, E. Livshits, and U. Salzner, Annu. Rev. Phys. Chem. **61**, 85 (2010).

[47] A. D. Becke, J. Chem. Phys. **119**, 2972 (2003).

[48] A. D. Becke, J. Chem. Phys. **122**, 064101 (2005).

[49] J. J. Sakurai and J. Napolitano, *Modern Quantum Mechanics*, International edition (Addison-Wesley, 2011).

[50] E. Runge and E. K. U. Gross, Phys. Rev. Lett. **52**, 997 (1984).

[51] R. van Leeuwen, Phys. Rev. Lett. **82**, 3863 (1999).

[52] M. E. Casida, "Time-dependent density functional response theory for molecules," in *Recent Advances in Computational Chemistry*, Vol. 1, edited by D. P. Chong (World Scientific, Singapore, 1995) p. 155.

[53] J. E. Rice, R. D. Amos, S. M. Colwell, N. C. Handy, and J. Sanz, J. Chem. Phys. **93**, 8828 (1990).

[54] A. Dreuw and M. Head-Gordon, J. Am. Chem. Soc. **126**, 4007 (2004).

[55] J. Blaizot and G. Ripka, *Quantum Theory of Finite Systems* (Cambridge, MA, 1986).

[56] W. H. Dickhoff and D. Van Neck, *Many-body Theory Exposed!: Propagator Description of Quantum Mechanics in Many-body Systems* (World Scientific, 2005).

[57] D. J. Rowe, Rev. Mod. Phys. **40**, 153 (1968).

[58] D. J. Rowe, *Nuclear Collective Motion: Models and Theory* (World Scientific, 2010).

[59] M. L. Tiago and J. R. Chelikowsky, Solid State Commun. **136**, 333 (2005).

[60] P. Chattaraj, *Chemical Reactivity Theory: A Density Functional View* (CRC PressINC, 2009).

[61] P. Geerlings and F. De Proft, Phys. Chem. Chem. Phys. **10**, 3028 (2008).

[62] R. G. Parr and W. Yang, J. Am. Chem. Soc. **106**, 4049 (1984).

[63] W. Yang, C. Lee, and S. K. Ghosh, J. Phys. Chem. **89**, 5412 (1985).

[64] W. Yang and R. G. Parr, Proc. Natl. Acad. Sci. USA **82**, 6723 (1985).

[65] W. Yang, R. G. Parr, and L. Uytterhoeven, Phys. Chem. Miner. **15**, 191 (1987).

[66] C. T. Lee, W. Yang, and R. G. Parr, J. Mol. Struc.-THEOCHEM **40**, 305 (1988).

[67] R. G. Parr and W. Yang, Annu. Rev. Phys. Chem. **46**, 701 (1995).

[68] F. De Proft and P. Geerlings, Chem. Rev. **101**, 1451 (2001).

[69] P. Geerlings, F. De Proft, and W. Langenaeker, Chem. Rev. **103**, 1793 (2003).

[70] J. S. M. Anderson, J. Melin, and P. W. Ayers, J. Chem. Theory Comput. **3**, 358 (2007).

[71] J. S. M. Anderson, J. Melin, and P. W. Ayers, J. Chem. Theory Comput. **3**, 375 (2007).

[72] P. W. Ayers, C. Morell, F. De Proft, and P. Geerlings, Chem.-Eur. J. **13**, 8240 (2007).

[73] S. B. Liu, Acta Phys.-Chim. Sin. **25**, 590 (2009).

[74] J. C. Slater, J. B. Mann, T. M. Wilson, and J. H. Wood, Phys. Rev. **184**, 672 (1969).

[75] J. F. Janak, Phys. Rev. B **18**, 7165 (1978).

[76] J. P. Perdew, R. G. Parr, M. Levy, and J. L. Balduz, Phys. Rev. Lett. **49**, 1691 (1982).

[77] W. Yang, Y. Zhang, and P. W. Ayers, Phys. Rev. Lett. **84**, 5172 (2000).

[78] Y. Tawada, T. Tsuneda, S. Yanagisawa, T. Yanai, and K. Hirao, J. Chem. Phys. **120**, 8425 (2004).

[79] E. Livshits and R. Baer, Phys. Chem. Chem. Phys. **9**, 2932 (2007).

[80] W. Yang, A. J. Cohen, F. D. Proft, and P. Geerlings, J. Chem. Phys. **136**, 144110 (2012).

[81] R. A. Donnelly and R. G. Parr, J. Chem. Phys. **69**, 4431 (1978).

[82] R. G. Parr and R. G. Pearson, J. Am. Chem. Soc. **105**, 7512 (1983).

[83] C. Morell, A. Grand, and A. Toro-Labbé, J. Phys. Chem. A **109**, 205 (2005).

[84] E. Chamorro, R. Contreras, and P. Fuentealba, J. Chem. Phys. **113**, 10861 (2000).

[85] E. Chamorro, P. Fuentealba, and R. Contreras, J. Chem. Phys. **115**, 6822 (2001).

[86] Y. K. Zhang and W. Yang, Theor. Chem. Acc. **103**, 346 (2000).

[87] K. Iverson, *A Programming Language* (Wiley, New York, 1962).

[88] P. W. Ayers, J. Math. Chem. **43**, 285 (2008).

[89] A. Seidl, A. Görling, P. Vogl, J. A. Majewski, and M. Levy, Phys. Rev. B **53**, 3764 (1996).

[90] W. Yang, A. J. Cohen, and P. Mori-Sánchez, J. Chem. Phys. **136**, 204111 (2012).

[91] J. E. Rice and N. C. Handy, J. Chem. Phys. **94**, 4959 (1991).

[92] S. M. Colwell, C. W. Murray, N. C. Handy, and R. D. Amos, Chem. Phys. Lett. **210**, 261 (1993).

[93] R. Flores-Moreno and A. M. Koster, J. Chem. Phys. **128**, 134105 (2008).

[94] R. Flores-Moreno, J. Melin, J. V. Ortiz, and G. Merino, J. Chem. Phys. **129**, 224105 (2008).

[95] U. Salzner and R. Baer, J. Chem. Phys. **131**, 231101 (2009).

[96] T. Stein, J. Autschbach, N. Govind, L. Kronik, and R. Baer, J. Phys. Chem. Lett. **3**, 3740 (2012).

[97] J. E. Rice and N. C. Handy, Int. J. Quantum Chem. **43**, 91 (1992).

[98] F. Furche and R. Ahlrichs, J. Chem. Phys. **117**, 7433 (2002).

[99] P. Mori-Sánchez, A. J. Cohen, and W. Yang, Phys. Rev. A **85**, 42507 (2012).

[100] W. Yang, P. Mori-Sánchez, and A. J. Cohen, J. Chem. Phys. **139**, 104114 (2013).

[101] W. Yang, P. Ayers, and Q. Wu, Phys. Rev. Lett. **92**, 146404 (2004).

[102] A. J. Cohen, P. Mori-Sánchez, and W. Yang, J. Chem. Theory Comput. **5**, 786 (2009).

[103] P. Bultinck, D. Clarisse, P. W. Ayers, and R. Carbo-Dorca, Phys. Chem. Chem. Phys. **13**, 6110 (2011).

[104] Q. Wu and W. Yang, J. Chem. Phys. **118**, 2498 (2003).

[105] E. E. Salpeter and H. A. Bethe, Phys. Rev. **84**, 1232 (1951).

[106] G. Onida, L. Reining, and A. Rubio, Rev. Mod. Phys. **74**, 601 (2002).

[107] U. von Barth and L. Hedin, J. Phys. C **5**, 1629 (1972).

[108] M. M. Pant and A. K. Rajagopal, Solid State Commun. **10**, 1157 (1972).

[109] D. H. Ess, E. R. Johnson, X. Q. Hu, and W. Yang, J. Phys. Chem. A **115**, 76 (2011).

[110] C. R. Jacob and M. Reiher, Int. J. Quantum Chem. **112**, 3661 (2012).

[111] N. Fukuda, F. Iwamoto, and K. Sawada, Phys. Rev. **135**, A932 (1964).

[112] W. J. Mulhall, R. J. Liotta, J. A. Evans, and R. P. Perazzo, Nucl. Phys. A **93**, 261 (1967).

[113] D. J. Rowe, Phys. Rev. **175**, 1283 (1968).

[114] J. Vary and J. N. Ginocchio, Nucl. Phys. A **166**, 479 (1971).

[115] J. C. Pacheco and N. Vinh Mau, Phys. Rev. C **65**, 44004 (2002).

[116] G. Blanchon, N. V. Mau, A. Bonaccorso, M. Dupuis, and N. Pillet, Phys. Rev. C **82**, 34313 (2010).

[117] P. Ring and P. Schuck, *The Nuclear Many-Body Problem* (Springer, 2004).

[118] H. van Aggelen, Y. Yang, and W. Yang, Phys. Rev. A **88**, 030501 (2013).

[119] Y. Yang, H. van Aggelen, S. N. Steinmann, D. Peng, and W. Yang, J. Chem. Phys. **139**, 174110 (2013).

[120] G. E. Scuseria, T. M. Henderson, and I. W. Bulik, J. Chem. Phys. **139**, 104113 (2013).

[121] Y. Yang, H. van Aggelen, and W. Yang, J. Chem. Phys. **139**, 224105 (2013).

[122] M. Lüders and E. Gross, Int. J. Quantum Chem. **56**, 521 (1995).

[123] M. Lüders, M. Marques, N. Lathiotakis, A. Floris, G. Profeta, L. Fast, A. Continenza, S. Massidda, and E. K. U. Gross, Phys. Rev. B **72**, 24545 (2005).

[124] S. Hirata and M. Head-Gordon, Chem. Phys. Lett. **302**, 375 (1999).

[125] M. a. L. Marques and E. K. U. Gross, Annu. Rev. Phys. Chem. **55**, 427 (2004).

[126] M. Marques, *Time-Dependent Density Functional Theory*, Lecture Notes in Physics (Springer, 2006).

[127] M. E. Casida, J. Mol. Struc.-THEOCHEM **914**, 3 (2009).

[128] M. A. L. Marques, N. T. Maitra, and F. M. S. Nogueira, *Fundamentals of Time-Dependent Density Functional Theory*, Lecture Notes in Physics (Springer Berlin Heidelberg, 2012).

[129] C. A. Ullrich, *Time-Dependent Density-Functional Theory: Concepts and Applications*, Oxford Graduate Texts (OUP Oxford, 2012).

[130] L. N. Oliveira, E. K. U. Gross, and W. Kohn, Phys. Rev. Lett. **60**, 2430 (1988).

[131] K. Capelle and E. K. U. Gross, Int. J. Quantum Chem. **61**, 325 (1997).

[132] O. J. Wacker, R. Kümmel, and E. K. U. Gross, Phys. Rev. Lett. **73**, 2915 (1994).

[133] S. Kurth, M. Marques, M. Lüders, and E. K. U. Gross, Phys. Rev. Lett. **83**, 2628 (1999).

[134] M. Lüders and E. K. U. Gross, *Density Functional Theory for Superconductors: a First Principles Approach to the Superconducting Phase*, Ph.D. thesis, der Bayerischen Julius-Maximilians-Universität Würzburg (1998).

[135] C.-M. Liegener, Chem. Phys. Lett. **90**, 188 (1982).

[136] C.-M. Liegener, J. Chem. Phys. **79**, 2924 (1983).

[137] C.-M. Liegener, J. Chem. Phys. **104**, 2940 (1996).

[138] J. V. Ortiz, J. Chem. Phys. **81**, 5873 (1984).

[139] M. Nooijen and R. J. Bartlett, J. Chem. Phys. **106**, 6441 (1997).

[140] M. Nooijen, Int. J. Mol. Sci. **3**, 656 (2002).

[141] J. Shen and P. Piecuch, J. Chem. Phys. **138**, 194102 (2013).

[142] E. K. U. Gross and S. Kurth, Int. J. Quantum Chem. **40**, 289 (1991).

[143] B. Verstichel, H. van Aggelen, D. Van Neck, P. W. Ayers, and P. Bultinck, J. Chem. Phys. **132**, 114113 (2010).

[144] E. H. Lieb, Int. J. Quantum Chem. **24**, 243 (1983).

[145] M. Marques and E. K. U. Gross, *Density Functional Theory for Superconductors: Exchange and Correlation Potentials for Inhomogeneous Systems*, Ph.D. thesis, der Bayerischen Julius-Maximilians-Universität Würzburg (2000).

[146] J. G. Valatin, Phys. Rev. **122**, 1012 (1961).

[147] F. Furche and T. Van Voorhis, J. Chem. Phys. **122**, 164106 (2005).

[148] A. Heß elmann and A. Görling, Mol. Phys. **109**, 2473 (2011).

[149] T. Gould and J. F. Dobson, J. Chem. Phys. **138**, 14109 (2013).

[150] K. W. Sattelmeyer, H. F. Schaefer III, and J. F. Stanton, Chem. Phys. Lett. **378**, 42 (2003).

[151] D. Bohm and D. Pines, Phys. Rev. **82**, 625 (1951).

[152] D. Pines and D. Bohm, Phys. Rev. **85**, 338 (1952).

[153] J. Lindhard, K. Dan. Vidensk. Selsk. Mat. Fys. Medd. **28**, 8 (1954).

[154] A. G. Eguiluz, Phys. Rev. Lett. **51**, 1907 (1983).

[155] D. C. Langreth and J. P. Perdew, Solid State Commun. **17**, 1425 (1975).

[156] G. F. Giuliani and G. Vignale, *Quantum Theory Of The Electron Liquid* (Cambridge University Press, 2005).

[157] D. Thouless, Nucl. Phys. **21**, 225 (1960).

[158] D. D. Thouless, Nucl. Phys. **22**, 78 (1961).

[159] D. Thouless and J. Valatin, Nucl. Phys. **31**, 211 (1962).

[160] E. R. Marshalek and J. Weneser, Ann. Phys. **53**, 569 (1969).

[161] H. Eshuis, J. Yarkony, and F. Furche, J. Chem. Phys. **132**, 234114 (2010).

[162] F. Furche, J. Chem. Phys. **129**, 114105 (2008).

[163] S. Kurth and J. P. Perdew, Phys. Rev. B **59**, 10461 (1999).

[164] F. Furche, Phys. Rev. B **64**, 195120 (2001).

[165] M. Fuchs, Y.-M. Niquet, X. Gonze, and K. Burke, J. Chem. Phys. **122**, 94116 (2005).

[166] H. Eshuis and F. Furche, J. Chem. Phys. **136**, 84105 (2012).

[167] X. Ren, P. Rinke, C. Joas, and M. Scheffler, J. Mater. Sci. **47**, 7447 (2012).

[168] W. Zhu, J. Toulouse, A. Savin, and J. G. Angyán, J. Chem. Phys. **132**, 244108 (2010).

[169] J. Toulouse, W. Zhu, J. G. Ángyán, and A. Savin, Phys. Rev. A **82**, 032502 (2010).

[170] M. Hellgren, D. R. Rohr, and E. K. U. Gross, J. Chem. Phys. **136**, 34106 (2012).

[171] O. Gunnarsson and B. Lundqvist, Phys. Rev. B **13**, 4274 (1976).

[172] J. Toivanen and J. Suhonen, Phys. Rev. Lett. **75**, 410 (1995).

[173] G. Ripka and R. Padjen, Nucl. Phys. A **132**, 489 (1969).

[174] K. A. Brueckner and C. A. Levinson, Phys. Rev. **97**, 1344 (1955).

[175] R. Eden, Proc. R. Soc. A **235**, 408 (1956).

[176] H. Bethe, Phys. Rev. **103**, 1353 (1956).

[177] J. Goldstone, Proc. R. Soc. A **239**, 267 (1957).

[178] M. Gell-Mann and K. Brueckner, Phys. Rev. **106**, 364 (1957).

[179] J. Čížek, J. Chem. Phys. **45**, 4256 (1966).

[180] G. E. Scuseria, T. M. Henderson, and D. C. Sorensen, J. Chem. Phys. **129**, 231101 (2008).

[181] E. Sanderson, Phys. Lett. **19**, 141 (1965).

[182] R. F. Bishop, W. Piechocki, and G. A. Stevens, Few-Body Systems **4**, 161 (1988).

[183] M. Nooijen and R. J. Bartlett, J. Chem. Phys. **102**, 3629 (1995).

[184] S. R. Gwaltney, R. J. Bartlett, and M. Nooijen, J. Chem. Phys. **111**, 58 (1999).

[185] H. Sekino and R. J. Bartlett, Int. J. Quantum Chem. **26**, 255 (1984).

[186] K. Kowalski, J. R. Hammond, and W. A. de Jong, J. Chem. Phys. **127**, 164105 (2007).

[187] N. J. Higham, *Functions of Matrices: Theory and Computation*, SIAM e-books (Society for Industrial and Applied Mathematics (SIAM, 3600 Market Street, Floor 6, Philadelphia, PA 19104), 2008).

[188] W. H. Adams, Phys. Rev. **127**, 1650 (1962).

[189] D. Dehareng and G. Dive, J. Comput. Chem. **21**, 483 (2000).

[190] W. Kutzelnigg, Theor. Chim. Acta **80**, 349 (1991).

[191] CFOUR, Coupled-Cluster techniques for Computational Chemistry, a quantum-chemical program package by J. F. Stanton, J. Gauss, M. E. Harding, P. G. Szalay with contributions from A. A. Auer, R. J. Bartlett, U. Benedikt, C. Berger, D. E. Bernholdt, Y. J. Bomble, L. Cheng, O. Christiansen, M. Heckert, O. Heun, C. Huber, T.-C. Jagau, D. Jonsson, J. Juselius, K. Klein, W. J. Lauderdale, D. A. Matthews, T. Metzroth, L. A. Muck, D. P. Oeill, D. R. Price, E. Prochnow, C. Puzzarini, K. Ruud, F. Schiffmann,W. Schwalbach, S. Stopkowicz, A. Tajti, J. Vazquez, F.Wang, J. D. Watts and the integral packages MOLECULE (J. Almlof and P. R. Taylor), PROPS (P. R. Taylor), ABACUS (T. Helgaker, H. J. Aa. Jensen, P. Jorgensen, and J. Olsen), and ECP routines by A. V. Mitin and C. van Wullen, see http://www.cfour.de for the current version.

[192] T. H. Dunning, J. Chem. Phys. **90**, 1007 (1989).

[193] D. E. Woon and T. H. Dunning, J. Chem. Phys. **98**, 1358 (1993).

[194] R. J. Bartlett, I. Grabowski, S. Hirata, and S. Ivanov, J. Chem. Phys. **122**, 34104 (2005).

[195] R. J. Bartlett, V. F. Lotrich, and I. V. Schweigert, J. Chem. Phys. **123**, 62205 (2005).

[196] J. D. Watts, J. Gauss, and R. J. Bartlett, J. Chem. Phys. **98**, 8718 (1993).

[197] G. J. O. Beran, S. R. Gwaltney, and M. Head-Gordon, Phys. Chem. Chem. Phys. **5**, 2488 (2003).

[198] J. D. Watts and R. J. Bartlett, J. Chem. Phys. **95**, 6652 (1991).

[199] L. A. Curtiss, K. Raghavachari, P. C. Redfern, and J. A. Pople, J. Chem. Phys. **112**, 7374 (2000).

[200] L. A. Curtiss, P. C. Redfern, and K. Raghavachari, J. Chem. Phys. **123**, 124107 (2005).

[201] J. A. Pople, M. Head-Gordon, D. J. Fox, K. Raghavachari, and L. A. Curtiss, J. Chem. Phys. **90**, 5622 (1989).

[202] L. A. Curtiss, C. Jones, G. W. Trucks, K. Raghavachari, and J. A. Pople, J. Chem. Phys. **93**, 2537 (1990).

[203] L. A. Curtiss, K. Raghavachari, P. C. Redfern, and J. A. Pople, J. Chem. Phys. **106**, 1063 (1997).

[204] C. Adamo, M. Ernzerhof, and G. E. Scuseria, J. Chem. Phys. **112**, 2643 (2000).

[205] T. Tamura and T. Udagawa, Nucl. Phys. **53**, 33 (1964).

[206] C. Yannouleas, Phys. Rev. C **35**, 1159 (1987).

[207] G. Lauritsch and P.-G. Reinhard, Nucl. Phys. A **509**, 287 (1990).

[208] D. Gambacurta and F. Catara, Journal of Physics: Conference Series **168**, 012012 (2009).

[209] D. L. Yeager and V. McKoy, J. Chem. Phys. **67**, 2473 (1977).

[210] D. Yeager, M. Nascimento, and V. McKoy, Phys. Rev. A **11**, 1168 (1975).

[211] A. Ipatov, F. Cordova, L. J. Doriol, and M. E. Casida, J. Mol. Struc.-THEOCHEM **914**, 60 (2009).

[212] E. R. Davidson, J. Comput. Phys. **17**, 87 (1975).

[213] L. Salem and C. Rowland, Angew. Chem. Int. Ed. **11**, 92 (1972).

[214] K. C. Nicolaou, W. M. Dai, S. C. Tsay, V. A. Estevez, and W. Wrasidlo, Science **256**, 1172 (1992).

[215] S. Pedersen, J. L. Herek, and A. H. Zewail, Science **266**, 1359 (1994).

[216] C. J. Cramer, J. Am. Chem. Soc. **120**, 6261 (1998).

[217] Z.-X. Yu, P. Caramella, and K. N. Houk, J. Am. Chem. Soc. **125**, 15420 (2003).

[218] A. Rajca, Chem. Rev. **94**, 871 (1994).

[219] K. Matsuda, M. Matsuo, and M. Irie, J. Org. Chem. **66**, 8799 (2001).

[220] D. Scheschkewitz, H. Amii, H. Gornitzka, W. W. Schoeller, D. Bourissou, and G. Bertrand, Science **295**, 1880 (2002).

[221] A. Rajca, K. Shiraishi, and S. Rajca, Chem. Commun. 4372 (2009).

[222] K. A. Williams, M. J. Nowak, E. Dormann, and F. Wudl, Synth. Met. **14**, 233 (1986).

[223] I. Kaur, M. Jazdzyk, N. N. Stein, P. Prusevich, and G. P. Miller, J. Am. Chem. Soc. **132**, 1261 (2010).

[224] W. Borden and E. R. Davidson, Annu. Rev. Phys. Chem. **30**, 125 (1979).

[225] R. R. Squires and C. J. Cramer, J. Phys. Chem. A **102**, 9072 (1998).

[226] S. N. Datta, P. P. Jha, and M. E. Ali, J. Phys. Chem. A **108**, 4087 (2004).

[227] E. R. Davidson and A. E. Clark, Int. J. Quantum Chem **103**, 1 (2005).

[228] P. Pulay and R. F. Liu, J. Phys. Chem. **94**, 5548 (1990).

[229] W. T. G. Johnson, D. A. Hrovat, A. Skancke, and W. T. Borden, Theor. Chem. Acc. **102**, 207 (1999).

[230] D. H. Ess, A. E. Hayden, F.-G. Klärner, and K. N. Houk, J. Org. Chem. **73**, 7586 (2008).

[231] J. Pittner, P. Nachtigall, P. Carsky, and I. Hubac, J. Phys. Chem. A **105**, 1354 (2001).

[232] X. Z. Li and J. Paldus, J. Chem. Phys. **129**, 054104 (2008).

[233] S. Yamanaka, T. Kawakami, H. Nagao, and K. Yamaguchi, Chem. Phys. Lett. **231**, 25 (1994).

[234] B. R. Beno, J. Fennen, K. N. Houk, H. J. Lindner, and K. Hafner, J. Am. Chem. Soc. **120**, 10490 (1998).

[235] A. D. Becke, A. Savin, and H. Stoll, Theor. Chem. Acc. **91**, 147 (1995).

[236] J. Wang, A. D. Becke, and J. Vedene H. Smith, J. Chem. Phys. **102**, 3477 (1995).

[237] A. Görling, Phys. Rev. Lett. **85**, 4229 (2000).

[238] T. Ziegler, A. Rauk, and E. J. Baerends, Theor. Chim. Acta **43**, 261 (1977).

[239] K. Yamaguchi, Y. Yoshioka, and T. Fueno, Chem. Phys. Lett. **46**, 360 (1977).

[240] I. Mayer, "The spin-projected extended hartree-fock method," in *Adv. Quantum Chem.*, Vol. Volume 12, edited by P.-O. Löwdin (Academic Press, 1980) p. 189.

[241] T. Saito, Y. Kataoka, Y. Nakanishi, T. Matsui, Y. Kitagawa, T. Kawakami, M. Okumura, and K. Yamaguchi, Chem. Phys. **368**, 1 (2010).

[242] A. I. Krylov, Chem. Phys. Lett. **338**, 375 (2001).

[243] A. I. Krylov, Chem. Phys. Lett. **350**, 522 (2001).

[244] L. V. Slipchenko and A. I. Krylov, J. Chem. Phys. **117**, 4694 (2002).

[245] J. S. Sears, C. D. Sherrill, and A. I. Krylov, J. Chem. Phys. **118**, 9084 (2003).

[246] Y. Shao, C. Saravanan, M. Head-Gordon, and C. A. White, J. Chem. Phys. **118**, 6144 (2003).

[247] Z. Li and W. Liu, J. Chem. Phys. **133**, 064106 (2010).

[248] E. R. Johnson and J. Contreras-Garcia, J. Chem. Phys. **135**, 081103 (2011).

[249] X. C. Zeng, H. Hu, X. Q. Hu, A. J. Cohen, and W. Yang, J. Chem. Phys. **128**, 124510 (2008).

[250] X. C. Zeng, H. Hu, X. Q. Hu, and W. Yang, J. Chem. Phys. **130**, 164111 (2009).

[251] P. W. Ayers and W. Yang, J. Chem. Phys. **124**, 224108 (2006).

[252] M. Filatov and S. Shaik, Chem. Phys. Lett. **288**, 689 (1998).

[253] M. Filatov and S. Shaik, J. Chem. Phys. **110**, 116 (1999).

[254] M. Filatov and S. Shaik, Chem. Phys. Lett. **304**, 429 (1999).

[255] M. Filatov and S. Shaik, J. Phys. Chem. A **104**, 6628 (2000).

[256] S. G. Wang and W. H. E. Schwarz, J. Chem. Phys. **105**, 4641 (1996).

[257] E. Baerends, J. Autschbach, A. Bérces, F. Bickelhaupt, C. Bo, P. Boerrigter, L. Cavallo, D. Chong, L. Deng, R. Dickson, D. Ellis, M. v. Faassen, L. Fan, T. Fischer, C. F. Guerra, S. v. Gisbergen, J. Groeneveld, O. Gritsenko, M. Grüning, F. Harris, P. v. d. Hoek, C. Jacob, H. Jacobsen, L. Jensen, G. v. Kessel, F. Kootstra, E. v. Lenthe, D. McCormack, A. Michalak, J. Neugebauer, V. Nicu, V. Osinga, S. Patchkovskii, P. Philipsen, D. Post, C. Pye, W. Ravenek, P. Ros, P. Schipper, G. Schreckenbach, J. Snijders, M. Solà, M. Swart, D. Swerhone, G. t. Velde, P. Vernooijs, L. Versluis, L. Visscher, O. Visser, F. Wang, T. Wesolowski, E. v. Wezenbeek, G. Wiesenekker, S. Wolff, T. Woo, A. Yakovlev, and T. Ziegler, ADF2010.02, SCM, Theoretical Chemistry, Vrije Universiteit, Amsterdam, The Netherlands, (2007), http://www.scm.com.

[258] T. Saito, S. Nishihara, S. Yamanaka, Y. Kitagawa, T. Kawakami, S. Yamada, H. Isobe, M. Okumura, and K. Yamaguchi, Theor. Chem. Acc. **130**, 749 (2011).

[259] W. T. Borden and E. R. Davidson, J. Am. Chem. Soc. **99**, 4587 (1977).

[260] A. Görling, Phys. Rev. A **47**, 2783 (1993).

[261] E. R. Davidson, "Singlet-triplet energy separation in carbenes and related diradicals," in *Diradicals*, edited by W. T. Borden (Wiley, Weinheim, Germany, 1982) p. 73.

[262] G. Osmann, P. R. Bunker, P. Jensen, and W. P. Kraemer, J. Mol. Spectrosc. **186**, 319 (1997).

[263] J. P. Gu, G. Hirsch, R. J. Buenker, M. Brumm, G. Osmann, P. R. Bunker, and P. Jensen, J. Mol. Struct. **517**, 247 (2000).

[264] P. R. Bunker and P. Jensen, *Molecular Symmetry and Spectroscopy, 2nd Ed* (NRC Research Press, 2006) p. 748.

[265] D. R. Yarkony, Rev. Mod. Phys. **68**, 985 (1996).

[266] J. Berkowitz, J. P. Greene, H. Cho, and B. Ruščić, J. Chem. Phys. **86**, 1235 (1987).

[267] R. Escribano and A. Campargue, J. Chem. Phys. **108**, 6249 (1998).

[268] J. Berkowitz and H. Cho, J. Chem. Phys. **90**, 1 (1989).

[269] P. H. Dederichs, S. Blügel, R. Zeller, and H. Akai, Phys. Rev. Lett. **53**, 2512 (1984).

[270] Y. Mo, L. Song, and Y. Lin, J. Phys. Chem. A **111**, 8291 (2007).

[271] Y. Geerts, G. Klärner, and K. Müllen, *Electronic Materials: The Oligomer Approach* (Weinheim, Germany, 1998).

[272] M. Bendikov, H. M. Duong, K. Starkey, K. N. Houk, E. A. Carter, and F. Wudl, J. Am. Chem. Soc. **126**, 7416 (2004).

[273] R. A. Horn and C. R. Johnson, *Matrix Analysis* (Cambridge University Press, 1990).

[274] S. Roman, *Advanced Linear Algebra*, Graduate texts in mathematics (Springer Science+Business Media, LLC, 2008).

[275] A. Ben-Israel and T. N. E. Greville, *Generalized Inverses: Theory and Applications* (Springer, 2003).

# Biography

Personal:

- Full Name: Degao Peng
- Date/Place of Birth: Dec 29, 1985, Wuchuan, Guangdong, China

Education:

- Ph.D in Chemistry, Duke University, 2014
- B.S. in Chemistry, Peking University, 2009

Honors and Awards:

- Conference Travel Fellowship, Duke University, 2014
- William Krigbaum and Marcus Hobbs Fellowship, Duke University, 2013
- Conference Travel Fellowship, Duke University, 2012
- Conference Travel Fellowship, National Science Foundation, 2012

Publications:

1. Degao Peng, Bo Zhao, Aron J. Cohen, Xiangqian Hu and Weitao Yang, "Optimized Effective Potential for Calculations with Orbital-Free Potential Functionals", *Mol. Phys.*, **110**, 925 (2012).

2. Degao Peng, Xiangqian Hu, Deepa Devarajan, Daniel H. Ess, Erin R. Johnson and Weitao Yang, "Variational Fractional-Spin Density-Functional Theory for Diradicals", *J. Chem. Phys.*, **137**, 114112 (2012).

3. Degao Peng and Weitao Yang, "Fukui Function and Response Function for Nonlocal and Fractional Systems", *J. Chem. Phys.*, **138**, 184108 (2013).

4. Degao Peng, Stephen N. Steinmann, Helen van Aggelen and Weitao Yang, "Equivalence of Particle-Particle Random Phase Approximation Correlation Energy and Ladder-Coupled-Cluster-Doubles", *J. Chem. Phys.*, **139**, 104112 (2013).

5. Yang Yang, Helen van Aggelen, Stephen N. Steinmann, Degao Peng and Weitao Yang, "Benchmark tests and spin adaptation for the particle-particle random phase approximation", *J. Chem. Phys.*, **139**, 174110 (2013).

6. Andrew T. Franks, Degao Peng, Weitao Yang and Katherine J. Franz, "Characterization of a Photoswitching Chelator with Light-Modulated Geometric, Electronic and Metal Binding Properties", *Inorg. Chem.*, **53**, 1397 (2014).

7. Degao Peng, Helen van Aggelen, Yang Yang and Weitao Yang, "Linear-Response Time-Dependent Density-Functional Theory with Pairing Fields", *J. Chem. Phys.*, **140**, 18A522 (2014).

8. Ali M. Malek, Degao Peng, Weitao Yang, Robert Balawender and Andrzej Holas, "Testing exchange-correlation functionals at fractional electron number", *J. Chem. Phys.*, submitted.

9. Hao Hu, Yuqian Jiang, Jun Gao and Degao Peng, "Minimum Free-Energy Path Method for Efficient Quantum Mechanical / Molecular Mechanical Computation of Vertical Excitation Energy in Solution", *J. Chem. Phys.*, submitted.

10. Degao Peng, Yang Yang, Peng Zhang and Weitao Yang "Second random phase approximations for single and double excitations", in preparation.